

# **ASYMMETRIC SYNTHESIS AND APPLICATIONS OF OCTAHEDRAL METAL COMPLEXES**

A DISSERTATION

In

Chemistry

Presented to the Faculties of Philipps-Universität Marburg in Partial Fulfillment  
of the Requirements for the Degree of Doctor of Science  
(Dr. rer. nat.)

**Zhijie Lin**

Beijing, P. R. China

Marburg/Lahn 2013

This thesis originated in the period from November 2009 to April 2013 under the direction of Prof. Dr. Eric Meggers the Department of Chemistry of the University of Marburg.

From the Department of Chemistry, Philipps-University Marburg

Accepted as a dissertation on \_\_\_\_\_

Defence committee: Prof. Dr. Gerhard Hilt

Prof. Dr. Jörg Sundermeyer

Prof. Dr. Bernhard Roling

Date of examination: April 30<sup>th</sup> 2013

## Acknowledgement

I'd like to express my deeply appreciation to my supervisor Prof. Meggers. I came to his lab at the end of 2009. And during these three years, he gave me so many valuable suggestions on my PHD thesis. With his helping, I published two papers on the good journals. And more importantly, he taught me how to do research in the right way. This will be the valuable wealth for me in the future.

Additionally, I would like to express my gratitude to my master research advisors, Peiqiang Huang and Hongkui Zhang. All of my basic skills for doing the chemical experiment were trained in their lab.

Besides, I would like to thank the Chinese government for providing scholarship to me.

While I worked in the lab, so many people have given me kindly helps, especially our secretary Ina Pinnschmidt, lab technician Katja Kr äing and my lab mate Pijus Sasmal. I also would like to express my appreciation to Dr. Xiulan Xie of the NMR facility and Dr. Klaus Harms in the X-ray crystallography department.

Finally, I want to thank my parents and my wife for their long time supporting. I want to say: I am very happy and feel very lucky to do chemical research in Meggers' group in Germany, and wish my friends here all the best.

**Part of this work has been already published:**

1) “Isomerization-Induced Asymmetric Coordination Chemistry: From Auxiliary Control to Asymmetric Catalysis”

L. Gong, Z. Lin, K. Harms, E. Meggers, *Angew. Chem. Int. Ed.* **2010**, *49*, 7955-7957.

2) “Asymmetric Coordination Chemistry by Chiral-Auxiliary-Mediated Dynamic Resolution under Thermodynamic Control”

Z. Lin, L. Gong, M. A. Celik, K. Harms, G. Frenking, E. Meggers, *Chem. Asian J.* **2011**, *6*, 474-481.

3) “*N*-Sulfinylcarboximidates as a Novel Class of Chiral Bidentate Ligands: Application to Asymmetric Coordination Chemistry”

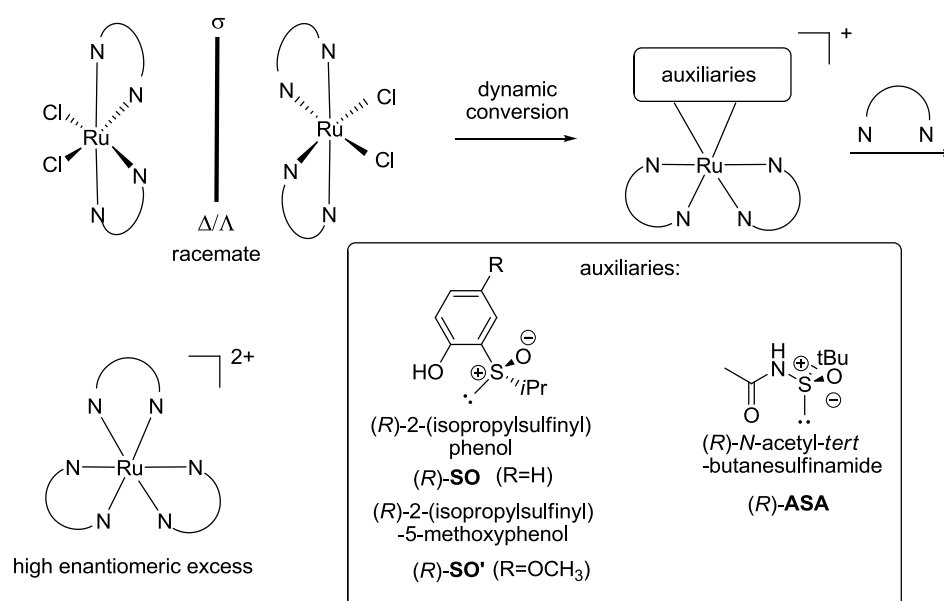
Z. Lin, M. A. Celik, C. Fu, K. Harms, G. Frenking, E. Meggers, *Chem. Eur. J.* **2011**, *17*, 12602-12605.

4) “Catalytic Azide Reduction in Biological Environments”

P. Sasmal, S. Carregal-Romero, A. Han, C. Streu, Z. Lin, E. Meggers, *ChemBioChem.* **2012**, *13*, 1116-1120.

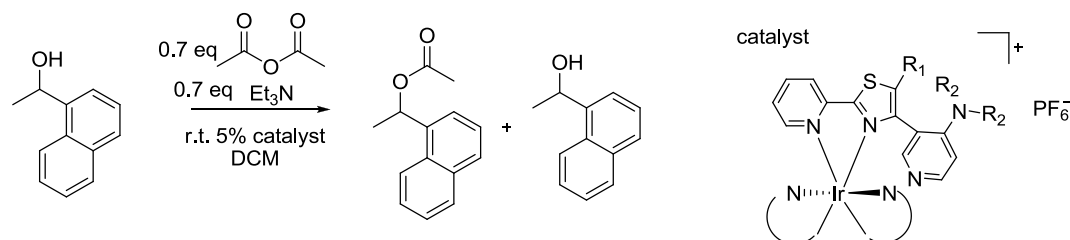
## Abstract

In this thesis, some methods for the asymmetric synthesis of octahedral metal complexes were developed by using chiral auxiliaries. These chiral auxiliaries are coordinating bidentate ligands which control the metal-centered configuration in the course of ligand exchange reactions or dynamic equilibria. Afterwards, the chiral auxiliaries can be removed in an acid-induced fashion under complete retention of configuration (Scheme I).



**Scheme I.** Auxiliary directed asymmetric synthesis of octahedral ruthenium complexes with high enantiomeric excess.

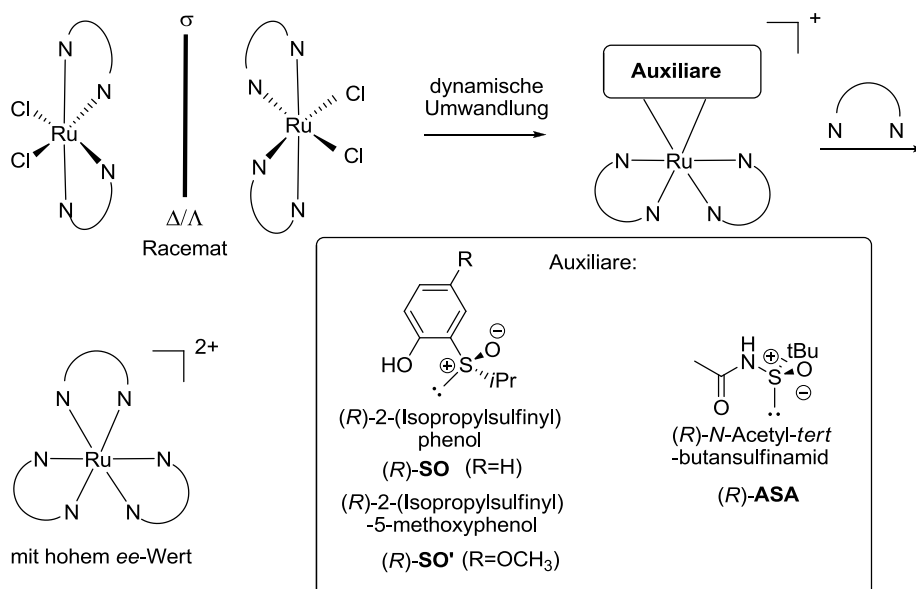
Additionally, we initially explored the applications of enantiomerically pure octahedral iridium complexes as catalysts for asymmetric transformations. In this direction, we focused on the asymmetric acyl transfer catalysis and synthesized different types of the catalysts for resolving racemic alcohols (Scheme II).



**Scheme II.** Kinetic resolution of racemic alcohols catalyzed by chiral Ir(III) catalysts.

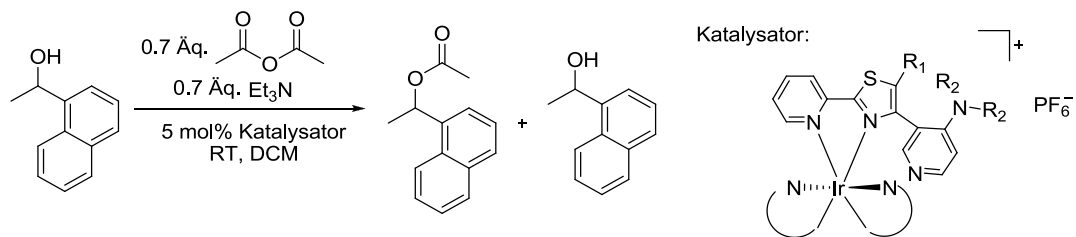
## Abstract auf Deutsch

In der vorliegenden Doktorarbeit wurden Methoden für die asymmetrische Synthese oktaedrischer Metallkomplexe entwickelt, welche auf der Anwendung chiraler Auxiliare basieren. Solche chiralen Auxiliare sind zweizähnige Liganden, die bei Koordination die Konfiguration des Metallzentrums durch Ligandenaustauschreaktion oder dynamisches Gleichgewicht kontrollieren. Die chiralen Auxiliare können anschließend unter sauren Bedingungen abgespalten werden, wobei die Konfiguration des Metallzentrums erhalten bleibt (Schema I).



**Schema I.** Auxiliare-vermittelte asymmetrische Synthese oktaedrischer Ruthenium-Komplexe mit hohem Enantiomerenüberschuss.

Desweiteren wurden Anwendungen enantiomerenreiner Iridium-Komplexe für die asymmetrische Katalyse erforscht. Es wurde sich auf die asymmetrische Acyltransfer-Katalyse konzentriert. Verschiedene Katalysatoren wurden synthetisiert und für die kinetische Racematspaltung sekundärer Alkohole untersucht (Schema II).



**Schema II.** Kinetische Racematspaltung eines sekundären Alkohols mittels chiraler Ir(III)-Katalysatoren.

---

## Table of Contents

<b>Chapter 1 Theoretical part</b> .....	<b>1</b>
1.1 Introduction .....	1
1.2 Preparation of non-racemic octahedral metal complexes .....	4
1.2.1 Resolution with chiral chromatography .....	4
1.2.2 Formation of diastereomeric salts .....	5
1.2.3 Diastereoselective coordination with chiral ligands .....	6
1.2.4 Chiral auxiliary directed asymmetric synthesis .....	10
1.3 Applications of enantiopure octahedral metal complexes in catalytic reactions .....	16
<b>Chapter 2 Aim of this work</b> .....	<b>19</b>
<b>Chapter 3 Results</b> .....	<b>21</b>
3.1 Novel chiral auxiliaries for the asymmetric synthesis of ruthenium polypyridyl complexes .....	21
3.1.1 Sulfinylphenol auxiliary system .....	21
3.1.2 Sulfinylacetone auxiliary system .....	47
3.1.3 N-Acetylsulfonamide auxiliary system .....	51
3.1.4 Cyclometalated phenyloxazoline auxiliary system .....	65
3.2 Development of octahedral chiral-at-metal complexes for asymmetric catalysis .....	70
3.2.1 Approach .....	70
3.2.2 Design, synthesis and evaluation of DMAP-iridium complexes .....	74
3.2.2.1 DMAP-picolinamide ligand .....	76
3.2.2.2 DMAP-pyridine-thiazole ligand .....	82
3.2.2.3 Polypyridyl ligand .....	92
3.2.2.4 Chiral bidentate ligand .....	96
<b>Chapter 4 Summary and outlook</b> .....	<b>102</b>
4.1 Asymmetric coordination chemistry .....	102
4.2 Applications of enantiomerically pure octahedral metal complexes .....	104
<b>Chapter 5 Experimental part</b> .....	<b>106</b>
5.1 Materials and Methods .....	106
5.2 Novel chiral auxiliaries for the asymmetric synthesis of ruthenium polypyridyl complexes .....	109
5.2.1 Ligand synthesis .....	109
5.2.2 Diastereoselective coordination chemistry .....	116
5.2.3 Auxiliary removal .....	128
5.3 Development of octahedral chiral-at-metal complexes for asymmetric catalysis .....	144
5.3.1 Synthesis of DMAP-ligands .....	144
5.3.2 Synthesis of metal chiral DMAP catalysts .....	156
5.3.2.1 Synthesis of enantiopure iridium precursor .....	156
5.3.2.2 General procedure for synthesis of chiral-at-metal DMAP catalysts .....	161
5.3.3 Evaluation of chiral-at-metal DMAP catalysts .....	169
<b>Chapter 6 References</b> .....	<b>172</b>
6.1 Literature .....	172



---

6.2 List of synthesized compounds .....	178
6.3 Abbreviations and symbols .....	183
6.4 Appendix .....	185

## ***Chapter 1 Theoretical part***

### **1.1 Introduction**

Mirror image objects, such as our hands, widely exist in nature. Scientists refer to these objects as having chirality, which was first defined by Lord Kelvin (1824-1907):

I call any geometrical figure, or group of points, chiral, and say that it has chirality, if its image in a plane mirror, ideally realized, cannot be brought to coincide with itself.

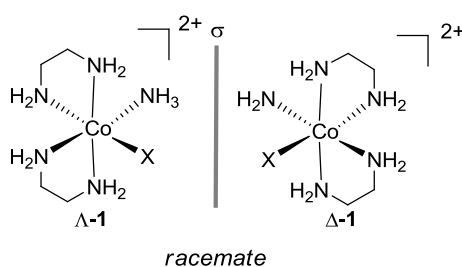
The word “chirality” comes from the Greek word “Khier,” meaning hand. Today, chirality is defined by the International Union of Pure and Applied Chemistry (IUPAC) as:

The geometric property of a rigid object (or spatial arrangement of points or atoms) of being nonsuperimposable on its mirror image; such an object has no symmetry elements of the second kind (a mirror plane,  $\sigma = S_1$ , a centre of inversion,  $i = S_2$ , a rotation reflection axis,  $S_{2n}$ ). If the object is superimposable on its mirror image the object is described as being achiral.

With the advances in science, chiral objects became an important issue in human life. For example, increasingly more enantiopure molecules are being used in the fields of pharmaceuticals and agriculture. Thus, the US Food and Drug Administration’s (FDA’s) policy statement for the development of new diastereomeric drugs recommends that, in the case of chiral molecules, the properties – particularly toxicity – of both enantiomers should be studied.

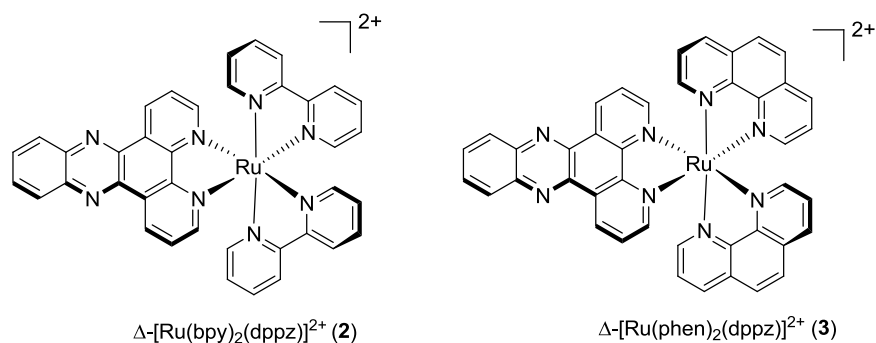
Organic stereochemistry in the twentieth century developed quickly, especially in the synthesis of natural compounds with large number of stereogenic centers. Additionally, for approximately the past 40 years, enantioselective catalysis has been researched to enrich the methods for obtaining enantiopure compounds. W. S. Knowles, R. Noyori and K. B. Sharpless won the Nobel Prize in this area in 2001. Similarly, inorganic stereochemistry also earned its own status. Alfred Werner first applied van’t Hoff and Le Bel’s stereochemical theories of the tetrahedral nature of

the carbon atom to the structure of octahedral metal complexes in 1893. He predicted that the octahedral coordination compounds could exist in an enantiomeric form with the power of optical rotation. This hypothesis was demonstrated in 1911 by resolution of the two enantiomers of the complexes  $[\text{Co}(\text{en})_2(\text{NH}_3)\text{X}]\text{X}_2$  ( $\text{X} = \text{Cl}, \text{Br}$ ;  $\text{en} =$  ethylene diamine) ( $\Lambda\text{-1}/\Delta\text{-1}$ ) (Figure 1)<sup>1-4</sup>, and won the Nobel Prize for these works in 1913.



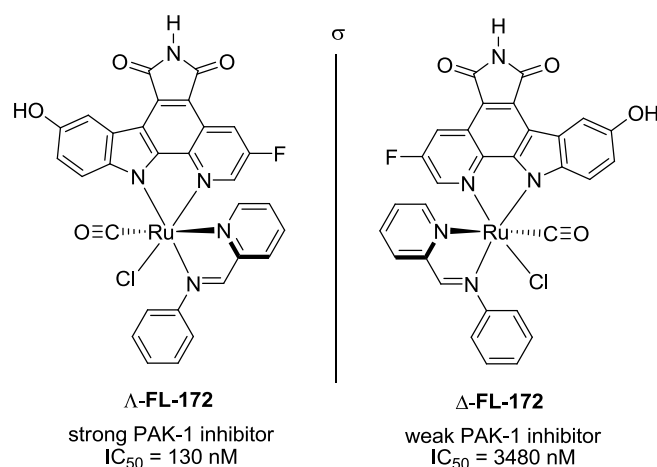
**Figure 1.** The two enantiomers of the cationic complexes of  $[\text{Co}(\text{en})_2(\text{NH}_3)\text{X}]^{2+}$ .

However, towards chirality, are there any specific properties of the coordination compounds? In inorganic stereochemistry, coordination compounds are more complicated than organic compounds, due to the high number of possible arrangements of atoms in molecules containing one or several centers of higher coordination numbers. For example, the octahedral metal complex has a maximum of 15 pairs of enantiomers (30 stereoisomers). Based on this range of possibilities, the coordination compounds display significant behavior in the life sciences and asymmetric catalysis reactions. For example, Barton et al. designed the enantiopure octahedral ruthenium complexes,  $\Delta\text{-2}$  and  $\Delta\text{-3}$ , which are capable of intercalating between stacked base pairs of B-DNA. In aqueous solutions, the complexes are nonluminescent, while in the presence of double-stranded nucleic acids, these compounds are strongly emissive and, thus, function as molecular light switches for DNA (Figure 2)<sup>5</sup>.



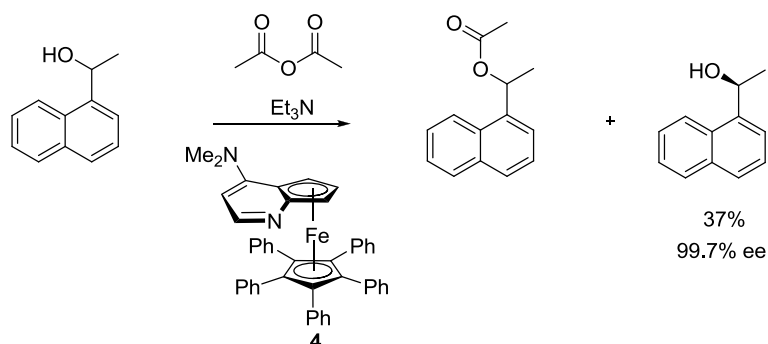
**Figure 2.** Molecular light switches for DNA.

Similarly, Meggers et al. invented inhibitors, such as  $\Lambda$ -**FL-172** and  $\Delta$ -**FL-172**, for protein kinases, which are based on the octahedral metal complexes. However, some results demonstrate that complexes with the same geometry, but different chirality, showed different biological activity (Figure 3)<sup>6</sup>.



**Figure 3.** The ruthenium complex  $\Lambda$ -**FL172** is a selective inhibitor of the protein kinase PAK-1 in contrast to the almost inactive mirror-imaged complex  $\Delta$ -**FL172** (1  $\mu$ M ATP).

A coordination compound in which the chiral element was a metallic center was also used in an organocatalytic reaction. For example, ferrocene has a rigid sandwich structure, which is highly stable and easily available. So, Fu et al. exploited this planar chirality in the resolution of acrylic alcohols (Scheme 1)<sup>7</sup>.



**Scheme 1.** Kinetic resolution of racemic alcohols catalyzed by the Fu-catalyst (**4**).

In summary, the chiral coordination compounds showed excellent behavior in the life sciences and metal based catalytic reactions. Considering the higher possibilities of stereoisomers, as opposed to chiral carbon, and the little attention these have received in the context of organic stereochemistry, this area merits further investigation.

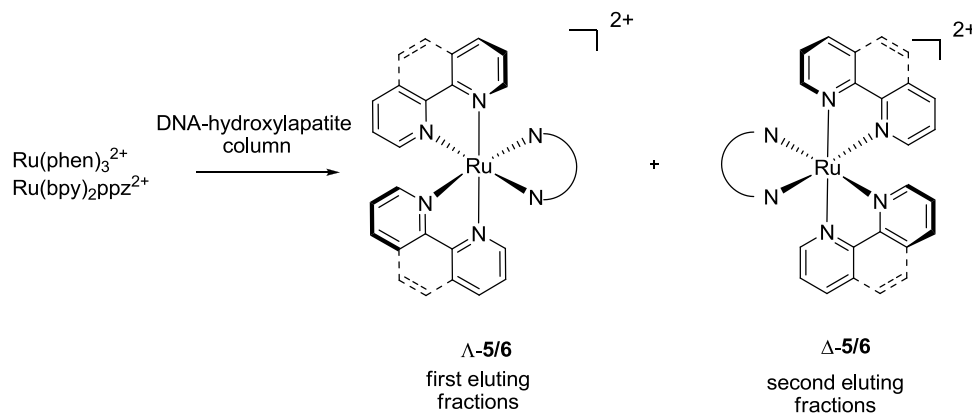
## 1.2 Preparation of non-racemic octahedral metal complexes

For investigating in the inorganic stereochemistry, we need to find the methods to obtain the non-racemic metal complexes. Considering our lab mainly researches on octahedral metal complexes, I will introduce the methods for asymmetric synthesis of octahedral metal complexes. Based on the different strategies for obtaining the enantiopure complexes, I will introduce them following in three directions.

### 1.2.1 Resolution with chiral chromatography

Strekas and co-workers invented DNA-hydroxylapatite column, since the various six-coordinate metal complexes in which the ligands are bidentate diimines with fused aromatic ring systems are capable of enantiomerically selective interaction with double-stranded DNAs<sup>8</sup>. The method is successfully resolved  $\text{Ru}(\text{phen})_3^{2+}$  (phen = 1,10-phenanthroline) (**5**) and  $\text{Ru}(\text{bpy})_2\text{ppz}^{2+}$  (bpy = 2,2'-bipyridine, ppz = pyrazino[2,3-f][4,7]phenanthroline) (**6**) with 90% ee (Scheme 2). Similarly, Villani and co-workers resolved the  $[\text{Fe}(\text{L})_3](\text{ClO}_4)_2$  (ligands L = 1,10-phenanthroline,

4,7-dimethyl-1,10-phenanthroline, 5,6-dimethyl-1,10-phenanthroline, 3,4,7,8-tetramethyl-1,10-phenanthroline, and 4,7-dichloro-1,10-phenanthroline) by using a Chiralcel OD RH column<sup>9</sup>.

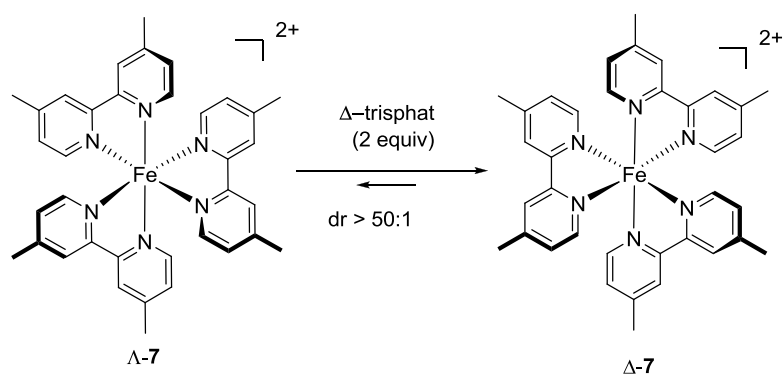


**Scheme 2.** Resolution of  $\text{Ru}(\text{phen})_3^{2+}$  (**5**) and  $\text{Ru}(\text{bpy})_2\text{ppz}^{2+}$  (**6**) by chiral chromatography (DNA-hydroxylapatite column).

### 1.2.2 Formation of diastereomeric salts

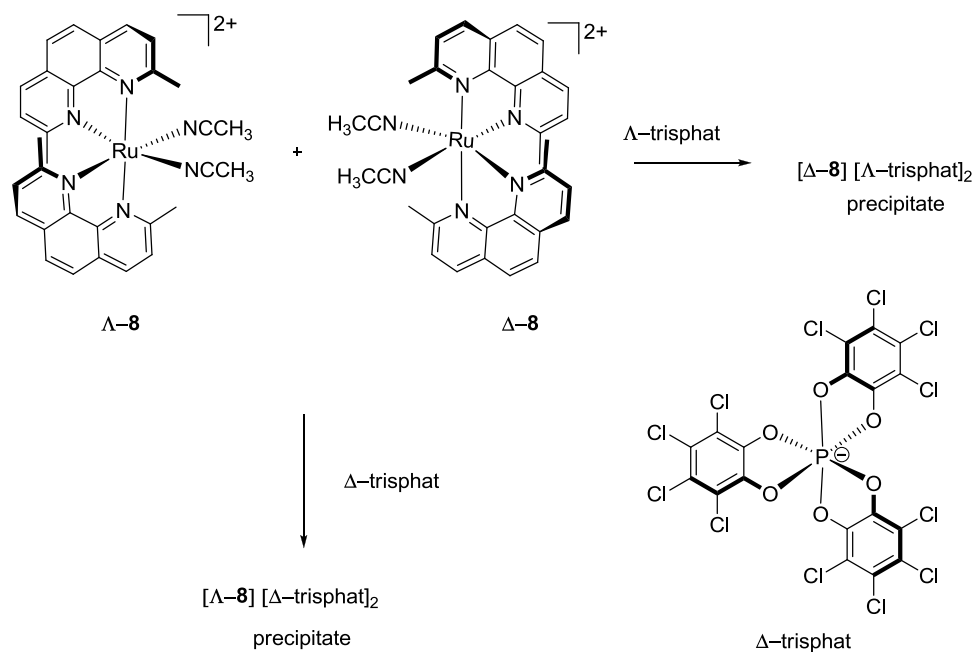
Lots of metal complexes have the charge around it; therefore they can form the ion pair using chiral cation or anion. These ion pair can be resolved by different techniques. Werner and co-workers first developed a method for resolving ion pair. In 1942, Werner's student King chose (+)-3-bromo-camphor-9-sulphonate anion to resolve the complexes  $[\text{Co}(\text{en})_2(\text{NH}_3)\text{X}]\text{X}_2$  ( $\text{X} = \text{Cl}, \text{Br}$ ; en = ethylene diamine) by crystallization successfully<sup>10</sup>. Followed this work, other chiral cations and anions were developed by scientists. For example: Chiral trisphats<sup>11-13</sup>, tartrate<sup>14-18</sup> are widely used as chiral anions in the resolution of metal complexes.  $[\text{Ni}^{\text{II}}(\text{phen})_3]^{2+}$ , or the derivatives from chiral amines are widely used as a chiral cations in the resolution of metal complexes<sup>19-21</sup>.

Among the above chiral resolution reagents, the chiral trisphat is commercially available and is used more frequently. For example: Lacour and coworkers found it can selectively control the equilibrium between the configurationally labile iron(II)-tris(diimine) enantiomers ( $\Lambda$ -**7** and  $\Delta$ -**7**). By using  $\Delta$ -trisphat, the complex  $\Delta$ -**7** reached a diastereomeric ratio greater than 50:1 (Scheme 3)<sup>22</sup>.



**Scheme 3.** Shifting the equilibrium between the  $\Lambda$ - and  $\Delta$ -configurations of a labile iron complex **7** with  $\Delta$ -trisphat.

Towards the resolution of diastereomerically ion pairs, Fontecave and co-workers selectively precipitated the *cis*- $[\Delta\text{-Ru}(\text{dmp})_2(\text{CH}_3\text{CN})_2][\Lambda\text{-trisphat}]_2$  ( $\Delta\text{-8}$ ) or *cis*- $[\Lambda\text{-Ru}(\text{dmp})_2(\text{CH}_3\text{CN})_2][\Delta\text{-trisphat}]_2$  ( $\Lambda\text{-8}$ ) by the  $[\text{n-Bu}_3\text{NH}][\Lambda\text{-trisphat}]$  or  $[\text{n-Bu}_4\text{NH}][\Delta\text{-trisphat}]$  owing to the different speed of the precipitation of two diastereomerically ion pair (Scheme 4)<sup>23</sup>.

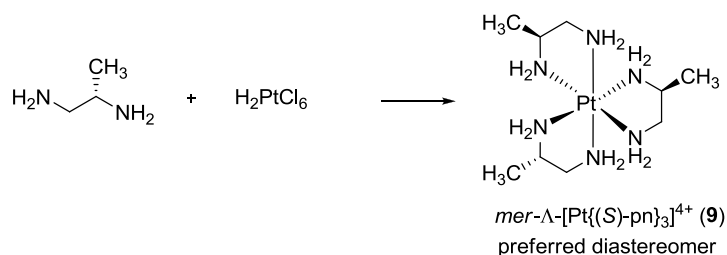


**Scheme 4.** Chiral trisphat resolved the  $\Lambda\text{-8}$  and  $\Delta\text{-8}$ .

### 1.2.3 Diastereoselective coordination with chiral ligands

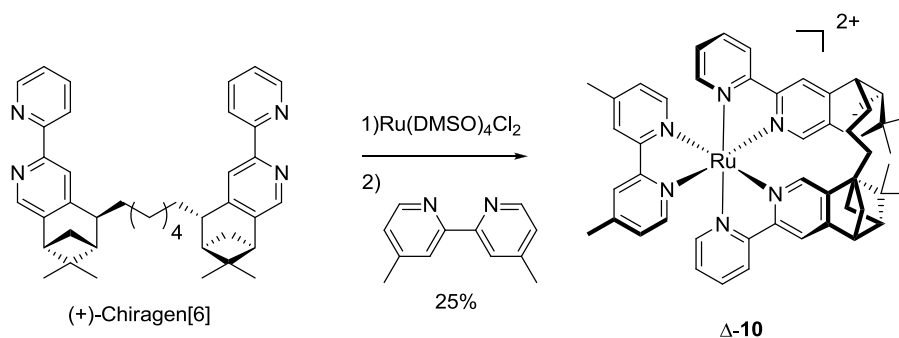
In the asymmetric synthesis, people use the metal without chirality and try to transfer the chiral information from chiral carbon to metal. This was first discovered by

Smirnoff and he used enantiopure propane-1,2-diamine (pn) to react with  $\text{H}_2\text{PtCl}_6$ , yielding octahedral complex which showed the optical rotation<sup>24</sup>. Von Zelewsky reinvestigated this work in detail 85 years later and found that the *mer*- $\Lambda$ -[Pt{(S)-pn}<sub>3</sub>]<sup>4+</sup> (**9**) was the favorable product in the reaction between the (S)-pn and  $\text{H}_2\text{PtCl}_6$  (Scheme 5)<sup>25</sup>.



**Scheme 5.** First example of asymmetric synthesis of chiral metal complex.

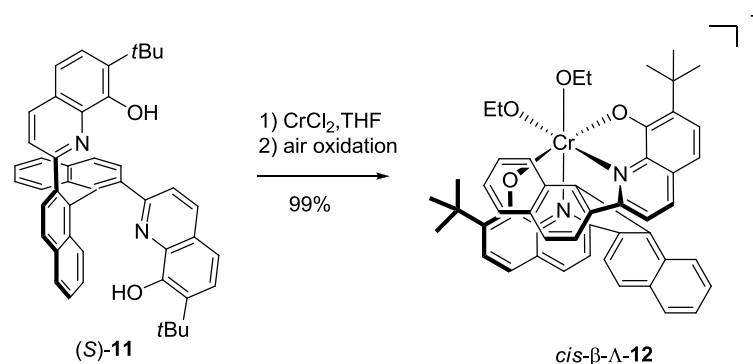
Above strategy is utilized by Von Zelewsky and he used terpene-derived chiral tetradentate bis(2,2'-bipyridine)s - so called CHIRAGENS (from CHIRAlity GENerator) to direct asymmetric coordination chemistry and obtained only one diastereomer<sup>26</sup>. In this reaction,  $[\text{Ru}(\text{DMSO})_4\text{Cl}_2]$  converted to the  $[\text{Ru}(\text{MeCN})_4\text{Cl}_2]$  and then the precursor was refluxed with the CHIRAGENS in ethanol, followed by heating with 4,4'-dimethyl-2,2'-bipyridine in ethyleneglycol, yielding complex  $\Delta$ -**10** with a 25% yield. According to the authors, this is the first example of asymmetric synthesis of an enantiomerically pure octahedral metal complex without the needing of chiral resolution (Scheme 6).



**Scheme 6.** Highly diastereoselective control of  $\text{Ru}^{\text{II}}$ -centered chirality by using the tetradentate CHIRAGENS ligand.

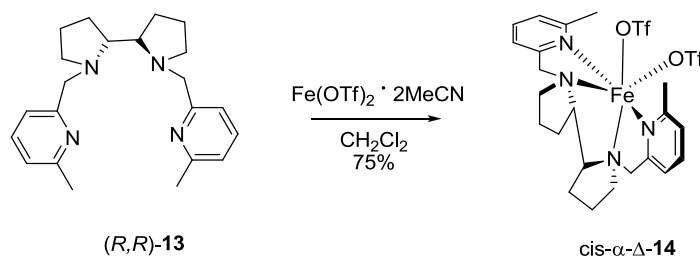


Similarly, Yamamoto and co-workers used the ligand (*S*)-**11** which contains axial chirality to asymmetrically synthesize the *cis*- $\beta$ - $\Lambda$ -[Cr{(*S*)-**11**(EtOH)<sub>2</sub>]Cl (*cis*- $\beta$ - $\Lambda$ -**12**) in almost quantitative yield as a single stereoisomer with *cis*- $\beta$  configuration of the tetradentate ligand and  $\Lambda$ -configuration at the Cr<sup>III</sup> center (Scheme 7)<sup>27</sup>.



**Scheme 7.** Highly diastereoselective control of Cr<sup>III</sup>-centered chirality by using the binaphthyl-tethered bis(8-hydroxyquinoline) ligand.

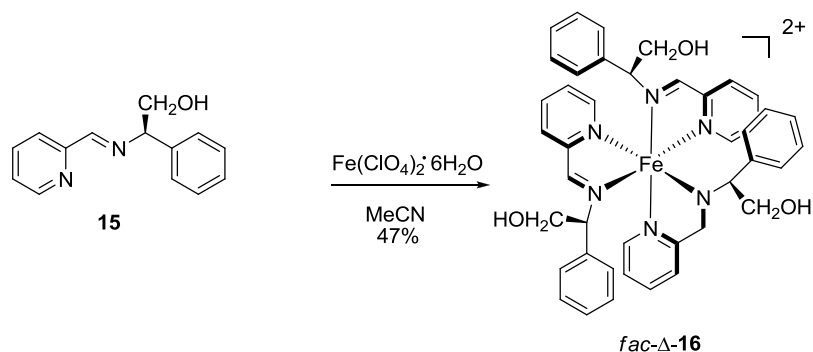
2,2'-Bipyrrolidine is another useful chiral linker for designing tetradentate ligand which can direct asymmetric coordination nicely. For example, Que Jr. and co-workers recently reported that the reaction of bipyrrolidine ligand (*R,R*)-**13** with Fe(OTf)<sub>2</sub> · 2MeCN provided exclusively the iron complex *cis*- $\alpha$ - $\Delta$ -[Fe{(*R,R*)-**13**}(OTf)<sub>2</sub>] (*cis*- $\alpha$ - $\Delta$ -(*R,R*)-**14**), which itself serves as a catalyst for asymmetric olefin *cis*-dihydroxylation (Scheme 8)<sup>28</sup>.



**Scheme 8.** Highly diastereoselective control of Fe<sup>II</sup>-centered chirality by explored the rigid 2,2'-bipyrrolidine backbone.

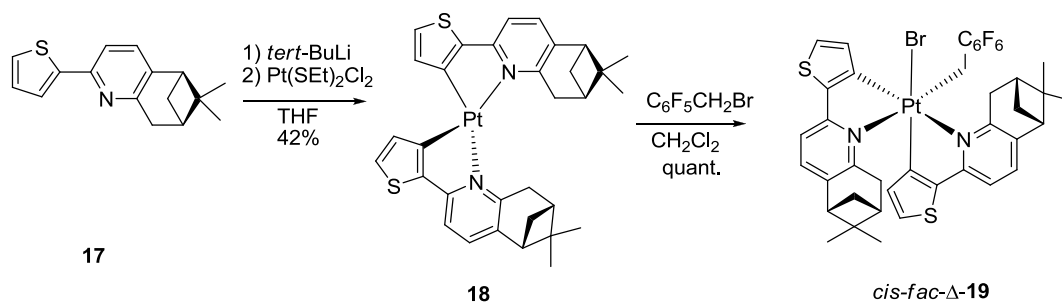
Besides relying on the steric hindrance from the multidentate ligands, aromatic

face-to-face  $\pi$ -stacking also can be exploited for the control of the absolute metal centered configuration. For instance, the Scott group used chiral iminopyridines **15** to react with  $\text{Fe}(\text{ClO}_4)_2 \cdot 6\text{H}_2\text{O}$  in MeCN and obtained the single diastereomer *fac*- $\Delta$ - $[\text{Fe}\{(R)\text{-15}\}_3](\text{ClO}_4)_2$  (*fac*- $\Delta$ -**16**) (Scheme 9)<sup>29</sup>.



**Scheme 9.** Diastereoselective coordination chemistry with  $\text{Fe}^{\text{II}}$  directed by aromatic face-to-face  $\pi$ -stacking.

Besides using the chiral ligand-substitution reaction, the oxidative addition reaction also can be used for synthesizing diastereoselective octahedral metal complex. An example of this approach was reported by Von Zelewsky and co-workers. In this method, the  $\text{Pt}^{\text{II}}$  starting complex *cis*- $\Delta$ -**18** was obtained by cyclometalation of the chiral thienylpyridine ligand (*R,R*)-**17** which was synthesized from (-)- $\alpha$ -pinene. Because of the steric constraints, this tetracoordinate  $\text{Pt}^{\text{II}}$  complex is  $\Delta$ -configuration. This  $\Delta$ -configuration is retained after oxidative addition with  $\text{C}_6\text{F}_5\text{CH}_2\text{Br}$ , yielding complex *cis*-*fac*- $\Delta$ -**19** as a single stereoisomer (Scheme 10)<sup>30</sup>.

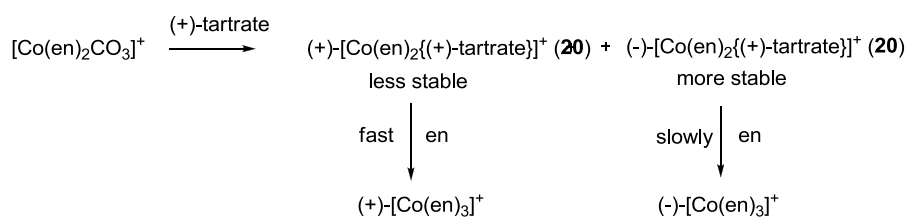


**Scheme 10.** Asymmetric synthesis of an octahedral  $\text{Pt}^{\text{IV}}$  complex by oxidative addition.

### 1.2.4 Chiral auxiliary directed asymmetric synthesis

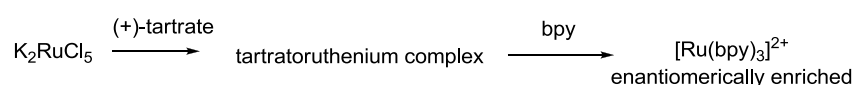
Chiral auxiliaries are optically active compounds and introduce chirality in racemic compounds, which are widespread used in the organic chemistry. They also play important roles for resolution of enantiomers of metal complexes. In this strategy, people use the chiral auxiliary which leads to diastereomers with different physico-chemical properties to separate them by variety ways.

In 1948, Bailar and co-workers first reported this strategy in the synthesis of octahedral metal complex. They used the (*R,R*)-(+)-tartrate to react with  $[\text{Co}(\text{en})_2\text{CO}_3]^+$ , yielding two diastereomers((+)-**20**/(-)-**20**), and one of them was less stable than the other diastereomer. So, when the en (ethylene diamine) substituted the (*R,R*)-(+)-tartrate, the less stable diastereomer reacted faster than the stable one, which afforded enantiomerically enriched (+)- $[\text{Co}(\text{en})_3]^{3+}$  (Scheme 6)<sup>31</sup>.



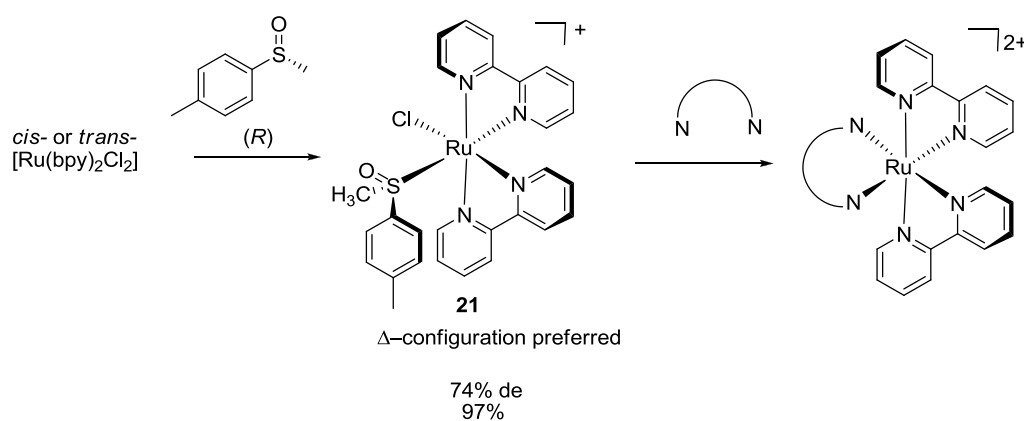
**Scheme 11.** (*R,R*)-(+)-tartrate as a chiral auxiliary for the asymmetric synthesis of cobalt complexes.

In 1964 Bailar and co-workers used the same strategy synthesis the enantiomerically enriched  $[\text{Ru}(\text{bpy})_3]^{2+}$  (bpy = 2,2'-bipyridine)<sup>32</sup>. In the synthesis,  $\text{K}_2\text{RuCl}_5$  hydrate was used as the starting material to react with the (*R,R*)-(+)-tartrate, followed by the addition of an excess of bpy to yield the ruthenium with an enantiomeric ratio of 63: 37 (Scheme 12).



**Scheme 12.** (*R,R*)-(+)-tartrate as a chiral auxiliary for the asymmetric synthesis of ruthenium complexes.

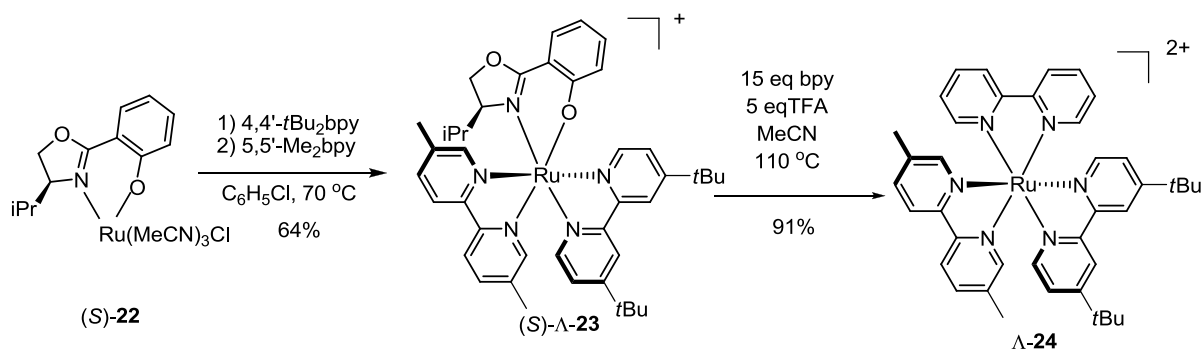
Similarly, based on the thermodynamically difference of the two diastereomers. Inoue and co-workers used the (*R*)-(+)-methyl *p*-tolyl sulfoxide as an auxiliary to obtain the ruthenium polypyridyl complexes (**21**) with enantiomerically enriched<sup>33</sup>. The result was optimized by using the microwave by Balavoine and co-workers<sup>34</sup>. Considering 1: 1 ratio of  $\Lambda$  and  $\Delta$  of the ruthenium as the starting materials to create 74% de, 97% yield of the product, there should be conversion between  $\Lambda$  and  $\Delta$  (Scheme 13). The reason for higher stability of the major diastereomer was presumed by Inoue and co-workers. They concluded two reasons: i)  $\pi$ - $\pi$  interactions between the tolyl group of the sulfoxide and one of the bpy ligands; ii) a hydrogen bond between the sulfoxide oxygen and a pyridyl ortho-proton in combination.



**Scheme 13.** Monodentate methyl *p*-tolyl sulfoxide as a chiral auxiliary for the asymmetric synthesis of ruthenium polypyridyl complexes.

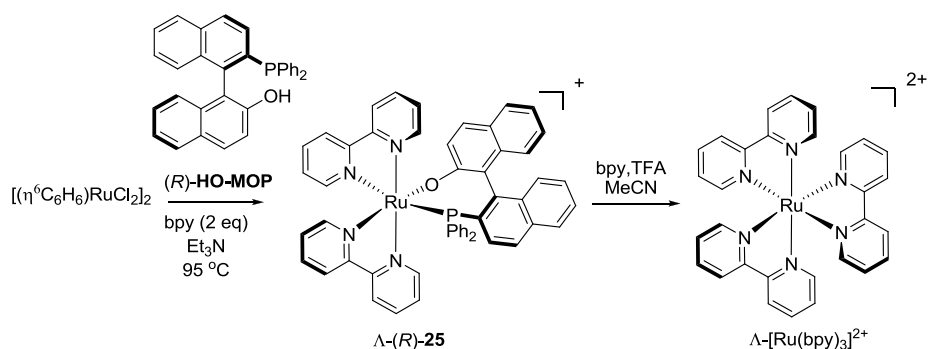
Even these methods are attractive to asymmetric synthesize different metal complexes. But for low ee value of the final compounds, there still lack of convenient and general method to enantioselectively synthesize metal complex until 2009. In 2009, Meggers group developed a general method to enantioselectively synthesize octahedral ruthenium polypyridyl complexes by using the bidentate ligand (Scheme 14). Compared to monodentate ligands, chiral bidentate chelates usually direct the asymmetric coordination chemistry better due to a restricted rotation around the M-L coordinative bonds that fixes the direction of the hindrance from the directing ligand. But the bidentate ligand coordinates much tightly with metal center. The main issue

was how to remove the directing ligand without isomerization of the metal-centered configuration in this area. Meggers and co-workers used salicyloxazoline for inducing the chiral information. Afterwards, the chair bidentate ligand was removed from the auxiliary-mediated-metal complex by acid. Importantly, the configuration of metal center was retained in this procession. In detail, by using (*S*)-2-(4-isopropyl-4,5-dihydrooxazol-2-yl)phenol as the auxiliary, the precursor (*S*)-**22** which has four labile ligands was obtained after two steps. And (*S*)-**22** can react with first one equivalent of 4,4'-di-*tert*-butyl-2,2'-bipyridine (4,4'-*t*Bu<sub>2</sub>bpy) in chlorobenzene at 70 °C and subsequent with one equivalent of 5,5'-dimethyl-2,2'-bipyridine (5,5'-Me<sub>2</sub>bpy) again in chlorobenzene at 70 °C, yielding only one diastereomer  $\Lambda$ -(*S*)-**23** under thermodynamically control. For the final step, the chiral-auxiliary-mediated complex reacted with the third ligand in the presence of acid, yielding the polypyridyl complex  $\Lambda$ -[Ru(pp)(pp')(pp'')]<sup>2+</sup> (pp, pp', pp'' = achiral 2,2'-bipyridines) ( $\Lambda$ -**24**) with enantiopurity<sup>35</sup>.



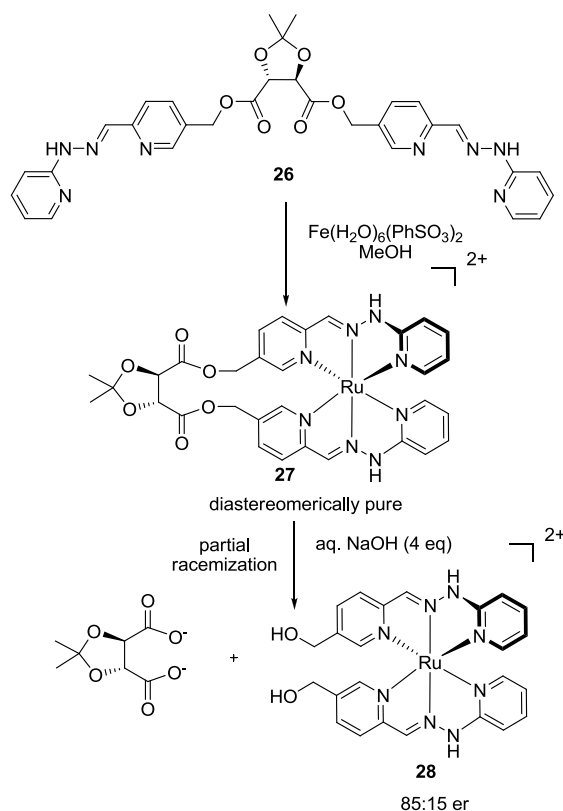
**Scheme 14.** Salicyloxazoline as a chiral auxiliary for the asymmetric synthesis of ruthenium polypyridyl complex.

After this work, Meggers group invented a new auxiliary (*R*)-2'-(diphenylphosphino)-1,1'-binaphthyl-2-ol ((*R*)-**HO-MOP**) and used in the same strategy. For example, (*R*)-**HO-MOP** reacted with commercial available half-sandwich complex [Ru( $\eta^6$ -C<sub>6</sub>H<sub>6</sub>)Cl<sub>2</sub>]<sub>2</sub> and bpy, yielding  $\Lambda$ -[Ru(bpy)<sub>2</sub>{(*R*)-**HO-MOP**}Cl] ( $\Lambda$ -(*R*)-**25**) with diastereomerically enriched (34: 1 dr) (Scheme 15)<sup>36</sup>. Then the directing auxiliary can be removed, yielding  $\Lambda$ -[Ru(bpy)<sub>3</sub>]<sup>2+</sup> with enantiomerically enriched.



**Scheme 15.** Transfer of axial chirality of (*R*)-HO-MOP to metal-centered chirality in a chiral-auxiliary-mediated asymmetric synthesis.

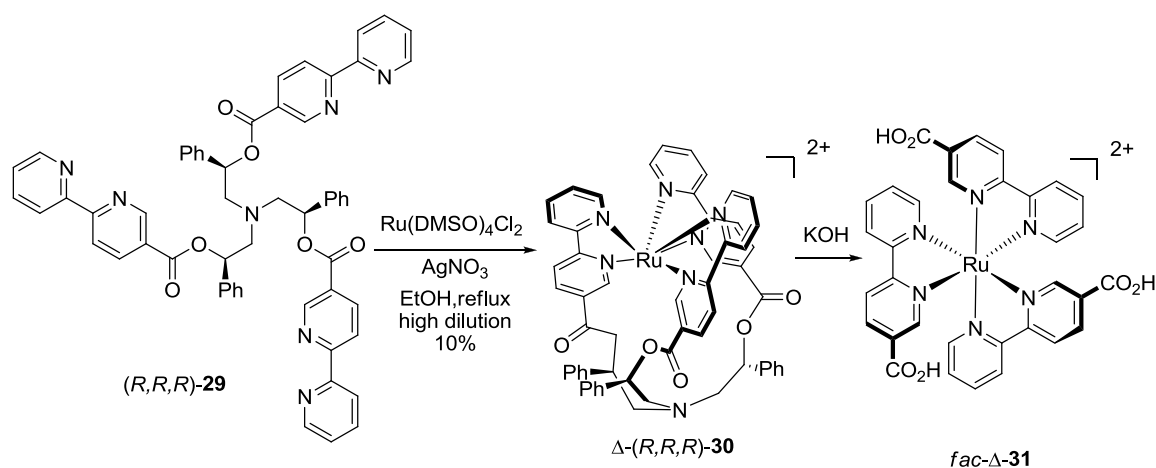
In the different approach, the chiral auxiliaries didn't coordinate to the metal directly. Instead, they are used as linkers between two ligands. In this direction, Wild and co-workers used chiral (*R,R*)-tartrate as linker to connect two tridentate pyridine-2-aldehyde-2'-pyridyl-hydrazone. Then the hexadentate ligand **26** was applied to react with the  $[\text{Fe}(\text{H}_2\text{O})_6](\text{PhSO}_3)_2$ , yielding octahedral metal complex **27** with diastereomeric purity (Scheme 16)<sup>37</sup>.



**Scheme 16.** Asymmetric synthesis of iron octahedral complex **28** by using a chiral linker as auxiliary.

Unfortunately, in the course of removing the auxiliary by hydrolysis of the ester linkages and deprotonation of the hydrazone NH groups, the configuration of the iron metal center **28** lost some chiral information, yielding only 85: 15 er.

In the same strategy, Fletcher and co-workers used chair tripodalk linker system to direct the asymmetric synthesis<sup>38</sup>. This time, hexadentate ligand controlled not only the metal centered configuration but also the geometry between the meridional (*mer*) and facial (*fac*). For example, the enantiopure tripodalk hexadentate ligand **29** was used to react with [Ru(DMSO)<sub>4</sub>Cl<sub>2</sub>] in the presence of AgNO<sub>3</sub> under refluxing in EtOH and high dilution, affording the ruthenium complex  $\Delta$ -(*R,R,R*)-**30** as mainly one diastereomer (>95:5 dr). After cleavage of the ester bonds with aqueous KOH, the reaction provided the compound *fac*- $\Delta$ -**31** (Scheme 17).

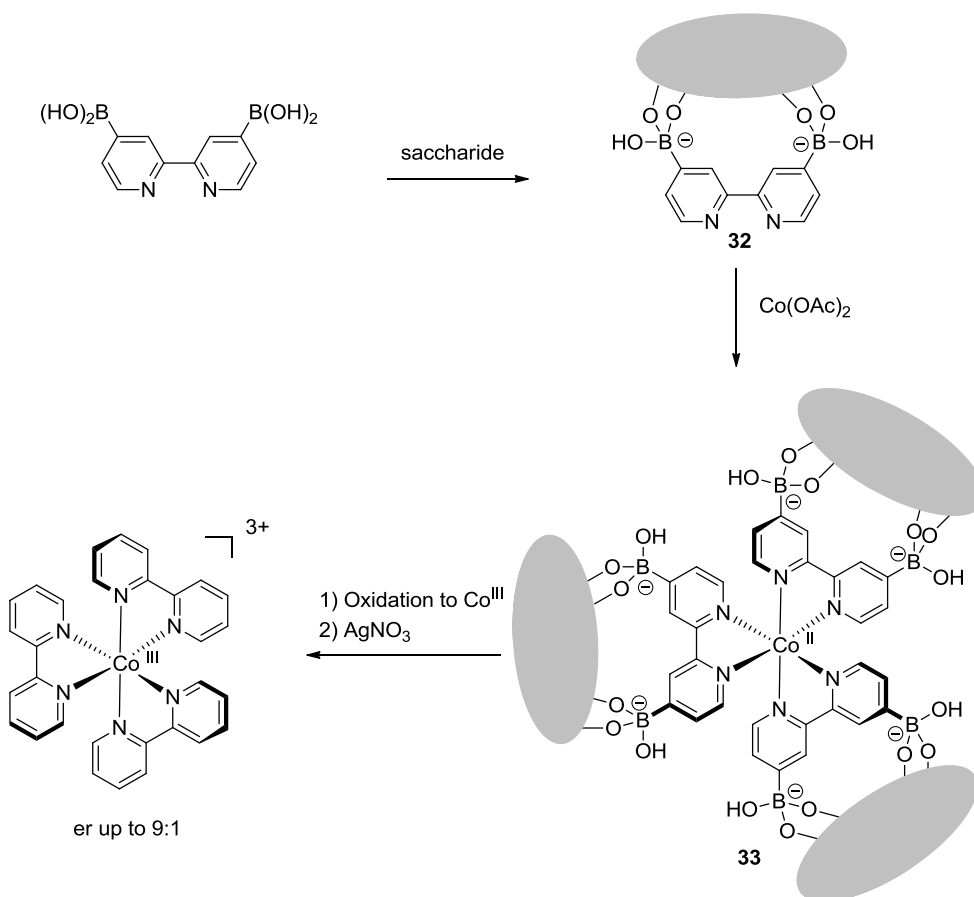


**Scheme 17.** Asymmetric synthesis of a *fac*- $\Delta$ -ruthenium polypyridyl complex with the cleavable linker approach.

Unfortunately, the yield of the coordination step was too low due to the hydrolytic instability of the ester bonds. Additionally, after purification of *fac*- $\Delta$ -**31**, the product still contained a high degree of water and salt, preventing detailed analysis, which makes this method unattractive.

Besides the methods of using auxiliaries directly to coordinate with the metal center and the chiral linker strategy, Shinkai and co-workers included the chiral auxiliary on the coordinated ligands<sup>39</sup>. For instance, the 2,2'-bipyridine-4,4'-diboronic

acid was used as the coordinated ligand to react with monosaccharides, yielding boronic esters **32** with 1: 1 complex formation. Then the complexes **32** reacted with  $\text{Co}(\text{OAc})_2$  to provide octahedral metal complex **33**. At last, the cobalt(II) was oxidized to the more inert cobalt(III), followed by a removal of the chiral auxiliary through reductive cleavage of the C-B bonds in the presence  $\text{AgNO}_3$  to yield  $[\text{Co}(\text{bpy})_3]^{3+}$  with enantiomerically enrich (Scheme 18).



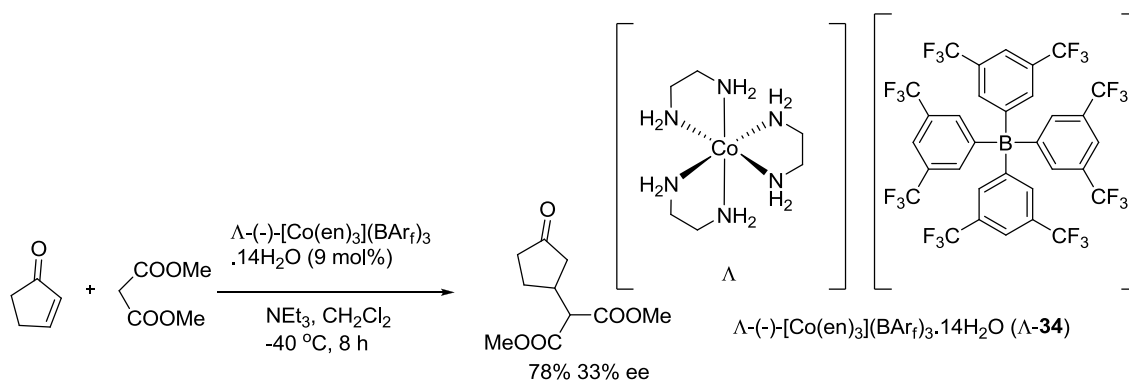
**Scheme 18.** Saccharides as chiral auxiliaries for the asymmetric synthesis of  $[\text{Co}(\text{bpy})_3]^{3+}$ .

In this method, the enantiomeric excess was dependent on the type of the saccharide and the reaction temperature. The best result was obtained with 79% ee when the reaction was carried out at  $-25\text{ }^\circ\text{C}$  using D-glucose.



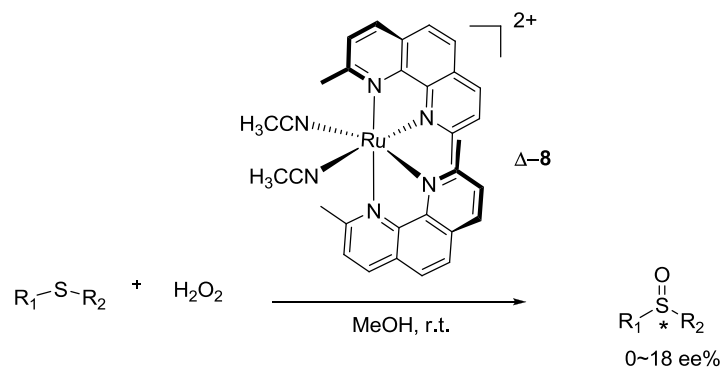
### 1.3 Applications of enantiopure octahedral metal complexes in catalytic reactions

Metal based catalysis reaction was developed so many years ago. The chiral information always comes from both the chiral ligand and the metal center. However, only chiral-at-metal complexes especially octahedral metal complexes are rarely used as the catalyst in the asymmetric synthesis. We just found few examples of using the enantiopure chiral-at-metal octahedral complexes to catalyze the organic reaction. For instance, Gladysz and co-workers used the complex  $\Delta(-)-[\text{Co}(\text{en})_3](\text{BAr}_f)_3 \cdot 14\text{H}_2\text{O}$  ( $\Delta$ -**34**) as the catalyst for the Michael addition. They successfully transferred the chiral information from the metal center to carbon. But unfortunately, the ee value of the product was very low (Scheme 19)<sup>40</sup>.



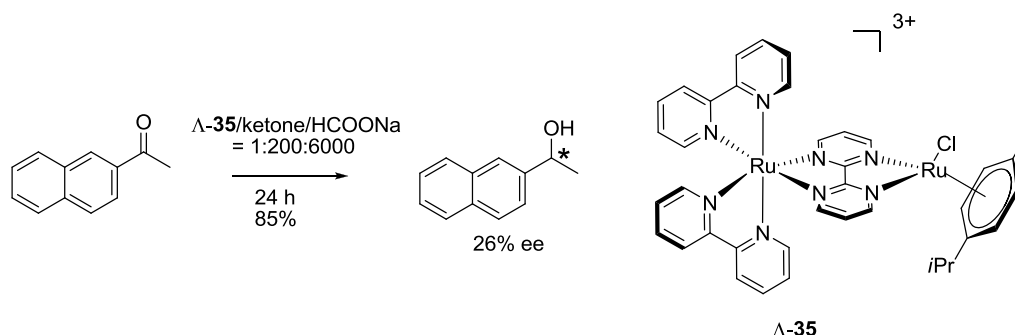
**Scheme 19.** Enantioselective catalysis of a Michael addition by  $\Delta(-)-[\text{Co}(\text{en})_3](\text{BAr}_f)_3 \cdot 14\text{H}_2\text{O}$  ( $\Delta$ -**34**).

Similarly, Fontecave and co-workers used complex  $[\Delta\text{-8}][\Delta\text{-trisphat}]_2$  to catalyze the oxidation reaction but did not obtain high ee values of the final sulfoxides (Scheme 20)<sup>23</sup>.



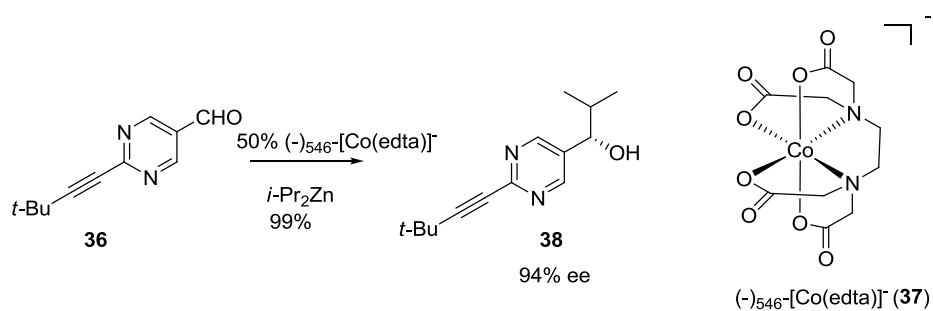
**Scheme 20.** Enantioselective oxidation of sulfides by  $\text{H}_2\text{O}_2$  catalyzed by a chiral-at-metal ruthenium complex.

In 2007, the same group invented a new catalyst  $\Lambda\text{-35}$  which has an enantiopure octahedral metal center<sup>41</sup>. They applied it in the enantioselective reduction of ketones, and the best result of the enantioselectivity just reached to 26% ee. In detail, the reaction was carried out at 80 °C using a 2'-acetonaphthone (0.43 mmol) in  $\text{H}_2\text{O}$  (6 mL) with  $\Lambda\text{-35}/\text{ketone}/\text{HCOONa} = 1: 200: 6000$ , which afforded methyl-2-naphthalene methanol with 26% ee (Scheme 21)



**Scheme 21.** Enantioselective transfer hydrogenation of ketones with complex  $[\Lambda\text{-35}][\text{NO}_3]_3$  as a catalyst.

In 2001, Soai and co-workers successfully induced the chair information to the substrates from the chair octahedral cobalt complex<sup>42</sup>. By the reaction of aldehyde **36** with  $i\text{-Pr}_2\text{Zn}$  in the presence of  $(-)\text{-}_{546}\text{-K}[\text{Co}(\text{edta})] \cdot 2\text{H}_2\text{O}$  (**(-)-37**), the enantiomer excess of the product pyrimidyl alkanol **38** can reach 94%. However, 50% of metal complex **(-)-37** was needed for the reaction (Scheme 22).



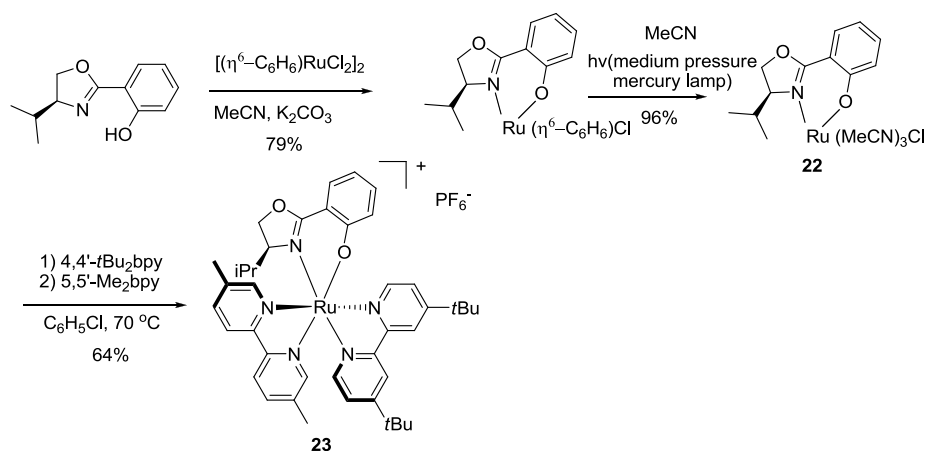
**Scheme 22.** Enantioselective addition of diisopropylzinc to aldehyde **36** in the presence of chiral octahedral cobalt complexes  $(-)\text{-37}$ .

It can be concluded that, the use of chirality of the octahedral complex in the asymmetric organic catalysis reaction is still a highly undeveloped area. The challenge lies in transferring the chiral information effectively from the catalytic metal to carbon or other stereocenters.

## Chapter 2 Aim of this work

Because of the high coordination number, octahedral metal complexes can form up to 15 diastereomers as pairs of enantiomers (30 stereoisomers). However, for applications in the life sciences and for asymmetric catalysis reactions, single stereoisomers are desired. Thus, developing methods for the stereoselective synthesis of octahedral metal complexes is an important and challenging objective. Considering existing strategies for the asymmetric synthesis of the enantiopure octahedral metal complexes, the methods recently developed by Meggers et al. showed advantages for the asymmetric synthesis of highly enantiopure complexes of the type  $[\text{Ru}(\text{pp})(\text{pp}')(\text{pp}'')]^{2+}$  ( $\text{pp}$ ,  $\text{pp}'$ ,  $\text{pp}''$  = achiral 2,2'-bipyridines or 1,10-phenanthrolines). Therefore, after the first example of using the (*S*)-2-(4-isopropyl-4,5-dihydrooxazol-2-yl)phenol as the auxiliary to direct asymmetric coordination chemistry, we want to rely on this strategy and modify this system in the following directions:

1) In the method developed by Meggers et al., three steps were needed starting from the chiral auxiliary for obtaining the chiral-auxiliary-mediated metal complex **23** (Scheme 23). Additionally, for synthesizing the acetonitrile precursor **22**, a medium pressure mercury lamp (an expensive instrument) was needed. Therefore, finding an alternative way to simplify the synthesis route to obtain the chiral-auxiliary-mediated metal complex without using this costly equipment is the first target in this thesis.

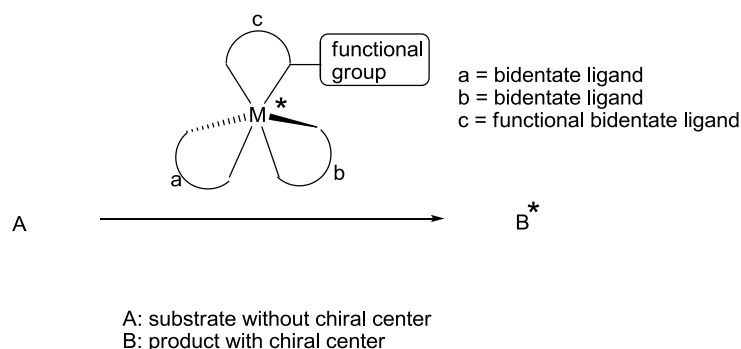


**Scheme 23.** Established but inconvenient asymmetric synthesis of the complex **23**.

2) The second target in this thesis is designing a chiral auxiliary that is very easy to synthesize.

3) In the salicyloxazoline system, a high temperature, combined with acid, was needed to remove the chiral auxiliary and substitute the third ligand (Scheme 14). Finding a mild and acid free condition to substitute the third ligand is, therefore, the ultimate goal in this part of the work.

After developing the methods for obtaining enantiopure octahedral metal complexes, we want to utilize them in some applications. There was not one useful example of transferring the chirality from the octahedral metal center to carbon center. Therefore, we will design different catalysts with enantiomerically pure octahedral metal centers, and focus on asymmetric acyl transfer catalysis to transfer chiral information from the metal to carbon (Scheme 24).



**Scheme 24.** Asymmetric catalysis reaction with chiral-at-metal catalyst.

## Chapter 3 Results

### 3.1 Novel chiral auxiliaries for the asymmetric synthesis of ruthenium polypyridyl complexes

#### 3.1.1 Sulfinylphenol auxiliary system

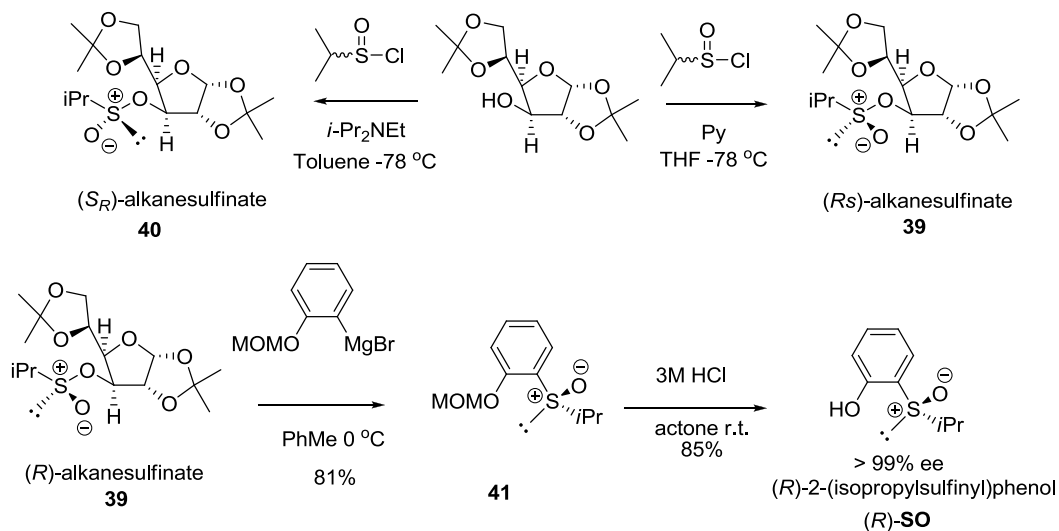
Having developed the method for asymmetric synthesis of ruthenium polypyridyl complexes by using the salicyloxazoline ligand (Scheme 14), we planned to discover some new auxiliaries similar to the salicyloxazoline ligand to enrich our system. In particular, we wanted to find a ligand that would allow the chiral center to be nearer to the ruthenium center, in the hope that the resulting reaction would provide better diastereoselectivity. Sulfoxide ligand appeared to us to be a suitable ligand. The sulfinyl group has certain advantages as a chiral controller. First, it possesses high optical stability. The sulfoxide ligand that we synthesized did not exhibit any racemization or decomposition, even at 170 °C. This was an important characteristic for our study<sup>43</sup>. Second, sulfoxide ligand is an efficient carrier of chiral information. The polarized S-O bond, with a net positive charge on sulfur, allows the sulfur atom to coordinate with transition metals and transfer the chiral information from sulfur to metal center easily<sup>44</sup> (Figure 4).



**Figure 4.** Facile chiral information transfer from a coordinated chelating sulfoxide to the neighboring octahedral metal center.

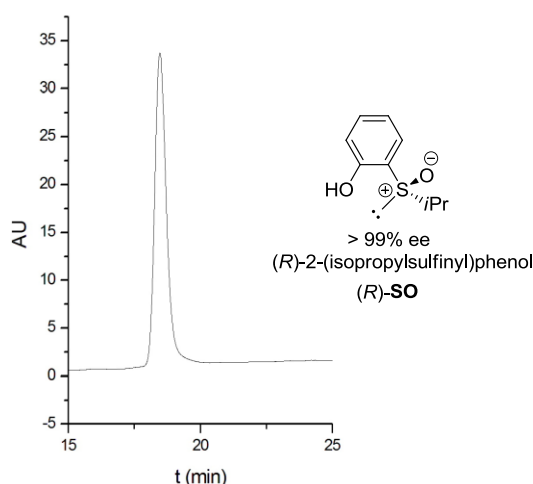
Third, both enantiomers can usually be synthesized in the same way<sup>45</sup>. For example, the reaction of diacetone-D-glucose with isopropylsulfinyl chlorides in THF

at  $-78\text{ }^{\circ}\text{C}$ , using pyridine as a base, gave the corresponding (*R*)-alkanesulfinate (**39**) with high yield and selectivity in favor of the (*R*)-isomer; whereas, Hunig's base (*i*-Pr<sub>2</sub>NEt) was used, the reaction gave an (*S*) configuration **40** as the main isomer (Scheme 25)<sup>46</sup>.



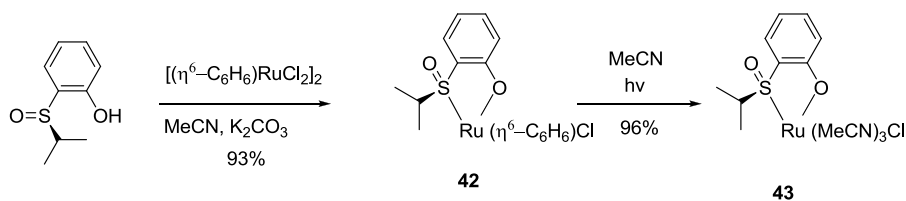
**Scheme 25.** Asymmetric synthesis of enantiopure sulfoxide ligand.

By using this method, we successfully synthesized diastereomerically pure (*R*)-alkanesulfonate (**39**). The Grignard reagent was then used to react with it, yielding the compound **41**. After deprotecting, the ligand (*R*)-2-(isopropylsulfinyl)phenol (*R*)-**SO** was obtained with high enantiomeric purity (> 99% ee) (Scheme 25). Figure 5 shows the enantiomeric purity of the (*R*)-**SO**.



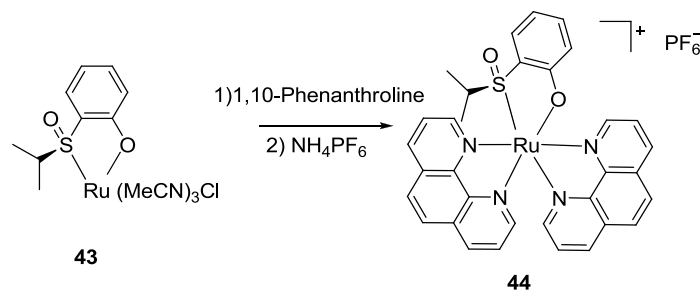
**Figure 5.** Shown is the chiral HPLC trace of (*R*)-**SO**. Conditions: Chiralpak IB (0.46cm×25cm) HPLC column on an Agilent 1200 Series HPLC System. The flow rate was 0.5 mL/min, the column temperature 40 °C, and UV-absorption was measured at 254 nm. Solvent A = hexane, solvent B = ethanol, with 6% B in 25 min.

Having the (*R*)-2-(isopropylsulfinyl)phenol [(*R*)-**SO**] ligand in hand, we planned to use it in the same system as salicyloxazoline. In a simulation of the structure of auxiliary mediated bisbipyridine ruthenium complex, the geometry showed that the isopropyl group is closer to the ruthenium than the salicyloxazoline ligand. Thus, it may introduce higher asymmetry. The directing ligand can be replaced afterwards by another polypyridyl ligand by reprotonating the phenol group. Based on these considerations, the (*R*)-**SO** ligand was converted to the precursor **43** by reaction with  $[(\eta^6\text{-C}_6\text{H}_6)\text{RuCl}_2]_2$  in the presence of  $\text{K}_2\text{CO}_3$ , which afforded **42** at yields of 93%, followed by photolysis with a medium pressure mercury lamp in acetonitrile (Scheme 26). For the next step, the precursor **42** reacted with 1,10-phenanthroline ligand in different conditions, yielding complex **44** with variable diastereoselectivity (Table 1).



**Scheme 26.** Synthesis of precursor **43**.



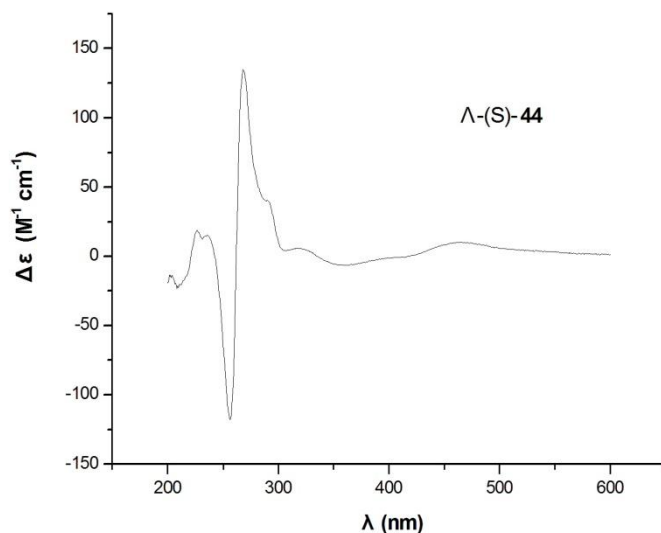


**Table 1.** Conditions dependence of diastereoselective formation of **44**<sup>a</sup>.

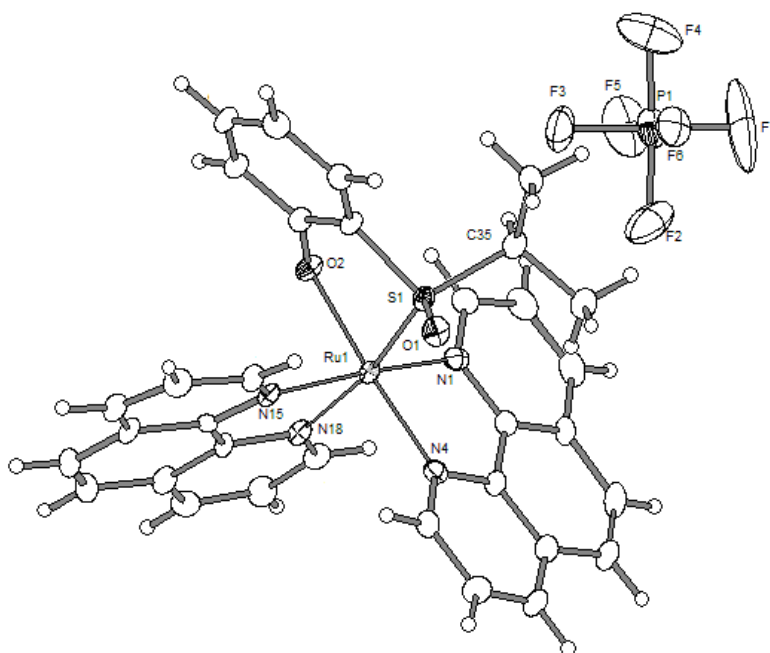
entry	solvent	conc.	phen	temp.	time	yield	dr <sup>b</sup>
1	EtOH	5mM	2.2eq	70°C	1h	45%	6:1
2	DMF	5mM	2.2eq	70°C	1h	95%	5:1
3	DMF	5mM	2.2eq	40°C	overnight	low	
4	PhCl	5mM	5eq	120°C	29h	70%	>99:1
5	PhCl	10mM	10eq	100°C	16h	80%	>99:1
6	Acetone	5mM	2.2eq	70°C	1h	low	

<sup>a</sup> Reaction conditions: Reaction of **43** with phen (1,10-phenanthroline) at the indicated time, equivalent of phen, solvent, concentration and temperature. <sup>b</sup> Diastereomeric ratios determined by crude <sup>1</sup>H NMR. The metal configuration of the main diastereomer was lambda.

The absolute metal configuration of the main diastereomer in Table 1 was determined by the crystal structure (Figure 7). This result also demonstrated that the (*R*)-configured 2-(isopropylsulfinyl)phenol ligand directed the  $\Lambda$ -configured ruthenium center, yielding  $\Lambda$ -(*S*)-**44** as the main stereoisomer. Note that, according to the Cahn–Ingold–Prelog priority rules, the assignment of the absolute stereo-chemistry at the sulfur changes from *R* to *S* upon coordination. Metal-centered configurations of all other complexes presented in this chapter were assigned relative to this crystal structure by means of CD spectroscopy. Figure 6 depicts the CD spectrum of the diastereomer  $\Lambda$ -(*S*)-**44**.



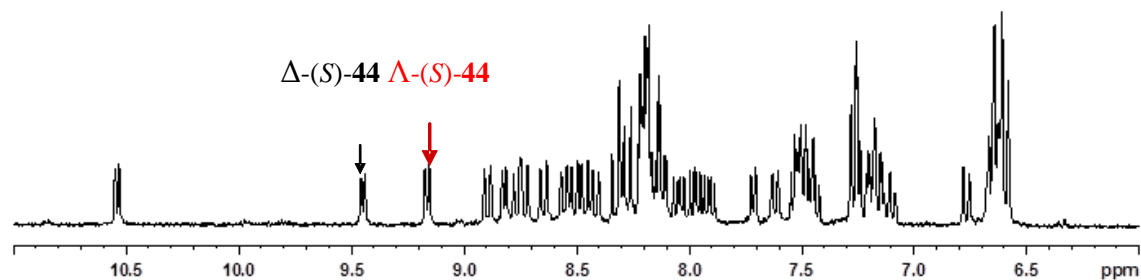
**Figure 6.** CD spectrum of the purified diastereomeric product  $\Lambda$ -(S)-**44**. The spectrum was measured in MeCN at concentrations of 0.1 mM.



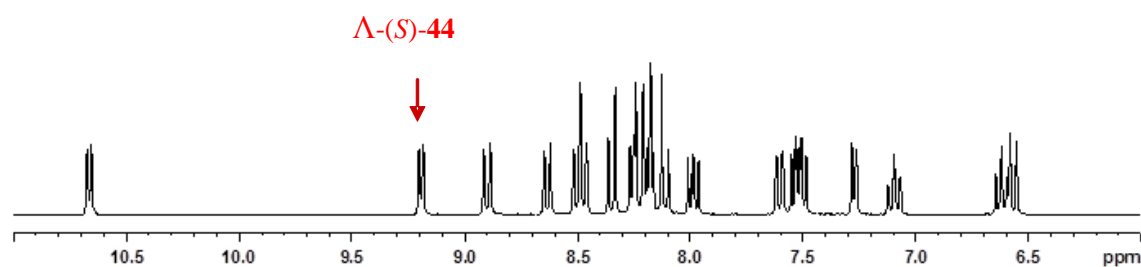
**Figure 7.** Crystal structure of  $\Lambda$ -(S)-**44** in which the absolute stereochemistry was determined. Solvent molecule is omitted for clarity. ORTEP drawing with 50% probability thermal ellipsoids. Selected bond distances ( $\text{\AA}$ ): C35-S1 = 1.823(4), N1-Ru1 = 2.042(4), O1-S1 = 1.491(3), O2-Ru1 = 2.089(3), S1-Ru1 = 2.2252(10), N4-Ru1 = 2.054(3), N15-Ru1 = 2.080(3), N18-Ru1 = 2.104(3).

The diastereoselectivity in the Table 1 was checked by the use of the proton NMR spectrum. Because the two chiral centers are close to each other in the chiral-auxiliary-mediated metal complex **44**, the two diastereomers differ strongly in the chemical shifts of their protons in the NMR spectra (Figure 8).

a) Mixtures of  $\Lambda/\Delta$ -(*S*)-**44**



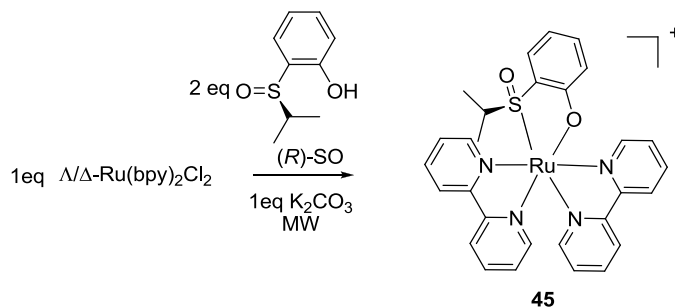
b)  $\Lambda$ -(*R*)-**44**



**Figure 8.**  $^1\text{H}$  NMR spectra excerpts of the diastereomeric products. a) 1:1  $\Lambda/\Delta$ -mixture; b)  $\Lambda$ -(*R*)-**44** after purification by column chromatography on silica gel.

After applying the (*R*)-**SO** auxiliary in the asymmetric synthesis of the octahedral metal complex by the same salicyloxazoline system method, we started to think about other applications of this ligand. Research by A ĩ-Haddou and colleagues suggested the next step to us. They reported the use of monodentate chiral sulfoxides as chiral auxiliaries to obtain enantiomerically enriched ruthenium polypyridyl complexes<sup>34</sup> (Scheme 13). Accordingly, we decided to replace the monodentate ligand (*R*)-(+)-methyl-*p*-tolylsulfoxide with the (*R*)-**SO** auxiliary. From previous results we know that this (*R*)-**SO** bidentate ligand can direct the asymmetric coordination chemistry efficiently. We used the same conditions as A ĩ-Haddou: the (*R*)-**SO** auxiliary (2 eq) reacted with (*rac*)-Ru(bpy)<sub>2</sub>Cl<sub>2</sub> (1 eq) in the presence of K<sub>2</sub>CO<sub>3</sub> (1 eq)

in ethyleneglycol on heating in a microwave oven. The result was surprisingly poor: there was hardly any conversion, even we extended the reaction time (Table 2).



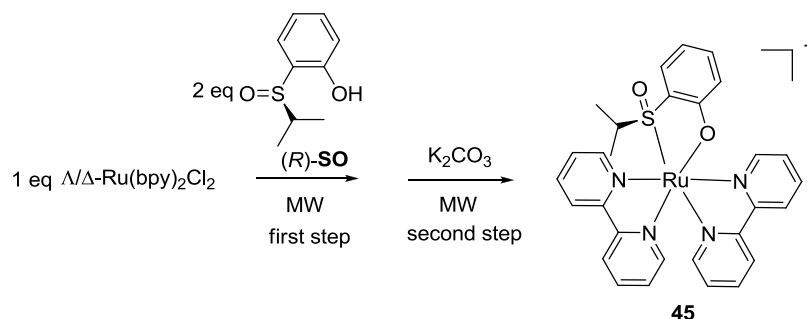
**Table 2.** Initial test of dynamic conversion of (*rac*)-Ru(bpy)<sub>2</sub>Cl<sub>2</sub><sup>a</sup>.

entry	solvent	equiv. ( <i>R</i> )-SO	conc.	time	dr <sup>b</sup>
1	ethylene glycol	2	100mM	1min	1:1
2	ethylene glycol	2	100mM	1.5min	1:1
3	ethylene glycol	2	100mM	2min	1:1
4	ethylene glycol	2	100mM	2.5min	1:1
5	ethylene glycol	2	100mM	3.5min	1:1

<sup>a</sup>Reaction conditions: Reaction of 100 mM (*rac*)-Ru(bpy)<sub>2</sub>Cl<sub>2</sub> with 2 equiv of (*R*)-SO and 1 equiv of the K<sub>2</sub>CO<sub>3</sub> in ethyleneglycol was heated by microwave oven [MADmm717 (M power)] at the indicated time. <sup>b</sup>Diastereomeric ratios determined by crude <sup>1</sup>H NMR.

Towards these results, we considered the problem was that the phenol group was deprotonated by the base, and this bidentate ligand fixed the metal center, which resulted in no conversion in the reaction. Postulating that the bidentate auxiliary fixed the configuration of the metal, we then carried out the reaction in two steps. In the first step, the reaction was carried out in microwave oven without any base, which

allowed the metal center to convert easily owing to the ligand just with monodentate fashion. In the second step, the  $K_2CO_3$  was added to fix the configuration of the metal center (Table 3).



**Table 3.** Influence of the equivalent of  $K_2CO_3$  and reaction time on the dynamic conversion of (*rac*)- $Ru(bpy)_2Cl_2$  in separate steps <sup>a</sup>.

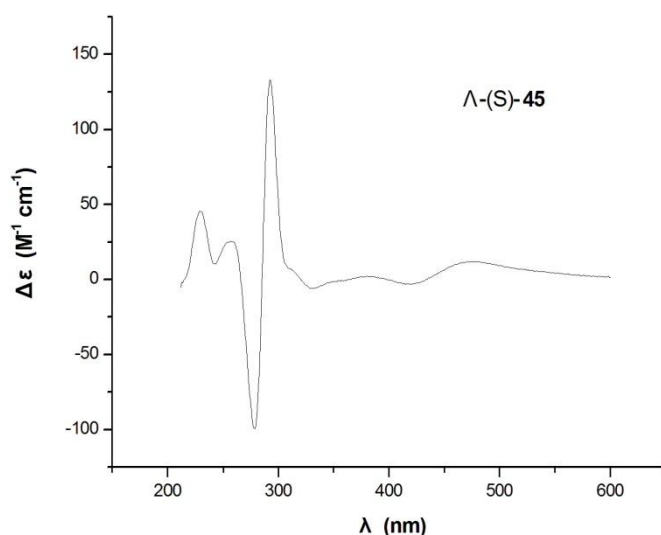
entry	solvent	equiv. ( <i>R</i> )-SO	conc.	time of first step	$K_2CO_3$	time of second step	dr <sup>b</sup>
1	ethyleneglycol	2	100mM	3min	1eq	2min	2:1
2	ethyleneglycol	2	100mM	7min	1eq	2min	3.3:1
3	ethyleneglycol	2	100mM	5min	0eq	2min	No product
4	ethyleneglycol	2	100mM	5min	0.5eq	2min	> 99:1
5	ethyleneglycol	2	100mM	5min	0.7eq	2min	2.5:1
6	ethyleneglycol	2	100mM	3min	0.5eq	2min	> 99:1
7	ethyleneglycol	2	100mM	2min	0.5eq	2min	>99:1

<sup>a</sup> Reaction conditions: Reaction of 100 mM (*rac*)- $Ru(bpy)_2Cl_2$  with 2 equiv of (*R*)-SO in ethyleneglycol was heated by microwave oven [MADmm717 (M power)] firstly at the indicated time followed by adding indicated equiv of the  $K_2CO_3$  and reacted for further indicated time. <sup>b</sup> Diastereomeric ratios determined by crude  $^1H$  NMR. The metal configuration of the main diastereomer was lambda.

Table 3 shows the importance of the equivalent of base. The more base was used,

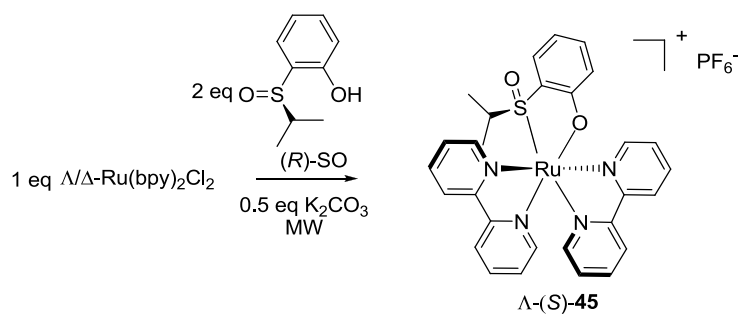
the worse the result it afforded, even though the 0.5 equivalent of  $\text{K}_2\text{CO}_3$  was perfect for this reaction. This phenomenon reflects what we had previously assumed, namely that too much base will fix the metal configuration. In this reaction, only one diastereomer was formed by the reaction with the auxiliary (2 eq) and (*rac*)- $\text{Ru}(\text{bpy})_2\text{Cl}_2$  (1 eq) on heating in a microwave oven for 2 min without any base, followed by adding  $\text{K}_2\text{CO}_3$  (0.5 eq) and stirring for 2 min in ethyleneglycol.

The absolute configuration of the complex **45** was determined by CD spectrum. Comparing with the complex  $\Lambda$ -(*S*)-**44**, the similar signal of the spectrum demonstrated the configuration of complex **45** was lambda (Figure 9).



**Figure 9.** CD spectrum of the purified diastereomeric product  $\Lambda$ -(*S*)-**45**. The spectrum was measured in MeCN at concentrations of 0.1 mM.

We finally found that the reaction can be carried out in one step by reacting with the auxiliary (2 eq), (*rac*)- $\text{Ru}(\text{bpy})_2\text{Cl}_2$  (1 eq), and  $\text{K}_2\text{CO}_3$  (0.5 eq) and heating in a microwave oven for 1 min. This also afforded only one diastereomer (Table 4).

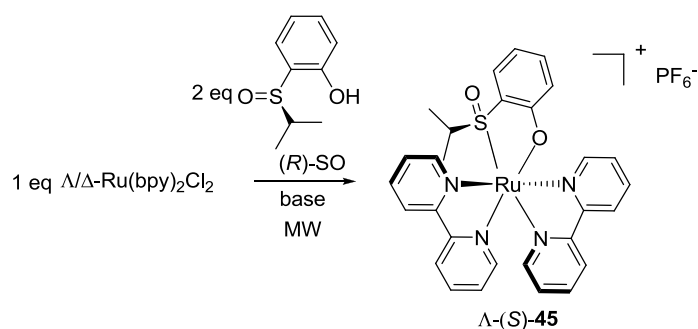


**Table 4.** Influence of reaction time on the dynamic conversion of (*rac*)-Ru(bpy)<sub>2</sub>Cl<sub>2</sub> in one step <sup>a</sup>.

entry	solvent	equiv. ( <i>R</i> )-SO	conc.	K <sub>2</sub> CO <sub>3</sub>	time	dr <sup>b</sup>	yield
1	ethyleneglycol	2	100mM	0.5eq	2min	>99:1	79%
2	ethyleneglycol	2	100mM	0.5eq	1min	>99:1	85%

<sup>a</sup> Reaction conditions: Reaction of 100 mM (*rac*)-Ru(bpy)<sub>2</sub>Cl<sub>2</sub> with 2 equiv of (*R*)-SO and 0.5 equiv of the K<sub>2</sub>CO<sub>3</sub> in ethyleneglycol was heated by microwave oven [MADmm717 (M power)] at the indicated time. <sup>b</sup> Diastereomeric ratios determined by crude <sup>1</sup>H NMR. The metal configuration of the main diastereomer was lambda.

Having discovered a method for achieving a good result in terms of diastereoselectivity, we tested a different equivalent of the ligand and the other base in this system, attempting to optimize the condition. This did not, however, work every well (Table 5).



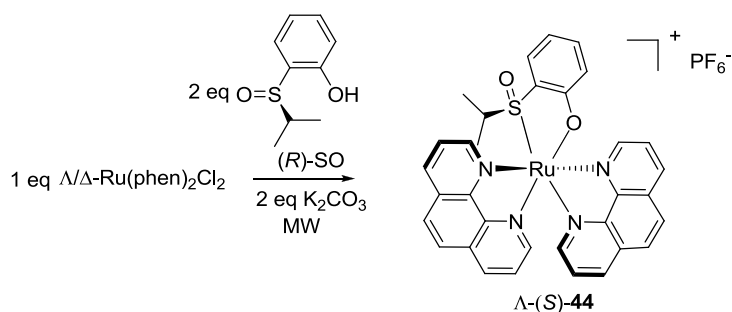
**Table 5.** Influence of the base and equivalent of the (*R*)-SO on the diastereoselective formation of  $\Lambda\text{-(S)-45}$ <sup>a</sup>.

entry	solvent	equiv. ( <i>R</i> )-SO	conc.	base	time	dr <sup>b</sup>
1	ethyleneglycol	1.1	100mM	0.5eq K <sub>2</sub> CO <sub>3</sub>	2min	3.8:1
2	ethyleneglycol	1.5	100mM	0.5eq K <sub>2</sub> CO <sub>3</sub>	2min	5.7:1
3	ethyleneglycol	2	100mM	0.5eq DABCO	2min	10:9

<sup>a</sup> Reaction conditions: Reaction of 100 mM (*rac*)-Ru(bpy)<sub>2</sub>Cl<sub>2</sub> with indicated equiv of (*R*)-SO and 0.5 equiv of indicated base in ethyleneglycol was heated by microwave oven [MADmm717 (M power)] in 2 min. <sup>b</sup> Diastereomeric ratios determined by crude <sup>1</sup>H NMR. The metal configuration of the main diastereomer was lambda.

The best reaction conditions were found to be those in which the auxiliary (2 eq), (*rac*)-Ru(bpy)<sub>2</sub>Cl<sub>2</sub> (1 eq) and K<sub>2</sub>CO<sub>3</sub> (0.5 eq) were heated in a microwave oven in ethyleneglycol for 1 min. Next, we turned our attention to the analogous substrate: (*rac*)-Ru(phen)<sub>2</sub>Cl<sub>2</sub> as the starting material reacted with the ligand (*R*)-SO (2 eq) in the presence of K<sub>2</sub>CO<sub>3</sub> (0.5 eq) in ethyleneglycol on heating in a microwave oven, in a different reaction time, yielding only one diastereomer (Table 6).





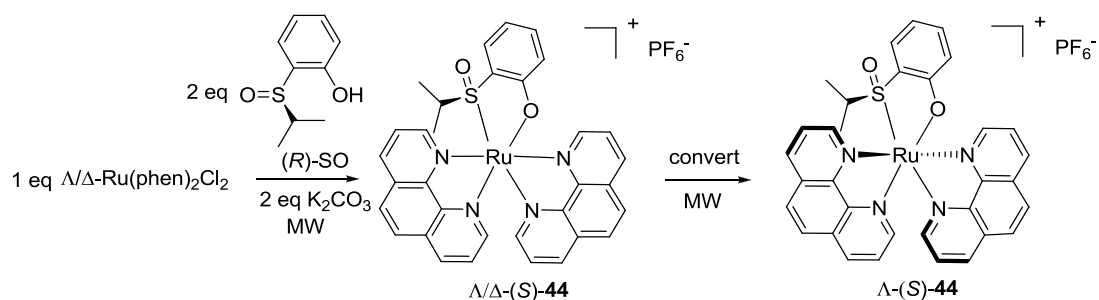
**Table 6.** Influence of reaction time on the dynamic conversion of  $(rac)\text{-Ru(phen)}_2\text{Cl}_2$ <sup>a</sup>

entry	solvent	equiv. ( <i>R</i> )-SO	conc.	base K <sub>2</sub> CO <sub>3</sub>	time	dr <sup>b</sup>	yield
1	ethylene glycol	2	100mM	0.5eq	2min	>99:1	Low
2	ethylene glycol	2	100mM	0.5eq	1min	>99:1	73%

<sup>a</sup> Reaction conditions: Reaction of 100 mM  $(rac)\text{-Ru(phen)}_2\text{Cl}_2$  with 2 equiv of  $(R)\text{-SO}$  and 0.5 equiv of the K<sub>2</sub>CO<sub>3</sub> in ethyleneglycol was heated by microwave oven [MADmm717 (M power)] at the indicated time. <sup>b</sup> Diastereomeric ratios determined by crude <sup>1</sup>H NMR. The metal configuration of the main diastereomer was lambda.

In the course of our research, we found that the conversion was not gradual but sudden. From Table 7, we can see that the ratio of  $\Lambda/\Delta$  was 1: 1 until 40 seconds, but suddenly became only one diastereomer at 50 seconds.

The question that now occurred to us was whether radiation from the microwave oven was the key factor in this reaction, whereas we had presumed that it was not radiation but temperature. A reasonable explanation of our findings is that conversion happens when the solvent reaches a certain temperature on heating in the microwave. Thus, since 40 seconds is not long enough to make the solvent reach the required temperature, the conversion cannot be triggered.

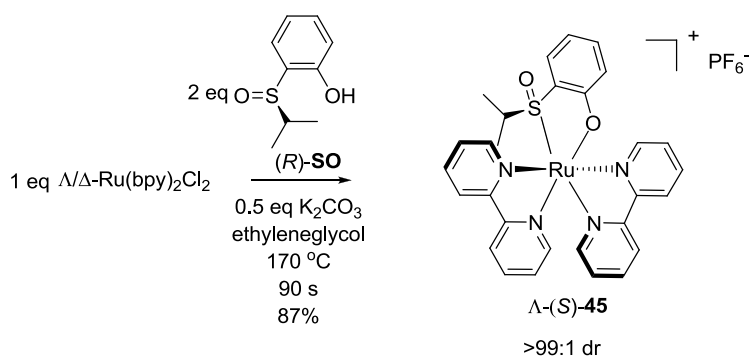


**Table 7.** Experiments to demonstrate the time-dependent conversion <sup>a</sup>.

entry	solvent	equiv. ( <i>R</i> )-SO	conc.	$\text{K}_2\text{CO}_3$	time	power of microwave	dr <sup>b</sup>
1	ethylene glycol	2	100mM	0.5eq	10s	M	1:1
2	ethylene glycol	2	100mM	0.5eq	20s	M	1:1
3	ethylene glycol	2	100mM	0.5eq	30s	M	1:1
4	ethylene glycol	2	100mM	0.5eq	40s	M	1:1
5	ethylene glycol	2	100mM	0.5eq	50s	M	>99:1

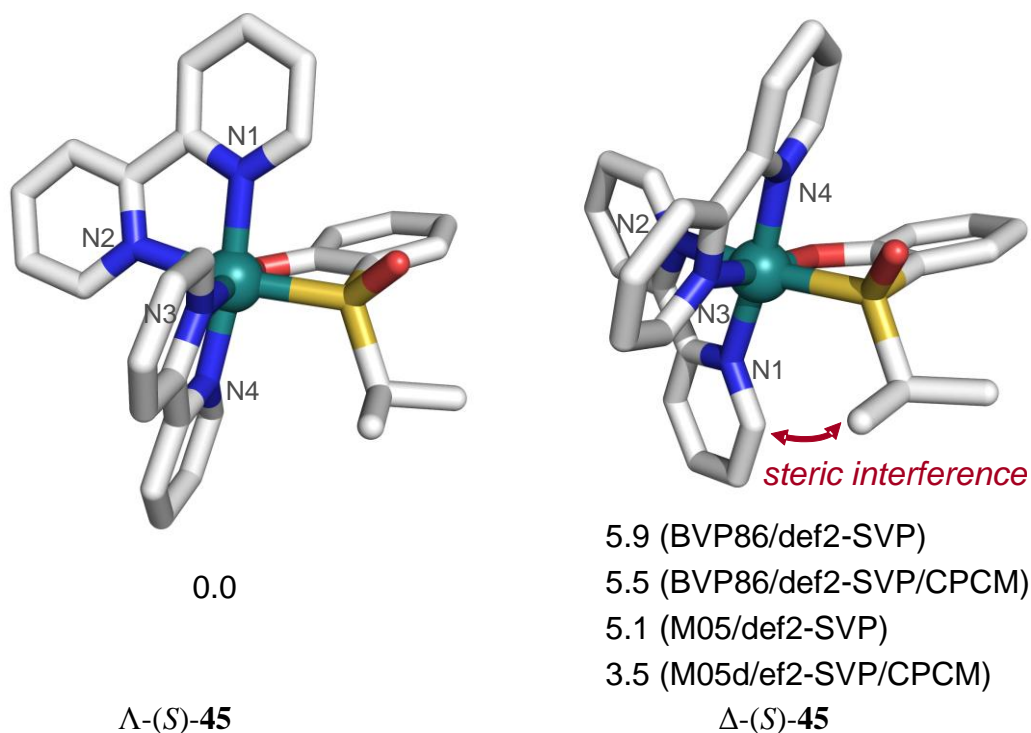
<sup>a</sup> Reaction conditions: Reaction of 100 mM (*rac*)-Ru(phen)<sub>2</sub>Cl<sub>2</sub> with 2 equiv of (*R*)-SO and 0.5 equiv of the K<sub>2</sub>CO<sub>3</sub> in ethyleneglycol was heated by microwave oven [MADmm717 (M power)] at the indicated time. <sup>b</sup> Diastereomeric ratios determined by crude <sup>1</sup>H NMR. The metal configuration of the main diastereomer was lambda.

In order to confirm this hypothesis, we decided to heat the reagents in an oil bath instead of a microwave oven. The reaction was first carried out at 150 °C, and yielded a ratio of  $\Lambda/\Delta$  of 2: 1. Allowing a longer reaction time produced a lot of decomposed compounds. Heating at 180 °C still yielded many decomposed compounds. After further testing, the best temperature for conversion was found to be 170 °C. At this temperature, only one diastereomer was achieved after stirring for 90 seconds in ethyleneglycol (Scheme 27).



**Scheme 27.** Dynamic conversion of (*rac*)-Ru(bpy)<sub>2</sub>Cl<sub>2</sub> by (*R*)-SO auxiliary.

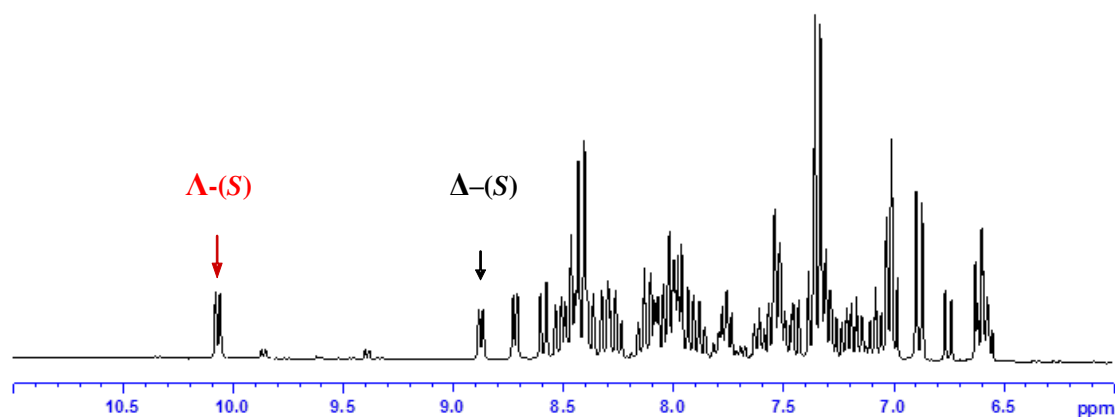
To better understand the different stability of the  $\Lambda$ -*S* and the  $\Delta$ -*S* diastereomers, Mehmet Ali Celik (Chemistry Department, Philipps-Universität) helped us calculate the geometries and Gibbs free energies of the  $\Lambda$ -(*S*)-**45** and the  $\Delta$ -(*S*)-**45** by using density functional theory (DFT) at the BP86/def2-SVP level. Figure 10 reveals that in the destabilized diastereomer  $\Delta$ -(*S*)-**45**, the isopropyl substituent sterically interferes with the CH group in the six-position of one bpy ligand. As a consequence, to escape this close contact, the entire coordination sphere of  $\Delta$ -(*S*)-**45** is distorted. For example, the chelate angle of S-Ru-N1 increases from 92.5° in  $\Lambda$ -(*S*)-**45** to 105.4° for the disfavored  $\Delta$ -(*S*)-**45**. At the same time, the dihedral angle S-O-N2-N3 changes by 12.1°. The resulting weakened coordinative bonds are reflected in the very large difference of the Gibbs free energies for the two diastereomers of 5.9 kcal mol<sup>-1</sup> (BP86/def2-SVP), thus explaining why the  $\Delta$ -*S* diastereomers are not observed under optimized reaction conditions, most likely because of thermal decomposition. The energy difference changes only slightly when solvent effects are considered or when different functionals are employed. The Gibbs free energy of  $\Delta$ -(*S*)-**45** is 5.5 kcal mol<sup>-1</sup> higher than  $\Lambda$ -(*S*)-**45** at BVP86/def2-SVP/CPCM. The energy difference at M05/def2-SVP becomes 5.1 kcal mol<sup>-1</sup> and it decreases to 3.5 kcal mol<sup>-1</sup> at M05/def2-SVP/CPCM. In all cases, we find a substantially lower stability of the  $\Delta$ -(*S*)-**45** isomer compared to  $\Lambda$ -(*S*)-**45**.



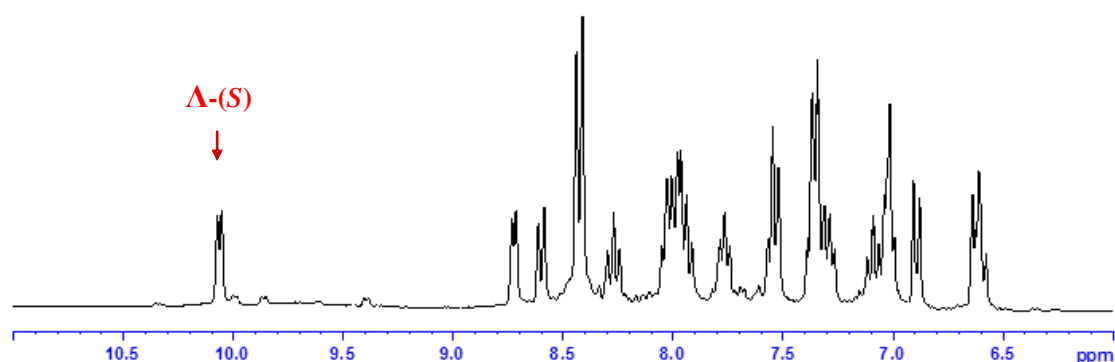
**Figure 10.** The optimized geometries of the two diastereomers  $\Lambda$ -(*S*)-**45** and  $\Delta$ -(*S*)-**45** at BVP86/def2-SVP. The differences in Gibbs free energies [kcal mol<sup>-1</sup>] between the two diastereomers were calculated at different levels of theory as indicated in parenthesis.

To further understand the mechanism, the following reactions have been done. Firstly, the (*R*)-**SO** auxiliary was reacted with (*rac*)-Ru(bpy)<sub>2</sub>Cl<sub>2</sub> in the presence of K<sub>2</sub>CO<sub>3</sub> (0.5 eq) in ethyleneglycol at 100 °C for 10 min, affording two diastereomers  $\Lambda$ -(*S*)-**45** and  $\Delta$ -(*S*)-**45** nearly 1: 1. Then this sample was heated continually at 170 °C for 90 seconds, only one diastereomer formed with a yield of 87%. Therefore, it demonstrates that the  $\Delta$ -(*S*)-**45** must have converted into the  $\Lambda$ -(*S*)-**45** instead of a simple decomposition of the less stable diastereomer (Figure 11).

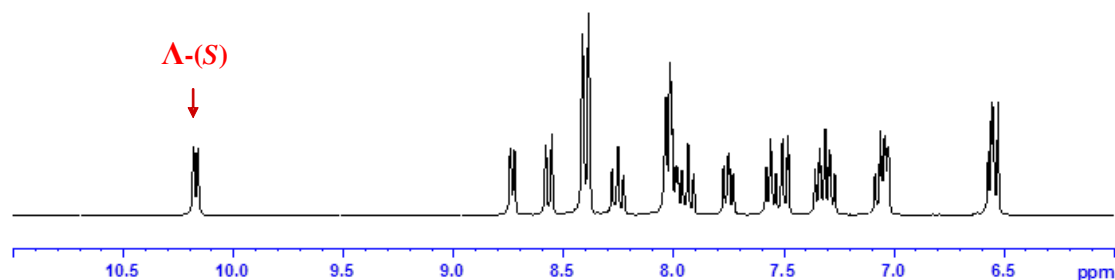
a) 100 °C 10 min



b) 170 °C 1.5 min



c) After purification

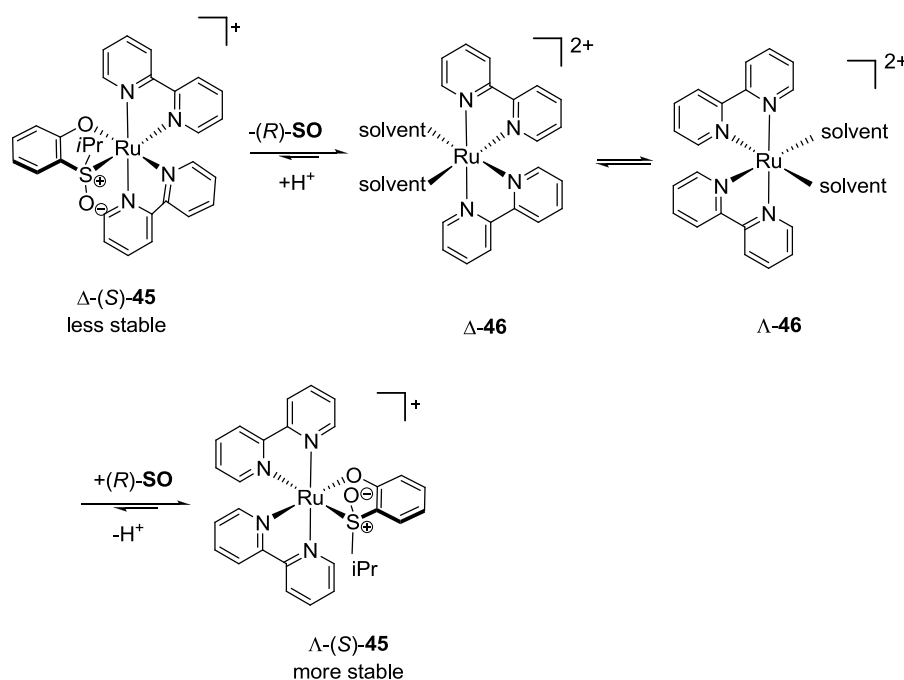


**Figure 11.** Excerpts of  $^1\text{H}$  NMR spectra of reaction  $(rac)\text{-Ru}(\text{bpy})_2\text{Cl}_2$  to  $\Lambda$ -(S)-**45**.

a) The reaction performed at 100 °C for 10 min afforded a mixture of compounds that are assigned to  $\Delta$ -(S)-**45** and  $\Lambda$ -(S)-**45**; b) After heating this mixture for another 1.5 min at 170 °C; c) Reference  $^1\text{H}$  NMR spectrum of  $\Lambda$ -(S)-**45** after purification by column chromatography on silica gel.

Based on the results in Figure 11, we proposed the following mechanism: initially, the (*R*)-**SO** auxiliary reacted with  $(rac)\text{-Ru}(\text{bpy})_2\text{Cl}_2$  to form two diastereomers,  $\Delta$ -(S)-**45** and  $\Lambda$ -(S)-**45**. Because of the large intramolecular hindrance of complex  $\Delta$ -(S)-**45**, it decomposed to intermediate complex  $\Delta$ -**46**, which was coordinated with the solvent at 170 °C. At high temperatures, complex  $\Delta$ -**46** can convert to complex

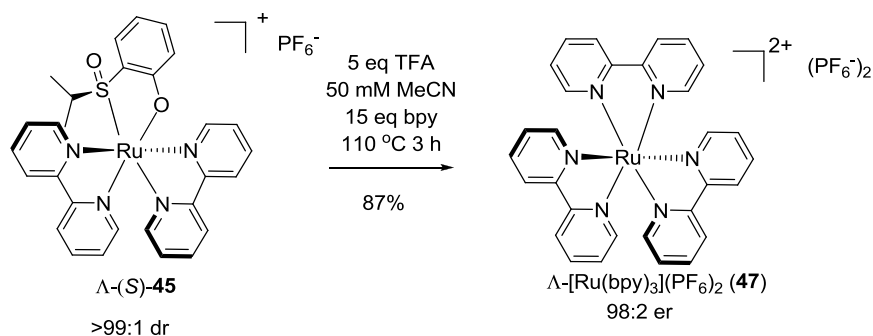
$\Lambda$ -**46**, most likely through pentacoordinated intermediates, and the equilibrium is reversible. At last, the free ligand catches intermediate complex  $\Lambda$ -**46**, providing the stable diastereomer  $\Lambda$ -(*S*)-**45**, which renders the equilibrium irreversible. Thus, the equilibrium shifted to the favored diastereomer in a dynamic transformation under thermodynamic control (Scheme 28).



**Scheme 28.** Proposed mechanism of the diastereoselective synthesis of complex  $\Delta$ -(*S*)-**45** and complex  $\Lambda$ -(*S*)-**45** via dynamic conversion under thermodynamic control.

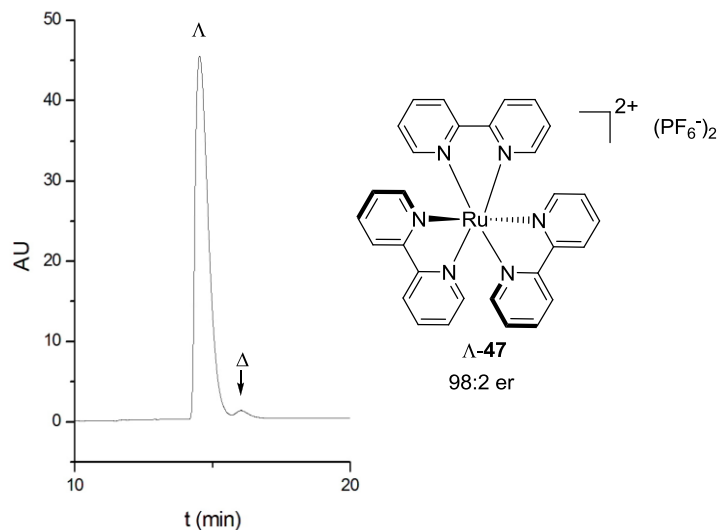
As a general method, the auxiliary not only controls the metal-centered chirality but can also be removed without affecting the metal-centered configuration. The (*R*)-SO auxiliary meets both requirements. According to the method published in salycaloxazoline system<sup>35</sup>, the auxiliary can be removed in the presence of TFA (5 eq) in acetonitrile (50 mM) and reacted with the bpy (2,2'-bipyridine) ligand (15 eq) at 110 °C, creating  $\Lambda$ -[Ru(bpy)<sub>3</sub>](PF<sub>6</sub>)<sub>2</sub> (**47**) with 98: 2 er (Scheme 29). The absolute stereochemistry of  $\Lambda$ -[Ru(bpy)<sub>3</sub>](PF<sub>6</sub>)<sub>2</sub> was verified via two aspects. Firstly, Figure 13 shows a similar CD spectrum to  $\Lambda$ -[Ru(4,4'-*t*Bu<sub>2</sub>bpy)(5,5'-Me<sub>2</sub>bpy)(bpy)]<sup>2+</sup> (4,4'-*t*Bu<sub>2</sub>bpy = 4,4'-di-*tert*-butyl-2,2'-bipyridine, 5,5'-Me<sub>2</sub>bpy =

5,5'-dimethyl-2,2'-bipyridine) which the configuration was confirmed via crystal structure<sup>35</sup>. Secondly, according to the work of Keene<sup>47</sup> and Hua<sup>48</sup>,  $\Lambda$ -[Ru(bpy)<sub>3</sub>](PF<sub>6</sub>)<sub>2</sub> will retain the configuration in the substitution reaction.

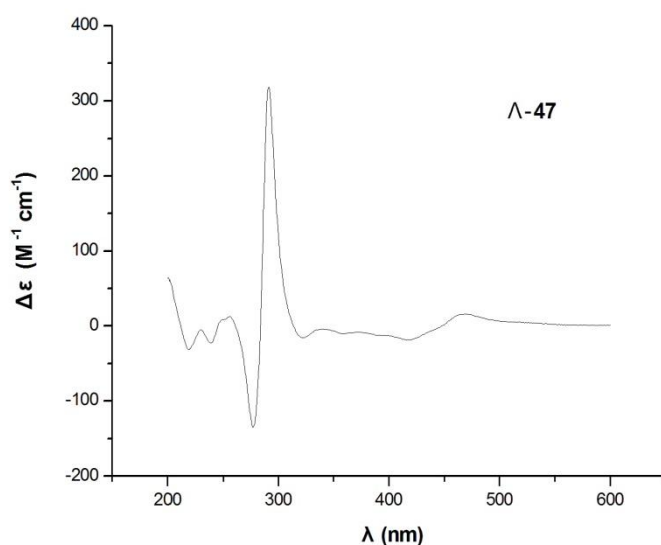


**Scheme 29.** Asymmetric synthesis of ruthenium polypyridyl complex  $\Lambda$ -47.

The enantiomeric excess of complex  $\Lambda$ -[Ru(bpy)<sub>3</sub>](PF<sub>6</sub>)<sub>2</sub> was determined via HPLC (Figure 12).



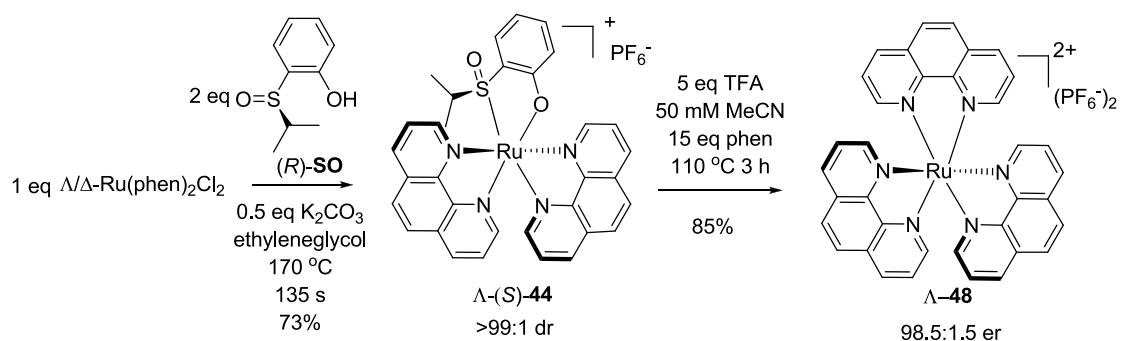
**Figure 12.** Shown is the chiral HPLC trace of the synthesized complex  $\Lambda$ -[Ru(bpy)<sub>3</sub>](PF<sub>6</sub>)<sub>2</sub>. Conditions: Daicel Chiralcel OD-R (250 × 4 mm) HPLC column, flow rate = 0.5 mL/min, column temperature 40 °C, and UV-absorption measured at 254 nm, solvent A = 0.087% aqueous H<sub>3</sub>PO<sub>4</sub>, solvent B = MeCN, with a linear gradient of 8% to 14% B in 20 min.



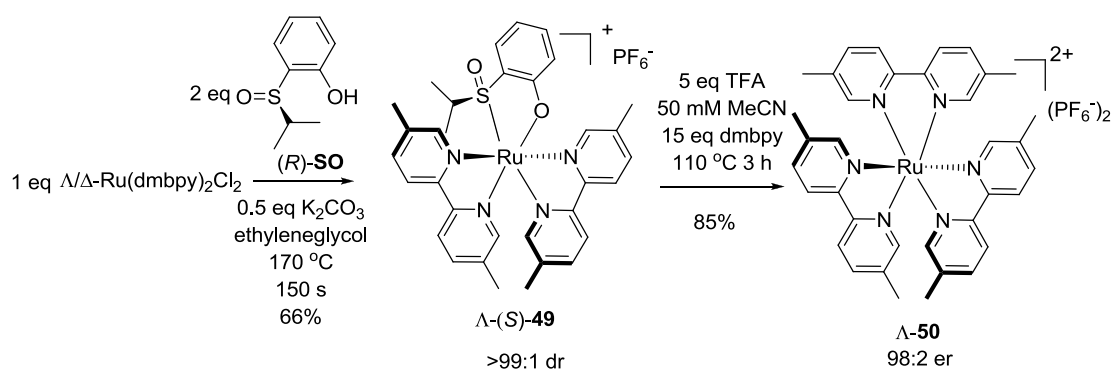
**Figure 13.** CD spectrum of the purified diastereomeric product  $\Lambda$ -47. The spectrum was measured in MeCN at concentrations of 0.1 mM.

The reason for the retention of the metal-centered configuration has been already explained in the salycaloxazoline system<sup>35</sup>: first, TFA weakened the chelate strength upon the protonation of the phenolate oxygen. Then, the coordination solvent substituted the auxiliary and fixed the metal-centered configuration. Finally, the third ligand coordinated with the metal to yield the enantiopure metal complex.

Via the same strategy, the analogous complexes  $(rac)$ -Ru(phen)<sub>2</sub>Cl<sub>2</sub> (phen = 1, 10-phenanthroline) and  $(rac)$ -Ru(dmbpy)<sub>2</sub>Cl<sub>2</sub> (dmbpy = 5,5'-dimethylbipyridine) have been resolved successfully (Scheme 30).

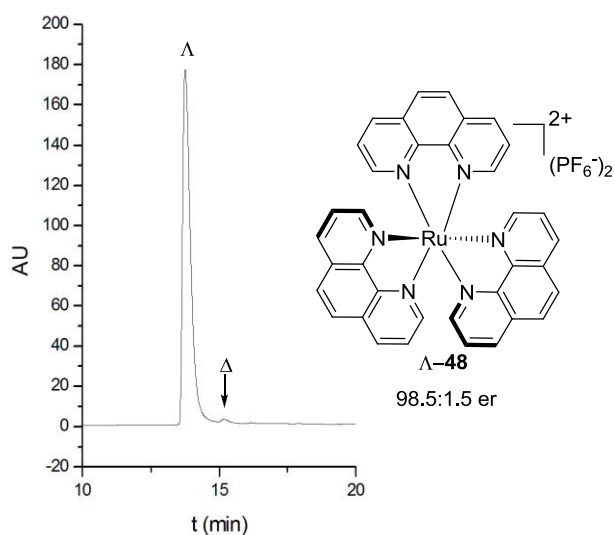


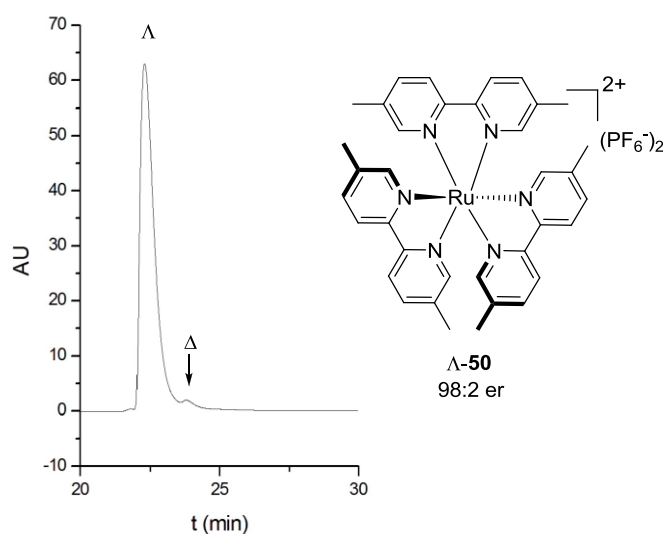




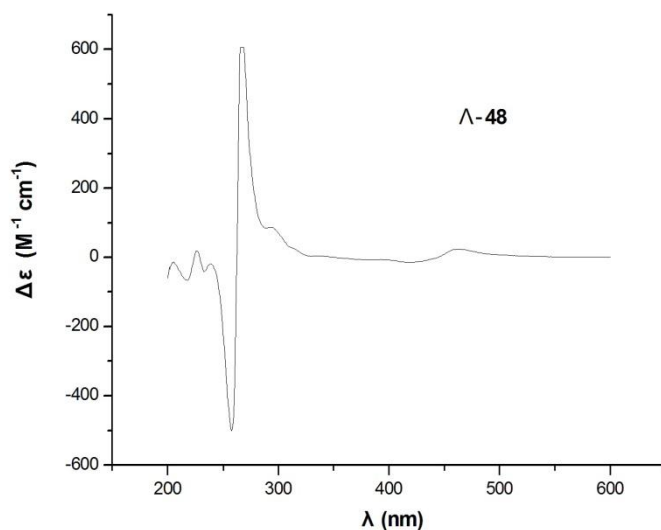
**Scheme 30.** Asymmetric synthesis of ruthenium polypyridyl complexes.

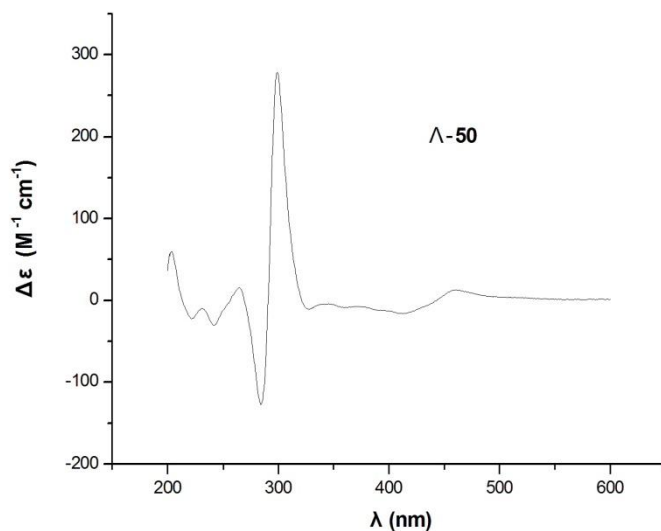
Similarly, the enantiomeric excess of complexes  $\Lambda$ -**48** and  $\Lambda$ -**50** were determined by HPLC (Figure 14). In addition, their CD spectra (Figure 15) were similar to that of  $\Lambda$ -**47**, which demonstrated that the absolute configurations of **48** and **50** were lambda.





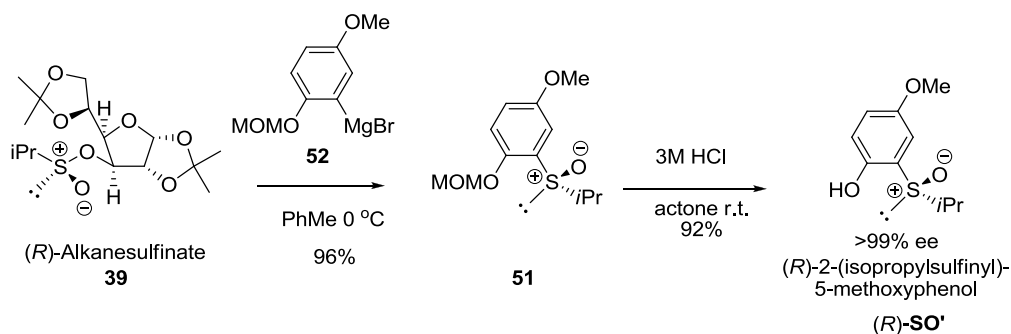
**Figure 14.** Shown is the chiral HPLC trace of the synthesized complexes  $\Lambda$ -[Ru(phen) $_3$ ](PF $_6$ ) $_2$  ( $\Lambda$ -48) and  $\Lambda$ -[Ru(dmbpy) $_3$ ](PF $_6$ ) $_2$  ( $\Lambda$ -50). Conditions: Daicel Chiralcel OD-R (250  $\times$  4 mm) HPLC column, flow rate = 0.5 mL/min, column temperature 40  $^\circ\text{C}$ , and UV-absorption measured at 254 nm, solvent A = 0.087% aqueous H $_3$ PO $_4$ , solvent B = MeCN, with a linear gradient of 15% to 40% B in 20 min for  $\Lambda$ -48; with a linear gradient of 14% to 27% B in 20 min, then 27% B in 5min for  $\Lambda$ -50.





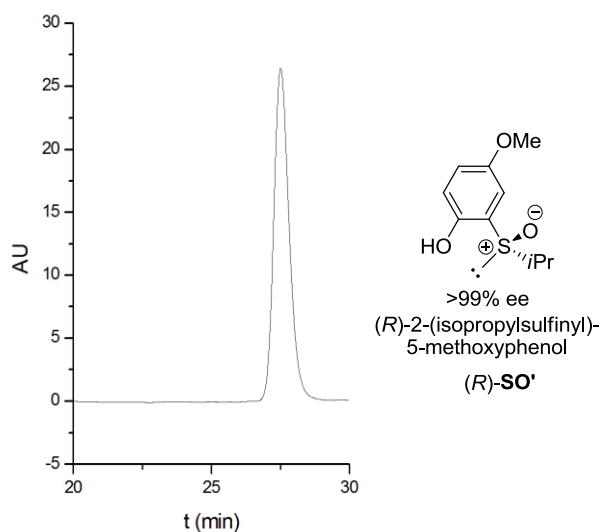
**Figure 15.** CD spectra of the purified diastereomeric products  $\Lambda$ -**48** and  $\Lambda$ -**50**. Spectra were measured in MeCN at concentrations of 0.1 mM.

Although the enantiopure ruthenium complex was obtained respectably, higher enantiopurities were desired for the final products. Considering the fact that a small amount of decomposed compound, such as  $\Delta$ -**46**, might make the  $\Lambda$ -(*S*)-**45** impure, which would reduce the enantiomeric ratios in the conversion, we purified  $\Lambda$ -(*S*)-**45** by using a gravitational column, but it did not work. Then, the complex  $\Lambda$ -(*S*)-**45** was purified via crystallization. In this way, completely enantiopure  $\Lambda$ -[Ru(bpy)<sub>3</sub>](PF<sub>6</sub>)<sub>2</sub> was obtained. However, this procedure lost many products in the solution and gave the crystal with low yield. In order to solve this problem, the modified ligand (*R*)-2-(isopropylsulfinyl)-5-methoxyphenol [(*R*)-**SO'**] was synthesized (Scheme 31), expecting the additional methoxy group to increase the purity of the intermediate diastereomers due to the cleaner formation or modified elution behavior during column chromatography on silica gel.



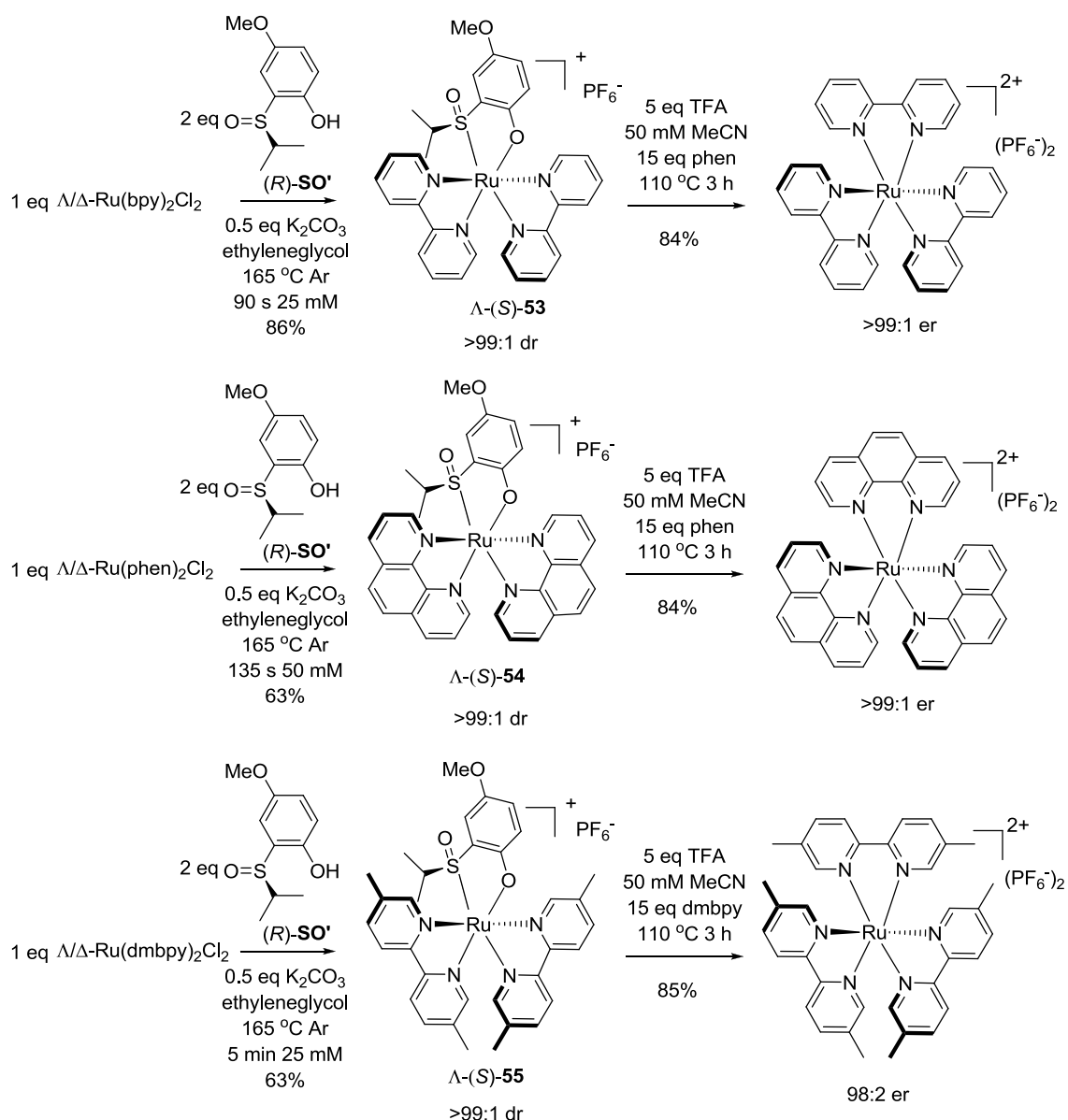
**Scheme 31.** Synthesis of (*R*)-SO'.

In order to synthesize (*R*)-SO', Grignard reagent **52** was made from 1-bromo-2-(methoxymethoxy)-5-methoxybenzene. After the addition of (*R*)-alkanesulfinate **39**, compound **51** was obtained. Finally, (*R*)-SO' was obtained via the deprotection of compound **51**. The enantiomeric purity of (*R*)-SO' was determined by HPLC (Figure 16), which was higher than 99% ee.



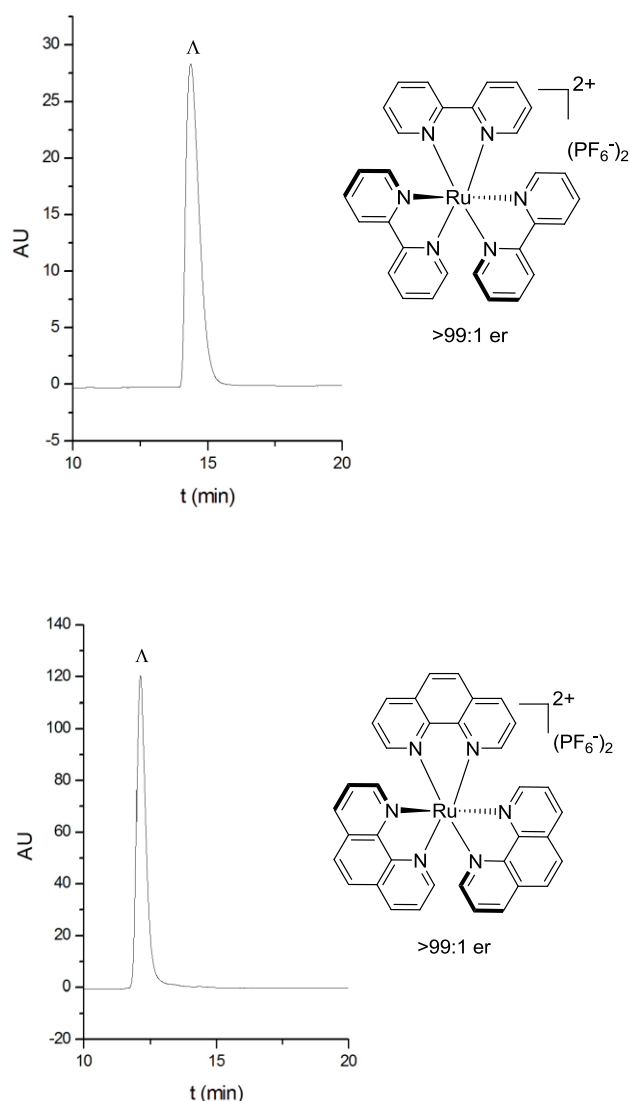
**Figure 16.** Shown is the chiral HPLC trace of (*R*)-SO'. Conditions: Chiralpak IB (0.46cm×25cm) HPLC column on an Agilent 1200 Series HPLC System. The flow rate was 0.5 mL/min, the column temperature 40 °C, and UV-absorption was measured at 254 nm. Solvent A = EtOH, solvent B = hexane, with 5% A in 30 min.

By using the new auxiliary (*R*)-SO' in this asymmetric coordination system, the final complexes became more enantiopure (Scheme 32).



**Scheme 32.** Asymmetric synthesis of ruthenium polypyridyl complexes by  $(R)$ -SO'.

From the HPLC trace, we can see that by using the new auxiliary  $(R)$ -SO', the  $\Lambda$ -[Ru(bpy) $_3$ ](PF $_6$ ) $_2$  and  $\Lambda$ -[Ru(phen) $_3$ ](PF $_6$ ) $_2$  became more pure that nearly only one stereoisomer was formed (Figure 17). Additionally, the behavior of the new auxiliary  $(R)$ -SO' was slightly different from that of  $(R)$ -SO. Because of the methoxy group on the  $(R)$ -SO', the  $(R)$ -SO' was oxidized more easily in the previous reaction conditions. Therefore, after screening the conditions, we found that the new auxiliary  $(R)$ -SO' needs to be used under argon and at a lower temperature.



**Figure 17.** HPLC traces of  $\Lambda$ -[Ru(bpy)<sub>3</sub>](PF<sub>6</sub>)<sub>2</sub> and  $\Lambda$ -[Ru(phen)<sub>3</sub>](PF<sub>6</sub>)<sub>2</sub> with high enantiopurity which were synthesized by using the new auxiliary (*R*)-SO'.

In summary, we developed a method for the asymmetric synthesis of ruthenium polypyridyl complexes based on thermodynamic control. In this method, the commercially available racemic complexes (*rac*)-Ru(bpy)<sub>2</sub>Cl<sub>2</sub>, (*rac*)-Ru(phen)<sub>2</sub>Cl<sub>2</sub>, and (*rac*)-Ru(dmbpy)<sub>2</sub>Cl<sub>2</sub> have been used as the starting materials in order to react with chiral sulfoxide ligand, providing only one diastereomer of the auxiliary-mediated metal complexes. Then, the auxiliary-mediated metal complexes are converted into their corresponding optically active ruthenium polypyridyl complexes with high enantiopurities (Table 8).

**Table 8.** Asymmetric synthesis of  $\Lambda$ -[Ru(pp)<sub>3</sub>](PF<sub>6</sub>)<sub>2</sub> from (*rac*)-Ru(pp)<sub>2</sub>Cl<sub>2</sub><sup>a</sup>.

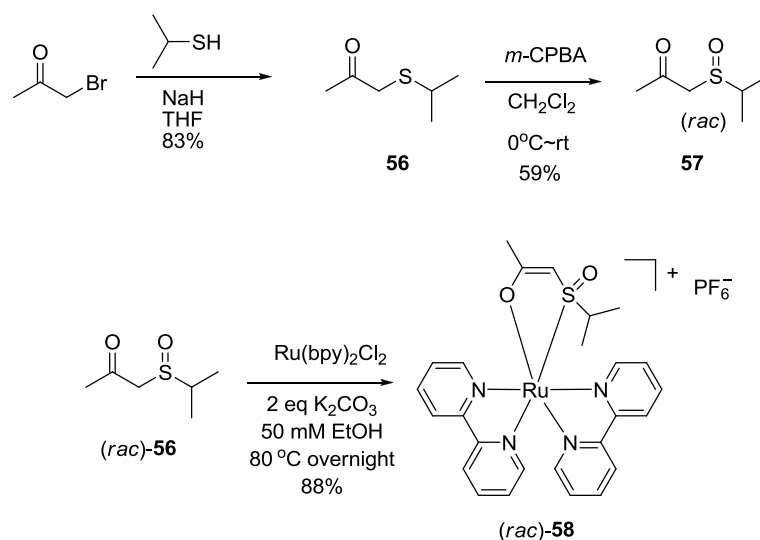
entry	[Ru(pp) <sub>2</sub> Cl <sub>2</sub> ]	auxiliary	$\Lambda$ -( <i>S</i> ) diastereomers <sup>b</sup>	$\Lambda$ -[Ru(pp) <sub>3</sub> ](PF <sub>6</sub> ) <sub>2</sub> products <sup>c</sup>
1	bpy	( <i>R</i> )-SO	$\Lambda$ -( <i>S</i> )-45 (87%)	87%, 98:2 er
2	phen	( <i>R</i> )-SO	$\Lambda$ -( <i>S</i> )-44 (73%)	85%, 98.5:1.5 er
3	5,5'-dmbpy	( <i>R</i> )-SO	$\Lambda$ -( <i>S</i> )-49 (66%)	91%, 98:2 er
4	bpy	( <i>R</i> )-SO'	$\Lambda$ -( <i>S</i> )-53 (86%)	84%, >99:1 er
5	phen	( <i>R</i> )-SO'	$\Lambda$ -( <i>S</i> )-54 (63%)	84%, >99:1 er
6	5,5'-dmbpy	( <i>R</i> )-SO'	$\Lambda$ -( <i>S</i> )-55 (63%)	85%, >98:2 er

<sup>a</sup> Reaction conditions: Reaction of racemic [Ru(pp)<sub>2</sub>Cl<sub>2</sub>] (pp = bpy, phen, dmbpy respectively) with (*R*)-SO or (*R*)-SO' (2 eq) and K<sub>2</sub>CO<sub>3</sub> (0.5 eq) at 165 or 170 °C in ethyleneglycol afforded chiral-auxiliary-mediated metal complexes. For the next step, chiral-auxiliary-mediated metal complexes reacted with pp (pp = bpy, phen, 5,5'-dmbpy) (15 eq) and TFA (5 eq) at 110 °C in MeCN, stirred for 3 hours, yielding  $\Lambda$ -[Ru(pp)<sub>3</sub>](PF<sub>6</sub>)<sub>2</sub>. <sup>b</sup> Diastereomeric ratios of chiral-auxiliary-mediated metal complexes were at least 99: 1 as determined by <sup>1</sup>H NMR spectroscopy. The metal configuration of the main diastereomer was lambda. <sup>c</sup> Enantiomeric ratios of  $\Lambda$ -[Ru(pp)<sub>3</sub>](PF<sub>6</sub>)<sub>2</sub> were determined by chiral HPLC analysis. The complexes were isolated as their PF<sub>6</sub> salts.

Up to now, we have carefully designed and synthesized sulfoxide auxiliary in order to let the sulfur-based stereo center come into the proximity of the ruthenium stereo center. Because of the steric crowding of the octahedral coordination sphere, there was a large difference in terms of the stability between the two diastereomers of the intermediate complexes. Based on these, the chiral-auxiliary-mediated dynamic conversion has been built up by us. This method opens a new door to achieving the enantiomerically pure octahedral complexes.

### 3.1.2 Sulfinylacetone auxiliary system

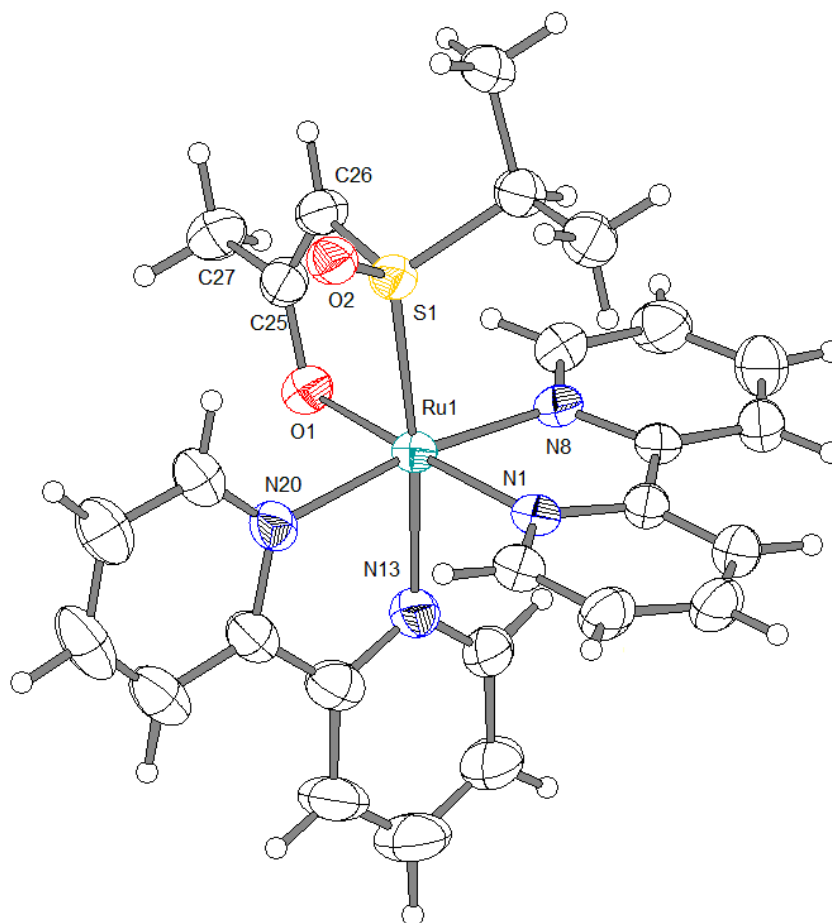
Although the (*R*)-2-(isopropylsulfinyl)phenol auxiliary directed asymmetric synthesis efficiently, the synthesis route was too long. This limited the application of this method. Thus, finding the auxiliary which was easy to synthesize became the new target for the next step. After screening different tapes of the ligands, the 1-(isopropylsulfinyl)propan-2-one (**57**) can coordinate with the ruthenium very well. The synthesis route of it was showed in the Scheme 33: propane-2-thiol reacted with 1-bromopropan-2-one, yielding compound **56**. It was then oxidized by *m*-CPBA, yielding 1-(isopropylsulfinyl)propan-2-one (**57**). By using the (*rac*)-Ru(bpy)<sub>2</sub>Cl<sub>2</sub> as the ruthenium source, the ligand **57** can react with it in the presence of K<sub>2</sub>CO<sub>3</sub> (2 eq), yielding complex **58** which was very stable. Interestingly, the two diastereomers of the complex **58** can be separated by column chromatography.



**Scheme 33.** Synthesis of complex **58**.

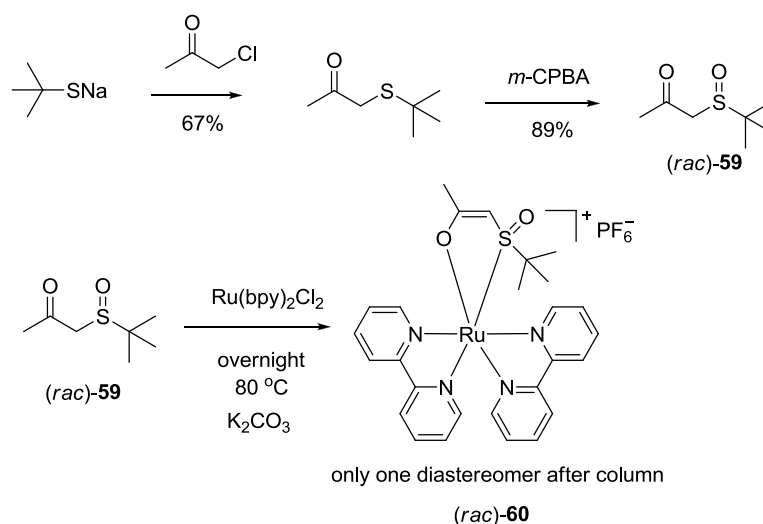
Figure 18 demonstrated that the ligand **57** coordinates with the metal by using the enolated oxygen and sulfoxide, forming five members chelate.





**Figure 18.** Crystal structure of complex **58** in which the absolute stereochemistry was determined. Counterion and solvent molecule are omitted for clarity. ORTEP drawing with 50% probability thermal ellipsoids. Selected bond distances ( $\text{\AA}$ ): N20-Ru1 = 2.083(3), N8-Ru1 = 2.049(3), N13-Ru1 = 2.094(3), N1-Ru1 = 2.047(3), O1-Ru1 = 2.077(3), O2-S1 = 1.496(3), S1-Ru1 = 2.2573(10), C26-S1 = 1.720(4), C25-C26 = 1.375(5), C25-O1 = 1.303(5), C25-C27 = 1.503(6).

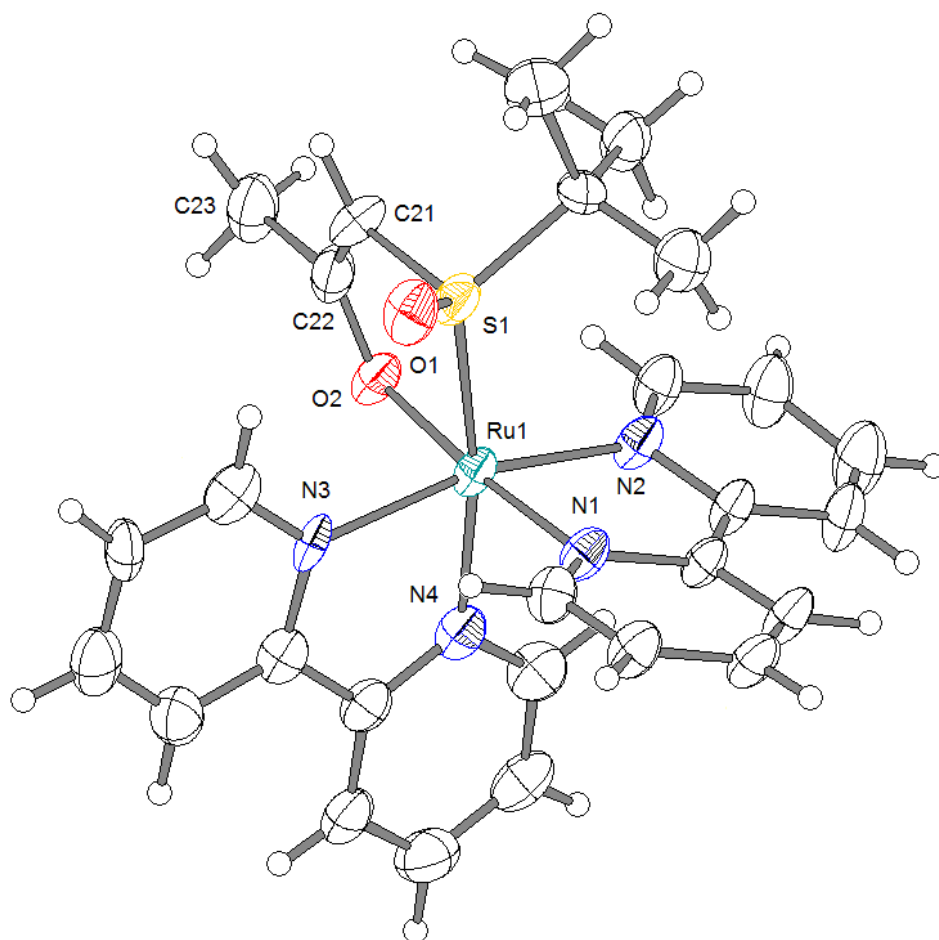
Having O,S-coordinated chelating ligand in hand, we decided to modify it with bigger hindrance group. Therefore, the ligand **59** was synthesized by the reaction with sodium 2-methylpropane-2-thiolate and acetone chloride followed by oxidizing with *m*-CPBA (Scheme 34).



**Scheme 34.** Synthesis of complex **60**.

This time, the ligand can still coordinate with  $\text{Ru}(\text{bpy})_2\text{Cl}_2$  and only one diastereomer was obtained after purification by column chromatography. The crystal structure of complex **60** showed that the large hindrance which gave by the *t*-Bu group distorted the plane of bpy strongly (Figure 19). This phenomenon indicated why one of the diastereomer was not stable and even decomposed in the column chromatography.

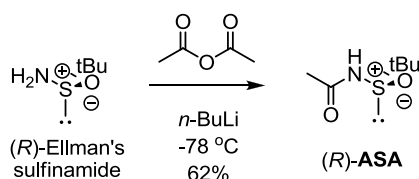
In conclusion, although the ligand **57** and **59** were racemic and the enantiopure sulfoxide center of them were not easy to synthesize, they showed us this important O,S-coordinated chelating way. Especially, the crystal structure of the complex **60** showed us how nicely this *t*-Bu group gave the hindrance and directed the asymmetric coordination chemistry. All of these results gave us strong groundwork to invent new chiral auxiliary in the next step.



**Figure 19.** Crystal structure of complex **60** in which the absolute stereochemistry was determined. Counterion and solvent molecule are omitted for clarity. ORTEP drawing with 50% probability thermal ellipsoids. Selected bond distances (Å): N1-Ru1 = 2.041(6), N2-Ru1 = 2.032(5), N3-Ru1 = 2.081(6), N4-Ru1 = 2.091(6), O1-S1 = 1.503(4), O2-Ru1 = 2.085(5), S1-Ru1 = 2.255(2), C21-S1 = 1.717(8), C22-O2 = 1.315(8), C21-C22 = 1.374(10), C22-C23 = 1.523(10).

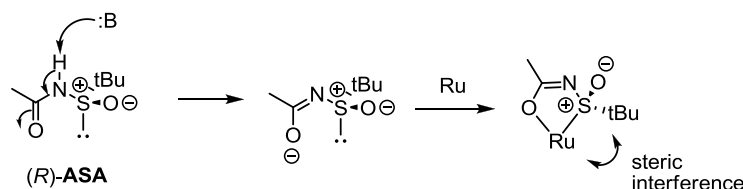
### 3.1.3 *N*-Acetylsulfinamide auxiliary system

Based on the results in the previous chapter, we invented the (*R*)-*N*-acetyl-*tert*-butanesulfinamide ((*R*)-**ASA**) auxiliary. It was synthesized in only a single step by acetylating commercially available Ellman's sulfinamide (Scheme 35).



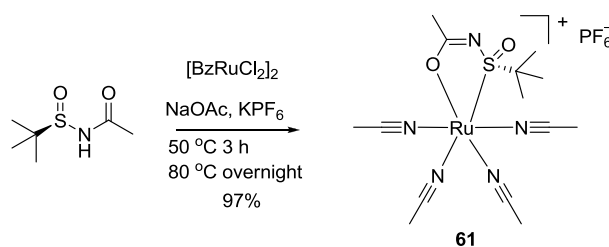
**Scheme 35.** Synthesis of (*R*)-**ASA** auxiliary.

We thought that the amide might enolate in the presence of a base and that it could use the oxygen of the carboximidate, together with sulfoxide, to coordinate with the metal, creating the same geometry as complex **60**. According to the previous results, this *t*-Bu group is in the proximity of the metal center, which can induce chirality into the system (Scheme 36).



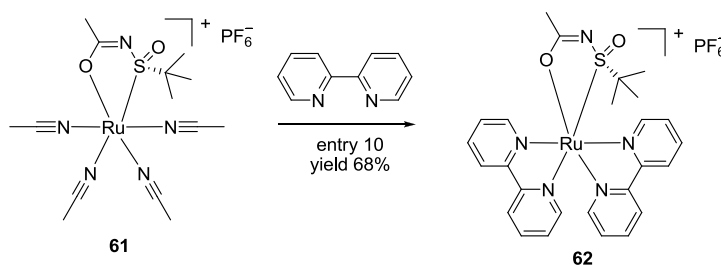
**Scheme 36.** (*R*)-**ASA** coordinates in a bidentate fashion through its deprotonated *N*-sulfinylcarboximidate form.

Because of these advantages, we investigated the asymmetric synthesis of ruthenium polypyridyl complex by using (*R*)-**ASA** auxiliary. Firstly, precursor **61** was synthesized via the optimization method, without using a pressure mercury lamp. Instead, NaOAc and KPF<sub>6</sub> were added to the solution of [(η<sup>6</sup>-C<sub>6</sub>H<sub>6</sub>)RuCl<sub>2</sub>]<sub>2</sub> in acetonitrile, which was heated to 50 °C and then refluxed at 80 °C, providing complex **61**, which was stable enough to purify via an aluminum column (Scheme 37). This reaction must be carried out under argon. Otherwise, it provided a very low yield.



**Scheme 37.** Synthesis of precursor **61**.

Then, we tested the asymmetric coordination chemistry of precursor **61**. It reacted with the bpy in various conditions, yielding various diastereoselectivities to form complex **62** (Table 9).

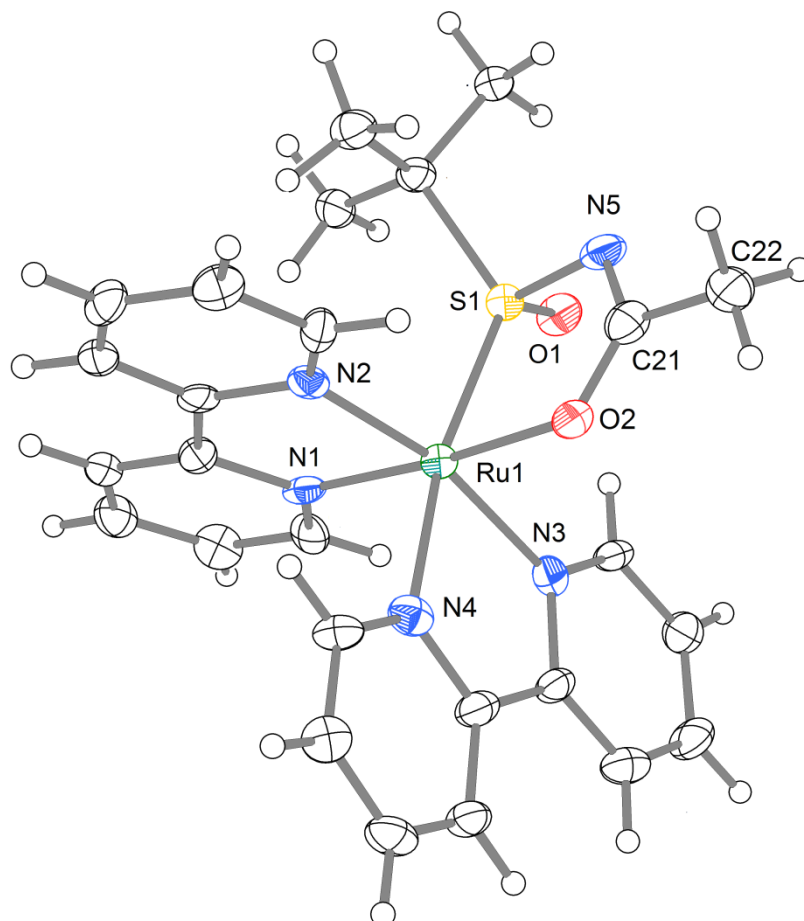


**Table 9.** Conditions dependence of the diastereoselective formation of **62**<sup>a</sup>.

entry	conc.	temp.	bpy	solvent	time	dr <sup>b</sup>
1	60mM	100°C	4eq	EtOH	5h	[Ru(bpy) <sub>3</sub> ] <sup>2+</sup>
2	60mM	100°C	4eq	ethyleneglycol	5h	[Ru(bpy) <sub>3</sub> ] <sup>2+</sup>
3	60mM	100°C	4eq	DMF	5h	3:1
4	60mM	100°C	4eq	PhCl	5h	30:1
5	30mM	100°C	4eq	PhCl	5h	4.6:1
6	90mM	100°C	4eq	PhCl	5h	4.3:1
7	60mM	100°C	8eq	PhCl	5h	3:1
8	60mM	100°C	2.5eq	PhCl	5h	3.6:1
9	60mM	80°C	4eq	PhCl	overnight	1.7:1
10	60mM	120°C	2.5eq	PhCl	overnight	>99:1

<sup>a</sup> Reaction conditions: Reaction of precursor **61** with bpy at the indicated time, equivalent of bpy, solvent, concentration and temperature. <sup>b</sup> Diastereomeric ratios determined by crude <sup>1</sup>H NMR. The metal configuration of the main diastereomer was lambda.

The absolute configuration of the main diastereomer in Table 9 was determined by the crystal structure (Figure 20). This result also demonstrated that the (*R*)-configured *N*-acetyl-*tert*-butanesulfonamide (**ASA**) ligand directed the  $\Lambda$ -configured ruthenium center by providing  $\Lambda$ -(*S*)-**62** as the main diastereomer.

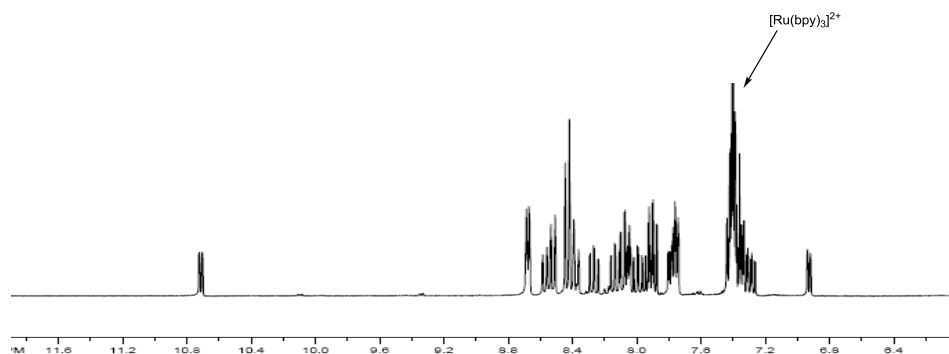


**Figure 20.** Crystal structure of  $\Lambda$ -(*S*)-**62**. Counterion and solvent molecule are omitted for clarity. ORTEP drawing with 50% probability thermal ellipsoids. Selected bond distances (Å): N1-Ru1 = 2.035(4), N2-Ru1 = 2.039(4), N3-Ru1 = 2.096(4), N4-Ru1 = 2.095(4), C21-C22 = 1.507(6), O1-S1 = 1.487(3), Ru1-O2 = 2.067(3), Ru1-S1 = 2.2543(13), C21-O2 = 1.290(6), C21-N5 = 1.319(6), N5-S1 = 1.659(4). CCDC 829833 contains additional supplementary crystallographic data which can be obtained free of charge from The Cambridge Crystallographic Data Centre via [www.ccdc.cam.ac.uk/data\\_request/cif](http://www.ccdc.cam.ac.uk/data_request/cif).

From the crystal structure of  $\Lambda$ -(*S*)-**62** (Figure 20), we can see the coordination

through the sulfur atom of the sulfinyl moiety and an additional oxygen atom of the carboximide. The structure also reveals that the C21-N5 (1.32 Å) and C21-O2 (1.28 Å) bonds of the chelate ring are shorter than single bonds and thus have a partial double bond character, formally indicating a resonance between a coordinated carboximide and carboxamide. To the best of our knowledge, such an O,S-coordinated chelating sulfinylcarboximide ligand has not been reported before. This five-membered ruthenium sulfinylcarboximide chelate ring is very stable. Complex  $\Lambda$ -(*S*)-**62** can be purified via regular silica gel chromatography, without any signs of decomposition.

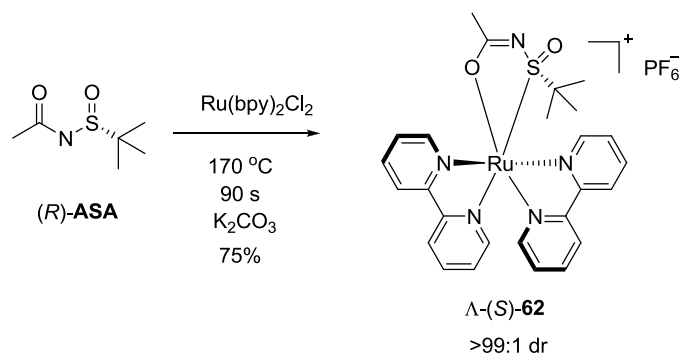
Table 9 noted that the  $[\text{Ru}(\text{bpy})_3]^{2+}$  was formed in entry 1 and entry 2. That means the (*R*)-**ASA** ligand of precursor **61** can be substituted in a proton solvent without acid. Additionally, a good diastereoselectivity result can be obtained in harsh conditions. From the crude NMR of entry 10 in Table 9, we found that there was a great deal of  $[\text{Ru}(\text{bpy})_3]^{2+}$ , in addition to complex **62** (Figure 21). To gain some insight into the mechanism, we separated the  $[\text{Ru}(\text{bpy})_3]^{2+}$  in the reaction of entry 10 and tested its enantiopurity. Surprisingly, it showed an enriched  $\Delta$ -configuration, which was the opposite of the main diastereomer of complex **62**. This means the  $\Delta$ -configuration of the diastereomer of complex **62** was not stable and bpy can be substituted for it, forming  $[\text{Ru}(\text{bpy})_3]^{2+}$  and leaving diastereomerically pure complex  $\Lambda$ -**62**.



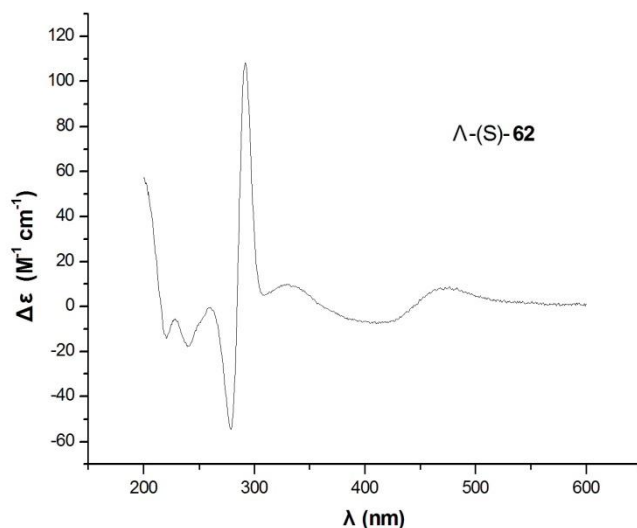
**Figure 21.** The crude proton NMR of complex **12**, which corresponds to Table 9, entry 10.

Next, we investigated the dynamic conversion of (*rac*)- $\text{Ru}(\text{bpy})_2\text{Cl}_2$  by using the

(*R*)-**ASA** auxiliary. According to the procedure that was developed in the (*R*)-2-(isopropylsulfinyl)phenol auxiliary system, the (*R*)-**ASA** auxiliary reacted with (*rac*)-Ru(bpy)<sub>2</sub>Cl<sub>2</sub> in the presence of K<sub>2</sub>CO<sub>3</sub> (0.5 eq) in ethyleneglycol at 170 °C for 90 seconds, creating only one diastereomer,  $\Lambda$ -(*S*)-**62** (Scheme 38). Figure 22 shows its CD spectrum.



**Scheme 38.** Dynamic conversion of (*rac*)-Ru(bpy)<sub>2</sub>Cl<sub>2</sub> by using the (*R*)-**ASA** auxiliary.

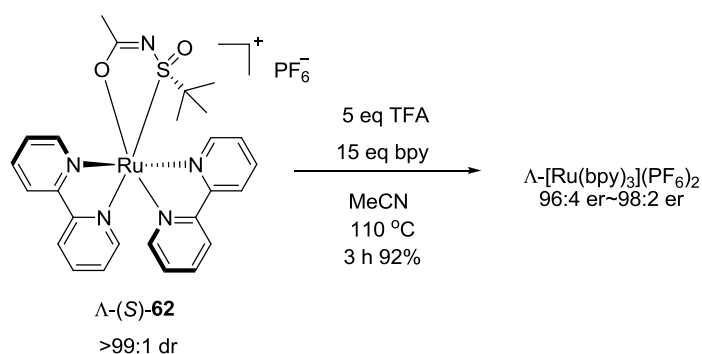


**Figure 22.** CD spectrum of the purified diastereomeric product  $\Lambda$ -(*S*)-**62**. The spectrum was measured in MeCN at concentrations of 0.1 mM.

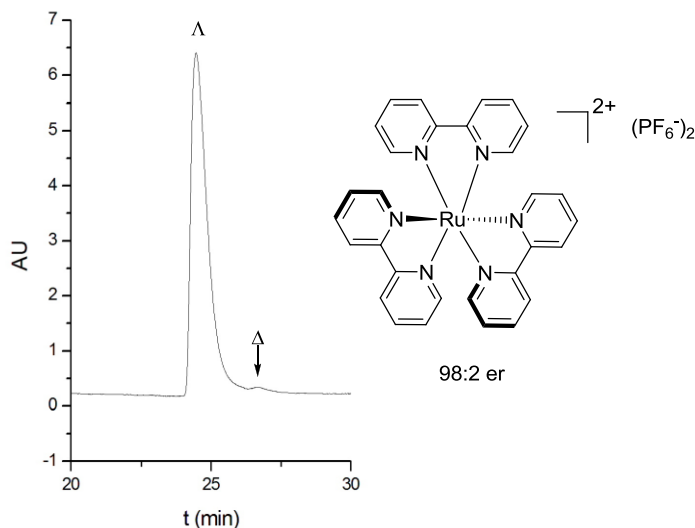
For the last step, bpy can be substituted for the (*R*)-**ASA** auxiliary by using the same procedure that was developed in the chiral sulfinylphenol auxiliary system.



However, the enantiopurity of the  $\Lambda$ -[Ru(bpy)<sub>3</sub>](PF<sub>6</sub>)<sub>2</sub> was not high; it was just 98:2 er. If the starting material  $\Lambda$ -(*S*)-**62** is used in the large-scale synthesis, the reaction provided a worse er value (96:4) for the final compound (Scheme 39). The absolute configuration and the ee value of [Ru(bpy)<sub>3</sub>](PF<sub>6</sub>)<sub>2</sub> were confirmed via HPLC trace (Figure 23). According to the HPLC trace in Figure 12, we know that the first signal in the HPLC trace was lambda and that the second signal was delta. Therefore, the configuration of [Ru(bpy)<sub>3</sub>](PF<sub>6</sub>)<sub>2</sub>, which was generated from  $\Lambda$ -(*S*)-**62**, was lambda.

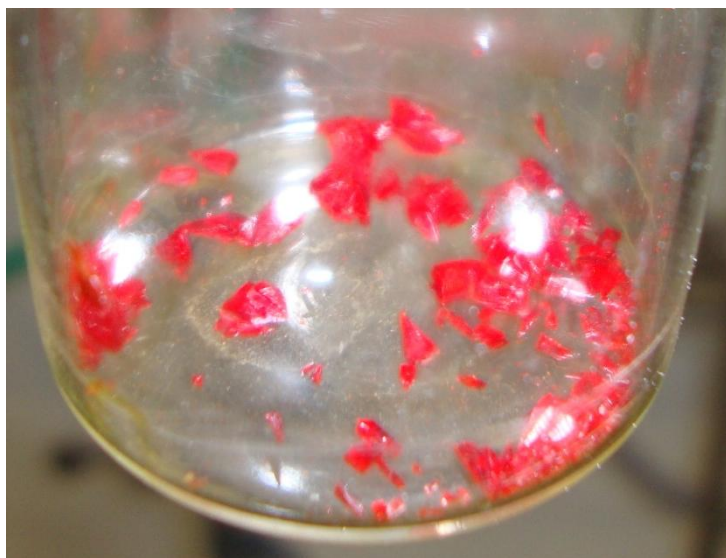


**Scheme 39.** Removing the (*R*)-ASA auxiliary by TFA.



**Figure 23.** HPLC traces of  $\Lambda$ -[Ru(bpy)<sub>3</sub>](PF<sub>6</sub>)<sub>2</sub> which was synthesized by using new auxiliary (*R*)-ASA. Conditions: Daicel Chiralcel OD-R (250 × 4 mm) HPLC column, flow rate = 0.5 mL/min, column temperature 40 °C, and UV-absorption measured at 254 nm, solvent A = 0.087% aqueous H<sub>3</sub>PO<sub>4</sub>, solvent B = MeCN, with a linear gradient of 4% to 10% B in 20 min.

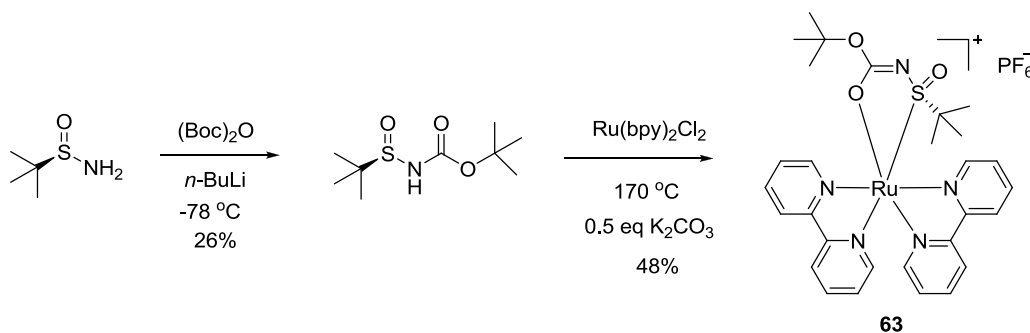
Considering the fact that only one diastereomer appeared in the NMR, we presumed a low ee value for the product due to the decomposition of  $\Delta$ -configured diastereomer mixing in the  $\Lambda$ -(*S*)-**62**, and it was difficult to separate them via column chromatography completely. Therefore, a method for purifying  $\Lambda$ -(*S*)-**62** more cleanly, even in the large scale synthesis, was needed. With this target,  $\Lambda$ -(*S*)-**62** was mixed with bpy and heated in EtOH for 2 hours. We expected that the bpy could consume the decomposition of  $\Delta$ -configuration diastereomer, leaving the  $\Lambda$ -(*S*)-**62** clean after being purified via column chromatography. Unfortunately, this strategy did not work at all. Then, we precipitated the  $\Lambda$ -(*S*)-**62** via Et<sub>2</sub>O from the DCM solution. In this way, the er value of [Ru(bpy)<sub>3</sub>](PF<sub>6</sub>)<sub>2</sub> increased a slightly. However, in order to enhance the er value from 96: 4 to 98: 2, the precipitation will need to be performed three times. In this process, much of the  $\Lambda$ -(*S*)-**62** was lost. Finally, we found that  $\Lambda$ -(*S*)-**62** can be crystallized easily from the THF with a high yield by adjusting the temperature properly. For example, 100 mg of  $\Lambda$ -(*S*)-**62** was first dissolved in DCM and evaporated via rotary evaporation, but not to complete dryness. The residue was dissolved in THF (2 mL) and heated to 80 °C. After slowly cooling this to the room temperature over a period of 1 hour, large crystals formed (Figure 24).



**Figure 24.** Crystals of  $\Lambda$ -(*S*)-**62**.

Eventually,  $[\text{Ru}(\text{bpy})_3](\text{PF}_6)_2$  with 98.5: 1.5 er was obtained by using these crystals of  $\Lambda$ -(*S*)-**62** in the substitution reaction.

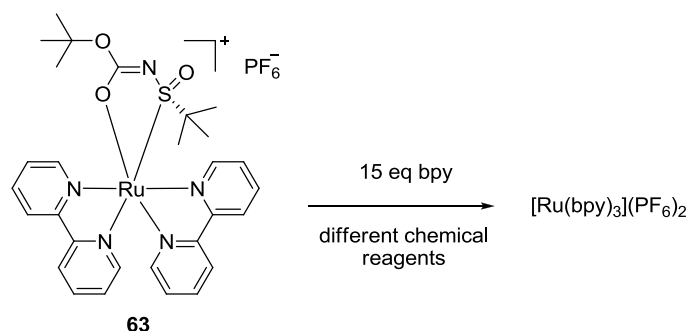
After finding the right auxiliary, for the next step, we wanted to develop some other methods for removing the directing ligand. Now, all the auxiliaries (salicyloxazoline auxiliary, isopropylsulfinylphenol auxiliary, and ASA auxiliary) were removed via acid after directing the asymmetric synthesis. However, we attempted to remove the acid-unstable ligand from the metal center without acid. In order to solve this problem, some modified ligands were synthesized. In the beginning, we changed the methyl group on the (*R*)-**ASA** into oxygen, expecting it to donate the electron density and stabilize the O-Ru bond of the five-member chelate (Scheme 40).



**Scheme 40.** Synthesis of complex **63**.

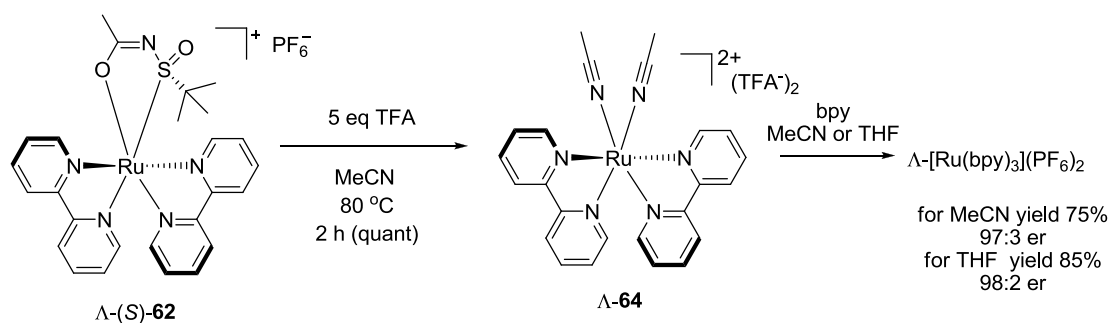
Then, compound **63** was mixed with bpy, using various chemical reagents to remove the auxiliary in an attempt to obtain  $[\text{Ru}(\text{bpy})_3](\text{PF}_6)_2$ . Unfortunately, this strategy did not work (Table 10).

Alternatively, we tried to synthesize enantiopure  $[\text{Ru}(\text{bpy})_3](\text{PF}_6)_2$  through another route. Firstly, complex  $\Lambda$ -(*S*)-**62** was dissolved in MeCN in the presence of TFA and heated at 80 °C for 2 hours, yielding acetonitrile complex  $\Lambda$ -**64**. Then, compound  $\Lambda$ -**64** can react with bpy to give enantiopure  $\Lambda$ - $[\text{Ru}(\text{bpy})_3](\text{PF}_6)_2$  in the neutral environment (Scheme 41). The absolute configuration and the ee value of  $[\text{Ru}(\text{bpy})_3](\text{PF}_6)_2$  were also determined by HPLC (for HPLC trace, see experiment part).

**Table 10.** Conditions screening for removing the directing ligand <sup>a</sup>.

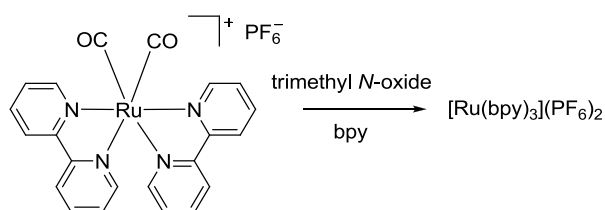
entry	chemical reagent	bpy	solvent	conc.	reaction time	temp.	results
1	5eq NaBH <sub>4</sub>	15eq	THF	50mM	overnight	rt	Decomposed <sup>b</sup> No[Ru(bpy) <sub>3</sub> ] <sup>2+</sup>
2	5eq LiAlH <sub>4</sub>	15eq	THF	50mM	1min	rt	Decomposed <sup>b</sup> No[Ru(bpy) <sub>3</sub> ] <sup>2+</sup>
3	5eq <i>m</i> CPBA	15eq	MeCN	50mM	overnight	110°C	Still had start material
4	5eq NaIO <sub>4</sub>	15eq	MeCN	50mM	overnight	110°C	Some Ru be oxidized
5	5eq MeMgBr	15eq	THF	50mM	1min	rt	A lot of salt generated

<sup>a</sup> Reaction conditions: Reaction of 50 mM **63** with 15 equiv of bpy at the indicated time, chemical reagent and temperature. <sup>b</sup> So many decomposed compounds were formed and difficulty to analyze what they are.

**Scheme 41.** Asymmetric synthesis of  $\Lambda\text{-}[\text{Ru}(\text{bpy})_3](\text{PF}_6)_2$  through the acetonitrile intermediate.

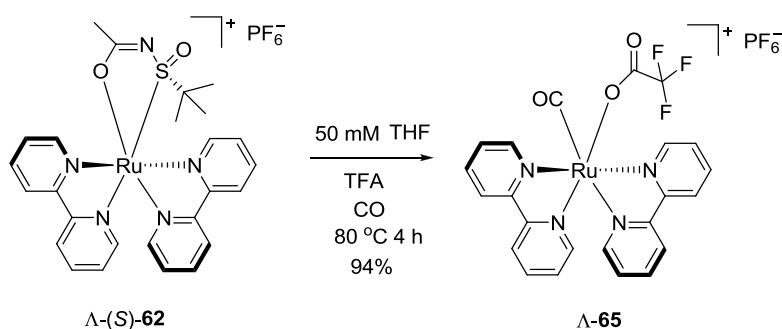
However, this reaction relies on acetonitrile and THF as solvents. Another limitation is the fact that the reaction must be carried out via heating. Thus, finding a solvent-free and method that works under mild conditions is the target for the next step.

According to Keene's work,  $[\text{Ru}(\text{bpy})_2(\text{CO})_2]^{2+}$  can react with bpy to form  $[\text{Ru}(\text{bpy})_3]^{2+}$  in the presence of  $\text{Me}_3\text{NO}$ , without adding any acid (Scheme 42)<sup>49</sup>.

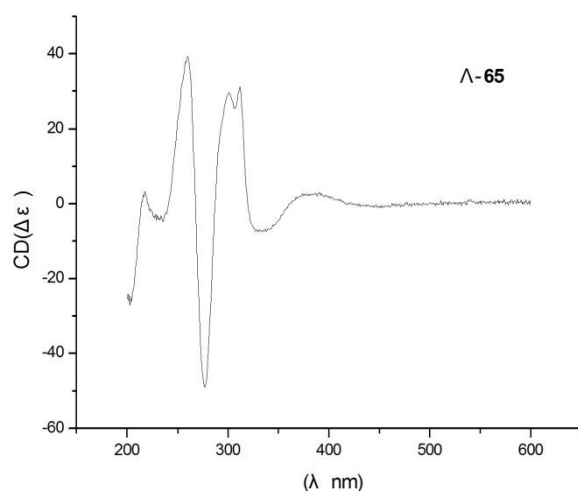


**Scheme 42.** Synthesis of  $[\text{Ru}(\text{bpy})_3]^{2+}$  according to Keene by using  $[\text{Ru}(\text{bpy})_2(\text{CO})_2]^{2+}$ .

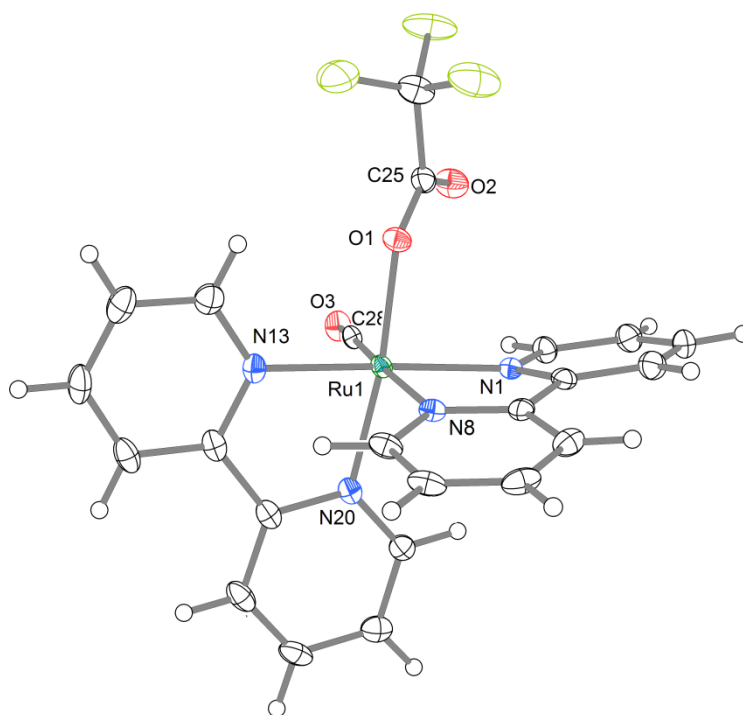
Based on this idea, we planned to synthesize  $[\text{Ru}(\text{bpy})_2(\text{CO})_2]^{2+}$  from  $\Lambda$ -(S)-**62** and retain the configuration with the metal center. Thus,  $\Lambda$ -(S)-**62** was mixed with TFA in the THF in a saturated CO atmosphere and heated for 4 hours. Surprisingly, instead of obtaining  $[\text{Ru}(\text{bpy})_2(\text{CO})_2]^{2+}$ , the CO/TFA precursor  $\Lambda$ -**65** was achieved (Scheme 43). The geometry and absolute configuration of the  $\Lambda$ -**65** was confirmed via the CD (Figure 25) and crystal structure (Figure 26).



**Scheme 43.** Synthesis of CO/TFA precursor  $\Lambda$ -**65**.

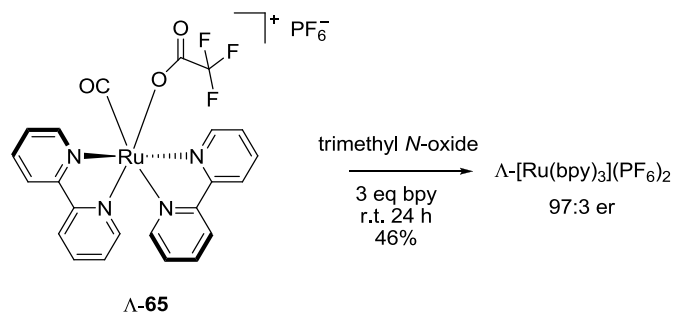


**Figure 25.** CD spectrum of the purified diastereomeric product  $\Lambda$ -65. The spectrum was measured in MeCN at concentrations of 0.1 mM.

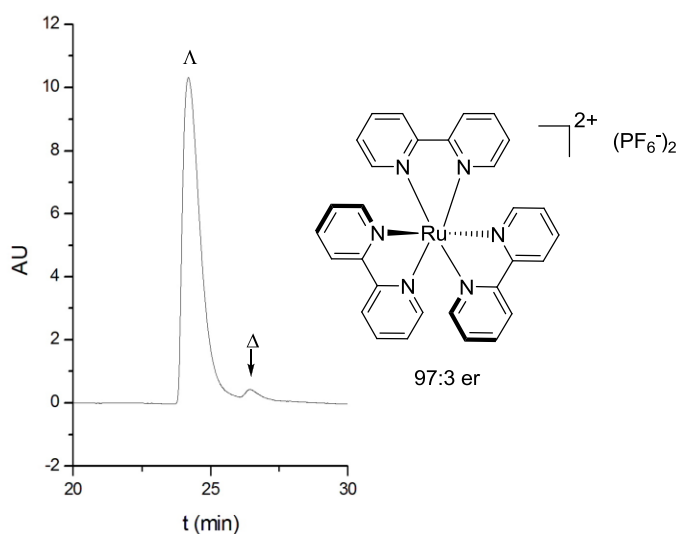


**Figure 26.** Crystal structure of  $\Lambda$ -65 for which the absolute configuration was determined. The  $\text{PF}_6$  counterion is omitted for clarity. ORTEP drawing with 50% probability thermal ellipsoids. Selected bond distances ( $\text{\AA}$ ): Ru1-C28 = 1.861(2), Ru1-N20 = 2.0520(17), Ru1-N13 = 2.0628(17), Ru1-N1 = 2.0756(18), Ru1-O1 = 2.0909(15), Ru1-N8 = 2.1223(17), O3-C28 = 1.143(3), O1-C25 = 1.271(3), O2-C25 = 1.214(3). CCDC 826723 contains additional supplementary crystallographic data which can be obtained free of charge from The Cambridge Crystallographic Data Centre via [www.ccdc.cam.ac.uk/data\\_request/cif](http://www.ccdc.cam.ac.uk/data_request/cif).

Fortunately, the CO/TFA precursor  $\Lambda$ -**65** was very stable and can be purified via column chromatography, without any decomposition. Another advantage is that it was more reactive than  $[\text{Ru}(\text{bpy})_2(\text{CO})_2]^{2+}$ , which can react with bpy, even at room temperature. Most interestingly, in the course of the ligand substitution, the metal did not lose any chiral information, yielding  $\Lambda$ - $[\text{Ru}(\text{bpy})_3](\text{PF}_6)_2$  (97: 3 er) (Scheme 44). This result was confirmed by HPLC (Figure 27).

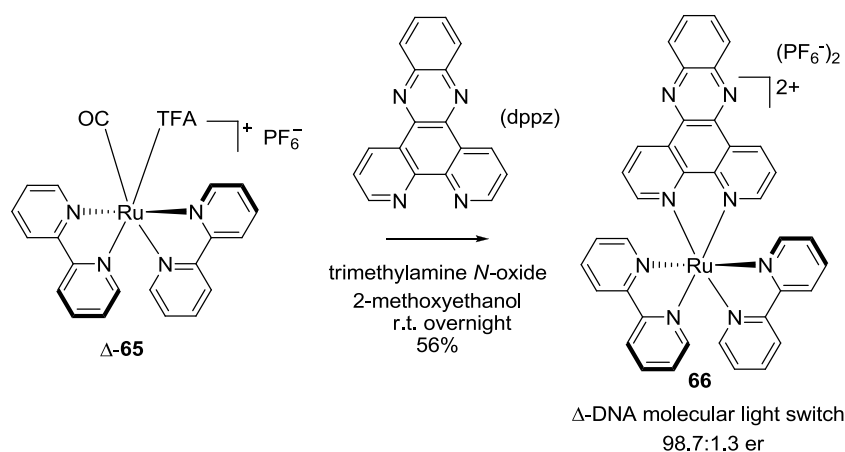


**Scheme 44.** Asymmetric synthesis of  $\Lambda$ - $[\text{Ru}(\text{bpy})_3](\text{PF}_6)_2$  through the CO/TFA precursor  $\Lambda$ -**65**.



**Figure 27.** HPLC traces of  $\Lambda$ - $[\text{Ru}(\text{bpy})_3](\text{PF}_6)_2$  which was synthesized from  $\Lambda$ -CO/TFA precursor. Conditions: Daicel Chiralcel OD-R (250 × 4 mm) HPLC column, flow rate = 0.5 mL/min, column temperature 40 °C, and UV-absorption measured at 254 nm, solvent A = 0.087% aqueous  $\text{H}_3\text{PO}_4$ , solvent B = MeCN, with a linear gradient of 4% to 10% B in 20 min.

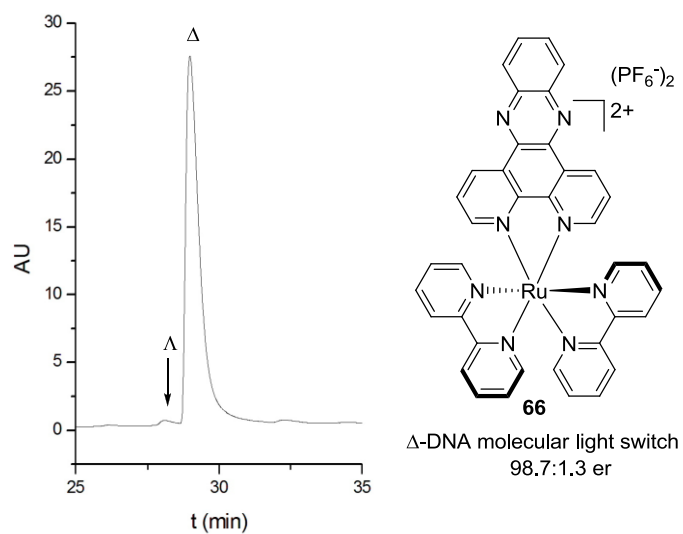
Finally, in order to see the applicability of CO/TFA precursor **65**, we used it to asymmetrically synthesize the DNA molecular light switch (Scheme 45). Because of the low solubility of the dppz (dipyrido[3,2-a:2',3'-c]phenazine) ligand in MeCN and THF, we did not successfully synthesize them via the previous methods. Thus, by using CO/TFA precursor  $\Delta$ -**65** as the starting material, the reaction can be carried out in 2-methoxyethanol, which can dissolve the dppz ligand and yield product  $\Delta$ -**66** at room temperature with 98.7: 1.3 er. The enantiomeric excess of the compound was determined via HPLC (Figure 28). The stereochemistry of  $\Delta$ -**65** was the same as that of precursor  $\Delta$ -**66** due to the configuration retention in the substituted reaction, which was confirmed in Scheme 39.



**Scheme 45.** Asymmetric synthesis of DNA molecular light switch.

In conclusion, we discovered a new auxiliary (**ASA**) that was very easy to synthesize. From commercially available Ellman's sulfinamide, we need only a single-step synthesis. The **ASA** auxiliary directed the asymmetrical synthesis nicely. After this, we developed a new method for obtaining enantiopure metal complex from CO/TFA precursor **65** in mild conditions. Finally, this method was applied in the synthesis of the DNA molecular light switch, creating a product with a high enantiopurity.

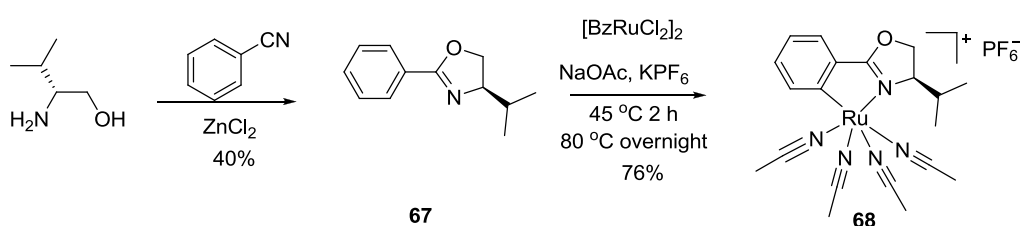




**Figure 28.** Enantioselective synthesis of Barton's "DNA molecular light switch",<sup>50</sup> ruthenium complex. Shown is the chiral HPLC trace of the synthesized complex  $\Delta$ -[Ru(bpy)<sub>2</sub>(dppz)](PF<sub>6</sub>)<sub>2</sub>. Conditions: Daicel Chiralcel OD-R (250 × 4 mm) HPLC column, flow rate = 0.5 mL/min, column temperature 40 °C, and UV-absorption measured at 254 nm, solvent A = 0.087% aqueous H<sub>3</sub>PO<sub>4</sub>, solvent B = MeCN, with a linear gradient of 4% to 10% B in 30 min.

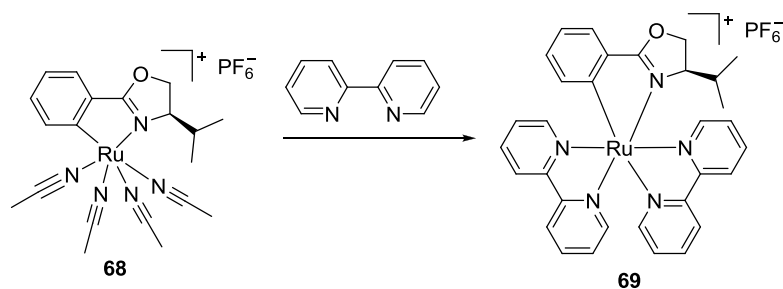
### 3.1.4 Cyclometalated phenyloxazoline auxiliary system

Based on the good results come from the (*S*)-2-(4-isopropyl-4,5-dihydrooxazol-2-yl)phenol ligand, the similar compound **67** has been synthesized by the reaction with the ammonic alcohol and benzonitrile. The complex  $[(\eta^6\text{-C}_6\text{H}_6)\text{RuCl}_2]_2$  was then to react with it in the presence of  $\text{KPF}_6$  and  $\text{NaOAc}$ , yielding precursor **68** (Scheme 46)<sup>51</sup>.



**Scheme 46.** Synthesis of precursor **68**.

Compound **68** was synthesized for two reasons. Firstly, the ligand will form a five-membered ring after coordinating with metal. There should be a bigger steric hindrance between the isopropyl group and metal than the previous (*S*)-2-(4-isopropyl-4,5-dihydrooxazol-2-yl)phenol ligand. Additionally, the coordination way of C-H bond activation should make the ligand more labile so as to be removed easily. Therefore, the diastereoselectivity of the precursor **68** was tested by reacting with the bpy (Table 11).

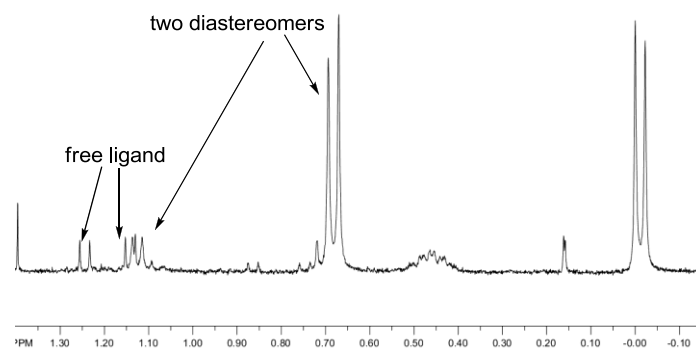


**Table 11.** Conditions dependence of diastereoselective formation of complex **69**<sup>a</sup>.

entry	solvent	time	temp.	conc.	dr <sup>b</sup>
1	PhCl	9h	80°C	5mM	3: 1
2	DMF	4.5h	80°C	5mM	3.2: 1
3	DCM	4.5h	80°C	5mM	1.5: 1
4	EtOH	4.5h	80°C	5mM	3.8: 1
5	THF	8h	80°C	5mM	3.2: 1
6	Actone	4h	80°C	5mM	3: 1

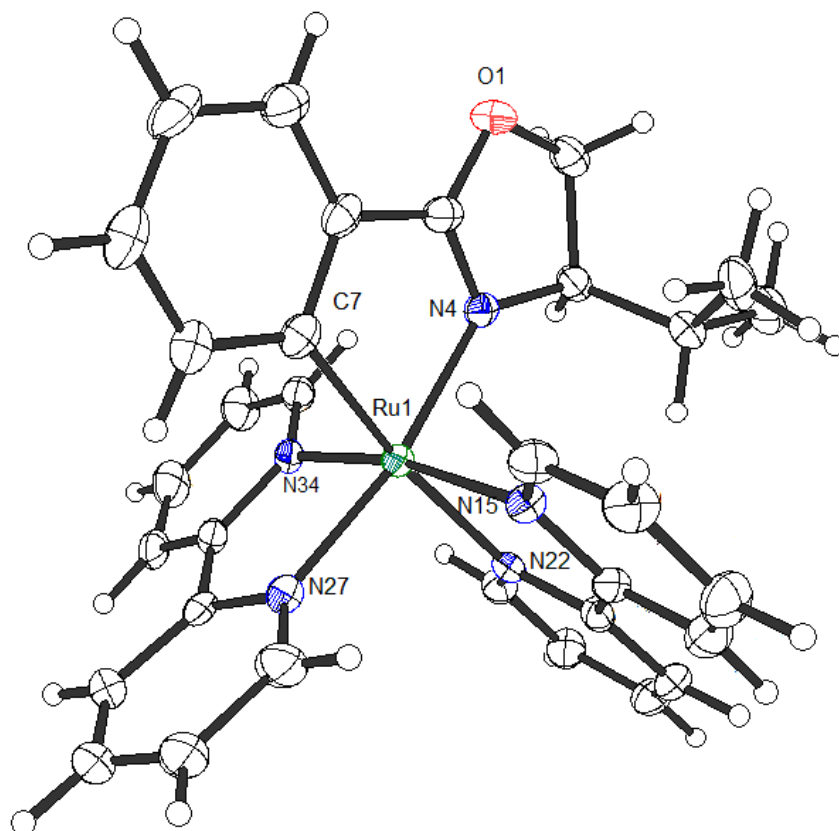
<sup>a</sup> Reaction conditions: Reaction of 5 mM **68** with 2.4 equiv of bpy at the indicated time and solvent. <sup>b</sup> Diastereomeric ratios determined by crude <sup>1</sup>H NMR. The metal configuration of the main diastereomer was not indicated here.

However, the diastereoselectivity of this reaction was not good. After analysis of the crude NMR of these reactions, we found that there was free ligand **67** in the NMR spectrum (Figure 29). That means this ligand was too liable in the asymmetric coordination reaction. This is also the main reason which leads to low ratio of the diastereoselectivity.



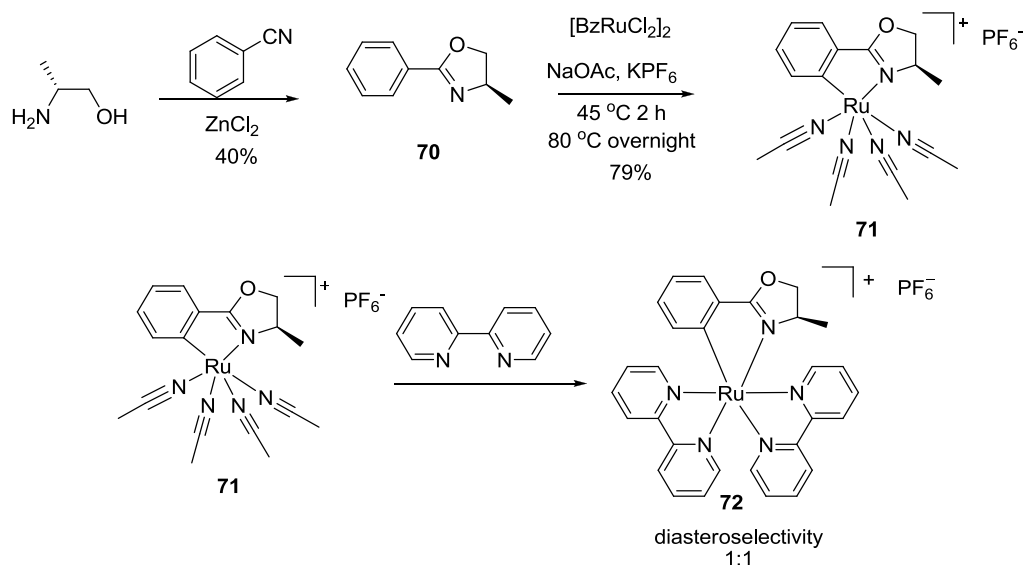
**Figure 29.** <sup>1</sup>H NMR spectrum excerpt of the diastereomeric product **69** together with free ligand **67**.

To gain some insight into the reasons for the instability, we crystallized the auxiliary-mediated complex **69** (Figure 30). And crystal structure demonstrated that the big steric hindrance even distorted the plane of the bpy, which can explain why this ligand was not stable on the ruthenium.



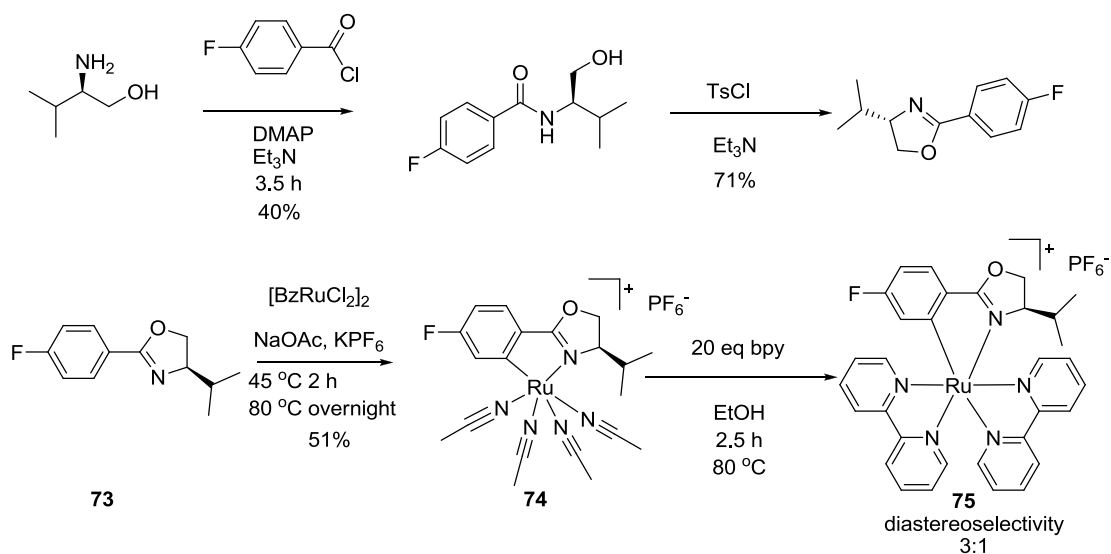
**Figure 30.** Crystal structure of complex **69** in which the absolute stereochemistry was determined. Counterion and solvent molecule are omitted for clarity. ORTEP drawing with 50% probability thermal ellipsoids. Selected bond distances ( $\text{\AA}$ ): N4-Ru1 = 2.098(3), N15-Ru1 = 2.059(3), N22-Ru1 = 2.135(3), N27-Ru1 = 2.037(3), N34-Ru1 = 2.045(3), C7-Ru1 = 2.058(3).

Next, in order to make octahedral coordination sphere less crowded, ligand **70** was synthesized by the reaction with the ammoniac alcohol and benzonitrile. This time, precursor **71** became very stable when it reacted with 3 eq of bpy in EtOH at 80 °C. But unfortunately, the reaction didn't show any diastereoselectivity, which provide complex **72** with 1: 1 dr (Scheme 47).



**Scheme 47.** Diastereoselectivity was directed by precursor **71**.

At last, precursor **74** which was more stable and together with the ability of the stereocontrol was synthesized (Scheme 48). But this system still had some problems. Firstly, even precursor **74** became more stable than precursor **71**, there were still some ligands decomposing from the ruthenium. Secondly, comparing with precursor **71**, the reaction was carried out very slowly. At last, the ratio of diastereoselectivity didn't increase by using precursor **74**, which provided complex **75** with 3: 1 dr after screening different conditions.



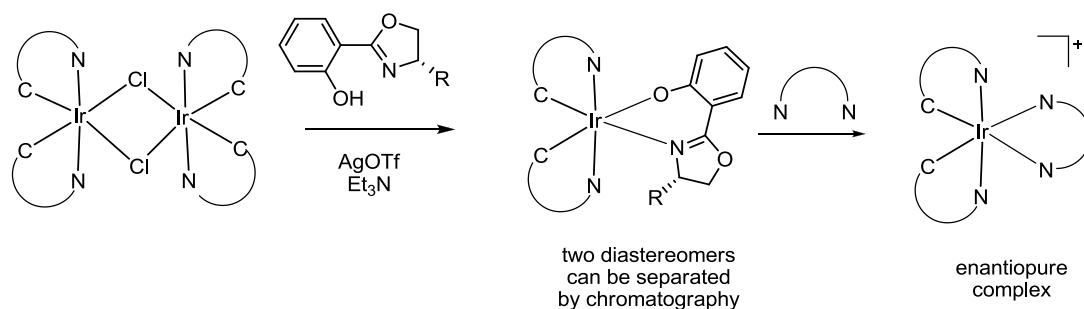
**Scheme 48.** Asymmetric synthesis of compound **75** by using the precursor **74**.

In conclusion, we modified the (*S*)-2-(4-isopropyl-4,5-dihydrooxazol -2-yl)phenol ligand to 4-isopropyl-2-phenyl-4,5-dihydrooxazole ligand expecting the good result owing to the more crowded octahedral coordination sphere. But the large internal steric hindrance together with the unstable coordination way of C-H bond activation afforded worse result than the pervious system. Then ligand **70** and **73** were synthesized, but still didn't direct the asymmetric coordination chemistry nicely.

## 3.2 Development of octahedral chiral-at-metal complexes for asymmetric catalysis

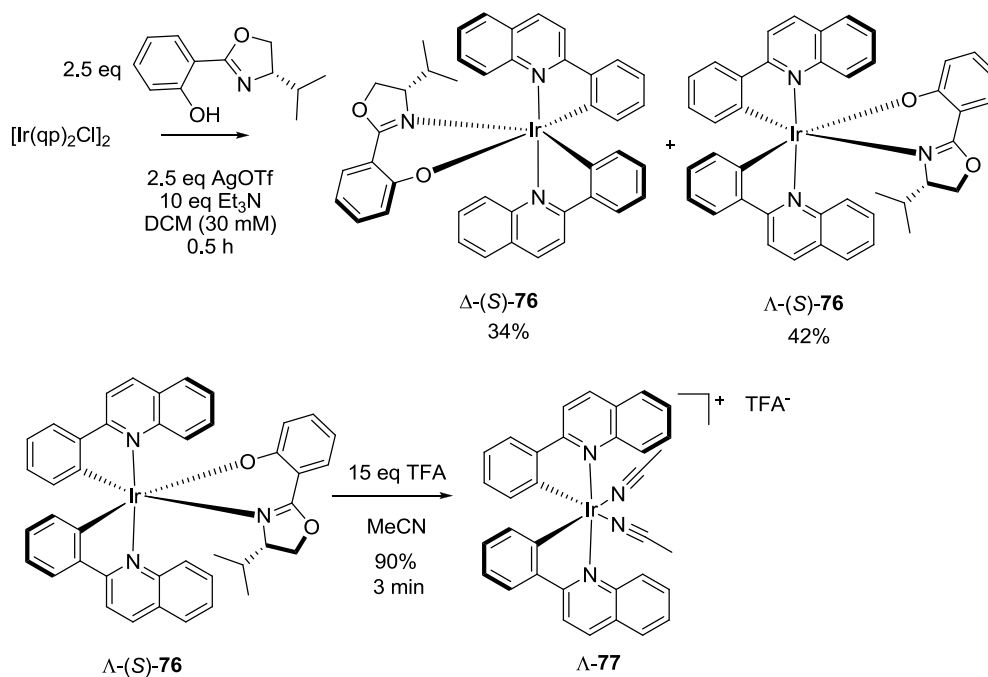
### 3.2.1 Approach

Although we can synthesize the octahedral ruthenium metal complexes with enantiopure by using the previous methods, easy racemization<sup>52-54</sup> of ruthenium will cause a negative effect if used as a catalyst. Fortunately, an alternative method for the resolution of the iridium dimer was found in our lab (Scheme 49). In this method, chiral salicyloxazoline was used first as the auxiliary to coordinate the iridium to form two diastereomers, which can be separated by column chromatography. Then, the salicyloxazoline ligand was easily substituted with the retained metal configuration<sup>55</sup>.



**Scheme 49.** Method for resolution of Ir-dimer.

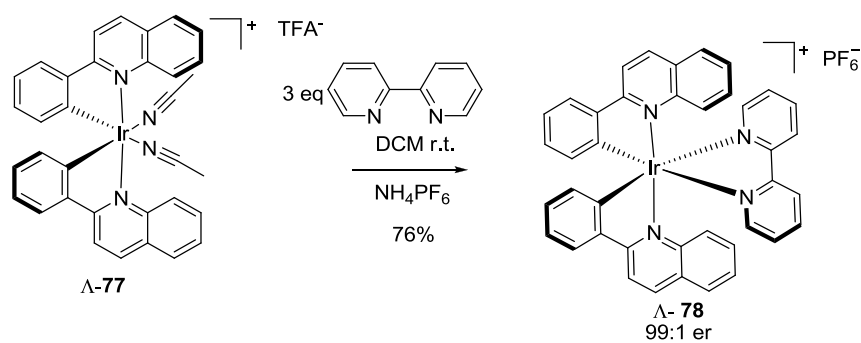
For example, by using this method, we synthesized the precursor complexes,  $\Lambda$ -(*S*)-**76** and  $\Delta$ -(*S*)-**76**, which were resolved from the  $[\text{Ir}(\text{qp})_2\text{Cl}]_2$  (qp = 2-phenylquinoline) dimer (Scheme 50) by column chromatography. The first fraction of complex **76** to emerge from the column was a  $\Lambda$ -configuration and the second fraction was a  $\Delta$ -configuration. Then the  $\Lambda$ -**77** was synthesized by removing the salicyloxazoline ligand in the presence of TFA in MeCN. In this chapter, the  $\Lambda$ -**77** complex was an important precursor for catalyst synthesis.



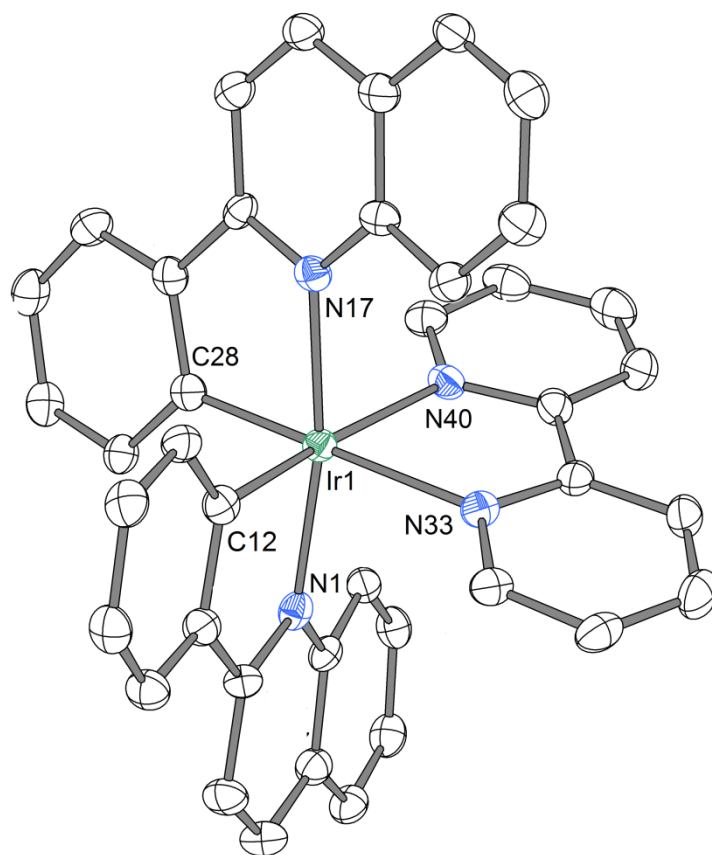
**Scheme 50.** Synthesis of precursor  $\Delta$ -77.

The absolute metal centered configuration of  $\Lambda$ -(S)-76 was verified by two aspects. First, it was confirmed by the crystal structure of the  $\Lambda$ -[Ir(bpy)(qp)<sub>2</sub>](PF<sub>6</sub>) (qp = 2-phenylquinoline) (78) (Figure 31), which was formed in the reaction with  $\Lambda$ -(S)-76. Second, the literature published by Chepelin et al. demonstrated that the configuration of the iridium center was retained during the substitution reaction<sup>55</sup>. The absolute stereochemistry of  $\Delta$ -(S)-76 was verified by the CD spectrum after comparing it with the  $\Lambda$ -(S)-76. Additionally, in order to determine the enantiopurity of the precursor  $\Delta$ -77, we used it to react with 2,2'-bipyridine to afford complex 78 (Scheme 51). The HPLC trace of complex 78 reflected the high enantiopurity of  $\Delta$ -77 (Figure 32). The stereochemistry of  $\Delta$ -77 was relative to the starting material  $\Lambda$ -(S)-76.

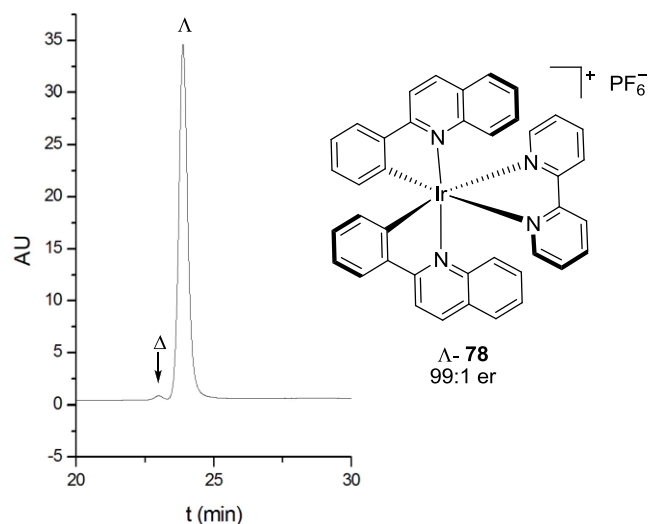




**Scheme 51.** Test enantiopurity of precursor  $\Delta$ -77.

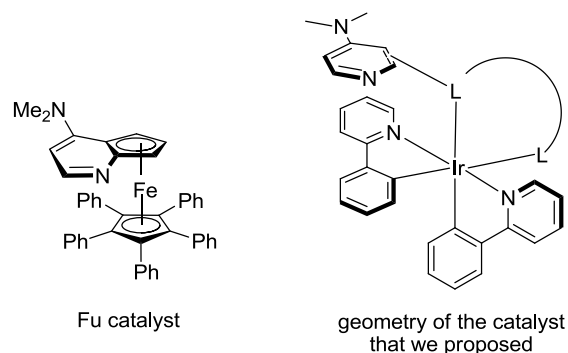


**Figure 31.** Crystal structure of complex **78** in which the absolute stereochemistry was determined. Counterion and solvent molecule are omitted for clarity. ORTEP drawing with 50% probability thermal ellipsoids. Selected bond distances ( $\text{\AA}$ ): C28-Ir1 = 1.995(4), N1-Ir1 = 2.092(3), N17-Ir1 = 2.102(3), N33-Ir1 = 2.163(3), N40-Ir1 = 2.180(2), C12-Ir1 = 2.010(3).



**Figure 32.** Shown is the chiral HPLC trace of the synthesized complex  $\Delta$ -78. Conditions: Chiralpak IA (250  $\times$  4 mm) HPLC column on an Agilent 1200 Series HPLC System. The flow rate was 0.5 mL/min, the column temperature 40  $^{\circ}$ C, and UV-absorption was measured at 254 nm. Solvent A = 0.1% TFA, solvent B = MeCN, with a linear gradient of 45% to 60% B in 20 min.

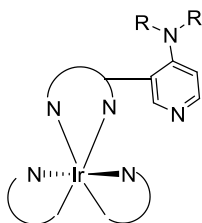
With the method of obtaining the enantiopure octahedral iridium complexes, we decided to focus on developing a chiral DMAP catalyst, which was based on the enantiopure Ir complex. This idea came from the Fu-catalyst<sup>7,56-67</sup> that resolves (*rac*)-alcohol very well (Scheme 1). By observing the geometry of the Fu-catalyst, we recognized that the key point of this asymmetric induction involved the bottom of the DMAP being blocked by the phenyl group; also, that this can be achieved using our polypyridyl ligand if the DMAP group is placed in the correct position around the metal sphere (Figure 33).



**Figure 33.** Similar structure between the Fu catalyst and the proposed catalyst.

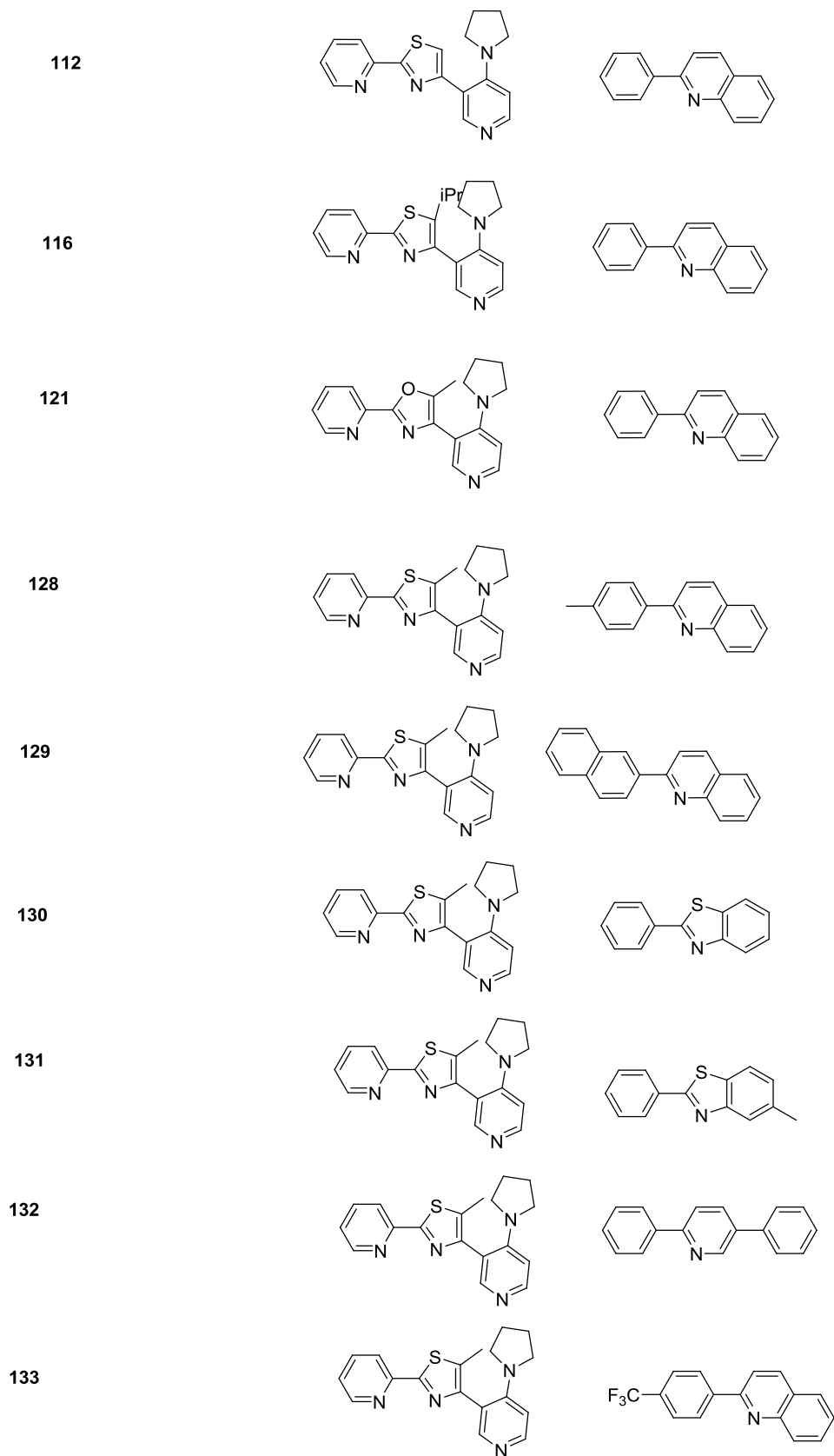
### 3.2.2 Design, synthesis and evaluation of DMAP-iridium complexes

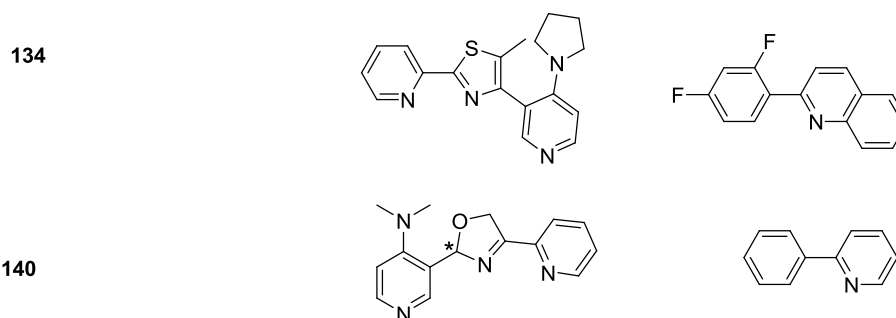
When we observed the structure of the DMAP-iridium complex in Figure 33, we determined two directions for its modification. First, a bidentate ligand that contains the DMAP segment could be carefully designed. Second, the 2-phenylpyridine could be changed to a different bidentate ligand. Based on this idea, 16 catalysts were invented (Table 12), which will be introduced one by one.



**Table 12.** Synthesized catalysts in this chapter <sup>a</sup>.

catalyst		
82 <sup>b</sup>		
90 <sup>c</sup>		
98		
101		
106		

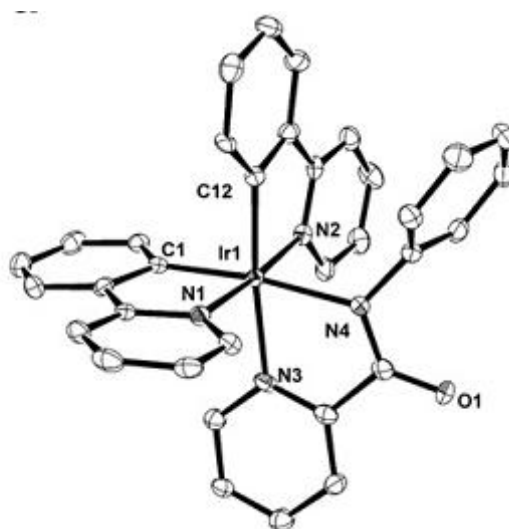




<sup>a</sup> Catalyst **82**, **90** were neuter, other catalysts were separated as PF<sub>6</sub> salt and have enantiopure iridium center. <sup>b</sup> Catalyst **82** has racemic iridium center. <sup>c</sup> Because the rotation of the DMAP segment, the two diastereomers of **90** can't be separated.

### 3.2.2.1 DMAP-picolinamide ligand

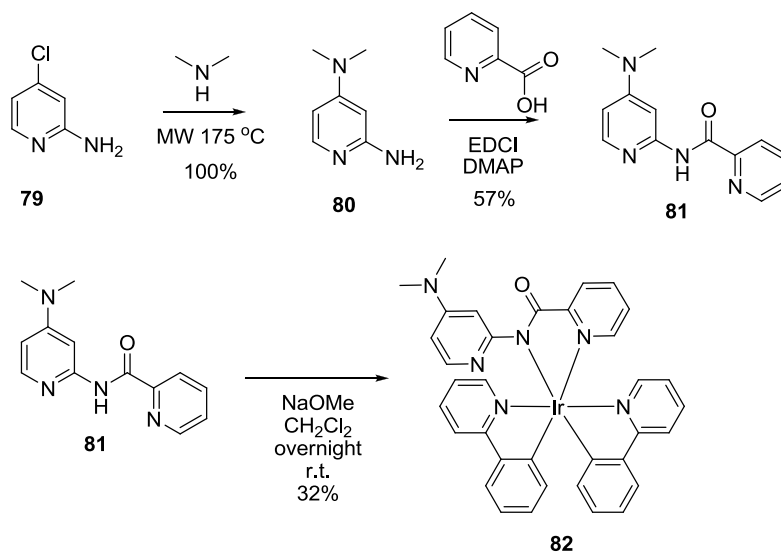
According to the crystal structure published by Chandrasekhar et al. (Figure 34)<sup>68</sup>, we see that the polypyridyl ligand blocked one side of the phenyl group, which was connected with the amide. The crystal structure also showed that the nitrogen from the amide, together with the pyridine, can coordinate the stability of the metal with a five-membered chelate.



**Figure 34.** The crystal structure which was published by Chandrasekhar et al<sup>68</sup>.

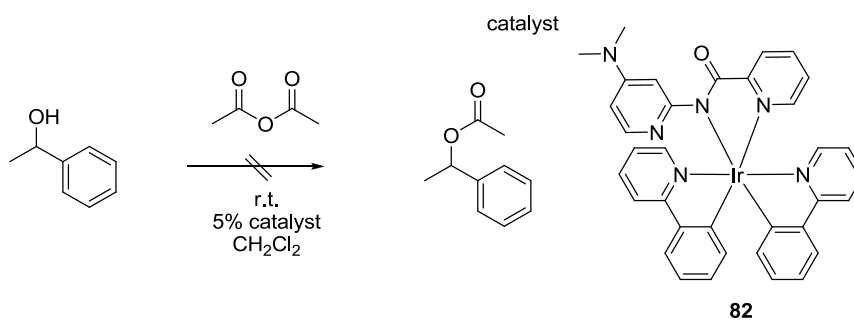
Therefore, we planned to synthesize complex **82** expecting it to be the same

geometry as in Figure 34 so as to block one side of the DMAP. In order to make this complex, compound **79** reacted with the diethylamine heated by MW, which afforded compound **80**. Then, by reacting with picolinic acid in the presence of EDCI and DMAP, the reaction provided ligand **81**. For the last step, the  $[\text{Ir}(\text{ppy})_2\text{Cl}]_2$  (ppy = 2-phenylpyridine) reacted with ligand **81** in the presence of NaOMe at room temperature, affording complex **82** with 32% yield (Scheme 52).



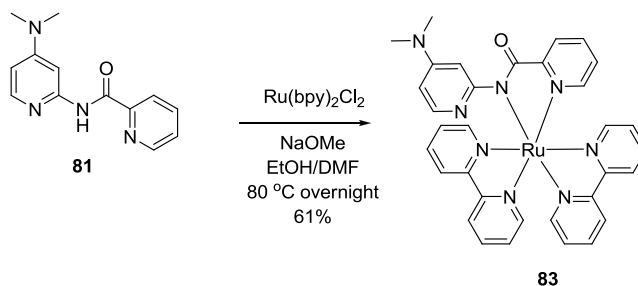
**Scheme 52.** Synthesis of complex **82**.

With complex **82** synthesized, we attempted to apply it in a catalytic reaction. For example, 1-phenylethanol and acetic anhydride were dissolved in  $\text{CH}_2\text{Cl}_2$  in the presence of a 5% complex **82** string at room temperature overnight. Surprisingly, the reaction was not carried out at all (Scheme 53).



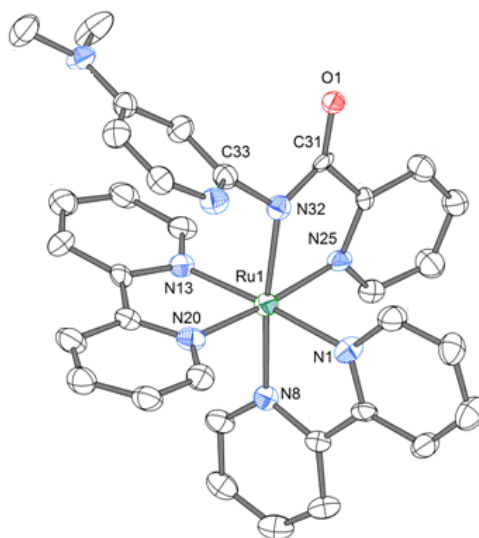
**Scheme 53.** The catalytic reaction tested by complex **82**.

Next, we changed the metal from iridium to ruthenium and synthesized catalyst **83**; however, this also did not catalyze the reaction. At the beginning, we presumed that the inactivity of the catalyst was attributed to the different ways of coordination. If ligand **81** coordinated by the DMAP and the enolated oxygen, activity may be lost (Scheme 54).



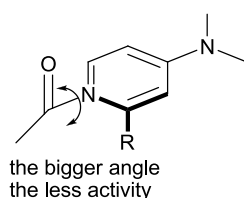
**Scheme 54.** Synthesis of the complex **83**.

In order to confirm this hypothesis, the crystal of compound **83** was obtained. From Figure 35, we noticed that ligand **81** coordinated by using the amide and pyridine to afford complex **83**, as illustrated in Scheme 54. This indicates that there should be other reasons for catalyst inactivity.



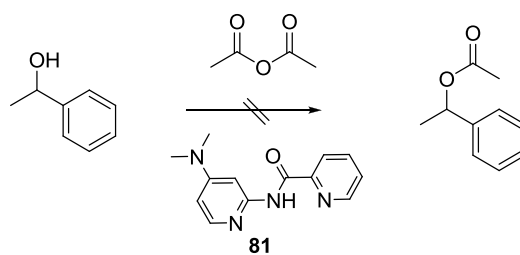
**Figure 35.** Crystal structure of complex **83** in which the absolute stereochemistry was determined. Counterion and solvent molecule are omitted for clarity. ORTEP drawing with 50% probability thermal ellipsoids. Selected bond distances (Å): C33-N32 = 1.414(11), N1-Ru1 = 2.045(8), N8-Ru1 = 2.039(7), N13-Ru1 = 2.037(8), N25-Ru1 = 2.060(8).

To gain some insight into the mechanism of the DMAP catalysis reaction, we reviewed some literatures focused on this area. We found that Zipse et al. provided a clear explanation for this phenomenon<sup>69</sup>. The acetylated DMAP was the key transition state in the catalytic circulation, and the dihedral angle between the acetyl group and the DMAP plan was also an important factor in the reaction. The literature showed that the higher the angle value the lower the activity of the catalyst (Figure 36). Therefore, substitution of the 2- and 6-positions of the DMAP will distort the acetyl group and allow for a greater dihedral angle, leading to low activity of the DMAP.



**Figure 36.** Activity influenced by dihedral angle between the acetyl group and the DMAP plane.

In order to confirm this, the free ligand **81** was used to catalyze the esterification reaction, but was not carried out at all (Scheme 55).

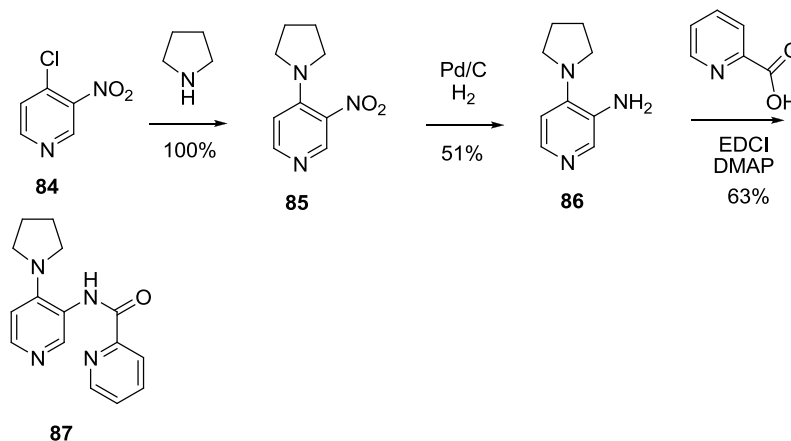


**Scheme 55.** The acyl transfer reaction which was catalyzed by free ligand **81**.

Therefore, we determined that the 2-position of the DMAP catalyst that we designed should not be substituted to keep it sufficiently active to catalyze the reaction. Subsequently, we planned to synthesize ligand **87** in which the 3-position was substituted. To obtain this compound, we used 4-chloro-3-nitropyridine (**84**) as the starting material to react with the pyrrolidine to make compound **85**. For the next step, compound **86** was obtained by palladifying the compound **85**. Finally, ligand **87**

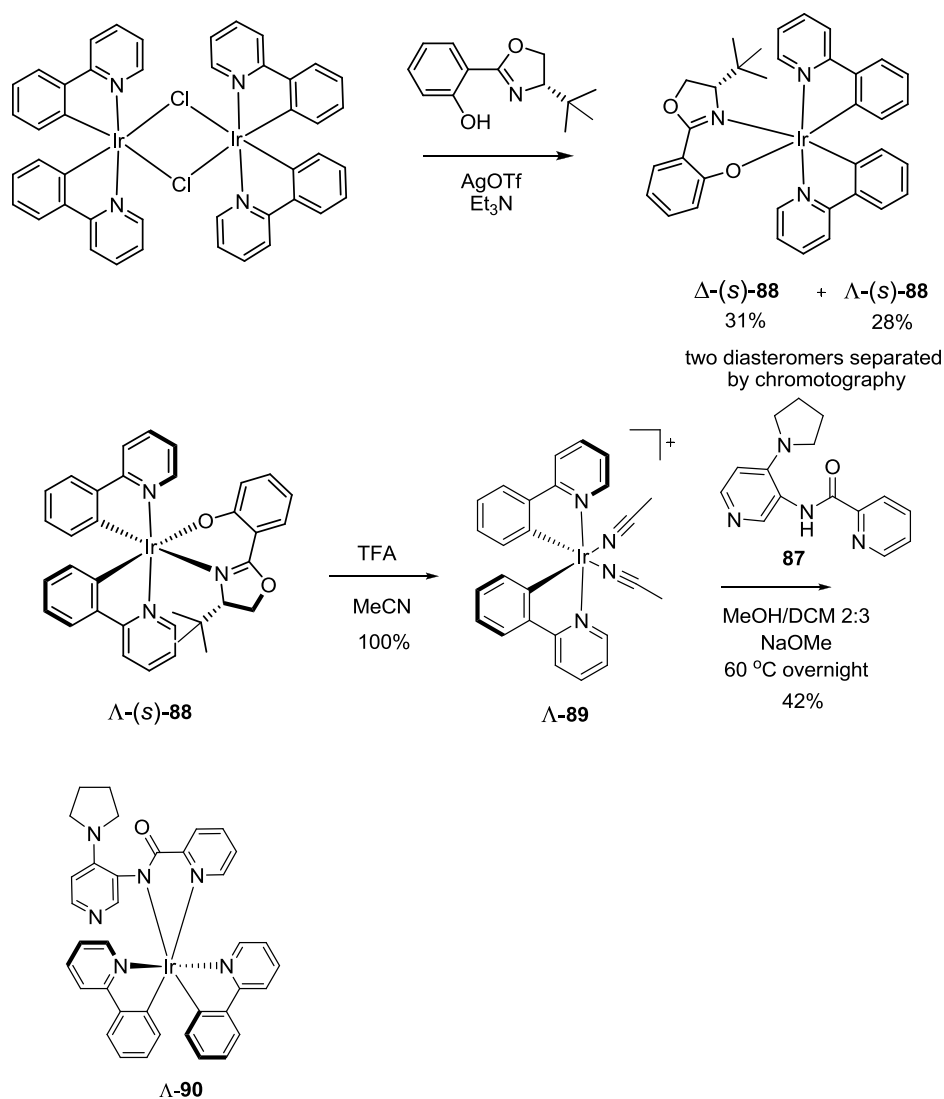


was achieved by coupling **86** with picolinic acid in the presence of EDCI and DMAP (Scheme 56).



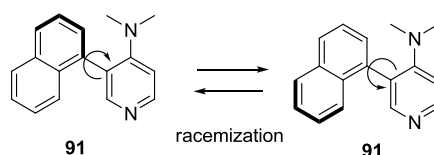
**Scheme 56.** Synthesis of ligand **87**.

After achieving the synthesis of ligand **87**, we tested its activity and found that it catalyzes the esterification reaction between the 1-phenylethanol and acetic anhydride very well. Next, we wanted to use ligand **87** to coordinate with the enantiopure Ir complex, and obtained a catalyst with an enantiopure metal center. Based on the resolution method developed in our lab, we started from the chiral-auxiliary-mediated metal complex  $\Lambda$ -(*S*)-**88**, which was obtained from resolving the  $[\text{Ir}(\text{ppy})_2\text{Cl}]_2$  (ppy = 2-phenylpyridine) dimer to synthesize complex  $\Lambda$ -**89**. This was then reacted with ligand **87** in the presence of NaOMe to obtain catalyst  $\Lambda$ -**90** (Scheme 57). The absolute configuration of the  $\Lambda$ -**90** was relative to the  $\Lambda$ -(*S*)-**88**, which was the first fraction to emerge from the column chromatography. This eluting phenomenon and the iridium configuration retained in the substitution reaction were confirmed in a manuscript by Melanie Helms in Meggers group.



**Scheme 57.** Asymmetric synthesis of catalyst  $\Lambda\text{-90}$ .

In this effort, the complex  $\Lambda\text{-90}$  catalyzed the esterification reaction; however, the catalyst's proton NMR spectrum was not clean, even after several purifications by column chromatography. Initially, we presumed that the impurity was due to decomposed residue from the catalyst as a result of an overly crowded hindrance around the metal sphere. However, after reading the literature published by Adams et al.<sup>70</sup>, we noticed that the axial chirality was easy to lose if the conformation could not adjust the rotation of the DMAP. As with Adams et al., by tracing the racemization through chiral HPLC, they found that compound **91** would lose axial chirality if it was heated slightly. This result was due to the low steric barrier of compound **91** (Scheme 58).

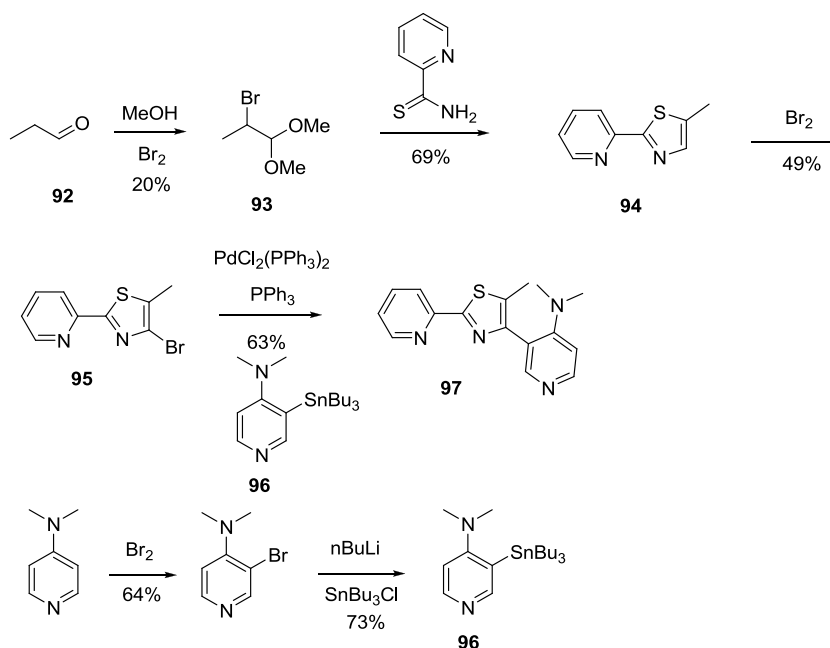


**Scheme 58.** Racemization of compound **91**.

The rotation of the DMAP in compound **90** resulted in the racemization of the axial chirality. Reflecting on the NMR spectrum, the impurity was another diastereomer.

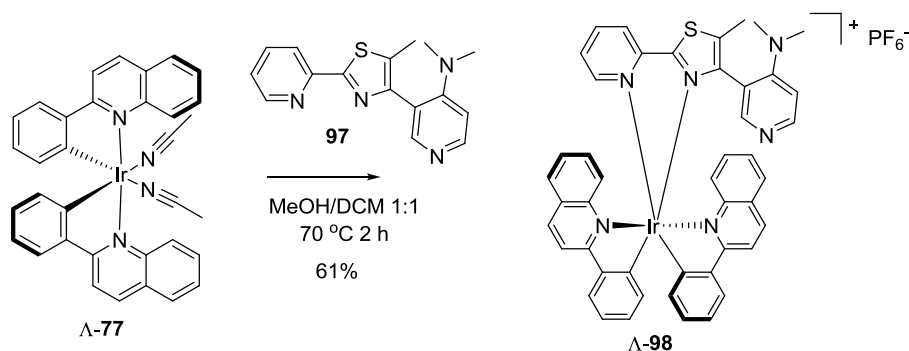
### 3.2.2.2 DMAP-pyridine-thiazole ligand

In order to restrict the rotation of the DMAP, ligand **97** was synthesized in six steps. First, propionaldehyde (**92**) reacted with bromine, affording compound **93** with a 20% yield. Then compound **94** was prepared by using pyridine-2-carbothioamide to react with compound **93**. Finally, after brominating compound **94**, one key fragment of ligand **95** was obtained. The DMAP portion was prepared by brominating the 4-position of free DMAP, followed by debromination and substitution, which afforded compound **96**. With both key fragments in place, we performed Stille coupling to obtain ligand **97** with a 63% yield (Scheme 59).



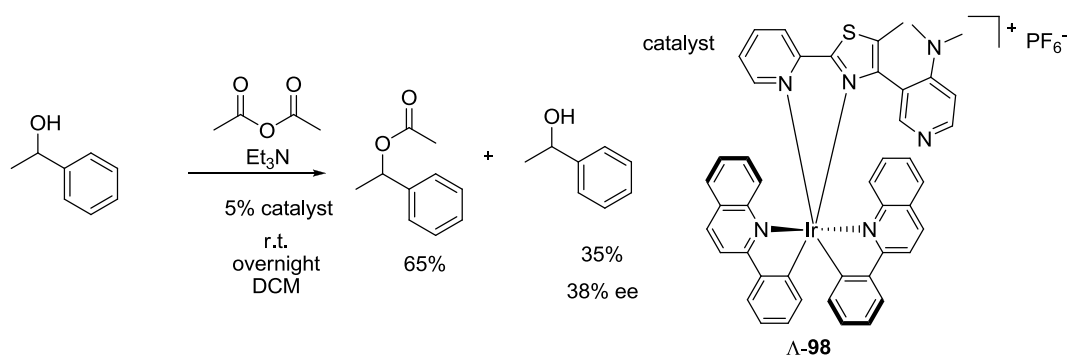
**Scheme 59.** Synthesis of bidentate ligand **97**.

Next, ligand **97** was used to react with precursor  $\Lambda$ -**77** affording the new catalyst,  $\Lambda$ -**98** (Scheme 60). Considering the metal configuration will be retained in the substitution reaction<sup>55</sup>, the catalyst  $\Lambda$ -**98**, which was formed from the precursor  $\Lambda$ -**77**, is a  $\Lambda$ -configuration.

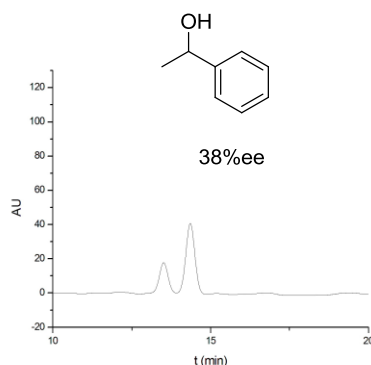


**Scheme 60.** Synthesis of catalyst  $\Lambda$ -**98**.

This catalyst was then applied in a catalytic resolution of alcohol. This time, the result showed obvious selectivity. After stirring at room temperature overnight, the remaining alcohol showed 38% ee with 65% conversion of the alcohol (Scheme 61). The enantioselectivity of this reaction was determined by HPLC, and all other catalytic resolution reactions in this chapter were determined in the same way (Figure 37).



**Scheme 61.** Kinetic resolution of racemic alcohols catalyzed by catalyst  $\Lambda$ -**98**.



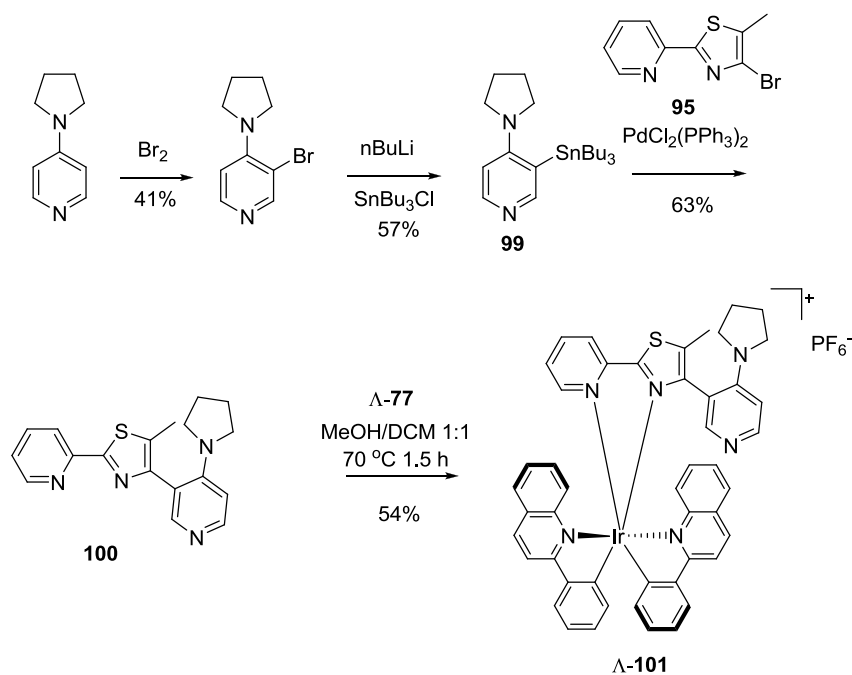
**Figure 37.** Shown is the chiral HPLC trace of remaining alcohol (1-phenylethanol) in the catalytic resolution reaction. Conditions: Chiralpak IB (0.46cm × 25cm) HPLC column on an Agilent 1200 Series HPLC System. The flow rate was 0.5 mL/min, the column temperature 40 °C, and UV-absorption was measured at 254 nm. Solvent A = iPrOH, solvent B = hexane, with 5% A in 20 min.

After achieving this promising result, we needed an accurate evaluation method. The selectivity factor is an important parameter for evaluating the kinetic resolution reaction. The formula for the selectivity factor is shown in Figure 38. A higher *s* value indicates better resolution ability.

$$\text{selectivity factor } s = \frac{K_{fast}}{K_{slow}} = \frac{\ln[(1-\text{conv})(1-\text{ee})]}{\ln[(1-\text{conv})(1+\text{ee})]}$$

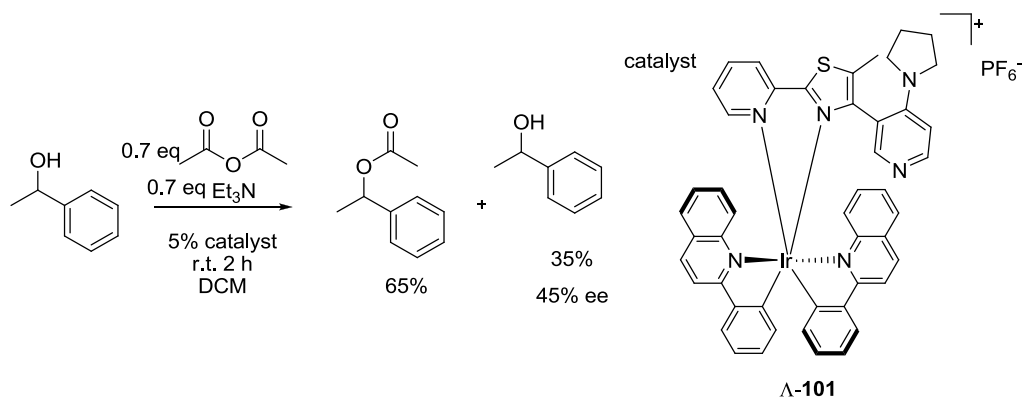
**Figure 38.** Formula for the selectivity factor<sup>71</sup>.

To obtain a more active catalyst, dimethylamine was changed with pyrrolidine on the pyridine. Then the catalyst **Λ-101** was synthesized using a similar procedure as **Λ-98** (Scheme 62).



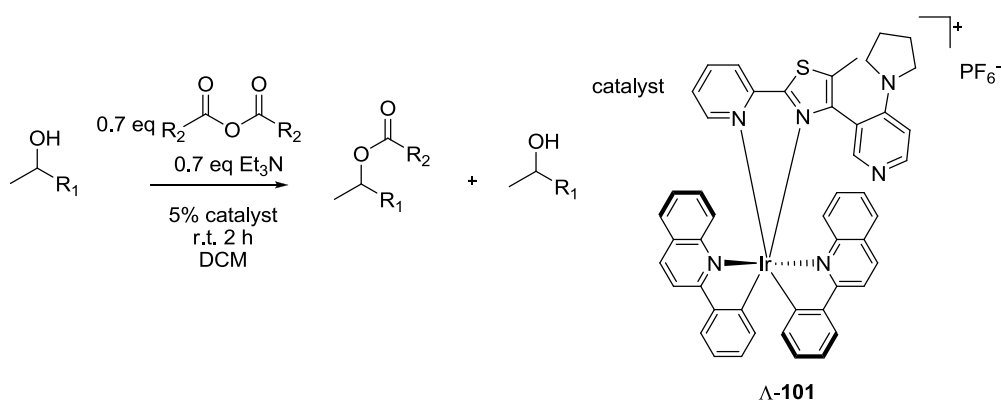
**Scheme 62.** Synthesis of complex  $\Lambda$ -101.

The catalyst  $\Lambda$ -101 was more active than the catalyst  $\Lambda$ -98. By using it, the reaction was completed in 2 hours at room temperature, affording 45% ee for the 35% remaining alcohol (Scheme 63). When this reaction was carried out at  $-30\text{ }^{\circ}\text{C}$  overnight, the selectivity factor increased from 2.4 to 3.0.



**Scheme 63.** Kinetic resolution of racemic alcohols catalyzed by chiral catalyst  $\Lambda$ -101.

In order to increase the selectivity factor of this reaction, we screened different substrates. The 1-(naphthalen-1-yl)ethanol and 1-(naphthalen-2-yl)ethanol were tested with different anhydrides. Table 13 shows the 1-(naphthalen-1-yl)ethanol with acetic anhydride providing the best result with catalyst  $\Lambda$ -101.

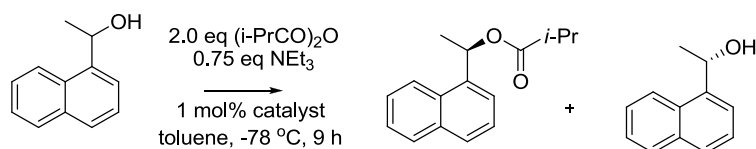
**Table 13.** Substrate screening <sup>a</sup>.

entry	R <sub>1</sub> =, R <sub>2</sub> =	remaining alcohol	ee of remaining alcohol	s
1	R <sub>1</sub> = phenyl R <sub>2</sub> = Me	35%	45%	2.4
2	R <sub>1</sub> = 2-naphthyl R <sub>2</sub> = <i>i</i> -Pr	48%	29%	2.2
3	R <sub>1</sub> = 2-naphthyl R <sub>2</sub> = Me	36%	49%	2.8
4	R <sub>1</sub> = 1-naphthyl R <sub>2</sub> = Me	35%	51%	2.9

<sup>a</sup> Reaction conditions: Reaction of 0.3 M aryl alcohol with 0.7 equiv of anhydride and 5% catalyst at room temperature in the CH<sub>2</sub>Cl<sub>2</sub> stirring for 2 hours.

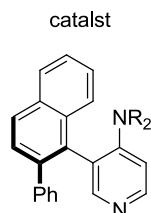
According to the literature by Spivey and co-workers, different substitutes on the 4-position of the pyridine significantly influenced the results (Table 14)<sup>72</sup>. Therefore, we planned to modify the diethylamine group on the DMAP segment.

We then attempted to synthesize complex **Δ-106**. In detail, the 3-bromo-4-chloropyridine (**102**) reacted with *N,N*-diethylformamide and Et<sub>2</sub>NH to afford compound **103**. This was followed by debromination and substitution, which provided the tin compound **104**. After Stille coupling, ligand **105** was obtained with a 55% yield. Finally, by reacting with the precursor **Δ-77**, complex **Δ-106** was formed (Scheme 64).

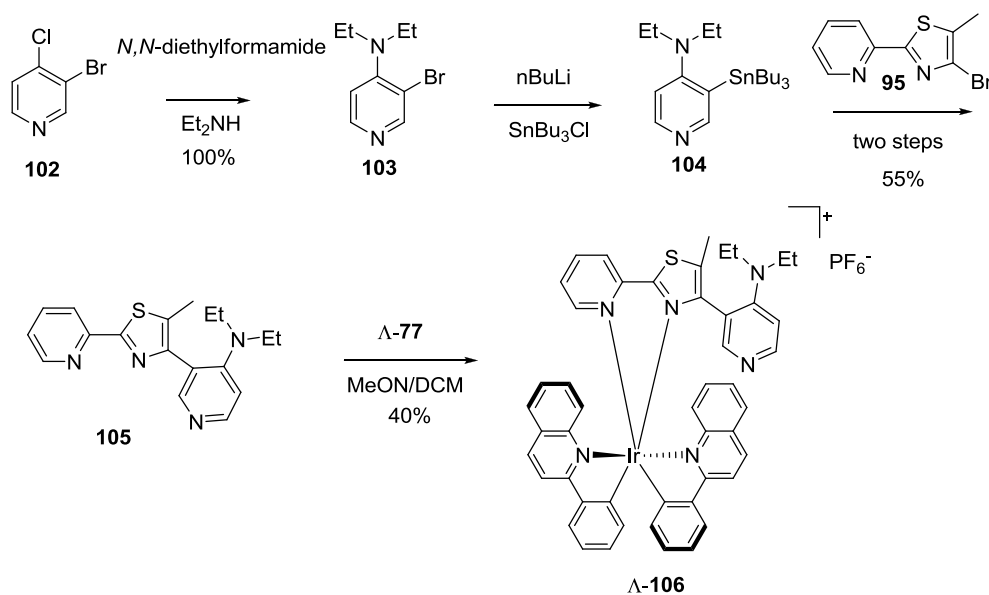


**Table 14.** Influence of the substitution of the R group on the DMAP segment <sup>a</sup>

catalyst	NR <sub>2</sub> =	Selectivity s
1	NMe <sub>2</sub>	10
2	NEt <sub>2</sub>	16
3	N(CH <sub>2</sub> ) <sub>4</sub>	3.5
4	NBu <sub>2</sub>	31
5	NPent <sub>2</sub>	30
6	NHex <sub>2</sub>	39



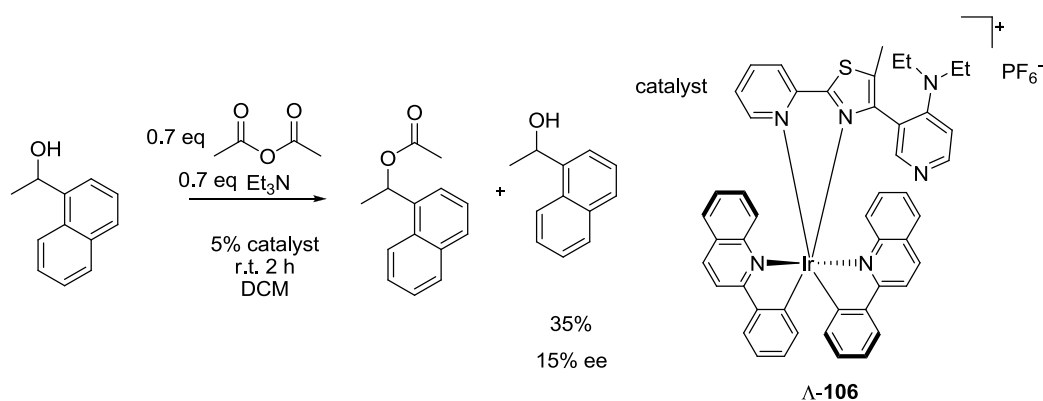
<sup>a</sup> Work published by Spivey et al<sup>72</sup>.



**Scheme 64.** Synthesis of complex  $\Lambda$ -106.

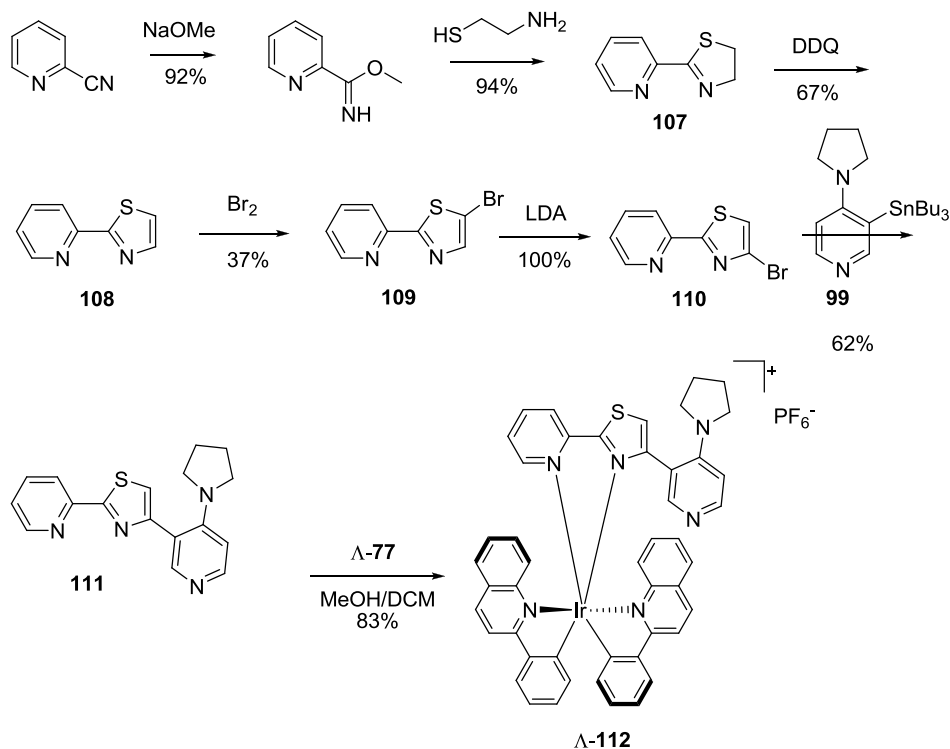
However, catalyst  $\Lambda$ -106 still did not show satisfactory enantioselectivity. After stirring at room temperature for 2 hours in the presence of 5% complex  $\Lambda$ -106, 1.3 of the selectivity factor was achieved for a resolution of (*rac*)-1-(naphthalen-2-yl)ethanol (Scheme 65).





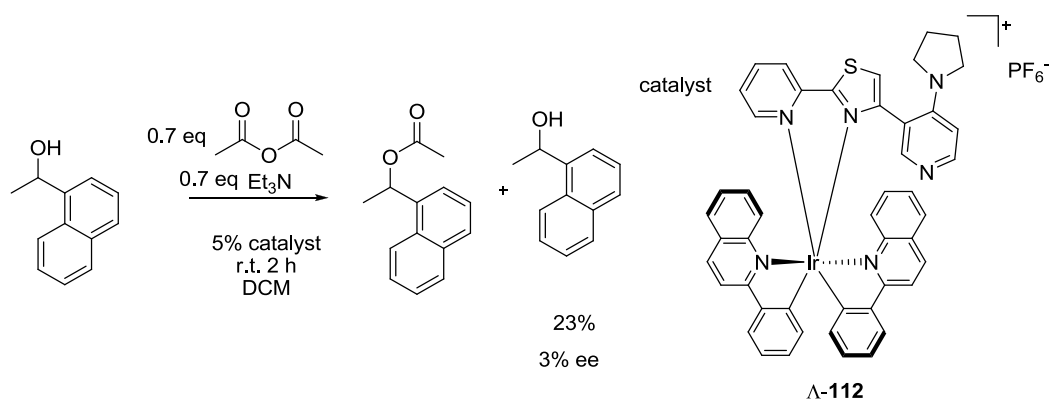
**Scheme 65.** Kinetic resolution of racemic alcohols catalyzed by chiral catalyst  $\Delta$ -106.

This negative result revealed that modifying the DMAP was not a suitable direction. To gain further insight into this system, we decided to modify the thiazole in the bidentate ligand. First, the influence of the methyl group on the thiazole was tested. Then, ligand **111** without the methyl group was synthesized (Scheme 66). In this synthesis, compound **107** was synthesized by the published method: picolinonitrile was treated with sodium methanolate following by cyclization with 2-aminoethanethiol, affording compound **107** with a high yield<sup>73</sup>. Then, the dihydrothiazole **107** was oxidized by DDQ providing 2-(pyridin-2-yl)thiazole **108**. Next, after brominating, compound **109** was obtained. To allow for bromo substitution at the 5-position of the thiazole, the halogen dance reaction was carried out, which provided compound **110** with a quant yield. Finally, compound **111** was achieved by coupling compound **110** and **99**. As with the previous work, with ligand **111** in place, the catalyst  $\Delta$ -**112** was synthesized.



**Scheme 66.** Synthesis of catalyst  $\Lambda$ -112.

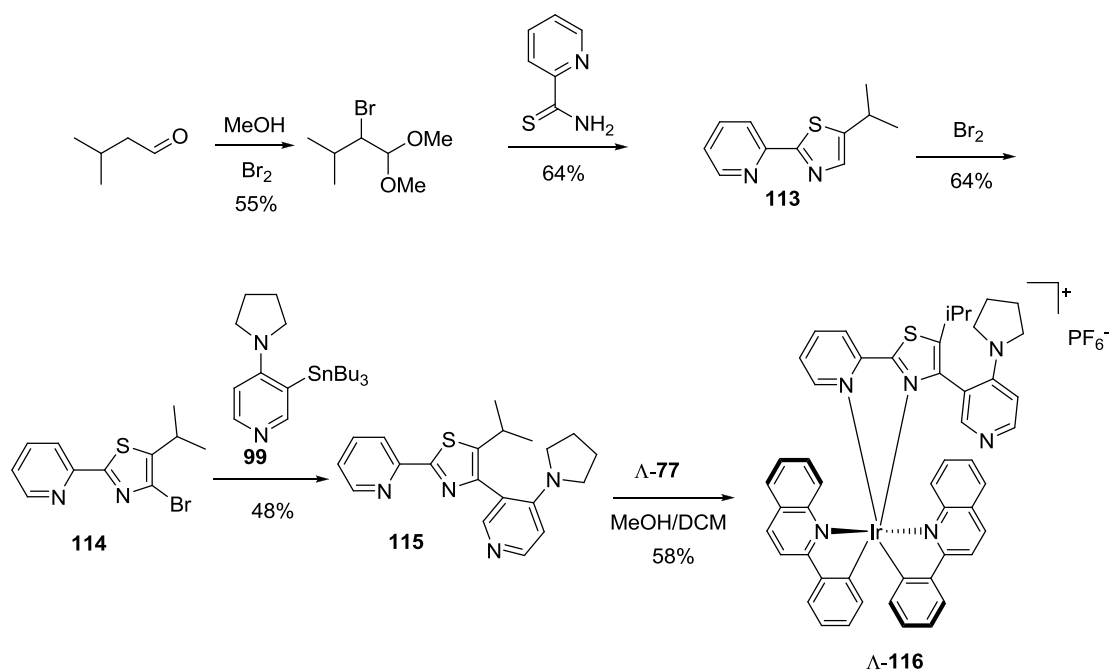
Surprisingly, the catalyst  $\Lambda$ -112 nearly did not show any enantioselectivity in the asymmetric acyl transfer catalysis (Scheme 67).



**Scheme 67.** Kinetic resolution of racemic alcohols catalyzed by chiral catalyst  $\Lambda$ -112.

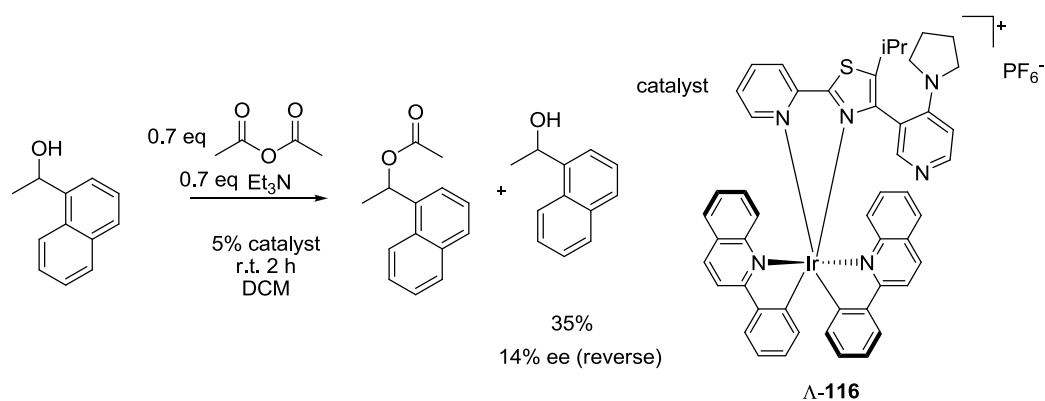
From our analysis, we presumed that the free rotation of the DMAP led to this negative result due to the blocking hindrance missing from the methyl group. Therefore, the methyl group was changed to isopropyl. In order to synthesize this catalyst, 3-methylbutanal was used as the starting material, and following the same procedure as ligand **95**, ligand **114** was obtained. For the next step, the targeting

ligand **115** was synthesized by coupling with the tin compound **99**. Then, catalyst  $\Lambda$ -**116** was obtained by reacting with the precursor  $\Lambda$ -**77** (Scheme 68).



**Scheme 68.** Synthesis of catalyst  $\Lambda$ -**116**.

However, catalyst  $\Lambda$ -**116** still did not provide a satisfactory result. Additionally, the selectivity of the (*R*) and (*S*) of the alcohol reversed compared with previous results (Scheme 69).

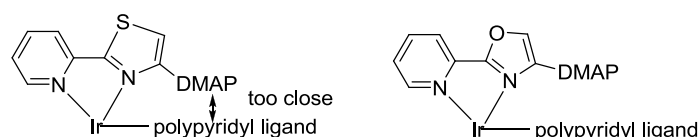


**Scheme 69.** Kinetic resolution of racemic alcohols catalyzed by chiral catalyst  $\Lambda$ -**116**.

After using the molecular model to simulate the structure of the compound  $\Lambda$ -**116**, we found the reason of the worse and reverse selectivity was that the isopropyl group made the less difference between two sides of the DMAP. Therefore, the methyl group

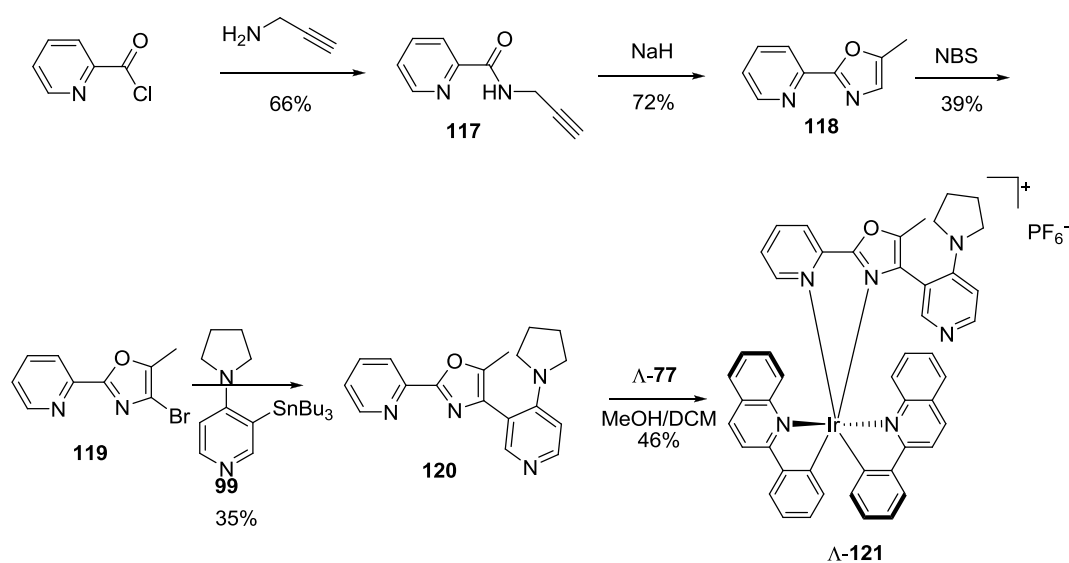
will be kept on the thiazole ring in the future.

Considering that a carbon-sulfur bond is longer than a carbon-oxygen bond, we presumed that the DMAP may be too close in proximity on the planned polypyridyl ligand, building an unfavorable structure compared with oxygen on the ligand (Figure 39).



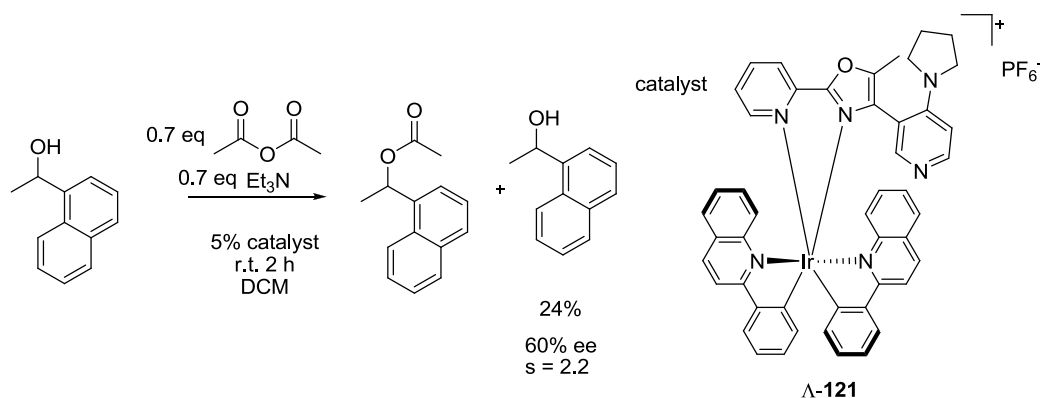
**Figure 39.** Proposed the influence of the sulfur on the ligand.

From this concept, catalyst  $\Lambda$ -**121** was synthesized using picolinoyl chloride as the starting material, which reacted with prop-2-yn-1-amine to afford compound **117** with a 66% yield. Then, the cyclization reaction was completed in the presence of compound NaH to give 2-pyridine oxazole **118**. Next, by brominating compound **118**, followed by coupling with the tin compound **99**, we obtained ligand **120** with the oxygen on the five-membered ring. Finally, by reacting with the precursor  $\Lambda$ -**77**, the complex  $\Lambda$ -**121** was obtained with a 46% yield (Scheme 70).



**Scheme 70.** Synthesis of complex  $\Lambda$ -**121**.

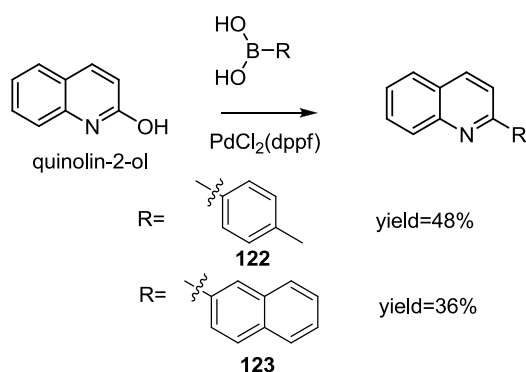
Afterwards, we tested the selectivity of the catalyst  $\Lambda$ -**121**, and it returned a similar result as with the catalyst  $\Lambda$ -**101** where sulfur was included. This result demonstrated that this was not the correct modification direction (Scheme 71).



**Scheme 71.** Kinetic resolution of racemic alcohols catalyzed by chiral catalyst  $\Lambda$ -**121**.

### 3.2.2.3 Polypyridyl ligand

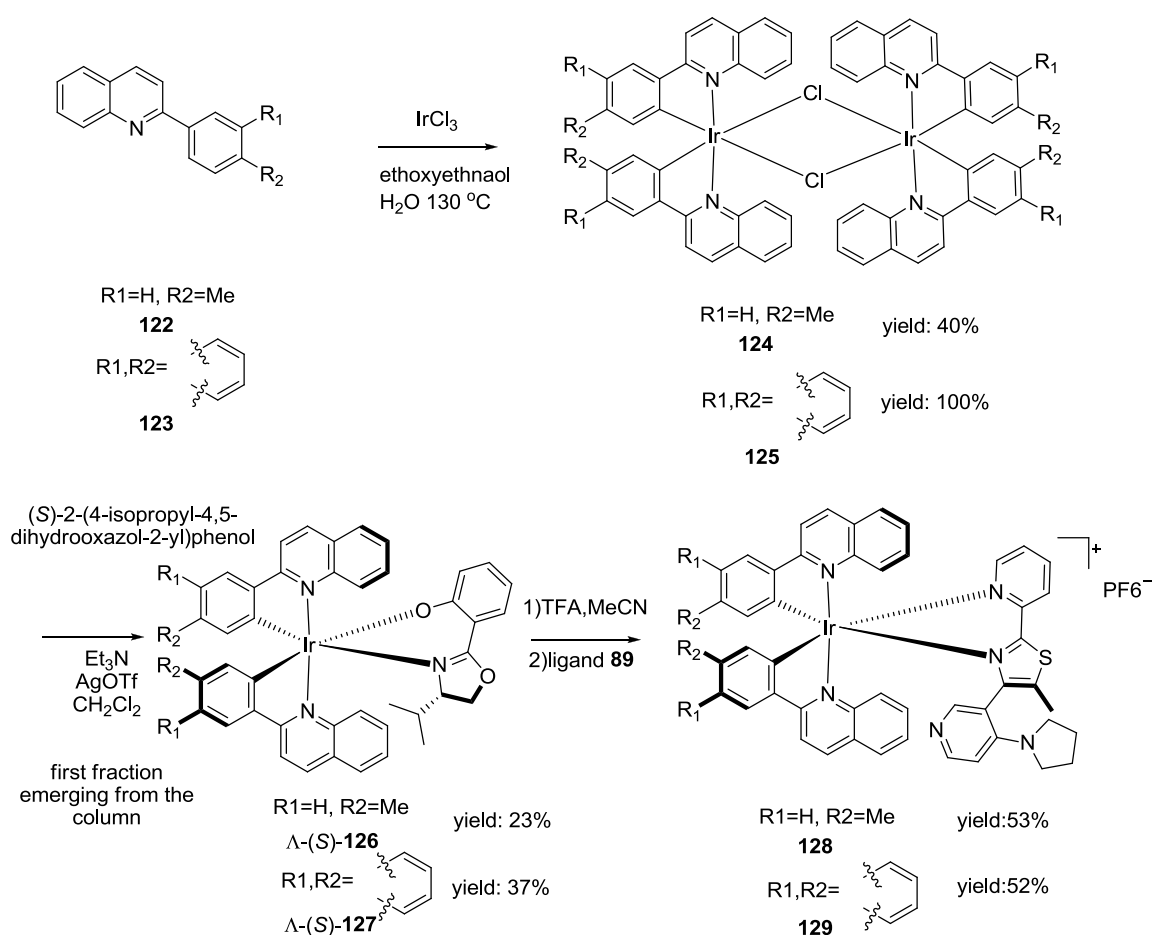
After modifying the DMAP-pyridine-thiazole ligand, we found that ligand **100** provided the best result. Based on this ligand, we used a larger polypyridyl ligand to block one side of the DMAP expecting it to induce better chiral information. Therefore, ligands **122** and **123** were synthesized using the published method<sup>74</sup>. The quinolin-2-ol reacted with boric acid in the presence of catalyst  $\text{PdCl}_2(\text{dppf})$ , affording different bidentate ligands (Scheme 72).



**Scheme 72.** Synthesis of ligands.

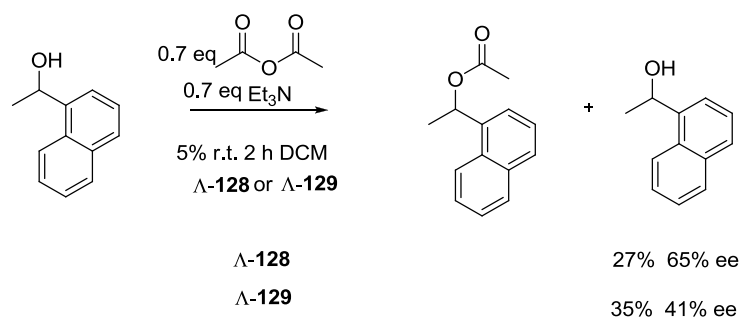
With the two ligands in place, the Ir-dimer **124**, **125** were synthesized. Following the same procedure as the precursor  $\Lambda$ -**76**, after resolving the dimer, the precursors,

$\Lambda$ -**126** and  $\Lambda$ -**127**, were obtained. Because of the similar structure of the polypyridyl ligand with  $\Lambda$ -**76**, we proposed that the first fraction emerging from the column in the resolved dimer was a  $\Lambda$ -configuration. After substituting with ligand **100**, the catalysts  $\Lambda$ -**128** and  $\Lambda$ -**129** were obtained (Scheme 73).



**Scheme 73.** Synthesis of modified catalysts  $\Lambda$ -**128**,  $\Lambda$ -**129**.

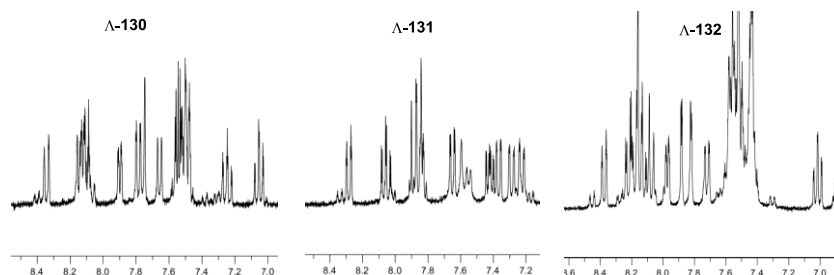
Unfortunately, when we applied these two catalysts in the asymmetric acyl transfer catalysis, the result also demonstrated that this was not the correct direction to modify the catalysts owing to only affording 2.9 and 2.2 selectivity factors, respectively (Scheme 74).



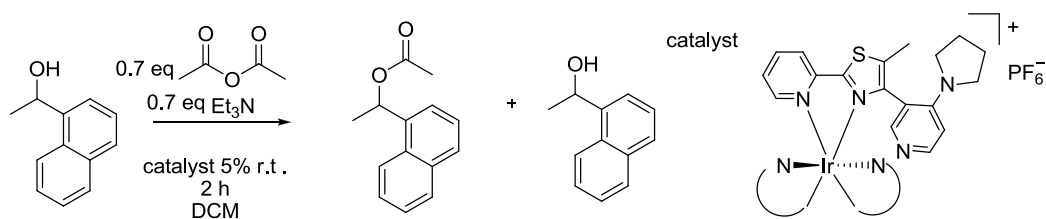
**Scheme 74.** Kinetic resolution of racemic alcohols catalyzed by chiral catalysts  $\Lambda$ -128,  $\Lambda$ -129.

After all previous works, we reviewed the influences that led to low enantioselectivity. When we rechecked the proton NMR of these catalysts, we found that impurities were regularly mixing with the catalysts. Additionally, there was slight yellow residue appearing in the alcohol in less polar fraction during the purification by column chromatography. Both of these phenomena revealed the catalyst's instability, indicating that achieving more stability was our target.


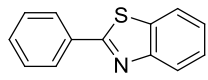
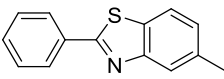
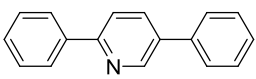
From analysis of the crystal structure of compound **78** (Figure 31), we noticed that quinoline greatly hindered the bpy ligand, and this hindrance was strong enough to distort the plane of the bpy. Therefore, we presumed that this was a key parameter to the catalyst's instability. Starting from this point, catalysts  $\Lambda$ -130,  $\Lambda$ -131, and  $\Lambda$ -132 were synthesized following the same procedure of catalysts **128** and **129**. This time, the catalysts were more stable, but another issue developed. This less hindered design allowed the DMAP to lose axial chirality and form two diastereomers, which cannot be separated. We can clearly see two sets of signals in the NMR spectra (Figure 40), indicating that we will not achieve satisfactory results using both diastereomers (Table 15).



**Figure 40.**  $^1\text{H}$  NMR spectra excerpts of catalysts  $\Lambda$ -130,  $\Lambda$ -131, and  $\Lambda$ -132 showing two set of signals.



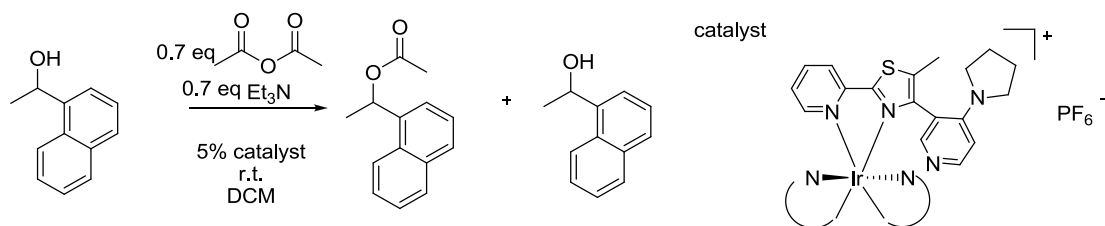
**Table 15.** Kinetic resolution of racemic alcohols catalyzed by chiral catalysts  $\Lambda$ -**130**,  $\Lambda$ -**131** and  $\Lambda$ -**132**<sup>a</sup>.

Catalyst		yield of remaining alcohol	ee of remaining alcohol	s
$\Lambda$ - <b>130</b> <sup>b</sup>		34%	40%	2.1
$\Lambda$ - <b>131</b> <sup>b</sup>		43%	30%	2.0
$\Lambda$ - <b>132</b> <sup>b</sup>		35%	6%	1.1

<sup>a</sup> Reaction conditions: Reaction of 0.3 M 1-(naphthalen-1-yl)ethanol with 0.7 equiv of acetic anhydride and 5% catalyst at room temperature in the  $\text{CH}_2\text{Cl}_2$  was stirred for 2 hours. <sup>b</sup> The absolute configuration of the catalysts  $\Lambda$ -**130**,  $\Lambda$ -**131** and  $\Lambda$ -**132** were relative to catalyst  $\Lambda$ -**100**. Because the similar structure of the polypyridyl ligand with  $\Lambda$ -**76**, we proposed the first fraction emerging from the column in the dimer resolving was  $\Lambda$ -configuration. They were synthesized following the same procedure of the catalyst **128** and **129**.

Expecting both of high stability and axial chirality retention, we changed the strategy by using a fluorine substitution to stabilize the catalyst. Based on this, the catalysts  $\Lambda$ -**133** and  $\Lambda$ -**134** were synthesized and applied to the asymmetric acyl transfer catalysis. The results revealed that increasing the stability of the catalyst can improve the selectivity factor (Table 16), but the result was still unsatisfactory. First, there were still some impurities as can be seen from the NMR spectrum. Second, the catalyst became less active when fluorine was on the ligand.





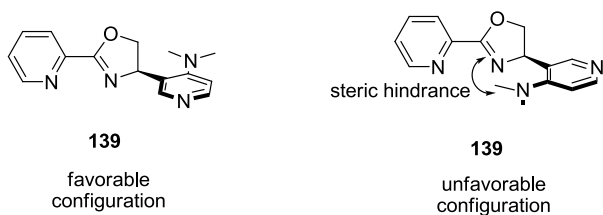
**Table 16.** Kinetic resolution of racemic alcohols catalyzed by chiral catalysts  $\Lambda$ -**133** and  $\Lambda$ -**134**<sup>a</sup>.

Catalyst		time	yield of remaining alcohol	ee of remaining alcohol	s
$\Lambda$ - <b>133</b> <sup>b</sup>		8h	40%	56%	3.7
$\Lambda$ - <b>134</b> <sup>b</sup>		2h	49%	21%	1.8

<sup>a</sup> Reaction conditions: Reaction of 0.3 M 1-(naphthalen-1-yl)ethanol with 0.7 equiv of acetic anhydride and 5% catalyst at room temperature in the  $\text{CH}_2\text{Cl}_2$  was stirred for indicated time. <sup>b</sup> The catalysts  $\Lambda$ -**133** and  $\Lambda$ -**134** were synthesized following the same procedure of the catalyst **128** and **129**. The absolute configuration of the catalysts  $\Lambda$ -**133** and  $\Lambda$ -**134** were relative to catalyst  $\Lambda$ -**100**. Because the similar structure of the polypyridyl ligand with  $\Lambda$ -**76**, we proposed the first fraction emerging from the column in the dimer resolving was  $\Lambda$ -configuration.

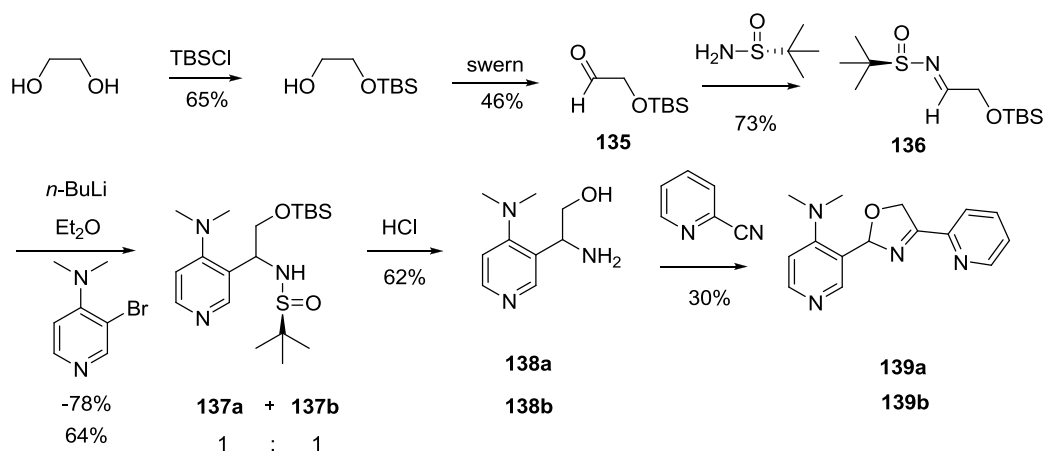
### 3.2.2.4 Chiral bidentate ligand

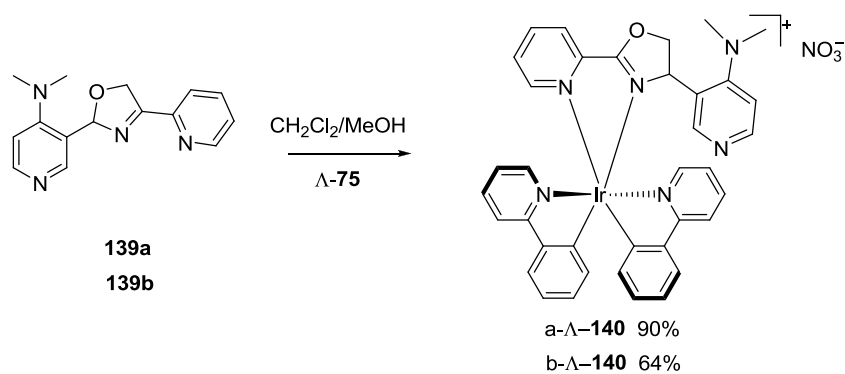
Up until now, we encountered some obstacles while attempting to design the catalyst. When it was less crowded around the metal sphere, the DMAP lost axial chirality. Paradoxically, when the metal sphere was crowded, the catalyst became unstable. Therefore, to restrict the rotation of the DMAP and release the hindrance around the metal sphere, we had to determine the correct approach. Finally, we decided to synthesize ligand **139**, expecting the DMAP to point to only one possibility due to the steric hindrance difference between these two diastereomers (Figure 41).



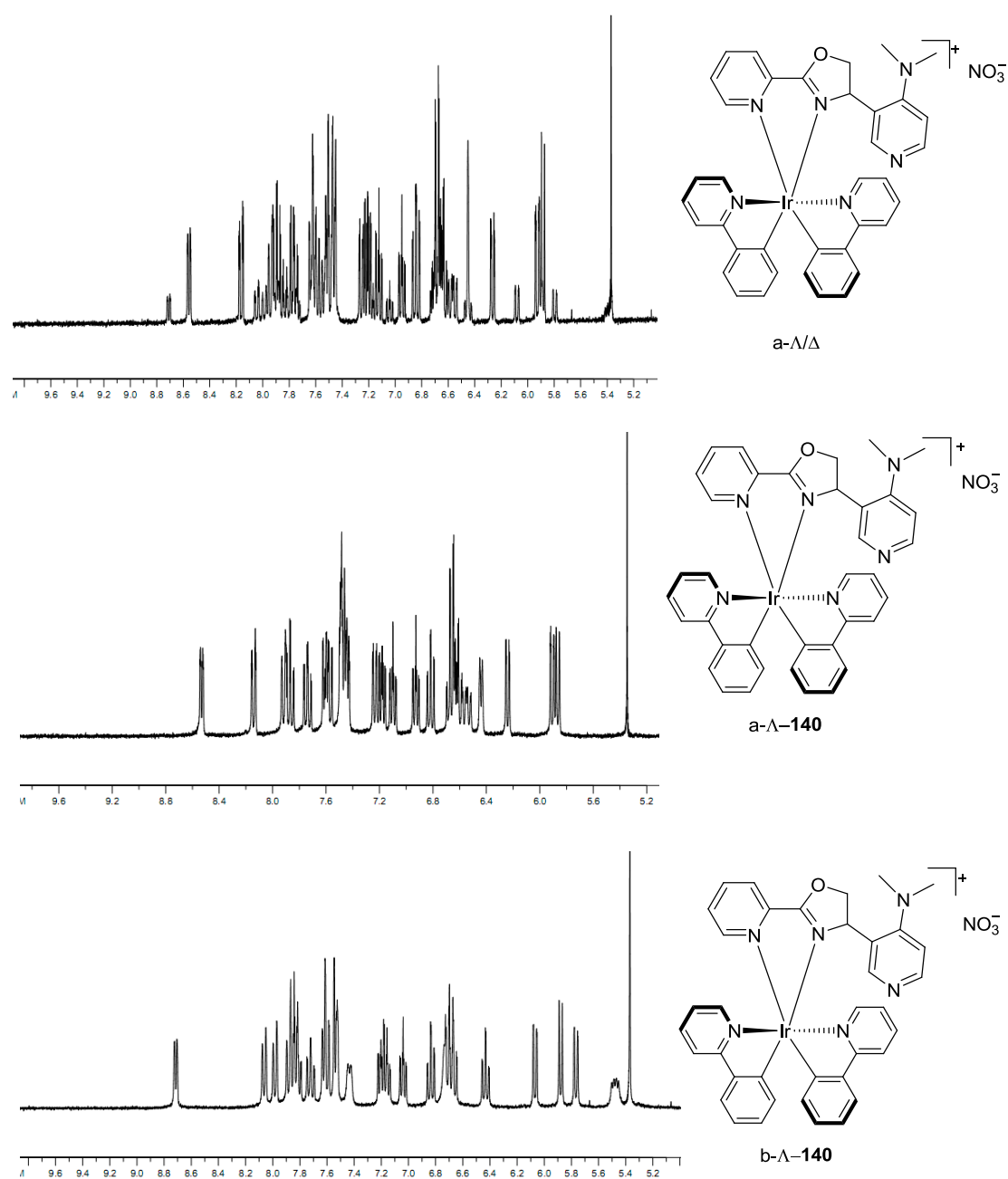
**Figure 41.** Two proposed configurations for compound **139**.

In order to asymmetrically synthesize compound **139**, compound **135** was synthesized first using the published method<sup>75</sup>, which monoprotected the ethylene glycol by TBS, followed by oxidizing the alcohol to aldehyde. Then, compound **135** reacted with (*R*)-2-methylpropane-2-sulfinamide, affording compound **136**. It also reacted with the 3-bromo DMAP in the presence of *n*-BuLi, providing two diastereomers, **137a** and **137b**, with a 1: 1 ratio, which can be easily separated by column chromatography. After deprotecting, followed by cyclizing in the presence of 2-cynopyridine, we obtained the final ligands, **139a** and **139b**, with enantiopurity and only one conformation of the DMAP. Finally, by reacting with the precursor  $\Lambda$ -**89**, the two diastereomers of the catalysts a- $\Lambda$ -**140** and b- $\Lambda$ -**140** were obtained, respectively (Scheme 75). The proton NMR shows that both a- $\Lambda$ -**140** and b- $\Lambda$ -**140** were enantiopure and diastereopure (Figure 42), and both showed good stability in the catalytic reaction. The  $\Lambda$ -configuration of the catalysts was relative to the precursor  $\Lambda$ -**89**. The absolute configuration of the chiral bidentate ligand **139** was not indicated here; therefore, we identified the two enantiomers by **a** and **b**.





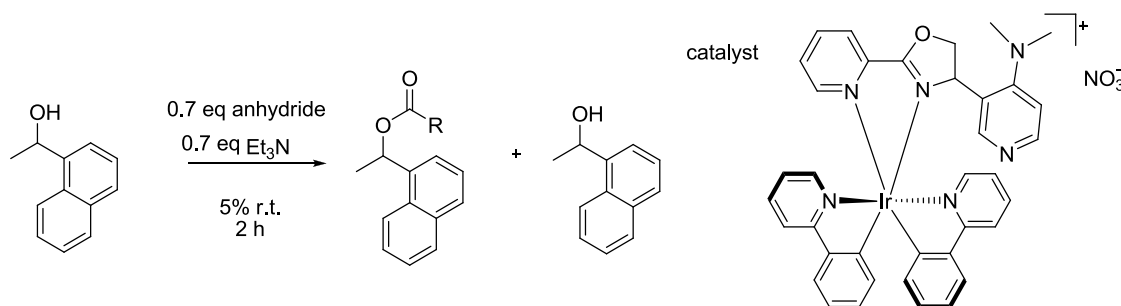
**Scheme 75.** Synthesis of complexes a- $\Lambda$ -140 and b- $\Lambda$ -140.



**Figure 42.** The proton NMR of the compounds a- $\Lambda$ -140 and b- $\Lambda$ -140.

From the analysis of the proton NMR, several conclusions can be drawn. First, both of the chiral carbon center and the iridium center of the catalysts were enantiopure. Second, the DMAP only had one conformation in this system. Third, the chiral iridium center was retained during substitution with the directing ligand.

With these advantages in the new catalysts, we applied them to the asymmetric acyl transfer catalysis; yet, the selective factor was still not high (Table 17).

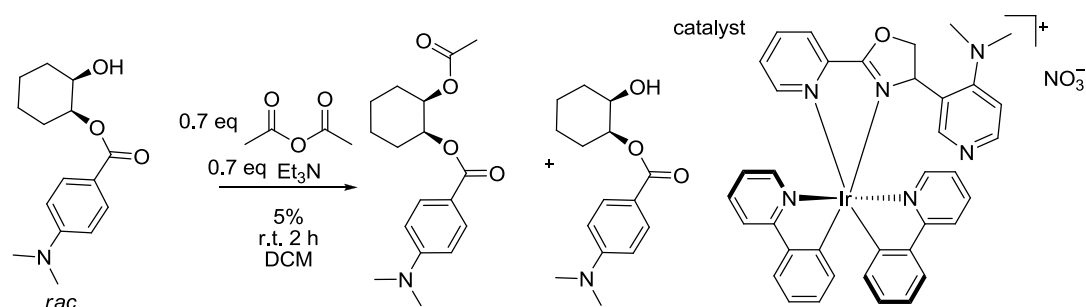


**Table 17.** Kinetic resolution of racemic alcohols catalyzed by chiral catalysts a-**Λ-140** and b-**Λ-140**<sup>a</sup>.

Catalyst	anhydride	yield of remaining alcohol	ee of remaining alcohol	s
a- <b>Λ-140</b> <sup>b</sup>	acetic anhydride	20%	60%	2.2
a- <b>Λ-140</b> <sup>b</sup>	isobutyric anhydride	42%	24%	1.75
b- <b>Λ-140</b> <sup>b</sup>	acetic anhydride	29%	27%	1.6

<sup>a</sup> Reaction conditions: Reaction of 0.3 M 1-(naphthalen-1-yl)ethanol with 0.7 equiv of acetic anhydride and 5% catalyst at room temperature in the CH<sub>2</sub>Cl<sub>2</sub> was stirred for 2 hours. <sup>b</sup> The absolute and relative configuration of the catalyst **140** was not indicated here.

Next, we changed the substrate to one with a greater hindrance, but still did not achieve positive results (Table 18).



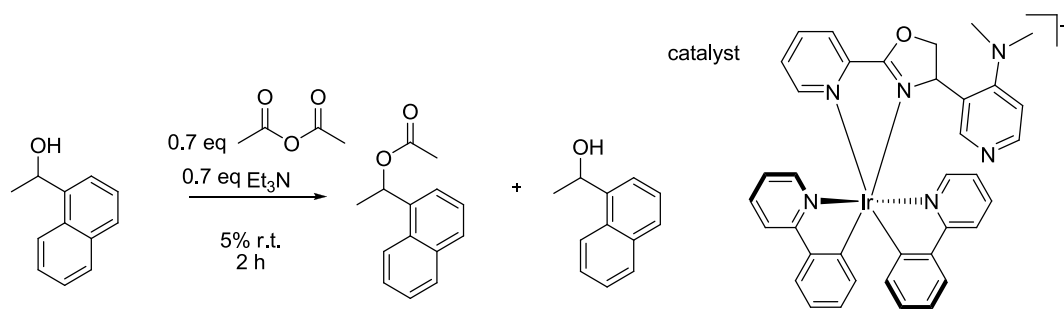
**Table 18.** Kinetic resolution of racemic alcohols catalyzed by chiral catalysts a- $\Lambda$ -**140** and b- $\Lambda$ -**140**<sup>a</sup>.

Catalyst	yield of remaining alcohol	ee of remaining alcohol	s
a- $\Lambda$ - <b>140</b> <sup>b</sup>	43%	27%	1.9
b- $\Lambda$ - <b>140</b> <sup>b</sup>	30%	0%	

<sup>a</sup> Reaction conditions: Reaction of 0.3 M (1*S*,2*R*)-2-hydroxycyclohexyl 4-(dimethylamino)benzoate with 0.7 equiv of acetic anhydride and 5% catalyst at room temperature in the CH<sub>2</sub>Cl<sub>2</sub> was stirred for 2 hours. <sup>b</sup> The absolute and relatively configuration of the catalyst **140** was not indicated here.

Finally, the anion of catalyst b- $\Lambda$ -**140** was changed from nitrate to borate, but we still did not obtain the expected result (Table 19).

In conclusion, we tested 16 different catalysts based on a chiral iridium complex. The most positive was the fluorine substitution catalyst,  $\Lambda$ -**134**, which showed a selectivity factor of 3.7 in the resolution reaction. However, the instability of these types of catalysts was still unresolved. On the other hand, although a- $\Lambda$ -**140** and b- $\Lambda$ -**140** were the stable catalysts, they showed low selectivity, and further investigation is required in this area.



**Table 19.** Kinetic resolution of racemic alcohols catalyzed by chiral catalysts a- $\Lambda$ -**140** and b- $\Lambda$ -**140**<sup>a</sup>.

Catalyst	anion	yield of remaining alcohol	ee of remaining alcohol	s
b- $\Lambda$ - <b>140</b> <sup>b</sup>	$\text{NO}_3^-$	29%	27%	1.6
b- $\Lambda$ - <b>140</b> <sup>b</sup>		29%	27%	1.6

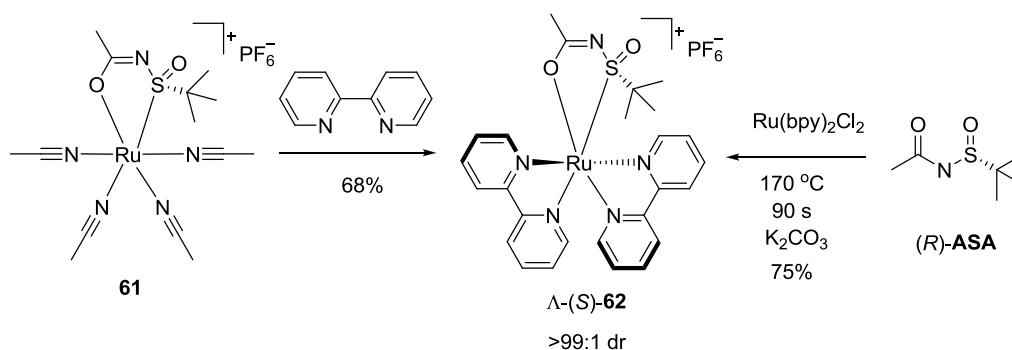
<sup>a</sup> Reaction conditions: Reaction of 0.3 M 1-(naphthalen-1-yl)ethanol with 0.7 equiv of acetic anhydride and 5% catalyst at room temperature in the  $\text{CH}_2\text{Cl}_2$  was stirred for 2 hours. <sup>b</sup> The absolute and relatively configuration of the catalyst **140** was not indicated here.

## Chapter 4 Summary and outlook

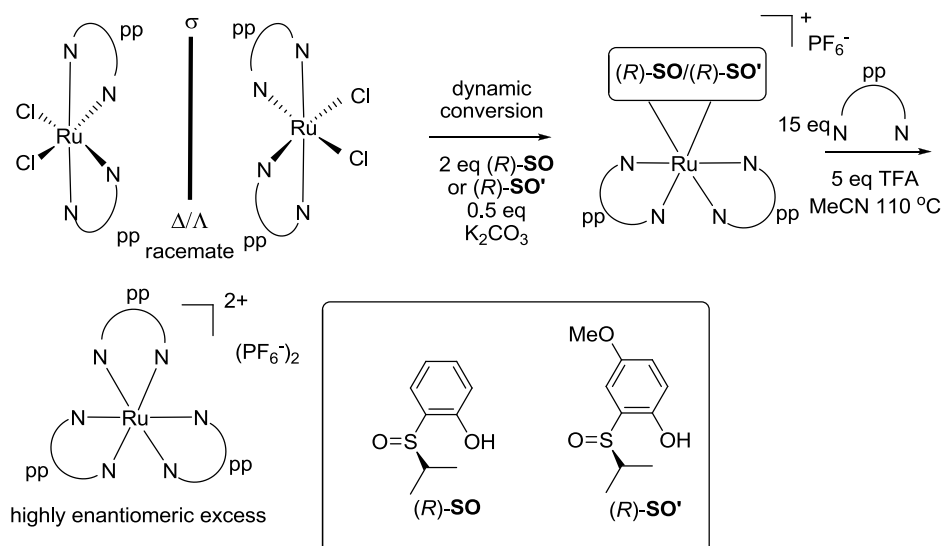
### 4.1 Asymmetric coordination chemistry

In this thesis, we explored chiral auxiliaries for the asymmetric synthesis of polypyridyl metal complexes. After the first useful method to obtain enantiopure polypyridyl ruthenium complexes based on salicyloxazoline auxiliaries developed by the Meggers group (Scheme 14), we expanded this area of research by using (*R*)-2-(isopropylsulfinyl)phenol [(*R*)-SO] and (*R*)-2-(isopropylsulfinyl)-5-methoxy phenol [(*R*)-SO'] for a dynamic conversion to obtain only one diastereomer of the chiral-auxiliary-mediated metal complexes. Then, the chiral-auxiliary-mediated metal complexes are converted into their corresponding optically active ruthenium polypyridyl complexes. The advantages of this new method are that the ruthenium precursors are commercially available, and the final polypyridyl ruthenium complexes are synthesized with high enantiopurity (Table 20).

Next, for synthesizing the auxiliary more easily, we invented the ASA ligand, which was a one step synthesis from the commercially available Ellman's sulfinamide. Then, the chiral-auxiliary-mediated metal complex,  $\Lambda$ -(*S*)-**62**, was obtained through either dynamic conversion or asymmetric synthesis (Scheme 77).



**Scheme 77.** Asymmetrically synthesized chiral-auxiliary-mediated metal complex,  $\Lambda$ -(*S*)-**62**, by using (*R*)-ASA auxiliary.



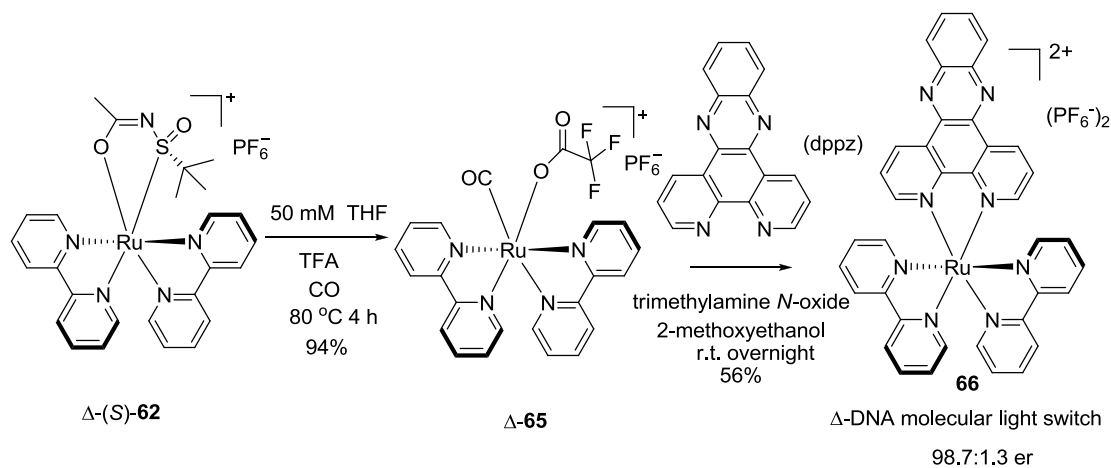
**Table 20.** Asymmetric synthesis of  $\Lambda$ -[Ru(pp)<sub>3</sub>](PF<sub>6</sub>)<sub>2</sub> from  $(rac)$ -Ru(pp)<sub>2</sub>Cl<sub>2</sub><sup>a</sup>.

entry	[Ru(pp) <sub>2</sub> Cl <sub>2</sub> ]	auxiliary	$\Lambda$ -(S) diastereomers <sup>b</sup>	$\Lambda$ -[Ru(pp) <sub>3</sub> ](PF <sub>6</sub> ) <sub>2</sub> products <sup>c</sup>
	pp =			
1	bpy	$(R)$ -SO	$\Lambda$ -(S)-45 (87%)	87%, 98:2 er
2	phen	$(R)$ -SO	$\Lambda$ -(S)-44 (73%)	85%, 98.5:1.5 er
3	5,5'-dmbpy	$(R)$ -SO	$\Lambda$ -(S)-49 (66%)	91%, 98:2 er
4	bpy	$(R)$ -SO'	$\Lambda$ -(S)-53 (86%)	84%, >99:1 er
5	phen	$(R)$ -SO'	$\Lambda$ -(S)-54 (63%)	84%, >99:1 er
6	5,5'-dmbpy	$(R)$ -SO'	$\Lambda$ -(S)-55 (63%)	85%, >98:2 er

<sup>a</sup> Reaction conditions: Reaction of racemic [Ru(pp)<sub>2</sub>Cl<sub>2</sub>] (pp = bpy, phen, 5,5'-dmbpy respectively) with  $(R)$ -SO or  $(R)$ -SO' (2 eq) and K<sub>2</sub>CO<sub>3</sub> (0.5 eq) at 165 or 170 °C in ethyleneglycol afforded chiral-auxiliary-mediated metal complexes. For the next step, chiral-auxiliary-mediated metal complexes reacted with pp (pp = bpy, phen, 5,5'-dmbpy) (15 eq) and TFA (5 eq) at 110 °C in MeCN, stirred for 3 hours, yielding  $\Lambda$ -[Ru(pp)<sub>3</sub>](PF<sub>6</sub>)<sub>2</sub>. <sup>b</sup> Diastereomeric ratios of chiral-auxiliary-mediated metal complexes were at least 99: 1 as determined by <sup>1</sup>H NMR spectroscopy. The metal configuration of the main diastereomer was lambda. <sup>c</sup> Enantiomeric ratios of  $\Lambda$ -[Ru(pp)<sub>3</sub>](PF<sub>6</sub>)<sub>2</sub> were determined by chiral HPLC analysis. The complexes were isolated as their PF<sub>6</sub> salts.



Finally, we synthesized the CO/TFA precursor  $\Delta$ -**65** from  $\Delta$ -(*S*)-**62** with a high yield. Additionally, precursor  $\Delta$ -**65** can react with other bidentate ligands in mild conditions. At last, we utilized  $\Delta$ -**65** for one application to synthesize the  $\Delta$ -DNA molecular light switch complex (**66**) (Scheme 78).



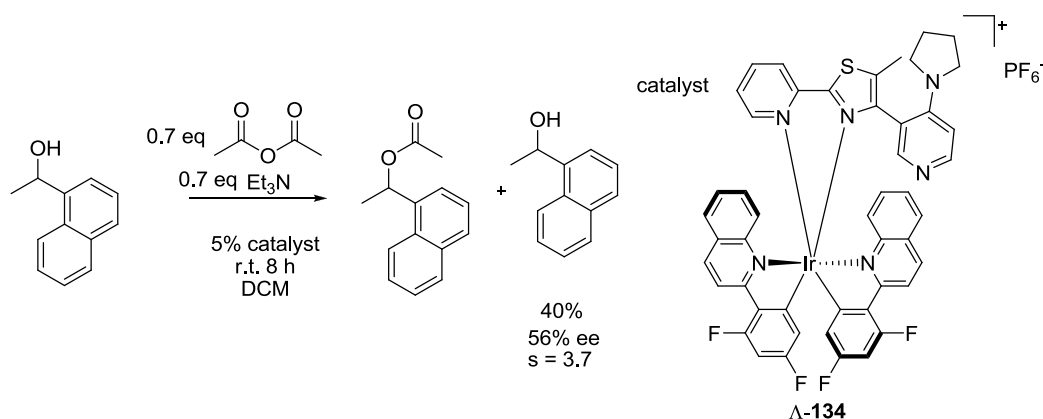
**Scheme 78.** Asymmetric synthesis of the DNA molecular light switch.

Although we obtained some positive results in controlling the chirality of the ruthenium complexes, there are still several undeveloped areas in this direction that require further investigation. First, up until now, the ligands we used for the reactions were limited to polypyridyl ligands. Further study is needed to determine how to synthesize chiral ruthenium with other ligands. Second, asymmetric synthesis of ruthenium complexes with a multidentate ligand is another undeveloped area. Third, we know that if all ligands are monodentate and coordinated to the ruthenium, there are 30 stereoisomers. Therefore, the ultimate goal is how to selectively synthesize a single isomer from these 30 stereoisomers.

## 4.2 Applications of enantiomerically pure octahedral metal complexes

In this thesis, we initially explored asymmetric catalytic synthesis by using the enantiomerically pure octahedral iridium complexes. Towards this direction, we focused on the asymmetric acyl transfer catalysis. After screening different types of

catalysts, catalyst **98** was obtained, which showed enantioselectivity in the acyl transfer reaction (Scheme 61). We then started to modify the catalyst based on this structure. At the beginning, we modified the DMAP-pyridine-thiazole ligand (Scheme 63, 65, 67, 69, and 71), and ligand **100** presented the best result. For the next step, based on ligand **100**, we synthesized the catalyst with a different polypyridyl ligand, and evaluated its selectivity in the asymmetric acyl transfer catalysis reaction (Scheme 73, Table 15, 16). However, with a selectivity factor no higher than 10, none of these results was as positive as expected. At last, the catalysts a- $\Lambda$ -**140** and b- $\Lambda$ -**140** with the chiral DMAP ligand were synthesized, but still did not provide good enantioselectivity (Table 17, Table 18). Therefore, up to this point, the best result in this system was derived from catalyst **134**, which showed a 3.7 selectivity factor (Scheme 79).



**Scheme 79.** The best result in the asymmetric acyl transfer catalysis reaction.

To improve these results, we need to solve two problems in the catalyst design. First, we need to synthesize a catalyst with highly stability. Second, the chirality on the DMAP should be at the correct position to influence the reaction's efficiency. It is also worth developing catalysts that are based on the chiral metal centers of other types of the reactions. Considering that there are several different types of catalytic reactions in organic chemistry, we can simulate their mechanisms and connect the octahedron chirality to design the chiral metal catalyst. We believe that this area will positively integrate organic and inorganic chemistry for an encouraging future.

## Chapter 5 Experimental part

### 5.1 Materials and Methods

#### Solvents and reagents

All asymmetric coordination reactions were carried out under nitrogen or argon atmosphere and ruthenium chemistry additionally in the dark. Solvents were distilled under nitrogen from calcium hydride ( $\text{CH}_3\text{CN}$ ,  $\text{CH}_2\text{Cl}_2$  and DMF) or sodium/benzophenone ( $\text{Et}_2\text{O}$ , THF). Chlorobenzene and acetone were used as HPLC grade without further drying. All reagents were purchased from Acros, Aldrich, Alfa, and fluorochem and used without further purification. Column chromatography was performed with silica gel (230-400 mesh). Compounds *cis*-[Ru(bpy) $_2$ Cl $_2$ ], *cis*-[Ru(dmbpy) $_2$ Cl $_2$ ], *cis*-[Ru(phen) $_2$ Cl $_2$ ]<sup>76</sup>, (*R*)-alkanesulfinate (**23**)<sup>46</sup>, 2-phenylbenzo[d]thiazole (Aldrich); 5-methyl-2-phenylbenzo[d]thiazole<sup>77</sup>, 2,5-diphenylpyridine<sup>78</sup>, 2-(4-(trifluoromethyl)phenyl)quinoline<sup>74</sup>, 2-(2,4-difluorophenyl)quinoline<sup>74</sup>, 2-p-tolylquinoline<sup>74</sup>, 2-(naphthalen-2-yl)quinoline<sup>74</sup>, **79**<sup>79</sup>, **82**<sup>80</sup>, **88**<sup>80</sup>, **101**<sup>73</sup> were synthesized as published.

#### Chromatographic methods

The course of the reactions and the column chromatographic elutions were traced by thin layer chromatography [Macherey-Nagel(ALUGRAM®Xtra Sil G/UV254) or Merck (aluminum silica gel 60 F254)] with Fluorescent indicator UV254 or color developing agent (cerium sulfate / ammonium molybdate solution). For column chromatography silica gel, Merck (particle size 0.040-0.063 mm) was used. The elution was performed at room temperature using a compressed air overpressure. The corresponding mobile phase was specified in the followed procedure. If substance has poor solubility, the crude product on silica gel was absorbed firstly, and then the adsorbed material was applied to the silica gel chromatographic column.

#### Nuclear magnetic resonance spectroscopy (NMR)

Bruker Advance 300 MHz ( $^1\text{H}$ -NMR: 300 MHz,  $^{13}\text{C}$ -NMR: 75 MHz)

Bruker DRX 400 MHz ( $^1\text{H-NMR}$ : 400 MHz,  $^{13}\text{C-NMR}$ : 100 MHz)

Bruker AM 500 MHz ( $^1\text{H-NMR}$ : 500 MHz,  $^{13}\text{C-NMR}$ : 126 MHz)

In the experiments, the spectroscopic NMR data are given as follows: "(MHz, deuterated solvent):  $\delta$  (ppm)". The calibration of the spectra was carried out according to the literature by Fulmer et al<sup>81</sup>. The characteristic signals were specified from the low field to high-field with the chemical shifts ( $\delta$  in ppm).  $^1\text{H-NMR}$  spectra peak multiplicities indicated as singlet (s), doublet (d), doublet of doublet (dd), doublet of doublet of doublet (ddd), triplet (t), doublet of triplet (dt), quartet (q), multiplet (m). The coupling constant  $J$  indicated in hertz (Hz). And  $^1\text{H-NMR}$  spectra peak also show the number of protons.

### High-performance liquid chromatography (HPLC)

Chiral HPLC chromatography was performed with an Agilent 1200 Series HPLC System. All the compounds in the thesis were detected by UV at  $\lambda = 254$  nm. The flow was 0.5 mL/min. The injection was 1~2  $\mu\text{L}$  for 2 mM solution. Y-axis range was adjusted to the 100~300 mAu. The corresponding mobile phase and the type of the columns were specified in the followed procedure.

### Circular dichroism (CD)

CD spectra were recorded on a JASCO J-810 CD spectropolarimeter. The parameter which we used was the following: from 600 nm to 200 nm; data pitch (0.5 nm); band with (1 nm); response (1 second); sensitivity (standard); scanning speed (50 nm/min); accumulation (5). The concentration of the compounds in the measurement was 0.1 mM (metal complex) and 1 mM (organic compound). The formula for converting  $\theta$  to  $\epsilon$  was showed in the Figure 43.

$$\Delta\epsilon = \frac{\theta \text{ [mdeg]}}{32980 \times c(\text{mol/L}) \times L(\text{cm})}$$

c: concentration of the sample

L: the thickness of the measurement vial

**Figure 43.** Formula for converting  $\theta$  to  $\epsilon$ .

### Infrared spectroscopy (IR)

The measurements were recorded on a Bruker Alpha-P FT-IR spectrometer. The

absorption bands were indicated in the wave number  $\nu$  ( $\text{cm}^{-1}$ ). All substances were measured as film or solid. For the film, the substance was dissolved in DCM or MeCN or suspended and the solution applied to the device. After evaporation of the solvent the sample is measured.

### **Crystal structure analysis**

Crystal X-ray measurements and the crystal structure analysis were carried out by Klaus Harms (Chemistry Department, Philipps University of Marburg) on the devices IPDS-II (Mo-K $\alpha$ -irradiation, bis  $2\Theta = 77^\circ$ , Oxford Cryosystem) or IPDS-IIT (Mo-K $\alpha$ -irradiation, bis  $2\Theta = 135^\circ$ , Oxford Cryosystem). The solution and refinement of the structures were carried with the corresponding programs. Details of crystal structures are in the Appendix.

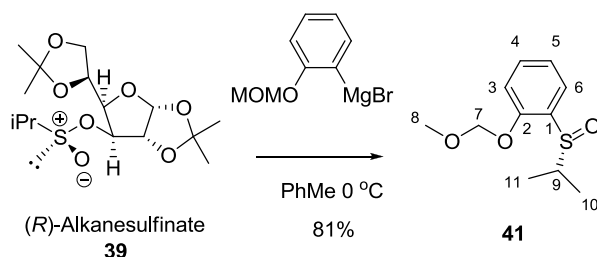
### **Microwave**

1) Microwave oven. Brand: MADmm717. The reactions in Table 2, 3, 4, 5, 6 and 7 were heated by microwave oven. The power of the microwave oven was selected to (M). The reactions were carried out under the air. And the reaction vial was roll edge glasses (45 x 22 mm) without cap. Before heating by microwave oven, the sample was shake in the ultrasound cleaner until the sample can equality distributed in the ethyleneglycol.

2) Microwave reactor. Brand: CEM discover. The compound **80** was synthesized by using Microwave reactor.

## 5.2 Novel chiral auxiliaries for the asymmetric synthesis of ruthenium polypyridyl complexes

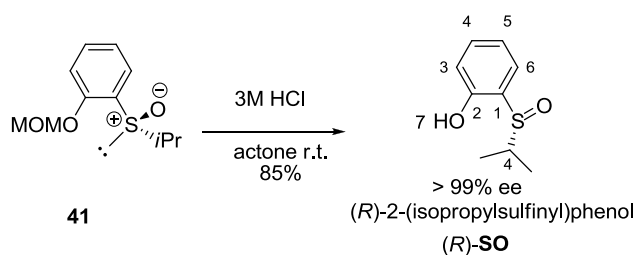
### 5.2.1 Ligand synthesis



#### **(*R*)-1-(Isopropylsulfinyl)-2-(methoxymethoxy)benzene (41).**

2-(Methoxymethoxy)phenylmagnesium bromide was freshly prepared from 1-bromo-2-(methoxymethoxy)benzene and magnesium turnings in anhydrous THF. Accordingly, magnesium turnings (122.8 mg, 5.1 mmol) were dried under vacuum with heating at 75 °C over night. After cooling to room temperature under nitrogen, 1-bromo-2-(methoxymethoxy)benzene (1000 mg, 4.6 mmol) in anhydrous THF (4.6 mL) was added slowly and the reaction initiated by heating. After the addition, the reaction mixture was stirred at 40 °C for 1 h after which almost all the magnesium was consumed to afford a yellow solution. This freshly prepared Grignard reagent was added dropwise to a solution of 1,2:5,6-di-*O*-isopropylidene- $\alpha$ -D-glucopyranosyl (+)-(*R*)-2-propanesulfinate (**39**) (1600 mg, 4.57 mmol) in toluene (91 mL) at 0 °C under nitrogen. The mixture was stirred at this temperature for 0.5 h, was then quenched with saturated aqueous NH<sub>4</sub>Cl, and extracted by EtOAc. The combined organic phase was dried over Na<sub>2</sub>SO<sub>4</sub>, filtered, concentrated, and subjected to silica gel chromatography with hexane: EtOAc = 3: 1 to yield (*R*)-1-(isopropylsulfinyl)-2-(methoxymethoxy)benzene as a colorless liquid (833 mg, 80%). The absolute configuration of the compound **41** was confirmed according to the literature by Alcuia et al<sup>46</sup>. According to the literature, after addition with the Grignard reagent, the sulfoxide exhibit the same configuration to the 1,2:5,6-di-*O*-isopropylidene- $\alpha$ -D-glucopyranosyl (+)-(*R*)-2-propanesulfinate (**39**).

$^1\text{H-NMR}$  (300.1 MHz,  $\text{CDCl}_3$ ):  $\delta$  (ppm) 7.68 (dd,  $J = 7.7, 1.7$  Hz, 1H, 6-H), 7.35 (m, 1H, 4-H), 7.15 (td,  $J = 7.6, 0.9$  Hz, 1H, 5-H), 7.07 (dd,  $J = 8.3, 0.7$  Hz, 1H, 3-H), 5.19 (d,  $J = 6.8$  Hz, 1H, 7-H), 5.14 (d,  $J = 6.8$  Hz, 1H, 7-H), 3.42 (s, 3H, 8-H), 3.30 (m, 1H, 9-H), 1.34 (d,  $J = 7.1$  Hz, 3H,  $\text{CH}(\text{CH}_3)_2$ ), 0.95 (d,  $J = 7.1$  Hz, 3H,  $\text{CH}(\text{CH}_3)_2$ ).  $^{13}\text{C-NMR}$  (75.5 MHz,  $\text{CDCl}_3$ ):  $\delta$  (ppm) 153.1 (C-1), 131.8 (C-2), 130.9 ( $\text{C}_{\text{arom}}$ ), 126.4 ( $\text{C}_{\text{arom}}$ ), 122.4 ( $\text{C}_{\text{arom}}$ ), 113.9 ( $\text{C}_{\text{arom}}$ ), 94.6 (C-7), 56.5 (C-9), 51.2 (C-8), 17.3 ( $\text{CH}(\text{CH}_3)_2$ ), 12.6 ( $\text{CH}(\text{CH}_3)_2$ ). IR (thin film):  $\nu$  ( $\text{cm}^{-1}$ ) 2965, 2930, 2827, 1584, 1472, 1441, 1404, 1382, 1364, 1310, 1268, 1226, 1198, 1154, 1130, 1082, 1071, 1022, 973, 924, 874, 791, 758, 644, 587, 558. HRMS (ESI) calcd for  $\text{C}_{11}\text{H}_{16}\text{SO}_3\text{Na}$  ( $\text{M}+\text{H}$ ) $^+$  229.0893, found: 229.0890.



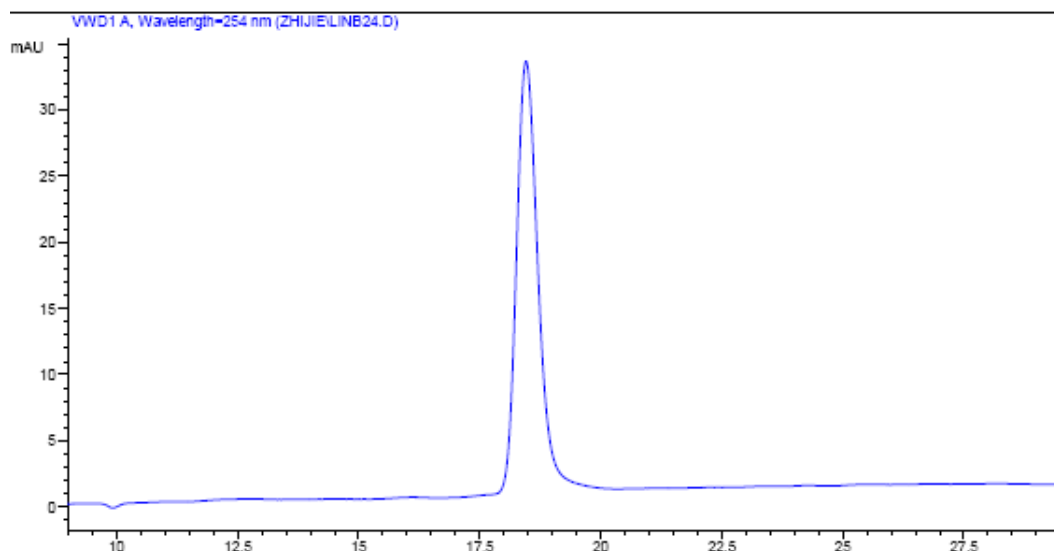
### **(R)-2-(Isopropylsulfinyl)phenol [(R)-SO].**

To a solution of (*R*)-1-(isopropylsulfinyl)-2-(methoxymethoxy)benzene (**41**) (833 mg, 2.0 mmol) in acetone (14 mL) was added 3 M HCl (14 mL). The mixture was stirred at room temperature for 36 h. Afterwards, acetone was evaporated and the aqueous phase was extracted with  $\text{CH}_2\text{Cl}_2$  (3 x 50 mL). The combined organic phase was washed by brine, dried over  $\text{MgSO}_4$ , and the residue after filtration and evaporation was subjected to silica gel chromatography with hexane: EtOAc = 2: 1. After evaporation the final product [(*R*)-SO] was collected as a white solid (571 mg, 85%). The compound was determined to have an er value of >99: 1 by chiral HPLC analysis (Figure 44). The absolute configuration was assigned relative to compound **41**.

$^1\text{H-NMR}$  (300.1 MHz,  $\text{CDCl}_3$ ):  $\delta$  (ppm) 10.57 (br, 1H, 7-H), 7.30 (ddd,  $J = 8.7, 7.3, 1.7$  Hz, 1H, 6-H), 6.93 (dd,  $J = 7.7, 1.7$  Hz, 1H,  $\text{H}_{\text{arom}}$ ), 6.83 (m, 2H,  $\text{H}_{\text{arom}}$ ), 3.14 (m, 1H, 4-H), 1.29 (d,  $J = 6.9$  Hz, 3H,  $\text{CH}(\text{CH}_3)_2$ ), 1.20 (d,  $J = 6.9$  Hz, 3H,  $\text{CH}(\text{CH}_3)_2$ ).  $^{13}\text{C-NMR}$  (75.5 MHz,  $\text{CDCl}_3$ ):  $\delta$  (ppm) 161.0 (C-1), 132.9 (C-2), 126.5

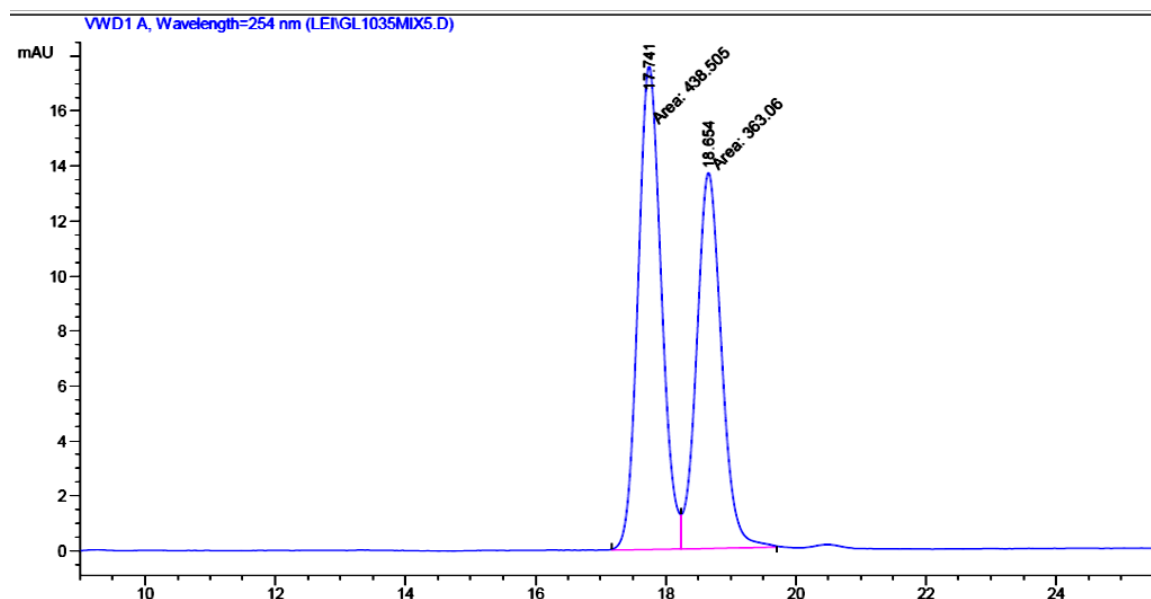
(C<sub>arom</sub>), 119.5 (C<sub>arom</sub>), 119.2 (C<sub>arom</sub>), 118.7 (C<sub>arom</sub>), 54.7 (C-4), 15.8 (CH(CH<sub>3</sub>)<sub>2</sub>), 15.0 (CH(CH<sub>3</sub>)<sub>2</sub>). IR (neat):  $\nu$  (cm<sup>-1</sup>) 2965, 2928, 2836, 2687, 2556, 1585, 1451, 1358, 1284, 1215, 1157, 1064, 1039, 993, 834, 760, 719, 680, 527. HRMS (ESI) calcd for C<sub>9</sub>H<sub>13</sub>SO<sub>2</sub> (M+H) 185.0631, found: 185.0631.

**Determination of the enantiopurity of (*R*)-2-(isopropylsulfinyl)phenol.** The sulfoxide ligands were analyzed with a Daicel Chiralpak IB (250 × 4.6 mm) HPLC column on an Agilent 1200 Series HPLC System. The flow rate was 0.5 mL/min, the column temperature 40 °C, UV-absorption was measured at 254 nm, and isocratic conditions with 6% ethanol and 94% hexane.

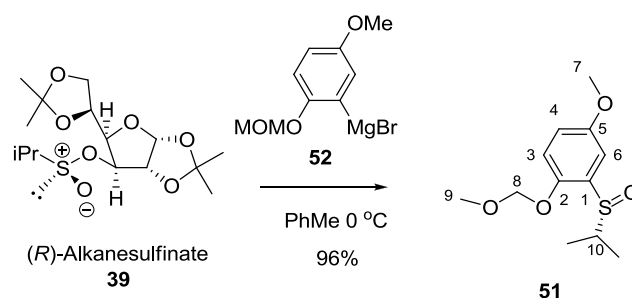


**Figure 44.** HPLC trace for (*R*)-2-(isopropylsulfinyl)phenol. Integration of peak areas: >99: 1 er.





**Figure 45.** HPLC trace for coinjection of the enantiomers (*S*)- and (*R*)-2-(isopropylsulfinyl)phenol.

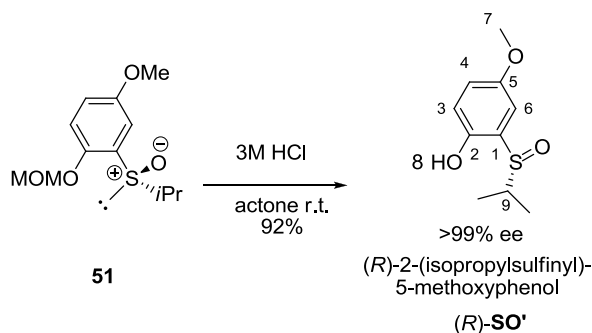


**(*R*)-2-(Isopropylsulfinyl)-4-methoxy-1-(methoxymethoxy)benzene (50).**

(5-Methoxy-2-(methoxymethoxy)phenyl)magnesium bromide (**52**) was freshly prepared from 2-bromo-4-methoxy-1-(methoxymethoxy)benzene and magnesium turnings in anhydrous THF. Accordingly, magnesium turnings (126.0 mg, 5.2 mmol) were dried under vacuum with heating at 75 °C over night. After cooling to room temperature under nitrogen, 2-bromo-4-methoxy-1-(methoxymethoxy)benzene (1000 mg, 4.1 mmol) in anhydrous THF (4.0 mL) was added slowly and the reaction initiated by heating. After the addition, almost all the magnesium was consumed to afford a yellow solution. (This freshly prepared Grignard reagent should be used intermediately.) This freshly prepared Grignard reagent was added dropwise to a solution of 1,2:5,6-di-*O*-isopropylidene- $\alpha$ -D-glucopyranosyl

(+)-(*R*)-2-propanesulfinate(**39**) (1000 mg, 2.84 mmol) in toluene (56 mL) at 0 °C under nitrogen. The mixture was stirred at this temperature for 1.5 h, was then quenched with saturated aqueous NH<sub>4</sub>Cl, and extracted by EtOAc. The combined organic phase was dried over Na<sub>2</sub>SO<sub>4</sub>, filtered, concentrated, and subjected to silica gel chromatography with hexane: EtOAc = 3: 1 to yield (*R*)-1-(isopropylsulfinyl)-2-(methoxymethoxy) benzene (**51**) as a colorless liquid (700.0 mg, 96%). The absolute configuration of the ligand **51** was confirmed according to the literature by Alcudia et al.<sup>46</sup>. According to the literature, after addition with the Grignard reagent, the sulfonide exhibit the same configuration to the 1,2:5,6-di-*O*-isopropylidene- $\alpha$ -D-glucofuranosyl (+)-(*R*)-2-propanesulfinate (**39**).

<sup>1</sup>H-NMR (300.1 MHz, CDCl<sub>3</sub>):  $\delta$  (ppm) 7.22 (d, *J* = 3.1 Hz, 1H, 6-H), 7.01 (d, *J* = 8.9 Hz, 1H, 3-H), 6.86 (dd, *J* = 8.9, 3.1 Hz, 1H, 4-H), 5.11 (d, *J* = 6.7 Hz, 1H, 8-H), 5.05 (d, *J* = 6.7 Hz, 1H, 8-H), 3.77 (s, 3H, 7-H), 3.41 (s, 3H, 9-H), 3.04 (m, 1H, 10-H), 1.35 (d, *J* = 7.1 Hz, 3H, CH(CH<sub>3</sub>)<sub>2</sub>), 0.96 (d, *J* = 7.1 Hz, 3H, CH(CH<sub>3</sub>)<sub>2</sub>). <sup>13</sup>C-NMR (75.5 MHz, CDCl<sub>3</sub>):  $\delta$  (ppm) 155.3 (C-1), 146.9 (C-2), 118.2 (C<sub>arom</sub>), 116.0 (C<sub>arom</sub>), 110.1 (C<sub>arom</sub>), 95.3 (C-8), 56.4 (C-7), 56.0 (C-10), 51.4 (C-9), 17.4 (CH(CH<sub>3</sub>)<sub>2</sub>), 12.6 (CH(CH<sub>3</sub>)<sub>2</sub>). IR (thin film):  $\nu$  (cm<sup>-1</sup>) 2963, 2932, 2831, 1603, 1584, 1484, 1440, 1400, 1364, 1295, 1266, 1214, 1193, 1155, 1138, 1080, 1067, 1042, 1020, 976, 923, 872, 814, 741, 714, 689, 675, 641, 494. HRMS (ESI) calcd for C<sub>12</sub>H<sub>18</sub>SO<sub>4</sub>Na (M+Na)<sup>+</sup> 281.0818, found: 281.0810.



### **(*R*)-2-(Isopropylsulfinyl)-4-methoxyphenol [(*R*)-SO']**

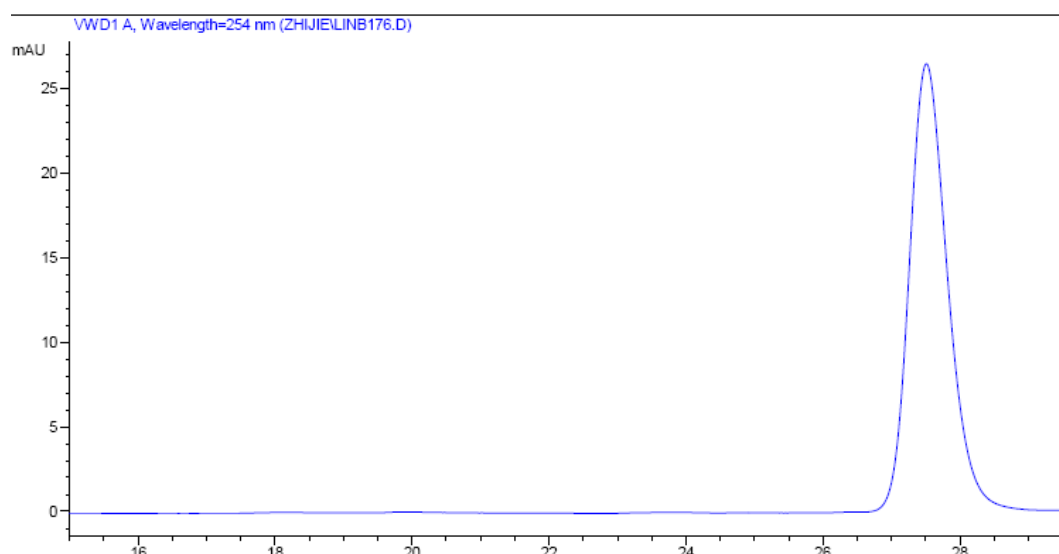
To a solution of (*R*)-1-(isopropylsulfinyl)-2-(methoxymethoxy)-5-methoxybenzene (**51**) (700 mg, 2.7 mmol) in acetone (12 mL) was added 3 M HCl (12 mL). The mixture was stirred at room temperature for 16 h. Afterwards, acetone was evaporated

and the aqueous phase was extracted with  $\text{CH}_2\text{Cl}_2$  (3 x 15 mL). The combined organic phase was washed by brine, dried over  $\text{MgSO}_4$ , and the residue after filtration and evaporation was subjected to silica gel chromatography with hexane: EtOAc = 2: 1. After evaporation the final product was collected as a white solid [(*R*)-SO'] (520 mg, 90%). The compound was determined to have an ee value of >99% by chiral HPLC analysis (Figure 46). The absolute configuration was assigned relative to compound **51**.

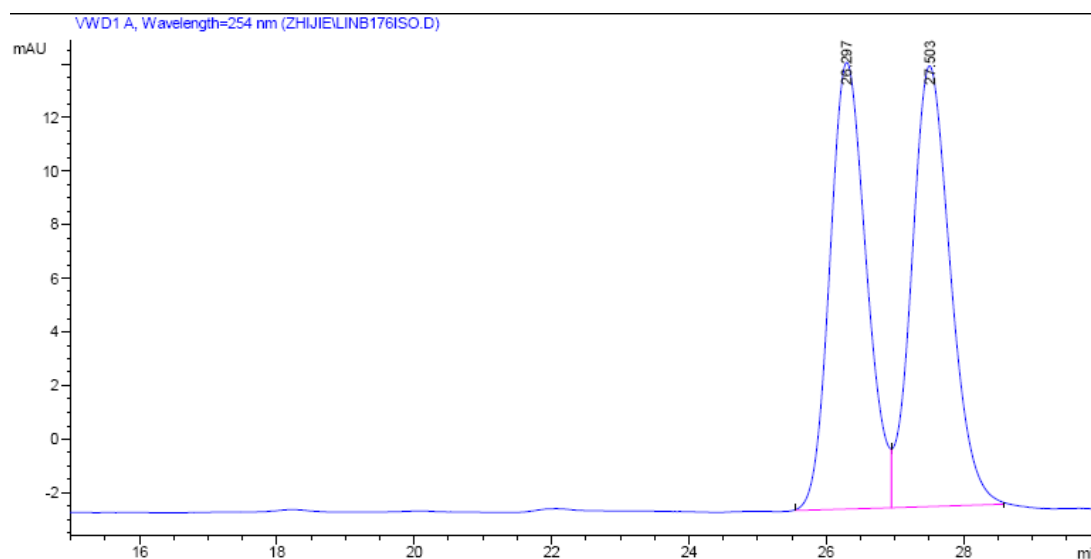
$^1\text{H-NMR}$  (300.1 MHz,  $\text{CDCl}_3$ ):  $\delta$  (ppm) 10.07 (br, 1H, 8-H), 6.95 (dd,  $J = 9.0, 3.0$  Hz, 1H, 3-H), 6.86 (d,  $J = 9.0$  Hz, 1H, 4-H), 6.51 (d,  $J = 3.0$  Hz, 1H, 6-H), 3.75 (s, 3H, 7-H), 3.21 (m, 1H, 9-H), 1.37 (d,  $J = 6.6$  Hz, 3H,  $\text{CH}(\text{CH}_3)_2$ ), 1.28 (d,  $J = 6.6$  Hz, 3H,  $\text{CH}(\text{CH}_3)_2$ ).  $^{13}\text{C-NMR}$  (75.5 MHz,  $\text{CDCl}_3$ ):  $\delta$  (ppm) 154.6 ( $\text{C}_{\text{arom}}$ ), 152.2 ( $\text{C}_{\text{arom}}$ ), 120.2 ( $\text{C}_{\text{arom}}$ ), 119.2 ( $\text{C}_{\text{arom}}$ ), 110.8 ( $\text{C}_{\text{arom}}$ ), 55.9 (C-7), 54.7 (C-9), 15.9 ( $\text{CH}(\text{CH}_3)_2$ ), 15.0 ( $\text{CH}(\text{CH}_3)_2$ ). IR (neat):  $\nu$  ( $\text{cm}^{-1}$ ) 2966, 2933, 2869, 2829, 2775, 1499, 1462, 1418, 1363, 1255, 1197, 1126, 1060, 1034, 1009, 997, 856, 819, 783, 709, 676, 492. HRMS (ESI) calcd for  $\text{C}_{10}\text{H}_{14}\text{SO}_3\text{Na}$  ( $\text{M}+\text{Na}$ ) $^+$  237.0556, found: 237.0547.

#### Determination of the enantiopurity of (*R*)-2-(isopropylsulfinyl)-4-methoxyphenol.

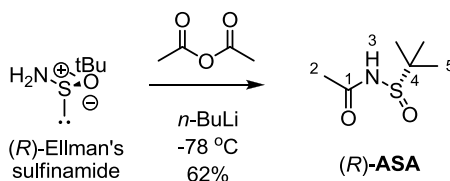
The sulfoxide ligands were analyzed with a Daicel Chiralpak IB (250 × 4.6 mm) HPLC column on an Agilent 1200 Series HPLC System. The flow rate was 0.5 mL/min, the column temperature 40 °C, UV-absorption was measured at 254 nm, and isocratic conditions with 5% ethanol and 95% hexane.



**Figure 46.** HPLC trace for (*R*)-2-(isopropylsulfinyl)-5-methoxyphenol [(*R*)-SO']. Integration of peak areas: >99:1 er.



**Figure 47.** HPLC trace for (*rac*)-2-(isopropylsulfinyl)-5-methoxyphenol.

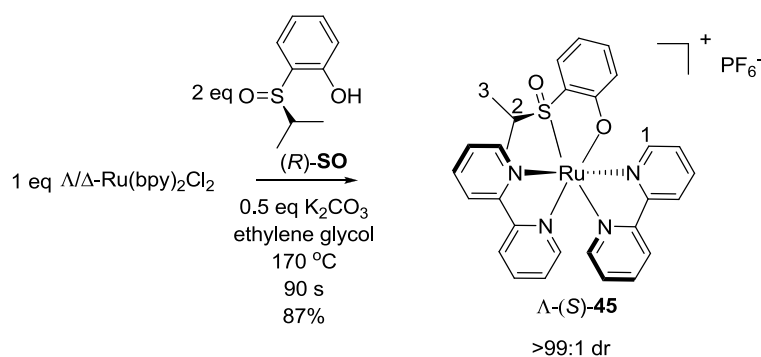


**(*R*)-*N*-Acetyl-*tert*-butansulfinamide ((*R*)-ASA).**

To a 50 mL round bottom flask was added (*R*)-*tert*-butansulfinamide (150 mg, 1.24 mmol) and THF (6.2 mL). The flask was cooled to -78 °C with a dry ice/acetone bath. *n*-BuLi (1.1 mL, 2.5 M in hexane) was added over 20 min followed by the rapid addition of acetic anhydride (0.17 mL, 1.86 mmol). After stirring at -78 °C for 5 hours, saturated aqueous NaHCO<sub>3</sub> (2 mL) and H<sub>2</sub>O (4 mL) was added, and the THF was removed by rotary evaporation. The aqueous phase was extracted with EtOAc (3 x 15 mL), dried over Na<sub>2</sub>SO<sub>4</sub>, concentrated, and subjected to flash silica gel chromatography with EtOAc to yield (*R*)-*N*-acetyl-*tert*-butansulfinamide {(*R*)-ASA} as a white solid (130 mg, 64%). The enantiopurity and absolute configuration was relative to the starting material (*R*)-*tert*-butansulfinamide which was purchased from Aldrich (>99% ee).

$^1\text{H-NMR}$  (300.1 MHz,  $\text{CD}_3\text{CN}$ ):  $\delta$  (ppm) 8.50 (br, 1H, 3-H), 2.15 (s, 3H, 2-H), 1.25 (s, 9H, 5-H).  $^{13}\text{C-NMR}$  (75.5 MHz,  $\text{CD}_3\text{CN}$ ):  $\delta$  (ppm) 172.0 (C-1), 57.2 (C-4), 23.2 (C-2), 22.1 ( $\text{C}(\text{CH}_3)_3$ ). IR (thin film):  $\nu$  ( $\text{cm}^{-1}$ ) 3218, 2967, 2925, 2870, 1696, 1469, 1395, 1365, 1215, 1182, 1057, 998, 809, 651, 604, 567, 488, 455, 417. CD ( $\Delta\epsilon/\text{M cm}^{-1}$ , MeCN): 215 nm (+14), 194 nm (-14). HRMS (ESI) calcd for  $\text{C}_6\text{H}_{13}\text{NO}_2\text{S}$  ( $\text{M}+\text{Na}$ ) $^+$ : 186.0559, found: 186.0559.

### 5.2.2 Diastereoselective coordination chemistry

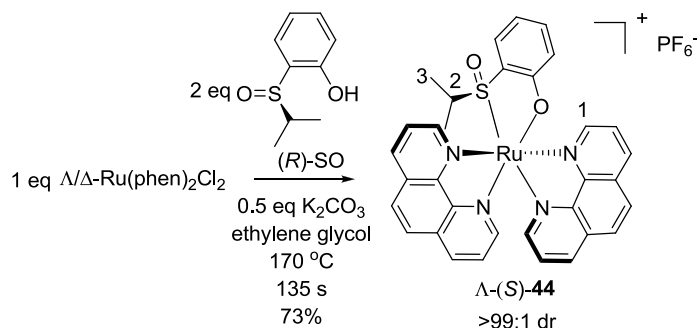


#### $\Lambda$ -[ $\text{Ru}(\text{bpy})_2((R)\text{-2-(isopropylsulfinyl)phenol})$ ]( $\text{PF}_6$ ) ( $\Lambda$ -(S)-45).

In a closed glass 1.5 mL vial fitted with a septum (brand: MACHEREY-NAGEL), a solution of  $(R)$ -2-(isopropylsulfinyl)phenol (10.0 mg, 0.054 mmol),  $\text{K}_2\text{CO}_3$  (1.9 mg, 0.013 mmol) (quality: fine powder) and  $cis$ -[ $\text{Ru}(\text{bpy})_2\text{Cl}_2$ ] (14.1 mg, 0.027 mmol) in ethylene glycol (0.27 mL) (quality: Aldrich anhydrous 99.8%) was degassed with argon and then was heated at 170 °C (oil bath temperature) for 1.5 min. The reaction mixture was cooled to room temperature. The crude material was mixed with 2 mL  $\text{CH}_3\text{CN}$  and subjected to flash silica gel chromatography. The elution was  $\text{CH}_3\text{CN}$ :  $\text{H}_2\text{O}$ :  $\text{KNO}_3(\text{sat}) = 50: 2: 1$ . The product eluents were concentrated to dryness by evaporator, the resulting material was dissolved in minimal amounts of ethanol/water = 1/10 (2~3 mL), and the product was precipitated by the addition of solid  $\text{NH}_4\text{PF}_6$  (add  $\text{NH}_4\text{PF}_6$  together with shaking until the precipitate came and the colour of the solution from the orange to light yellow). The orange precipitate was centrifuged, washed twice with water, and dried under high vacuum to afford complex  $\Lambda$ -(S)-45

(17.6 mg, 87%). The absolute stereochemistry of  $\Lambda$ -(*S*)-**45** was verified by X-ray crystallography of  $\Lambda$ -(*S*)-**44** and CD analysis.

$^1\text{H-NMR}$  (500.1 MHz,  $\text{CD}_3\text{CN}$ ):  $\delta$  (ppm) 10.19 (dd,  $J = 6.0, 0.9$  Hz, 1H, 1-H), 8.75 (dd,  $J = 5.7, 0.6$  Hz, 1H), 8.57 (d,  $J = 8.1$  Hz, 1H), 8.35 – 8.44 (m, 3H), 8.26 (td,  $J = 7.8, 1.5$  Hz, 1H), 7.90 – 8.04 (m, 4H), 7.75 (ddd,  $J = 7.2, 5.7, 1.2$  Hz, 1H), 7.55 (ddd,  $J = 7.2, 5.7, 1.5$  Hz, 1H), 7.50 (dd,  $J = 8.4, 1.5$  Hz, 1H), 7.26 – 7.35 (m, 2H), 7.02 – 7.09 (m, 2H), 6.52 – 6.59 (m, 2H), 2.87 (m, 1H, 2-H), 1.02 (d,  $J = 6.7$  Hz, 3H,  $\text{CH}(\text{CH}_3)_2$ ), 0.34 (d,  $J = 6.7$  Hz, 3H,  $\text{CH}(\text{CH}_3)_2$ ).  $^{13}\text{C-NMR}$  (125.8 MHz,  $\text{CD}_3\text{CN}$ )  $\delta$  (ppm) 173.0, 158.2, 157.9, 157.7, 156.4, 156.1, 153.4, 152.5, 149.1, 138.7, 138.3, 137.5, 137.1, 133.4, 129.4, 127.6, 126.8, 126.7, 126.5, 125.9, 124.3, 123.9, 123.6, 123.5, 120.4, 113.7, 60.3, 16.0, 15.4. IR (neat):  $\nu$  ( $\text{cm}^{-1}$ ) 3081, 1604, 1463, 1446, 1425, 1313, 1268, 1242, 1163, 1125, 1064, 1047, 893, 879, 833, 756, 729, 659, 648, 555, 491, 469, 443, 412, 400. CD ( $\Delta\epsilon/\text{M}^{-1}\text{cm}^{-1}$ , MeCN): 292 nm (+132), 278 nm (-98). HRMS (ESI) calcd for  $\text{RuO}_2\text{N}_4\text{SC}_{29}\text{H}_{27}$  ( $\text{M-PF}_6$ ) $^+$  597.0900, found: 597.0905.

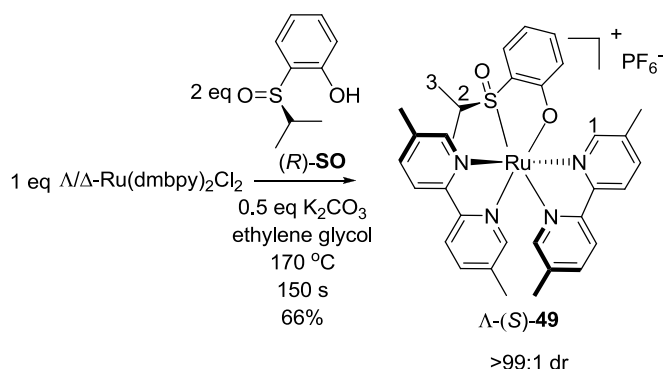


#### $\Lambda$ -[ $\text{Ru}(\text{phen})_2$ -(*R*)-2-(isopropylsulfinyl)phenol]( $\text{PF}_6$ ) ( $\Lambda$ -(*S*)-**44**).

In a closed glass 1.5 mL vial fitted with a septum (brand: MACHEREY-NAGEL), a solution of (*R*)-2-(isopropylsulfinyl)phenol (10.0 mg, 0.054 mmol),  $\text{K}_2\text{CO}_3$  (1.9 mg, 0.013 mmol) (quality: fine powder) and *cis*-[ $\text{Ru}(\text{phen})_2\text{Cl}_2$ ] (15.4 mg, 0.027 mmol) in ethylene glycol (0.27 mL) (quality: Aldrich anhydrous 99.8%) was degassed with argon and then was heated at 170 °C (oil bath temperature) for 135 seconds. The reaction mixture was cooled to room temperature. The crude material was mixed with 2 mL  $\text{CH}_3\text{CN}$  and subjected to flash silica gel chromatography. The elution was  $\text{CH}_3\text{CN}:\text{H}_2\text{O}:\text{KNO}_3(\text{sat}) = 50:2:1$ . The product eluents were concentrated to

dryness by evaporator, the resulting material was dissolved in minimal amounts of ethanol/water = 1/10 (2~3 mL), and the product was precipitated by the addition of solid  $\text{NH}_4\text{PF}_6$  (add  $\text{NH}_4\text{PF}_6$  together with shaking until the precipitate came and the colour of the solution from the orange to light yellow). The orange precipitate was centrifuged, washed twice with water, and dried under high vacuum to afford complex  $\Lambda$ -(*S*)-**44** (15.6 mg, 73%). The absolute stereochemistry of  $\Lambda$ -(*S*)-**44** was verified by X-ray crystallography (Figure 7).

$^1\text{H-NMR}$  (300.1 MHz,  $\text{CD}_3\text{CN}$ ):  $\delta$  (ppm) 10.61 (dd,  $J = 5.4, 1.1$  Hz, 1H, 1-H), 9.15 (dd,  $J = 5.2, 1.1$  Hz, 1H), 8.85 (dd,  $J = 8.3, 1.1$  Hz, 1H), 8.60 (dd,  $J = 8.2, 1.1$  Hz, 1H), 8.45 (td,  $J = 8.4, 1.1$  Hz, 2H), 8.30 (d,  $J = 8.9$  Hz 1H), 8.05 -8.25 (m, 5H), 7.95 (dd,  $J = 8.2, 5.4$  Hz, 1H), 7.56 (dd,  $J = 8.0, 1.6$  Hz, 1H), 7.44-7.51 (m, 2H), 7.22 (dd,  $J = 5.2, 1.1$  Hz, 1H), 7.05 (m, 1H), 6.50-6.61 (m, 2H), 2.87 (m, 1H, 2-H), 0.80 (d,  $J = 6.7$  Hz, 3H,  $\text{CH}(\text{CH}_3)_2$ ), 0.00 (d,  $J = 6.7$  Hz, 3H,  $\text{CH}(\text{CH}_3)_2$ ).  $^{13}\text{C-NMR}$  (125.8 MHz,  $\text{CD}_3\text{CN}$ )  $\delta$  (ppm) 174.3, 158.1, 155.0, 154.4, 150.9, 149.9, 149.7, 149.6, 147.7, 138.7, 138.4, 137.8, 137.0, 134.3, 132.0, 131.8, 131.4, 130.4, 129.2, 129.0, 128.7, 128.4, 127.3, 126.9, 126.5, 126.4, 126.0, 121.4, 114.8, 61.6, 16.7, 16.2. IR (neat):  $\nu$  ( $\text{cm}^{-1}$ ) 3052, 1629, 1580, 1545, 1455, 1427, 1410, 1321, 1275, 1146, 1126, 1072, 1028, 826, 753, 720, 688, 637, 621, 555, 524, 506, 467, 401. CD ( $\Delta\epsilon/\text{M}^{-1}\text{cm}^{-1}$ , MeCN): 268 nm (+134), 256 nm (-117). HRMS (ESI) calcd for  $\text{C}_{33}\text{H}_{27}\text{N}_4\text{O}_2\text{RuS}$  ( $\text{M-PF}_6$ ) $^+$  645.0896, found: 645.0886.



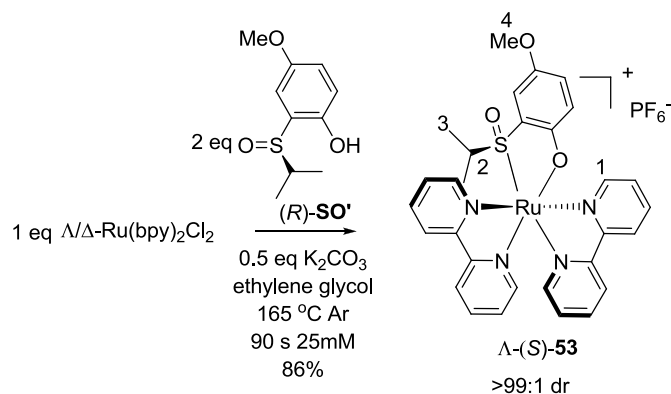
**$\Lambda$ -[Ru(dmbpy) $_2$ ((*R*)-2-(isopropylsulfinyl)phenol)](PF $_6$ ) ( $\Lambda$ -(*S*)-**49**).**

In a closed glass 1.5 mL vial fitted with a septum (brand: MACHEREY-NAGEL), a solution of (*R*)-2-(isopropylsulfinyl)phenol (10.0 mg, 0.054 mmol),  $\text{K}_2\text{CO}_3$  (1.9 mg, 0.013 mmol) (quality: fine powder) and *cis*-[Ru(dmbpy) $_2$ Cl $_2$ ] (16.2 mg, 0.027 mmol)

in ethylene glycol (0.27 mL) (quality: Aldrich anhydrous 99.8%) was degassed with argon and then was heated at 170 °C (oil bath temperature) for 150 seconds. The reaction mixture was cooled to room temperature. The crude material was mixed with 2 mL CH<sub>3</sub>CN and subjected to flash silica gel chromatography. The elution was CH<sub>3</sub>CN: H<sub>2</sub>O: KNO<sub>3</sub>(sat) = 100: 4: 1. The product eluents were concentrated to dryness by evaporator, the resulting material was dissolved in minimal amounts of ethanol/water = 1/10 (2~3 mL), and the product was precipitated by the addition of solid NH<sub>4</sub>PF<sub>6</sub> (add NH<sub>4</sub>PF<sub>6</sub> together with shaking until the precipitate came and the colour of the solution from the orange to light yellow). The orange precipitate was centrifuged, washed twice with water, and dried under high vacuum to afford complex  $\Lambda$ -(*S*)-**49** (14.3 mg, 73%). The absolute stereochemistry of  $\Lambda$ -(*S*)-**49** was verified by X-ray crystallography of  $\Lambda$ -(*S*)-**44** and CD analysis.

<sup>1</sup>H-NMR (500.1 MHz, CD<sub>3</sub>CN):  $\delta$  (ppm) 10.00 (s, 1H), 8.50 (s, 1H, 1-H), 8.40 (d, *J* = 8.4 Hz, 1H), 8.18-8.28 (m, 3H), 8.05 (dd, *J* = 8.6, 1.5 Hz 1H), 7.71-7.83 (m, 4H), 7.50 (dd, *J* = 7.8, 1.1 Hz 1H), 7.05 (dt, *J* = 6.9, 1.6 Hz, 1H), 6.73 (s, 1H), 6.50-6.513 (m, 2H), 2.89 (m, 1H), 2.48 (s, 3H, C-CH<sub>3</sub>), 2.35 (s, 3H, C-CH<sub>3</sub>), 2.18 (s, 3H, C-CH<sub>3</sub>), 2.13 (s, 3H, C-CH<sub>3</sub>), 1.06 (d, *J* = 6.7 Hz, 3H, CH(CH<sub>3</sub>)<sub>2</sub>), 0.39 (d, *J* = 6.7 Hz, 3H, CH(CH<sub>3</sub>)<sub>2</sub>). <sup>13</sup>C-NMR (125.8 MHz, CD<sub>3</sub>CN)  $\delta$  (ppm) 173.9, 157.2, 156.8, 156.4, 156.2, 155.1, 154.0, 152.9, 149.8, 140.1, 139.8, 139.3, 138.7, 138.6, 138.4, 138.0, 137.8, 134.2, 130.8, 127.0, 124.3, 123.9, 123.5, 123.4, 121.3, 114.5, 60.9, 18.9, 18.8, 18.7, 18.4, 17.0, 16.3. IR (neat):  $\nu$  (cm<sup>-1</sup>) 3040, 2927, 1605, 1581, 1545, 1474, 1455, 1384, 1321, 1274, 1240, 1152, 1126, 1075, 1027, 835, 753, 729, 688, 621, 556, 519, 467, 459, 432, 405. CD ( $\Delta\epsilon$ /M<sup>-1</sup>cm<sup>-1</sup>, MeCN): 298 nm (+125), 283 nm (-109). HRMS (ESI) calcd for C<sub>33</sub>H<sub>35</sub>N<sub>4</sub>O<sub>2</sub>RuS (M-PF<sub>6</sub>)<sup>+</sup> 653.1527, found: 653.1526.



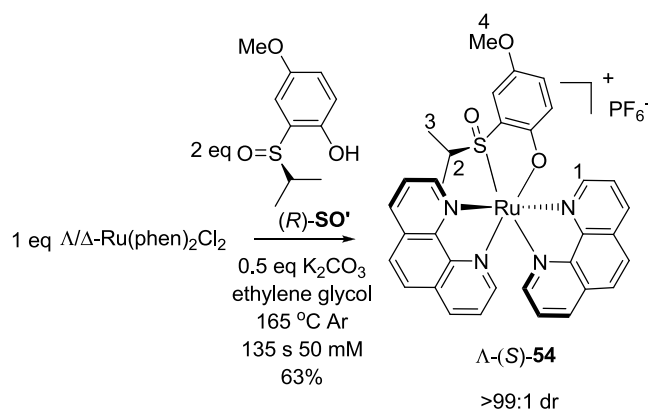


**$\Lambda$ -[Ru(bpy)<sub>2</sub>((R)-2-(isopropylsulfinyl)-4-methoxyphenol)](PF<sub>6</sub>) ( $\Lambda$ -(S)-53).**

In a closed glass 1.5 mL vial fitted with a septum (brand: MACHEREY-NAGEL), a solution of (*S*)-1-(isopropylsulfinyl)-2-(methoxymethoxy) benzene (20.0 mg, 0.093 mmol), K<sub>2</sub>CO<sub>3</sub> (3.2 mg, 0.023 mmol) (quality: fine powder) and *cis*-[Ru(bpy)<sub>2</sub>Cl<sub>2</sub>] (24.3 mg, 0.047 mmol) in ethylene glycol (1.86 mL) (quality: Aldrich anhydrous 99.8%) was degassed with argon then heated at 165 °C (oil bath temperature) for 90 seconds. The reaction mixture was cooled to room temperature. The crude material was mixed with 2 mL CH<sub>3</sub>CN and subjected to flash silica gel chromatography. The elution was CH<sub>3</sub>CN: H<sub>2</sub>O: KNO<sub>3</sub>(sat) = 100: 4: 1. The product eluents were concentrated to dryness by evaporator, the resulting material was dissolved in minimal amounts of ethanol/water = 1/10 (2~3 mL), and the product was precipitated by the addition of solid NH<sub>4</sub>PF<sub>6</sub> (add NH<sub>4</sub>PF<sub>6</sub> together with shaking until the precipitate came and the colour of the solution from the orange to light yellow). The orange precipitate was centrifuged, washed twice with water, and dried under high vacuum to afford complex  $\Lambda$ -(*S*)-53 (31.0 mg, 86%). The absolute stereochemistry of  $\Lambda$ -(*S*)-53 was verified by X-ray crystallography of  $\Lambda$ -(*S*)-44 and CD analysis.

<sup>1</sup>H-NMR (300.1 MHz, CD<sub>3</sub>CN):  $\delta$  (ppm) 10.19 (dd,  $J = 5.2, 1.3$  Hz, 1H, 1-H), 8.75 (dq,  $J = 5.5, 0.6$  Hz, 1H), 8.57 (d,  $J = 8.1$  Hz, 1H), 8.36 – 8.43 (m, 3H), 8.26 (td,  $J = 7.7, 1.5$  Hz, 1H), 7.90 – 8.05 (m, 4H), 7.75 (ddd,  $J = 7.2, 5.7, 1.2$  Hz, 1H), 7.55 (ddd,  $J = 7.2, 5.7, 1.5$  Hz, 1H), 7.26 – 7.35 (m, 2H), 7.01 (dq,  $J = 6.2, 0.6$  Hz, 1H), 6.92 (d,  $J = 3.1$  Hz, 1H), 6.76 (dd,  $J = 9.1, 3.1$  Hz, 1H), 6.47 (d,  $J = 9.1$  Hz, 1H), 3.70 (s, 3H, 4-H), 2.95 (m, 1H, 2-H), 1.02 (d,  $J = 6.7$  Hz, 3H, CH(CH<sub>3</sub>)<sub>2</sub>), 0.34 (d,  $J = 6.7$  Hz, 3H, CH(CH<sub>3</sub>)<sub>2</sub>). <sup>13</sup>C-NMR (125.8 MHz, CD<sub>3</sub>CN)  $\delta$  (ppm) 169.1, 159.2, 158.9, 158.7,

157.4, 157.0, 154.4, 153.5, 149.9, 149.8, 139.6, 139.3, 138.4, 138.0, 128.7, 128.5, 127.7, 127.6, 127.4, 125.3, 124.9, 124.6, 124.4, 123.6, 121.4, 108.1, 61.6, 56.8, 17.2, 16.4. IR (neat):  $\nu(\text{cm}^{-1})$  2929, 1602, 1471, 1441, 1310, 1266, 1212, 1161, 1123, 1060, 1023, 832, 761, 730, 685, 643, 611, 555, 538, 516, 465, 420, 402. CD ( $\Delta\epsilon/\text{M}^{-1}\text{cm}^{-1}$ , MeCN): 280 nm (-64), 293 nm (+96). HRMS (ESI) calcd for  $\text{C}_{33}\text{H}_{35}\text{N}_4\text{O}_2\text{RuS}$  ( $\text{M-PF}_6$ )<sup>+</sup> 627.1006, found: 627.0995.

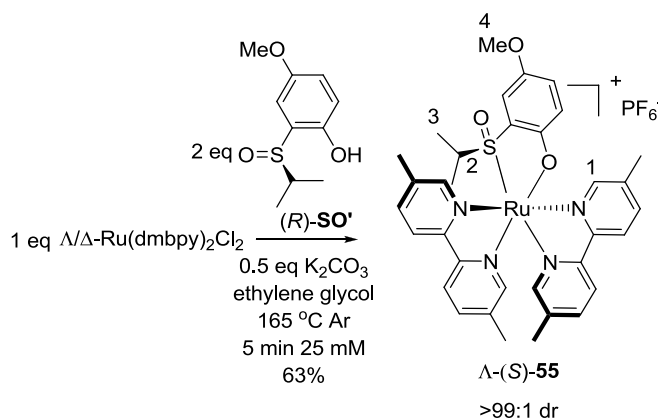


**$\Lambda$ -[Ru(phen)<sub>2</sub>((R)-2-(isopropylsulfinyl)-4-methoxyphenol)](PF<sub>6</sub>) ( $\Lambda$ -(S)-**54**).**

In a closed glass 1.5 mL vial fitted with a septum (brand: MACHEREY-NAGEL), a solution of (*S*)-1-(isopropylsulfinyl)-2-(methoxymethoxy) benzene (20.0 mg, 0.093 mmol), K<sub>2</sub>CO<sub>3</sub> (3.2 mg, 0.023 mmol) (quality: fine powder) and *cis*-[Ru(Phen)<sub>2</sub>Cl<sub>2</sub>] (26.6 mg, 0.047 mmol) in ethylene glycol (1.86 mL) (quality: Aldrich anhydrous 99.8%) was degassed with argon then heated at 165 °C (oil bath temperature) for 135 seconds. The reaction mixture was cooled to room temperature. The crude material was mixed with 2 mL CH<sub>3</sub>CN and subjected to flash silica gel chromatography. The elution was CH<sub>3</sub>CN: H<sub>2</sub>O: KNO<sub>3</sub>(sat) = 100: 4: 1. The product eluents were concentrated to dryness by evaporator, the resulting material was dissolved in minimal amounts of ethanol/water = 1/10 (2~3 mL), and the product was precipitated by the addition of solid NH<sub>4</sub>PF<sub>6</sub> (add NH<sub>4</sub>PF<sub>6</sub> together with shaking until the precipitate came and the colour of the solution from the orange to light yellow). The orange precipitate was centrifuged, washed twice with water, and dried under high vacuum to afford complex  $\Lambda$ -(S)-**54** (23.0 mg, 61%). The absolute stereochemistry of  $\Lambda$ -(S)-**54** was verified by X-ray crystallography of  $\Lambda$ -(S)-**44** and CD analysis.

<sup>1</sup>H-NMR (300.1 MHz, CD<sub>3</sub>CN):  $\delta$  (ppm) 10.63 (dd, *J* = 5.4, 1.3 Hz, 1H, 1-H), 9.17

(dd,  $J = 5.2, 1.3$  Hz, 1H), 8.85 (dd,  $J = 8.3, 1.3$  Hz, 1H), 8.57 (dd,  $J = 8.2, 1.3$  Hz, 1H), 8.45 (td,  $J = 7.2, 1.0$  Hz, 2H), 8.00 -8.33 (m, 6H), 7.94 (dd,  $J = 8.2, 5.4$  Hz, 1H), 7.40-7.51 (m, 2H), 7.19 (dd,  $J = 5.2, 1.3$  Hz, 1H), 7.05 (d,  $J = 3.0$  Hz, 1H), 6.75 (dd,  $J = 9.2, 3.1$  Hz, 2H), 6.45 (d,  $J = 9.2$  Hz, 1H), 3.73 (s, 1H, 4-H), 2.95 (m, 1H, 2-H), 0.78 (d,  $J = 6.7$  Hz, 3H, CH(CH<sub>3</sub>)<sub>2</sub>), - 0.05 (d,  $J = 6.7$  Hz, 3H, CH(CH<sub>3</sub>)<sub>2</sub>). <sup>13</sup>C-NMR (125.8 MHz, CD<sub>3</sub>CN)  $\delta$  (ppm) 158.1, 155.2, 155.0, 154.5, 154.1, 150.8, 150.1, 150.0, 149.7, 149.6, 147.6, 138.6, 138.4, 137.7, 137.0, 132.0, 131.8, 131.7, 131.3, 129.2, 129.0, 128.8, 128.7, 128.3, 127.2, 126.5, 126.3, 126.0, 124.0, 123.7, 121.4, 108.1, 62.1, 56.8, 16.9, 16.3. IR (neat):  $\nu$  (cm<sup>-1</sup>) 2927, 1630, 1579, 1471, 1427, 1407, 1269, 1212, 1147, 1068, 1055, 1025, 826, 739, 720, 686, 648, 555, 525, 508, 471, 401. CD ( $\Delta\epsilon/M^{-1}cm^{-1}$ , MeCN): 267 nm (+141), 256 nm (-122). HRMS (ESI) calcd for C<sub>33</sub>H<sub>27</sub>N<sub>4</sub>O<sub>2</sub>RuS (M-PF<sub>6</sub>)<sup>+</sup> 675.1007, found: 675.1006.

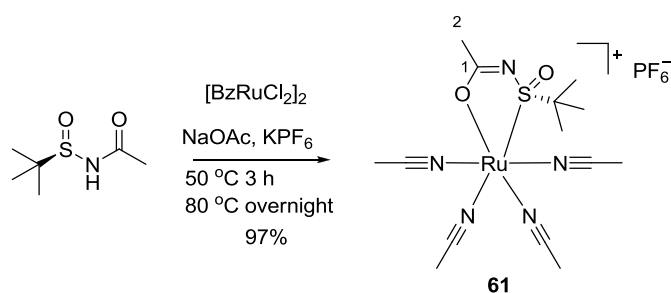


### $\Lambda$ -[Ru(dmbpy)<sub>2</sub>((*R*)-2-(isopropylsulfinyl)-4-methoxyphenol)]PF<sub>6</sub> ( $\Lambda$ -(*S*)-55).

In a closed glass 1.5 mL vial fitted with a septum (brand: MACHEREY-NAGEL), a solution of (*S*)-1-(isopropylsulfinyl)-2-(methoxymethoxy) benzene (20.0 mg, 0.093 mmol), K<sub>2</sub>CO<sub>3</sub> (3.2 mg, 0.023 mmol) (quality: fine powder) and *cis*-[Ru(dmbpy)<sub>2</sub>Cl<sub>2</sub>] (28.0 mg, 0.047 mmol) in ethylene glycol (1.86 mL) (quality: Aldrich anhydrous 99.8%) was degassed with argon then heated at 165 °C (oil bath temperature) for 5 min. The reaction mixture was cooled to room temperature. The crude material was mixed with 2 mL CH<sub>3</sub>CN and subjected to flash silica gel chromatography. The elution was CH<sub>3</sub>CN: H<sub>2</sub>O: KNO<sub>3</sub>(sat) = 100: 4: 1. The product eluents were concentrated to dryness by evaporator, the resulting material was dissolved in minimal

amounts of ethanol/water = 1/10 (2~3 mL), and the product was precipitated by the addition of solid  $\text{NH}_4\text{PF}_6$  (add  $\text{NH}_4\text{PF}_6$  together with shaking until the precipitate came and the colour of the solution from the orange to light yellow). The orange precipitate was centrifuged, washed twice with water, and dried under high vacuum to afford complex  $\Lambda$ -(*S*)-**55** (25.0 mg, 64%). The absolute stereochemistry of  $\Lambda$ -(*S*)-**55** was verified by X-ray crystallography of  $\Lambda$ -(*S*)-**44** and CD analysis.

$^1\text{H-NMR}$  (500.1 MHz,  $\text{CD}_3\text{CN}$ ):  $\delta$  (ppm) 10.01 (dd,  $J = 1.3, 0.7$  Hz 1H, 1-H), 8.51 (dd,  $J = 1.3, 0.6$  Hz 1H), 8.39 (d,  $J = 8.4$  Hz, 1H), 8.17-8.25 (m, 3H), 8.05 (ddd,  $J = 8.3, 1.9, 0.6$  Hz 1H), 7.70-7.83 (m, 4H), 6.96 (d,  $J = 3.1$  Hz 1H), 6.75 (dd,  $J = 9.1, 3.1$  Hz, 1H), 6.70 (dd,  $J = 1.2, 0.7$  Hz, 1H), 6.46 (d,  $J = 9.1$  Hz 1H), 3.71 (s, 3H, 4-H), 2.95 (m, 1H, 2-H), 2.47 (s, 3H, C- $\text{CH}_3$ ), 2.37 (s, 3H, C- $\text{CH}_3$ ), 2.18 (s, 3H, C- $\text{CH}_3$ ), 2.12 (s, 3H, C- $\text{CH}_3$ ), 1.06 (d,  $J = 6.7$  Hz, 3H,  $\text{CH}(\text{CH}_3)_2$ ), 0.36 (d,  $J = 6.7$  Hz, 3H,  $\text{CH}(\text{CH}_3)_2$ ).  $^{13}\text{C-NMR}$  (125.8 MHz,  $\text{CD}_3\text{CN}$ )  $\delta$  (ppm) 169.0, 157.2, 156.8, 156.5, 156.2, 155.1, 154.1, 154.0, 153.0, 152.8, 149.8, 149.7, 140.1, 139.8, 139.6, 139.3, 139.2, 138.7, 138.6, 138.4, 137.9, 137.8, 129.3, 124.3, 123.9, 123.5, 123.4, 121.3, 108.4, 61.4, 59.9, 18.9, 18.8, 18.7, 18.4, 17.1, 16.5. CD ( $\Delta\epsilon/\text{M}^{-1}\text{cm}^{-1}$ , MeCN): 299 nm (+82), 285 nm (-62). HRMS (ESI) calcd for  $\text{C}_{33}\text{H}_{35}\text{N}_4\text{O}_2\text{RuS}$  ( $\text{M-PF}_6$ ) $^+$  683.1633, found: 683.1619.

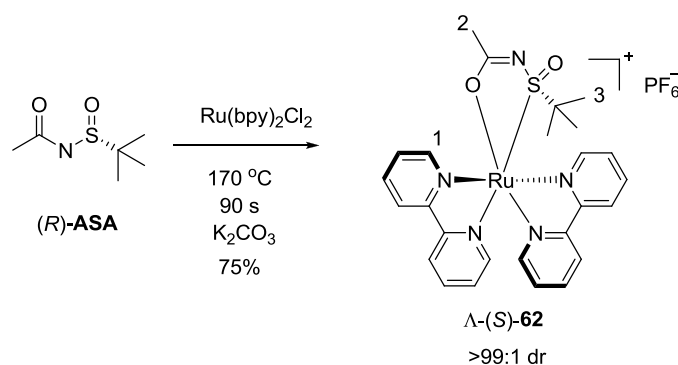


**[Ru(*R*)-ASA)(MeCN) $_4$ ](PF $_6$ ) (**61**).**

To a round bottom flask was added (*R*)-*N*-acetyl-*tert*-butansulfonamide (20 mg, 1.22 mmol),  $[\text{Ru}(\eta^6\text{-C}_6\text{H}_6)\text{Cl}_2]_2$  (45.9 mg, 0.09 mmol), NaOAc  $3\text{H}_2\text{O}$  (50.2 mg, 0.37 mmol),  $\text{KPF}_6$  (45.1 mg, 0.24 mmol) and MeCN (3 mL). Then, the solution was carefully degassed with argon for 30 min. After stirring at 50 °C for 3 hours, the

mixture heated at 80 °C overnight. The reaction mixture was cooled to room temperature and the crude material subjected to flash neutral aluminum oxide chromatography with MeCN to yield complex **61** as yellow solid (68 mg, 97%).

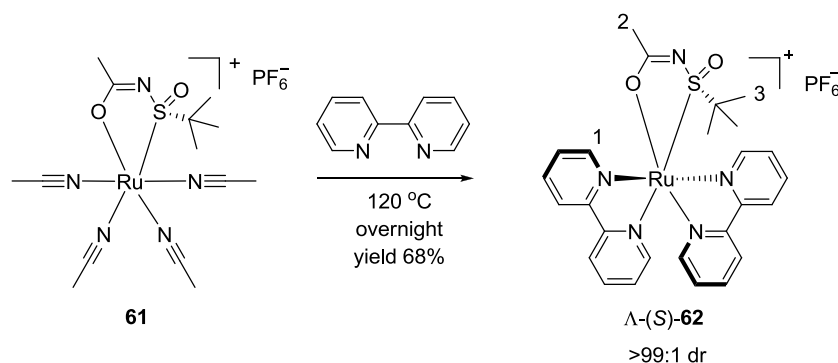
<sup>1</sup>H-NMR (300.1 MHz, CD<sub>3</sub>CN): δ (ppm) 2.44 (s, 3H, 2-H), 2.42 (s, 3H, CNCH<sub>3</sub>), 2.37 (s, 3H, CNCH<sub>3</sub>), 2.18 (s, 3H, CNCH<sub>3</sub>), 2.12 (s, 3H, CNCH<sub>3</sub>), 1.29 (s, 9H, C-(CH<sub>3</sub>)<sub>3</sub>). <sup>13</sup>C-NMR (75.5 MHz, CD<sub>3</sub>CN): δ (ppm) 188.3 (C-1), 128.3 (CNCH<sub>3</sub>), 126.8 (CNCH<sub>3</sub>), 125.0 (CNCH<sub>3</sub>), 124.6 (CNCH<sub>3</sub>), 65.6 (C-(CH<sub>3</sub>)<sub>3</sub>), 24.1 (C-(CH<sub>3</sub>)<sub>3</sub>), 20.9 (C-(CH<sub>3</sub>)<sub>3</sub>), 4.5 (CNCH<sub>3</sub>), 4.2 (CNCH<sub>3</sub>), 4.1 (CNCH<sub>3</sub>), 1.8 (CNCH<sub>3</sub>). IR (thin film): ν (cm<sup>-1</sup>): 2986, 2933, 1488, 1394, 1343, 1116, 830, 793, 637, 555, 512. CD (Δε/M<sup>-1</sup>cm<sup>-1</sup>, MeCN): 189 nm (+35), 228 nm (-15), 253 nm (+8). HRMS (ESI) calcd for C<sub>14</sub>H<sub>24</sub>N<sub>5</sub>O<sub>2</sub>RuS (M)<sup>+</sup>: 428.0692, found: 428.0688.



### $\Delta$ -[Ru(bpy)<sub>2</sub>((R)-ASA)](PF<sub>6</sub>) ( $\Delta$ -(S)-**62**).

*Synthesis from racemic cis-[Ru(bpy)<sub>2</sub>Cl<sub>2</sub>]*: In a closed glass 8 mL vial fitted with a septum (brand: CS-chromatographie serrice GmbH), a solution of (R)-N-acetyl-tert-butansulfonamide (62.5 mg, 0.38 mmol), K<sub>2</sub>CO<sub>3</sub> (13.2 mg, 0.095 mmol) (quality: fine powder), and *cis*-[Ru(bpy)<sub>2</sub>Cl<sub>2</sub>] (100 mg, 0.19 mmol) in ethylene glycol (3.8 mL) (quality: Aldrich anhydrous 99.8%) was degassed with argon and then heated at 170 °C (oil bath temperature) for 2 min. [NOTE: The optimal reaction time can change as a function of the used reaction vessel and scale.] The reaction mixture was cooled to room temperature. The crude material was mixed with 4 mL CH<sub>3</sub>CN and subjected to flash silica gel chromatography (25 x 5 cm). The elution was CH<sub>3</sub>CN: H<sub>2</sub>O: KNO<sub>3</sub>(sat) = 50: 3: 1. And collect isolate the orange-red fraction. The product eluents were concentrated to dryness by evaporator, the resulting material was

dissolved in 10 mL water, and the product was precipitated by the addition of solid  $\text{NH}_4\text{PF}_6$  (add  $\text{NH}_4\text{PF}_6$  together with shaking until the precipitate came and the colour of the solution from the orange to light yellow). Then,  $\text{CH}_2\text{Cl}_2$  (10 mL) was added and the layers were separated. The aqueous phase was extracted with  $\text{CH}_2\text{Cl}_2$  (2 x 10 mL), and the combined organic extracts were dried ( $\text{Na}_2\text{SO}_4$ ), filtered, and concentrated to give complex  $\Lambda$ -(S)-**62** as its  $\text{PF}_6^-$  salt (red solid, 107 mg, 77%). The product purity could be further improved by recrystallization from THF. For this,  $\Lambda$ -(S)-**62** was first dissolved in  $\text{CH}_2\text{Cl}_2$  and evaporated by rotary evaporation, but not to complete dryness. The residue was dissolved in THF (2 mL) and heated to 80 °C. After slow cooling to room temperature over a time period of 1 hour, the formed large crystals were filtered off and washed with small amounts of THF.

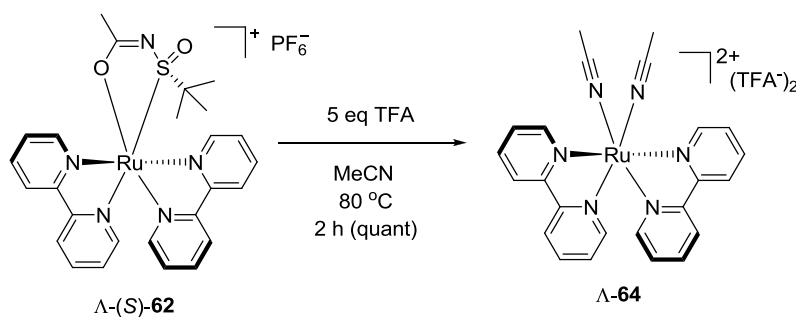


#### $\Lambda$ -[Ru(bpy)<sub>2</sub>((R)-ASA)](PF<sub>6</sub>) ( $\Lambda$ -(S)-**62**).

*Synthesis from complex 61:* In a closed glass 1.5 mL vial fitted with a septum (brand: MACHEREY-NAGEL), a solution of complex **61** (20 mg, 0.035 mmol) and 2,2'-bipyridine (13.6 mg, 0.087 mmol) in chlorobenzene (0.6 mL) was degassed with argon and then heated at 120 °C (oil bath temperature) for 16 hours. The reaction mixture was cooled to room temperature and the crude material subjected to flash silica gel chromatography eluting with  $\text{CH}_3\text{CN}:\text{H}_2\text{O}:\text{KNO}_3(\text{sat}) = 50:3:1$ . The product eluents were concentrated to dryness by evaporator, the resulting material was dissolved in 10 mL water, and solid  $\text{NH}_4\text{PF}_6$  was added (add  $\text{NH}_4\text{PF}_6$  together with shaking until the precipitate came and the colour of the solution from the orange to light yellow). From this mixture, the complex was extracted with  $\text{CH}_2\text{Cl}_2$  (3 x 10 mL) and the combined organic extracts were dried over  $\text{Na}_2\text{SO}_4$ , filtered, and concentrated to give complex  $\Lambda$ -(S)-**61** as its  $\text{PF}_6^-$  salt and as a single diastereomer (red solid, 17 mg,

68%). The absolute stereochemistry of  $\Lambda$ -(*S*)-**61** was verified by X-ray crystallography (Figure 20).

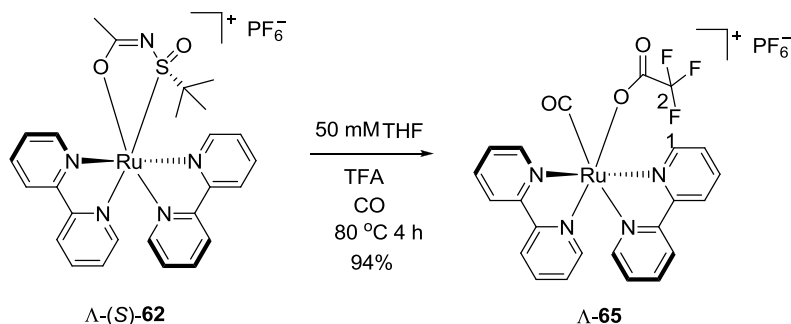
$^1\text{H-NMR}$  (300.1 MHz,  $\text{CD}_3\text{CN}$ ):  $\delta$  (ppm) 10.68 (ddd,  $J = 5.9, 1.4, 0.5$  Hz, 1H, 1-H), 8.65 (ddd,  $J = 5.6, 1.4, 0.7$  Hz, 1H), 8.55 (d,  $J = 8.0$  Hz, 1H), 8.33 – 8.44 (m, 3H), 8.24 (td,  $J = 7.8, 1.5$  Hz, 1H), 8.12 (td,  $J = 7.6, 1.5$  Hz, 1H), 8.02 (ddd,  $J = 5.7, 1.4, 0.7$  Hz, 1H), 7.97 (td,  $J = 7.7, 1.5$  Hz, 1H), 7.89 (td,  $J = 7.7, 1.5$  Hz, 1H), 7.72 – 7.79 (m, 2H), 7.24 – 7.35 (m, 2H), 6.90 (ddd,  $J = 5.7, 1.4, 0.7$  Hz, 1H), 2.17 (s, 3H, 2-H), 0.64 (s, 9H, 3-H).  $^{13}\text{C-NMR}$  (75.5 MHz,  $\text{CD}_3\text{CN}$ ):  $\delta$  (ppm) 187.5, 159.4, 158.8, 158.5, 157.8, 157.6, 154.5, 154.1, 149.8, 139.5, 138.9, 137.9, 128.5, 127.8, 127.7, 127.6, 125.6, 124.8, 124.4, 124.3, 68.1, 23.8, 21.6. IR (thin film):  $\nu$  ( $\text{cm}^{-1}$ ) 3119, 3056, 3036, 2966, 2852, 1603, 1479, 1464, 1446, 1417, 1395, 1364, 1348, 1266, 1227, 1168, 1089, 1062, 1025, 903, 878, 833, 781, 767, 731, 665, 636, 599, 556, 504, 447, 426. CD ( $\Delta\epsilon/\text{M}^{-1}\text{cm}^{-1}$ , MeCN): 292 nm (+108), 278 nm (-54). HRMS (ESI) calcd for  $\text{C}_{26}\text{H}_{28}\text{N}_5\text{O}_2\text{RuS}$  ( $\text{M}$ ) $^+$ : 576.1008, found: 576.0097.



#### $\Lambda$ -[Ru(bpy) $_2$ (MeCN) $_2$ ](TFA) $_2$ ( $\Lambda$ -**64**).

The following reaction was executed in the dark, while workup and purification were performed under reduced light. In a closed 1.5 mL brown glass vial fitted with a septum (brand: Agilent), a solution of complex  $\Lambda$ -(*S*)-**62** (20.0 mg, 0.028 mmol) and TFA (17  $\mu\text{L}$ , 0.22 mmol) in MeCN (0.55 mL) was heated at 80  $^\circ\text{C}$  (oil bath temperature) for 2 hours. The reaction mixture was cooled to room temperature and concentrated to give an orange solid. The solid was washed with  $\text{Et}_2\text{O}$  and dried in high vacuum to afford the reported complex  $\Lambda$ -**64** as a mixed  $\text{PF}_6^-/\text{trifluoroacetate}$  salt (20 mg, 100%).<sup>27</sup> The absolute configuration of the complex  $\Lambda$ -**64** was relative from

the starting material  $\Lambda$ -(*S*)-**62** together with the configuration retention in the substitution reaction<sup>47,48</sup>. The analytical data was already published<sup>82</sup>.



### $\Lambda$ -[Ru(bpy)<sub>2</sub>(CO)(TFA)](PF<sub>6</sub>) ( $\Lambda$ -**65**).

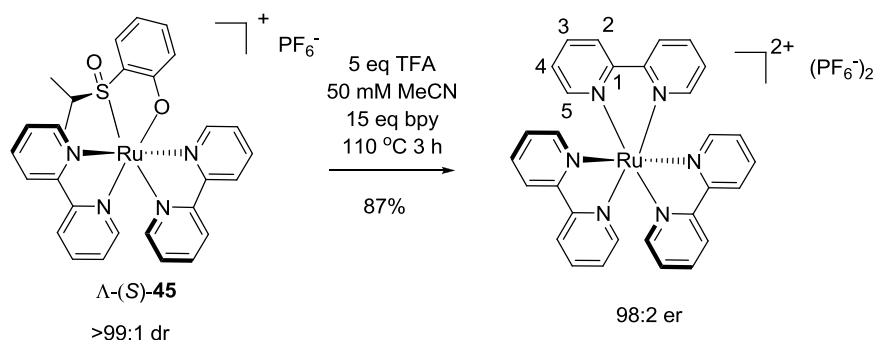
The following reaction was executed in the dark, while workup and purification were performed under reduced light. In a sealed tube (10 mL) covered with aluminium foil, a solution of complex  $\Lambda$ -(*S*)-**62** (35.0 mg, 0.048 mmol) and TFA (29.7  $\mu$ L, 0.39 mmol) in THF (0.48 mL) was purged with CO and then heated at 80 °C (oil bath temperature) for 4 hours. The reaction mixture was cooled to room temperature and the crude material subjected to flash silica gel chromatography eluting with CH<sub>3</sub>CN: H<sub>2</sub>O: KNO<sub>3</sub>(sat) = 50: 3: 1. The product eluents were concentrated to dryness by evaporator, the resulting material was dissolved in minimal amounts of ethanol/water = 1/10 (3~ 4 mL), and the product was precipitated by the addition of solid NH<sub>4</sub>PF<sub>6</sub> (add NH<sub>4</sub>PF<sub>6</sub> together with shaking until the precipitate came and the colour of the solution from the yellow to colourless). The yellow precipitate was centrifuged, washed twice with water, and dried under high vacuum to afford complex  $\Lambda$ -**65** as its PF<sub>6</sub> salt (31 mg, 92%). The absolute stereochemistry of  $\Lambda$ -**65** was verified by X-ray crystallography.

<sup>1</sup>H-NMR (500.1 MHz, CD<sub>3</sub>CN):  $\delta$  (ppm) 9.57 (d,  $J$  = 5.1 Hz, 1H, 1-H), 8.77 (d,  $J$  = 4.9 Hz, 1H), 8.53 (d,  $J$  = 8.1 Hz, 1H), 8.46 (t,  $J$  = 8.8 Hz, 2H), 8.33 – 8.39 (m, 2H), 8.21 (td,  $J$  = 8.0, 1.3 Hz, 1H), 8.16 (td,  $J$  = 8.0, 1.5 Hz, 1H), 8.03 (td,  $J$  = 7.9, 1.5 Hz, 1H), 7.88 (m, 1H), 7.74 (m, 1H), 7.69 (d,  $J$  = 5.5 Hz, 1H), 7.53 (d,  $J$  = 4.7 Hz, 1H), 7.47 (m, 1H), 7.30 (m, 1H). <sup>13</sup>C-NMR (125.8 MHz, CD<sub>3</sub>CN):  $\delta$  (ppm) 200.5 (CO), 163.7 (quartet,  $J$  = 35.7 Hz, CO-CF<sub>3</sub>), 158.3, 158.0, 157.7, 157.3, 156.2, 154.1, 152.5, 149.4, 141.7, 141.2, 140.3, 140.26, 129.1, 128.6, 128.45, 128.41, 125.5, 125.3, 125.2,



124.7,157.6 (quartet,  $J = 290.4$  Hz,  $\text{CF}_3$ ). IR (thin film):  $\nu$  ( $\text{cm}^{-1}$ ) 3088, 2961, 2922, 1975, 1697, 1605, 1471, 1447, 1401, 1240, 1183, 1129, 829, 762, 726, 643, 591, 553, 502, 455, 417. CD ( $\Delta\epsilon/\text{M}^{-1}\text{cm}^{-1}$ , MeCN): 260 nm (+40), 278 nm (-49), 300 nm (+30), 312 nm (+31). HRMS (ESI) calcd for  $\text{C}_{23}\text{H}_{16}\text{F}_3\text{N}_4\text{O}_3\text{Ru}$  ( $\text{M}$ )<sup>+</sup>: 555.0219, found: 555.0207.

### 5.2.3 Auxiliary removal



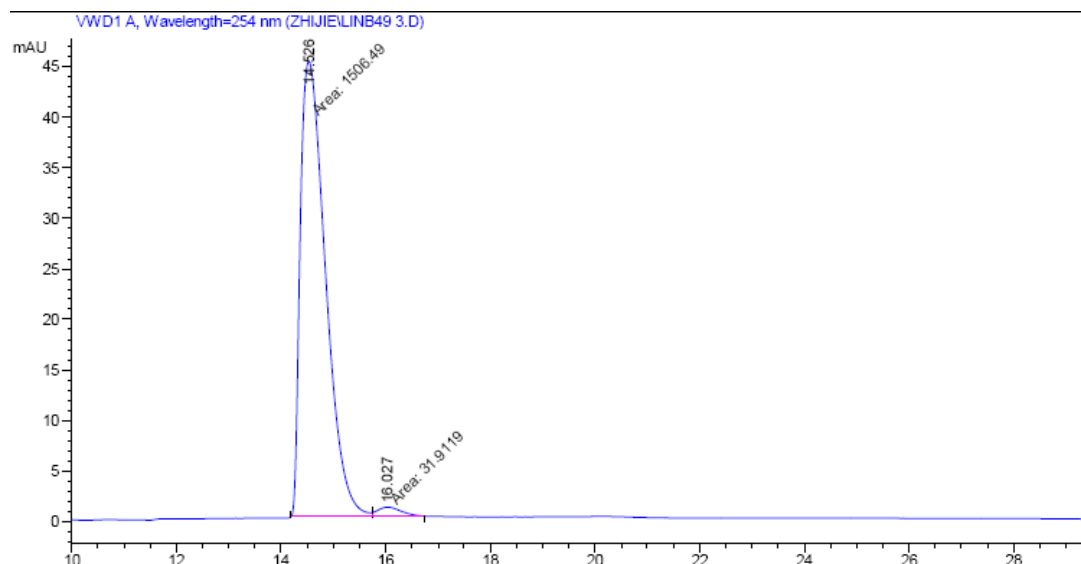
#### $\Lambda\text{-[Ru(bpy)}_3\text{](PF}_6\text{)}_2$ .

In a closed 1.5 mL brown glass vial fitted with a septum (brand: Agilent), a solution of  $\Lambda\text{-(S)-45}$  (14.0 mg, 0.018 mmol), 2,2'-bipyridine (44.1 mg, 0.28 mmol), and TFA (0.0072 mL, 0.09 mmol) in  $\text{CH}_3\text{CN}$  (0.36 mL) (quality: anhydrous) was heated at 110 °C (oil bath temperature) for 2 h under a nitrogen atmosphere. The reaction mixture was cooled to room temperature. The crude material was subjected to silica gel chromatography eluting with  $\text{CH}_3\text{CN}:\text{H}_2\text{O}:\text{KNO}_3(\text{sat}) = 50:6:2$ . The product eluents were concentrated to dryness by evaporator, the resulting material was dissolved in minimal amounts of ethanol/water = 1/10 (2~3 mL), and the product was precipitated by the addition of solid  $\text{NH}_4\text{PF}_6$  (add  $\text{NH}_4\text{PF}_6$  together with shaking until the precipitate came and the colour of the solution from the orange to light yellow). The orange precipitate was centrifuged, washed twice with water, and dried under high vacuum to afford  $\Lambda\text{-[Ru(bpy)}_3\text{](PF}_6\text{)}_2$  (14.0 mg, 87%). The absolute stereochemistry of the  $\Lambda\text{-[Ru(bpy)}_3\text{](PF}_6\text{)}_2$  was verified by two aspects. Firstly,  $\Lambda\text{-[Ru(bpy)}_3\text{](PF}_6\text{)}_2$  shows the similar CD spectrum to the  $\Lambda\text{-[Ru(4,4'-}i\text{Bu}_2\text{bpy)(5,5'-Me}_2\text{bpy)(bpy)]}^{2+}$  (4,4'-*tert*-butyl-2,2'-bipyridine, 5,5'-*Me*<sub>2</sub>bpy)

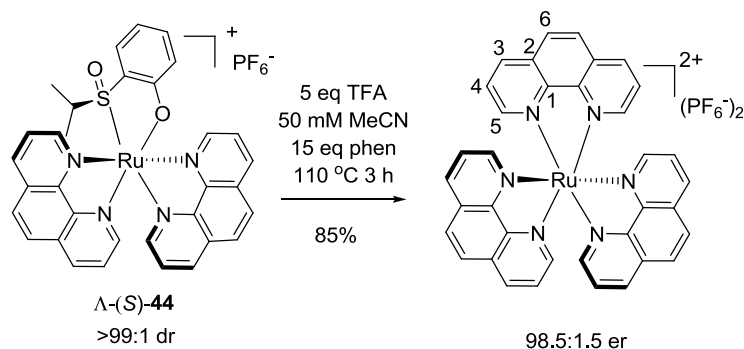
= 5,5'-dimethyl-2,2'-bipyridine) which the configuration was confirmed by crystal structure. Secondly, according to the work from Keene<sup>47</sup> and Hua<sup>48</sup>, the  $\Lambda$ -[Ru(bpy)<sub>3</sub>](PF<sub>6</sub>)<sub>2</sub> will retain the configuration in the substitution reaction. The enantiopurity (98: 2 er) was determined by chiral HPLC analysis (Figure 48).

<sup>1</sup>H-NMR (300.1 MHz, CD<sub>3</sub>CN):  $\delta$  (ppm) 8.53 (d,  $J$  = 8.1 Hz, 6H, 5-H), 8.08 (td,  $J$  = 8.0, 1.4 Hz, 6H, 4-H), 7.76 (d,  $J$  = 5.6 Hz, 6H, 2-H), 7.42 (ddd,  $J$  = 7.4, 5.6, 1.0 Hz, 6H, 3-H). <sup>13</sup>C-NMR (100.6 MHz, CD<sub>3</sub>CN):  $\delta$  (ppm) 157.0 (C-1), 151.7 (C-5), 137.8, 127.5, 124.3. IR (neat):  $\nu$  (cm<sup>-1</sup>) 1446, 833, 756, 555. CD ( $\Delta\epsilon$ /M<sup>-1</sup>cm<sup>-1</sup>, MeCN): 278 nm (-155), 292 nm (+365). HRMS (ESI) calcd for RuF<sub>6</sub>N<sub>6</sub>C<sub>30</sub>H<sub>24</sub>P (M-PF<sub>6</sub>) 715.0747, found: 715.0724.

**Determination of enantiomeric ratio of  $\Lambda$ -[Ru(bpy)<sub>3</sub>](PF<sub>6</sub>)<sub>2</sub> by chiral HPLC.** The ruthenium complex was analyzed with a Daicel Chiralcel OD-R (250 × 4 mm) HPLC column on an Agilent 1200 Series HPLC System. The flow rate was 0.5 mL/min, the column temperature 40 °C, and UV-absorption was measured at 254 nm. Solvent A = 0.087% H<sub>3</sub>PO<sub>4</sub>, solvent B = MeCN, with a linear gradient of 8% to 14% B in 20 min.



**Figure 48.** HPLC trace for [Ru(bpy)<sub>3</sub>]<sup>2+</sup>. Integration of peak areas: 98: 2 er.



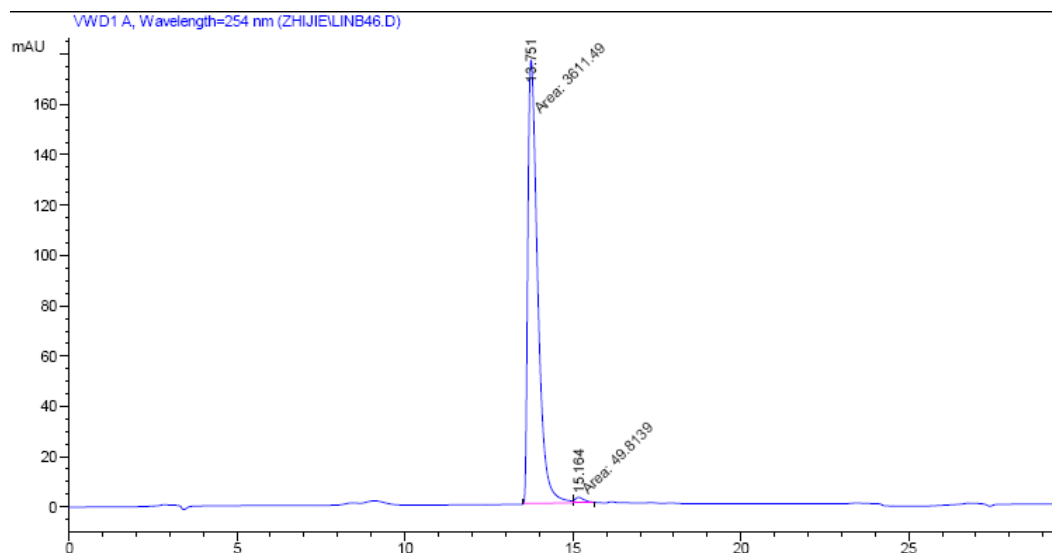
### $\Lambda$ -[Ru(phen)<sub>3</sub>](PF<sub>6</sub>)<sub>2</sub>.

In a closed 1.5 mL brown glass vial fitted with a septum (brand: Agilent), a solution of  $\Lambda$ -(S)-**44** (12.0 mg, 0.015 mmol), 1,10-phenanthroline (41.0 mg, 0.23 mmol) and TFA (0.0058 mL, 0.07 mmol) in CH<sub>3</sub>CN (0.3 mL) (quality: anhydrous) was heated at 110 °C (oil bath temperature) for 2 h under a nitrogen atmosphere. The reaction mixture was cooled to room temperature. The crude material was subjected to silica gel chromatography eluting with CH<sub>3</sub>CN: H<sub>2</sub>O: KNO<sub>3</sub>(sat) = 50: 6: 2. The product eluents were concentrated to dryness by evaporator, the resulting material was dissolved in minimal amounts of ethanol/water = 1/10 (2~3 mL), and the product was precipitated by the addition of solid NH<sub>4</sub>PF<sub>6</sub> (add NH<sub>4</sub>PF<sub>6</sub> together with shaking until the precipitate came and the colour of the solution from the orange to light yellow). The orange precipitate was centrifuged, washed twice with water, and dried under high vacuum to afford  $\Lambda$ -[Ru(phen)<sub>3</sub>](PF<sub>6</sub>)<sub>2</sub> (12.0 mg, 85%). The  $\Lambda$ -configuration of  $\Lambda$ -[Ru(phen)<sub>3</sub>](PF<sub>6</sub>)<sub>2</sub> was verified by comparing CD spectrum with  $\Lambda$ -[Ru(bpy)<sub>3</sub>](PF<sub>6</sub>)<sub>2</sub> and the enantiopurity (98.5: 1.5 er) was determined by chiral HPLC analysis (Figure 49).

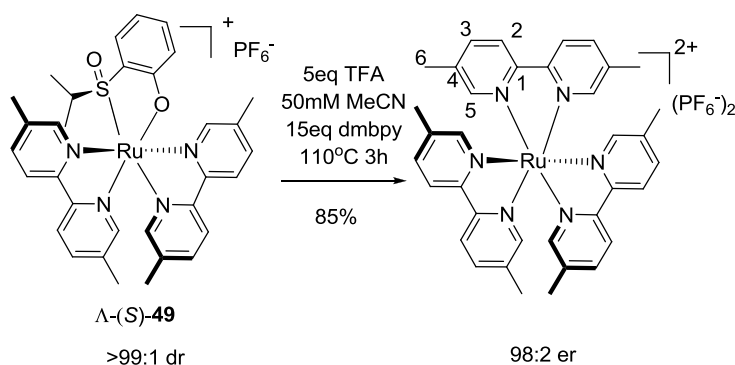
<sup>1</sup>H-NMR (500.1 MHz, CD<sub>3</sub>CN):  $\delta$  (ppm) 8.59 (dd,  $J = 8.3$  Hz,  $J = 1.1$  Hz, 6H, 5-H), 8.25 (s, 6H, 6-H), 8.01 (dd,  $J = 5.3$  Hz,  $J = 1.1$  Hz, 6H, 3-H), 7.62 (dd,  $J = 8.2$  Hz,  $J = 5.2$  Hz, 6H, 4-H). <sup>13</sup>C-NMR (100.6 MHz, CD<sub>3</sub>CN):  $\delta$  (ppm) 154.0, 149.0, 137.8, 132.0, 129.0, 126.9. IR (neat):  $\nu$  (cm<sup>-1</sup>) 1427, 831, 718, 555. CD ( $\Delta\epsilon/M^{-1}cm^{-1}$ , MeCN): 267 nm (+606), 257 nm (-496). HRMS (ESI) calcd for C<sub>37</sub>H<sub>27</sub>F<sub>6</sub>N<sub>6</sub>PRu (M-PF<sub>6</sub>) 787.0752, found: 787.0735.

**Determination of enantiomeric ratio of  $\Lambda$ -[Ru(phen)<sub>3</sub>](PF<sub>6</sub>)<sub>2</sub> by chiral HPLC.** The

ruthenium complex was analyzed with a Daicel Chiralcel OD-R (250 × 4 mm) HPLC column on an Agilent 1200 Series HPLC System. The flow rate was 0.5 mL/min, the column temperature 40 °C, and UV-absorption was measured at 254 nm. Solvent A = 0.087% H<sub>3</sub>PO<sub>4</sub>, solvent B = MeCN, with a linear gradient of 15% to 40% B in 20 min.



**Figure 49.** HPLC trace for [Ru(phen)<sub>3</sub>]<sup>2+</sup>. Integration of peak areas: 98.5: 1.5 er.



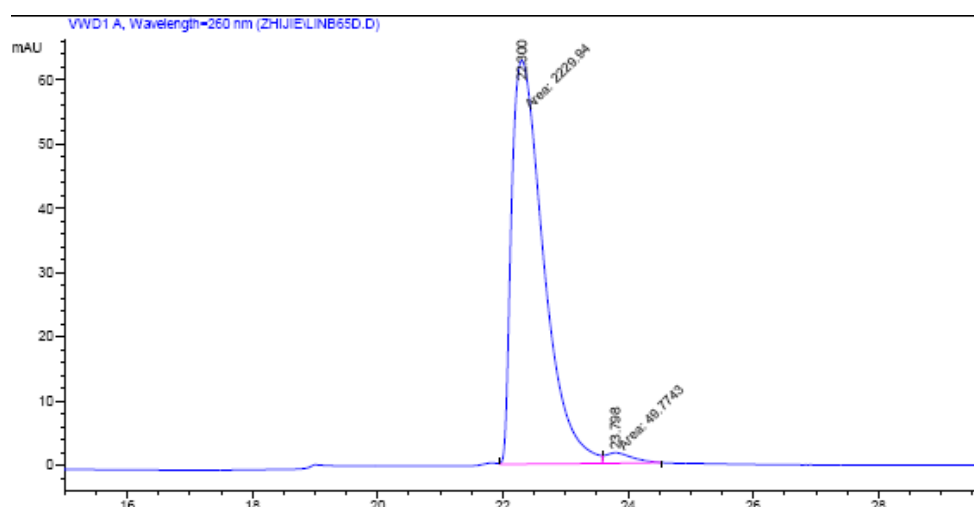
### $\Lambda$ -[Ru(dmbpy)<sub>3</sub>](PF<sub>6</sub>)<sub>2</sub>

In a closed 1.5 mL brown glass vial fitted with a septum (brand: Agilent), a solution of  $\Lambda$ -(S)-**49** (12 mg, 0.015 mmol), 5,5'-dimethyl-2,2'-bipyridine (41.5 mg, 0.225 mmol) and TFA (0.0057 mL, 0.07 mmol) in CH<sub>3</sub>CN (0.3 mL) (quality: anhydrous) was heated at 110 °C (oil bath temperature) for 2 h under a nitrogen atmosphere. The reaction mixture was cooled to room temperature. The crude material was subjected to silica gel chromatography eluting with CH<sub>3</sub>CN: H<sub>2</sub>O: KNO<sub>3</sub>(sat) = 50: 6: 2. The

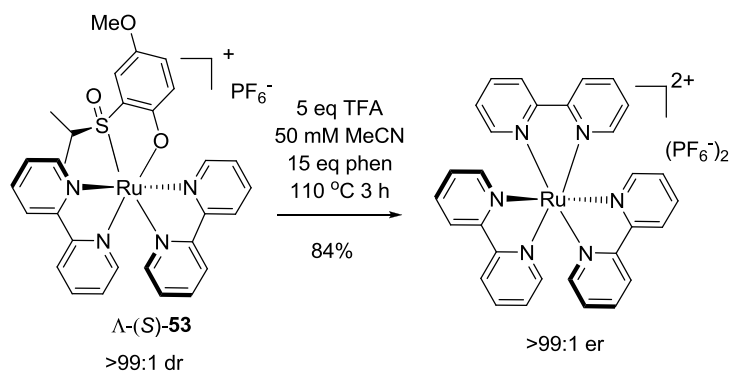
product eluents were concentrated to dryness by evaporater, the resulting material was dissolved in minimal amounts of ethanol/water = 1/10 (2~3 mL), and the product was precipitated by the addition of solid  $\text{NH}_4\text{PF}_6$  (add  $\text{NH}_4\text{PF}_6$  together with shaking until the precipitate came and the colour of the solution from the orange to light yellow). The orange precipitate was centrifuged, washed twice with water, and dried under high vacuum to afford  $\Lambda$ -[Ru(dmbpy) $_3$ ](PF $_6$ ) $_2$  (13 mg, 91%). The  $\Lambda$ -configuration of  $\Lambda$ -[Ru(dmbpy) $_3$ ](PF $_6$ ) $_2$  was verified by comparing CD spectrum with  $\Lambda$ -[Ru(bpy) $_3$ ](PF $_6$ ) $_2$  and the enantiopurity (98: 2 er) was determined by chiral HPLC analysis (Figure 50).  $^1\text{H-NMR}$  (400 MHz, CD $_3\text{CN}$ ):  $\delta$  (ppm) 8.29 (d,  $J$  = 8.4 Hz, 6H, 2-H), 7.83 (d,  $J$  = 8.3 Hz, 6H, 3-H), 7.43 (s, 6H, 5-H), 2.19 (s, 18 H, 6-H).  $^{13}\text{C-NMR}$  (100.6 MHz, CD $_3\text{CN}$ ):  $\delta$  (ppm) 155.6, 152.3, 139.0, 124.2, 18.6. IR (neat):  $\nu$  (cm $^{-1}$ ) 1475, 1242, 820, 556, 520, 433. CD ( $\Delta\epsilon/\text{M}^{-1}\text{cm}^{-1}$ , MeCN): 299 nm (+276), 284 nm (-127). HRMS (ESI) calcd for C $_{37}\text{H}_{39}\text{F}_6\text{N}_6\text{PRu}$  (M-PF $_6$ ) 799.1687, found: 799.1664.

#### Determination of enantiomeric ratio of $\Lambda$ -[Ru(dmbpy) $_3$ ](PF $_6$ ) $_2$ by chiral HPLC.

The ruthenium complex was analyzed with a Daicel Chiralcel OD-R (250  $\times$  4 mm) HPLC column on an Agilent 1200 Series HPLC System. The flow rate was 0.5 mL/min, the column temperature 40  $^\circ\text{C}$ , and UV-absorption was measured at 254 nm. Solvent A = 0.087% H $_3\text{PO}_4$ , solvent B = MeCN, with a linear gradient of 14% to 27% B in 20 min, then 27% B in 5min.



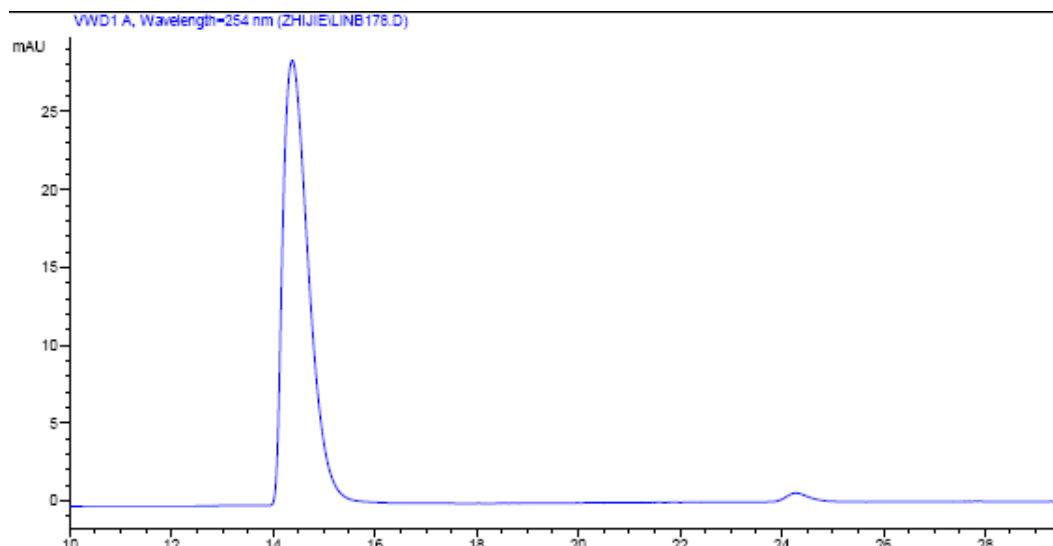
**Figure 50.** HPLC trace for [Ru(dmbpy) $_3$ ] $^{2+}$ . Integration of peak areas: 98 : 2 er.



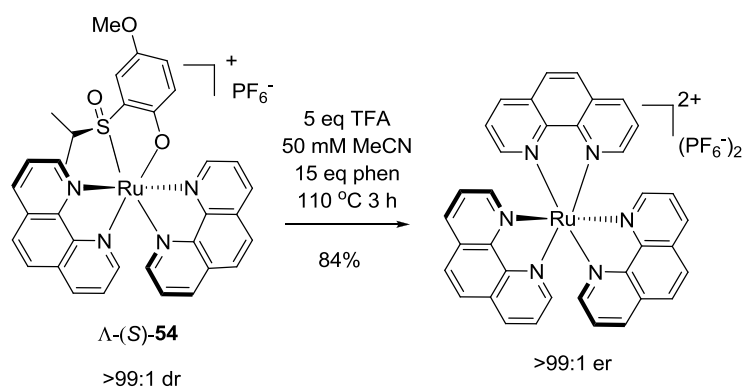
### $\Lambda$ -[Ru(bpy)<sub>3</sub>](PF<sub>6</sub>)<sub>2</sub>.

In a closed 1.5 mL brown glass vial fitted with a septum (brand: Agilent), a solution of  $\Lambda$ -(S)-**53** (7 mg, 0.009 mmol), 2,2'-bipyridine (21 mg, 0.136 mmol), and TFA (0.0034 mL, 0.045 mmol) in CH<sub>3</sub>CN (0.18 mL) (quality: anhydrous) was heated at 110 °C (oil bath temperature) for 2 h under a nitrogen atmosphere. The reaction mixture was cooled to room temperature. The crude material was subjected to silica gel chromatography eluting with CH<sub>3</sub>CN: H<sub>2</sub>O: KNO<sub>3</sub>(sat) = 50: 6: 2. The product eluents were concentrated to dryness by evaporator, the resulting material was dissolved in minimal amounts of ethanol/water = 1/10 (2~3 mL), and the product was precipitated by the addition of solid NH<sub>4</sub>PF<sub>6</sub> (add NH<sub>4</sub>PF<sub>6</sub> together with shaking until the precipitate came and the colour of the solution from the orange to light yellow). The orange precipitate was centrifuged, washed twice with water, and dried under high vacuum to afford  $\Lambda$ -[Ru(bpy)<sub>3</sub>](PF<sub>6</sub>)<sub>2</sub> (6.6 mg, 84%). The  $\Lambda$ -configuration of  $\Lambda$ -[Ru(bpy)<sub>3</sub>](PF<sub>6</sub>)<sub>2</sub> was verified by comparing CD spectrum with  $\Lambda$ -[Ru(bpy)<sub>3</sub>](PF<sub>6</sub>)<sub>2</sub> which was synthesized from complex  $\Lambda$ -(S)-**45** and the enantiopurity (>99:1 er) was determined by chiral HPLC analysis (Figure 51).

**Determination of enantiomeric ratio of  $\Lambda$ -[Ru(bpy)<sub>3</sub>](PF<sub>6</sub>)<sub>2</sub> by chiral HPLC.** The ruthenium complex was analyzed with a Daicel Chiralcel OD-R (250 × 4 mm) HPLC column on an Agilent 1200 Series HPLC System. The flow rate was 0.5 mL/min, the column temperature 40 °C, and UV-absorption was measured at 254 nm. Solvent A = 0.087% H<sub>3</sub>PO<sub>4</sub>, solvent B = MeCN, with a linear gradient of 8% to 14% B in 20 min.



**Figure 51.** HPLC trace for  $[\text{Ru}(\text{bpy})_3]^{2+}$ . Integration of peak areas: >99:1 er.

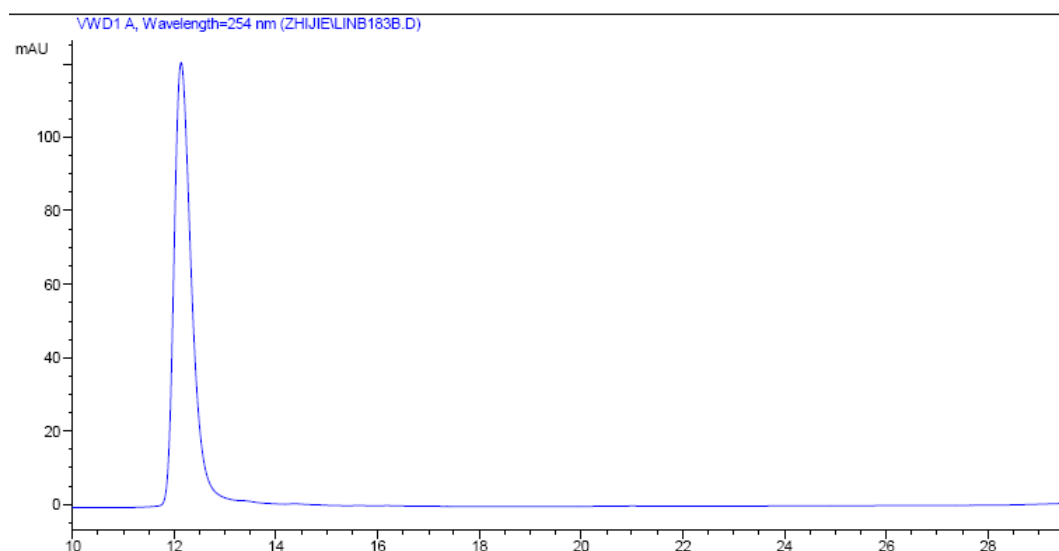


### $\Lambda$ -[Ru(phen)<sub>3</sub>](PF<sub>6</sub>)<sub>2</sub>.

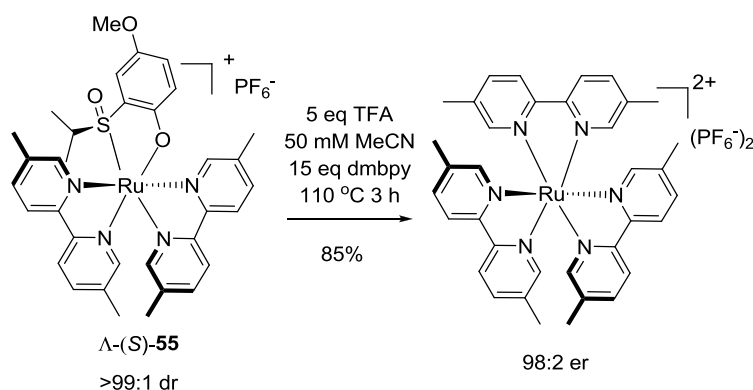
In a closed 1.5 mL brown glass vial fitted with a septum (brand: Agilent), a solution of  $\Lambda$ -(S)-**54** (5.0 mg, 0.0063 mmol), 1,10-phenanthroline (17.1 mg, 0.0949 mmol) and TFA (0.0024 mL, 0.0315 mmol) in CH<sub>3</sub>CN (0.15 mL) (quality: anhydrous) was heated at 110 °C (oil bath temperature) for 2 h under a nitrogen atmosphere. The reaction mixture was cooled to room temperature. The crude material was subjected to silica gel chromatography eluting with CH<sub>3</sub>CN: H<sub>2</sub>O: KNO<sub>3</sub>(sat) = 50: 6: 2. The product eluents were concentrated to dryness by evaporator, the resulting material was dissolved in minimal amounts of ethanol/water = 1/10 (2~3 mL), and the product was precipitated by the addition of solid NH<sub>4</sub>PF<sub>6</sub> (add NH<sub>4</sub>PF<sub>6</sub> together with shaking until the precipitate came and the colour of the solution from the orange to light yellow). The orange precipitate was centrifuged, washed twice with water, and dried under

high vacuum to afford  $\Lambda$ -[Ru(phen)<sub>3</sub>](PF<sub>6</sub>)<sub>2</sub> (4.9 mg, 82%). The  $\Lambda$ -configuration of  $\Lambda$ -[Ru(phen)<sub>3</sub>](PF<sub>6</sub>)<sub>2</sub> was verified by comparing CD spectrum with  $\Lambda$ -[Ru(phen)<sub>3</sub>](PF<sub>6</sub>)<sub>2</sub> which was synthesized from compound  $\Lambda$ -(S)-**44** and the enantiopurity (>99:1 er) was determined by chiral HPLC analysis (Figure 52).

**Determination of enantiomeric ratio of  $\Lambda$ -[Ru(phen)<sub>3</sub>](PF<sub>6</sub>)<sub>2</sub> by chiral HPLC.** The ruthenium complex was analyzed with a Daicel Chiralcel OD-R (250 × 4 mm) HPLC column on an Agilent 1200 Series HPLC System. The flow rate was 0.5 mL/min, the column temperature 40 °C, and UV-absorption was measured at 254 nm. Solvent A = 0.087% H<sub>3</sub>PO<sub>4</sub>, solvent B = MeCN, with a linear gradient of 15% to 40% B in 20 min.



**Figure 52.** HPLC trace for [Ru(phen)<sub>3</sub>]<sup>2+</sup>. Integration of peak areas: >99:1 er.



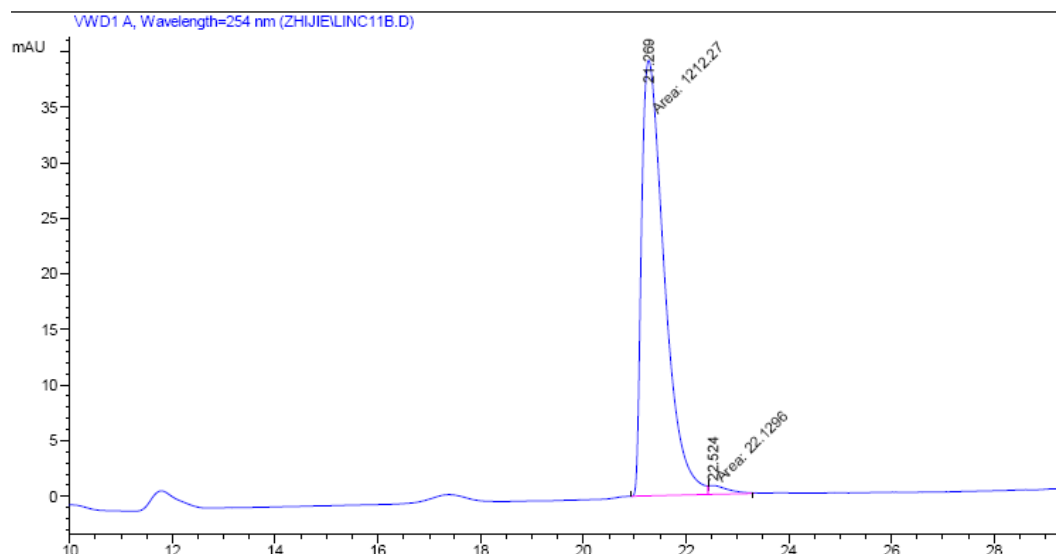
$\Lambda$ -[Ru(dmbpy)<sub>3</sub>](PF<sub>6</sub>)<sub>2</sub>.



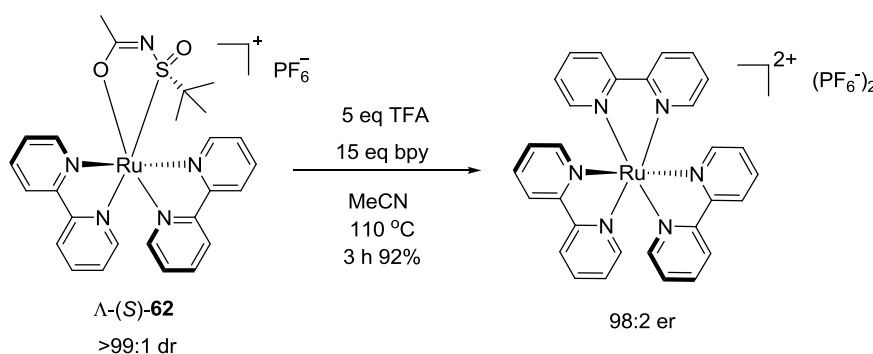
In a closed 1.5 mL brown glass vial fitted with a septum (brand: Agilent), a solution of  $\Lambda$ -(*S*)-**55** (5 mg, 0.006 mmol), 5,5'-dimethyl-2,2'-bipyridine (16.7 mg, 0.09 mmol) and TFA (0.0023 mL, 0.03 mmol) in CH<sub>3</sub>CN (0.15 mL) (quality: anhydrous) was heated at 110 °C (oil bath temperature) for 2 h under a nitrogen atmosphere. The reaction mixture was cooled to room temperature. The crude material was subjected to silica gel chromatography eluting with CH<sub>3</sub>CN: H<sub>2</sub>O: KNO<sub>3</sub>(sat) = 50: 6: 2. The product eluents were concentrated to dryness by evaporator, the resulting material was dissolved in minimal amounts of ethanol/water = 1/10 (2~3 mL), and the product was precipitated by the addition of solid NH<sub>4</sub>PF<sub>6</sub> (add NH<sub>4</sub>PF<sub>6</sub> together with shaking until the precipitate came and the colour of the solution from the orange to light yellow). The orange precipitate was centrifuged, washed twice with water, and dried under high vacuum to afford  $\Lambda$ -[Ru(dmbpy)<sub>3</sub>](PF<sub>6</sub>)<sub>2</sub> (4.9 mg, 85%). The  $\Lambda$ -configuration of  $\Lambda$ -[Ru(dmbpy)<sub>3</sub>](PF<sub>6</sub>)<sub>2</sub> was verified by comparing CD spectrum with  $\Lambda$ -[Ru(dmbpy)<sub>3</sub>](PF<sub>6</sub>)<sub>2</sub> which was synthesized from compound  $\Lambda$ -(*S*)-**49** and the enantiopurity (98: 2 er) was determined by chiral HPLC analysis (Figure 53).

**Determination of enantiomeric ratio of  $\Lambda$ -[Ru(dmbpy)<sub>3</sub>](PF<sub>6</sub>)<sub>2</sub> by chiral HPLC.**

The ruthenium complex was analyzed with a Daicel Chiralcel OD-R (250 × 4 mm) HPLC column on an Agilent 1200 Series HPLC System. The flow rate was 0.5 mL/min, the column temperature 40 °C, and UV-absorption was measured at 254 nm. Solvent A = 0.087% H<sub>3</sub>PO<sub>4</sub>, solvent B = MeCN, with a linear gradient of 14% to 27% B in 20 min, then 27% B in 5min.



**Figure 53.** HPLC trace for  $[\text{Ru}(\text{dmbpy})_3]^{2+}$ . Integration of peak areas: 98: 2 er.

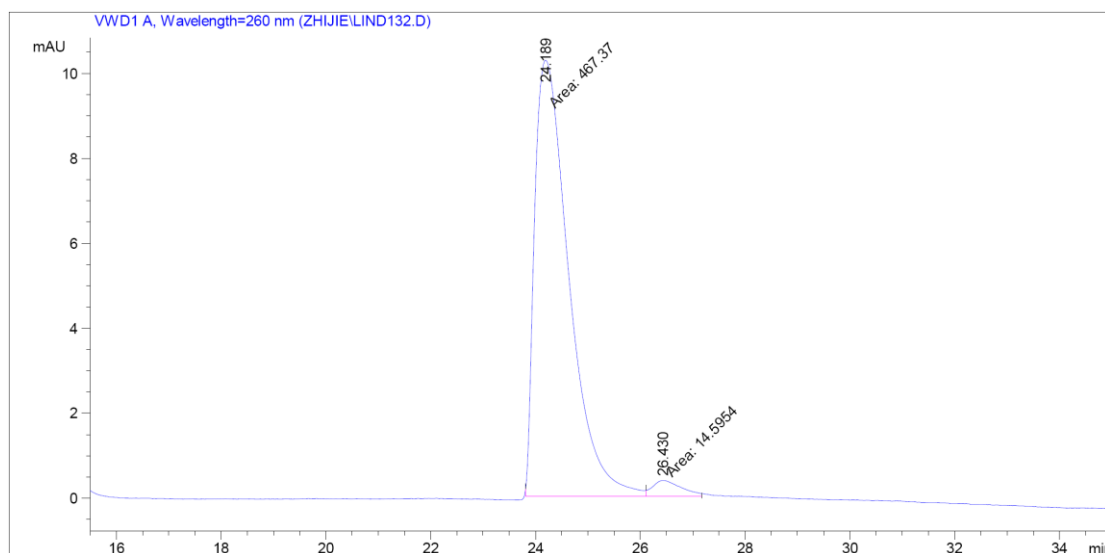


### $\Lambda\text{-}[\text{Ru}(\text{bpy})_3](\text{PF}_6)_2$

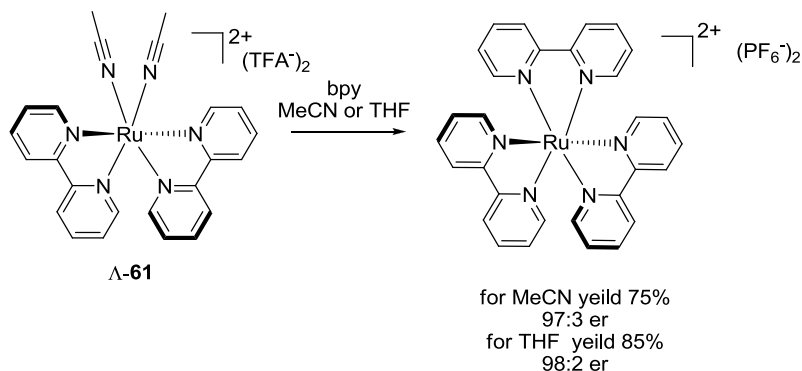
*Synthesis from complex  $\Lambda\text{-(S)-62}$ :* The following reaction was executed in the dark, while workup and purification were performed under reduced light. In a closed 1.5 mL brown glass vial fitted with a septum (brand: Agilent), a solution of complex  $\Lambda\text{-(S)-62}$  (10.0 mg, 0.014 mmol), 2,2'-bipyridine (32.5 mg, 0.21 mmol), and TFA (0.0053 mL, 0.07 mmol) in  $\text{CH}_3\text{CN}$  (0.27 mL) (quality: anhydrous) was heated at 110 °C (oil bath temperature) for 3 hours under a nitrogen atmosphere. The reaction mixture was cooled to room temperature. The crude material was subjected to silica gel chromatography eluting with  $\text{CH}_3\text{CN}:\text{H}_2\text{O}:\text{KNO}_3(\text{sat}) = 50:6:2$ . The product eluents were concentrated to dryness by evaporator, the resulting material was dissolved in minimal amounts of ethanol/water = 1/10 (2~3 mL), and the product was precipitated by the addition of solid  $\text{NH}_4\text{PF}_6$  (add  $\text{NH}_4\text{PF}_6$  together with shaking until the precipitate came and the colour of the solution from the orange to light yellow).

The orange precipitate was centrifuged, washed twice with water, and dried under high vacuum to afford  $\Lambda$ -[Ru(bpy)<sub>3</sub>](PF<sub>6</sub>)<sub>2</sub> (11.0 mg, 92%). The enantiomeric ratio (98:2 er) was determined by chiral HPLC analysis (Figure 54). The  $\Lambda$ -configuration of  $\Lambda$ -[Ru(bpy)<sub>3</sub>](PF<sub>6</sub>)<sub>2</sub> was verified by comparing CD spectrum with  $\Lambda$ -[Ru(bpy)<sub>3</sub>](PF<sub>6</sub>)<sub>2</sub> which was synthesized from complex  $\Lambda$ -(S)-45.

**Determination of enantiomeric ratios of ruthenium complexes by chiral HPLC analysis.** The analysis was performed with a Daicel Chiralcel OD-R (250 × 4 mm) HPLC column on an Agilent 1200 Series HPLC System. The flow rate was 0.5 mL/min, the column temperature 40 °C, and UV-absorption was measured at 254 nm. Solvent A = 0.087% H<sub>3</sub>PO<sub>4</sub>, solvent B = MeCN, with a linear gradient of 4% to 10% B in 30 min for  $\Lambda$ -[Ru(bpy)<sub>3</sub>](PF<sub>6</sub>)<sub>2</sub>.



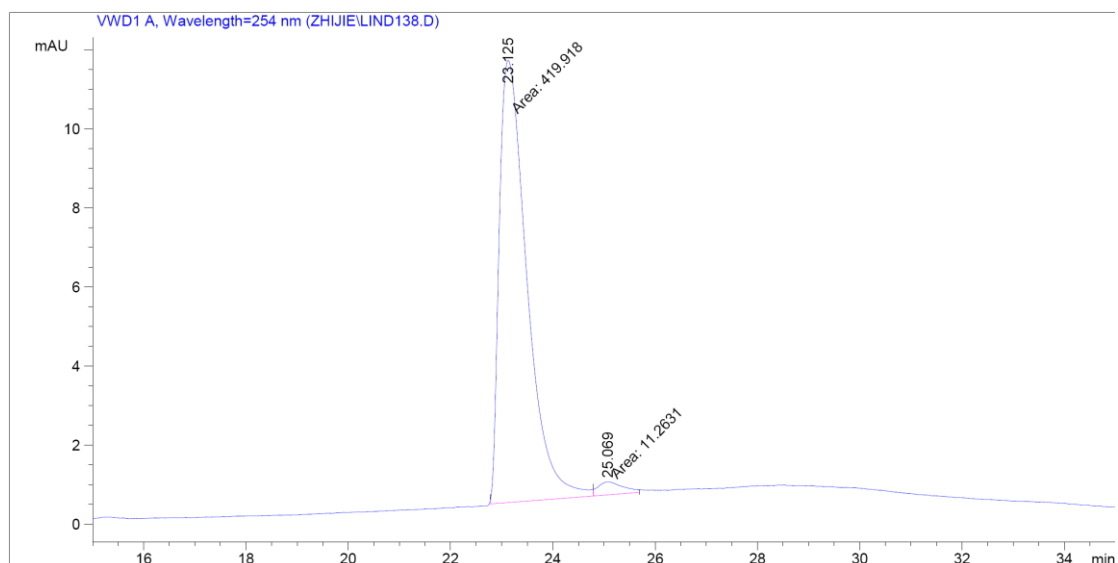
**Figure 54.** Synthesis of  $\Lambda$ -[Ru(bpy)<sub>3</sub>](PF<sub>6</sub>)<sub>2</sub> from  $\Lambda$ -(S)-62. Integration of peak areas = 98: 2.



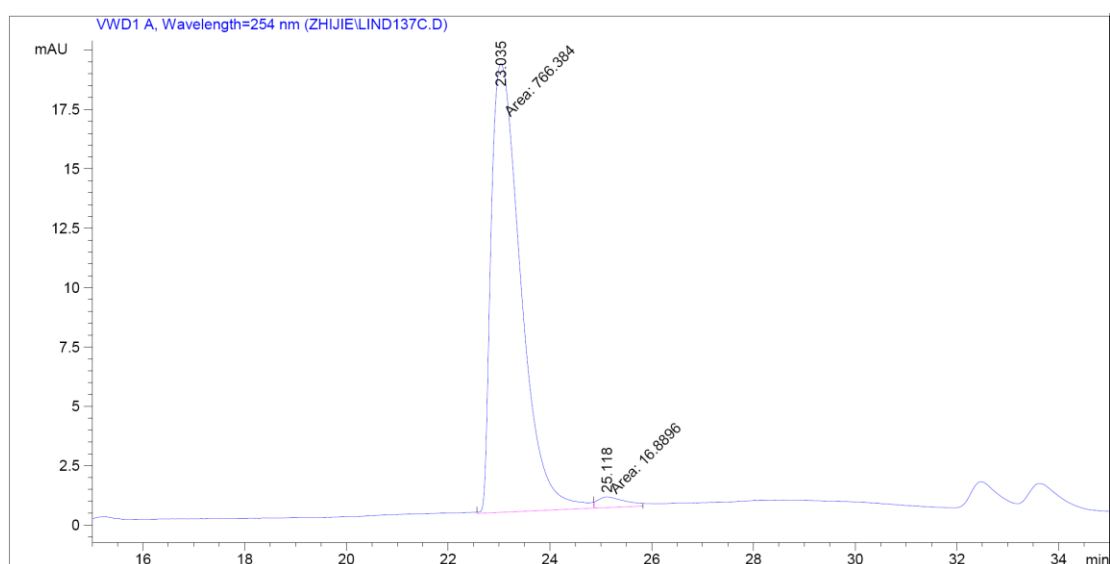
**$\Lambda$ -[Ru(bpy)<sub>3</sub>](PF<sub>6</sub>)<sub>2</sub>.**

*Synthesis from the acetonitrile-complex  $\Lambda$ -61*: The following reaction was executed in the dark, while workup and purification were performed under reduced light. In a closed 1.5 mL brown glass vial fitted with a septum (brand: Agilent), a solution of complex  $\Lambda$ -61 (5.0 mg, 0.0069 mmol) and 2,2'-bipyridine (16.2 mg, 0.1 mmol) in CH<sub>3</sub>CN (0.14 mL) (quality: anhydrous) was heated at 110 °C (oil bath temperature) for 2.5 hours under a nitrogen atmosphere. The reaction mixture was cooled to room temperature. The crude material was subjected to silica gel chromatography eluting with CH<sub>3</sub>CN: H<sub>2</sub>O: KNO<sub>3</sub>(sat) = 50: 6: 2. The product eluents were concentrated to dryness by evaporator, the resulting material was dissolved in minimal amounts of ethanol/water = 1/10 (2~3 mL), and the product was precipitated by the addition of solid NH<sub>4</sub>PF<sub>6</sub> (add NH<sub>4</sub>PF<sub>6</sub> together with shaking until the precipitate came and the colour of the solution from the orange to light yellow). The orange precipitate was centrifuged, washed twice with water, and dried under high vacuum to afford  $\Lambda$ -[Ru(bpy)<sub>3</sub>](PF<sub>6</sub>)<sub>2</sub> (4.5 mg, 75%). The enantiomeric ratio (97: 3 er) was determined by chiral HPLC analysis (Figure 55). The reaction was also performed in an analogous fashion in THF which afforded  $\Lambda$ -[Ru(bpy)<sub>3</sub>](PF<sub>6</sub>)<sub>2</sub> (5 mg, 85%) with 98: 2 er (Figure 56). The  $\Lambda$ -configuration of  $\Lambda$ -[Ru(bpy)<sub>3</sub>](PF<sub>6</sub>)<sub>2</sub> was verified by comparing CD spectrum with  $\Lambda$ -[Ru(bpy)<sub>3</sub>](PF<sub>6</sub>)<sub>2</sub> which was synthesized from compound  $\Lambda$ -(S)-45.

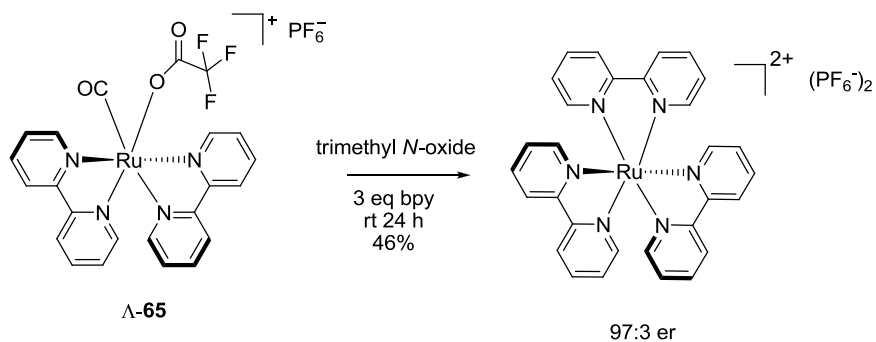
**Determination of enantiomeric ratios of ruthenium complexes by chiral HPLC analysis.** The analysis was performed with a Daicel Chiralcel OD-R (250 × 4 mm) HPLC column on an Agilent 1200 Series HPLC System. The flow rate was 0.5 mL/min, the column temperature 40 °C, and UV-absorption was measured at 254 nm. Solvent A = 0.087% H<sub>3</sub>PO<sub>4</sub>, solvent B = MeCN, with a linear gradient of 4% to 10% B in 30 min for  $\Lambda$ -[Ru(bpy)<sub>3</sub>](PF<sub>6</sub>)<sub>2</sub>.



**Figure 55.** Synthesis of  $\Lambda$ -[Ru(bpy)<sub>3</sub>](PF<sub>6</sub>)<sub>2</sub> from acetonitrile complex  $\Lambda$ -61 in MeCN. Integration of peak areas = 97: 3.



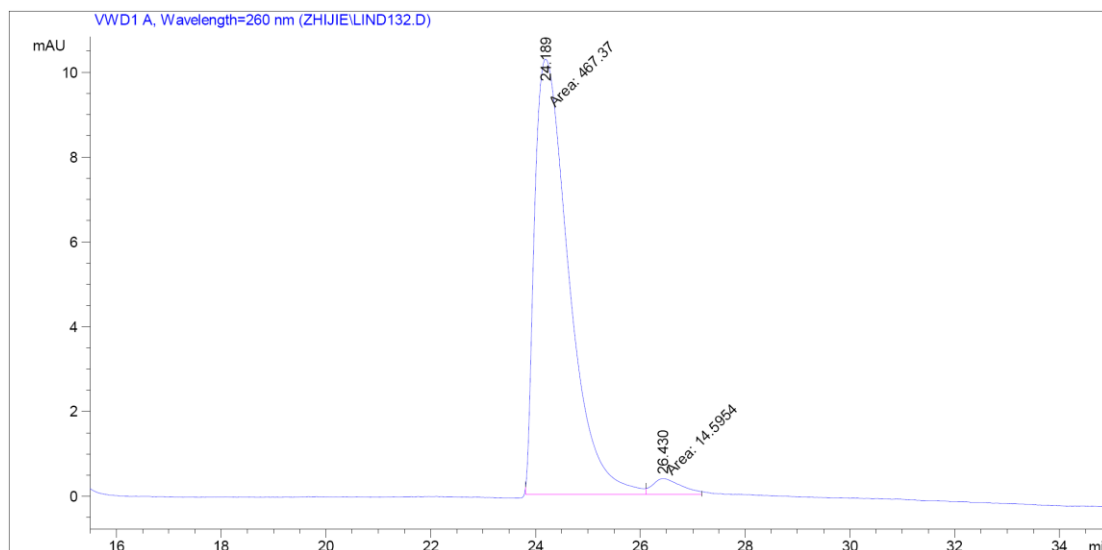
**Figure 56.** Synthesis of  $\Lambda$ -[Ru(bpy)<sub>3</sub>](PF<sub>6</sub>)<sub>2</sub> from acetonitrile complex  $\Lambda$ -61 in THF. Integration of peak areas = 98: 2.



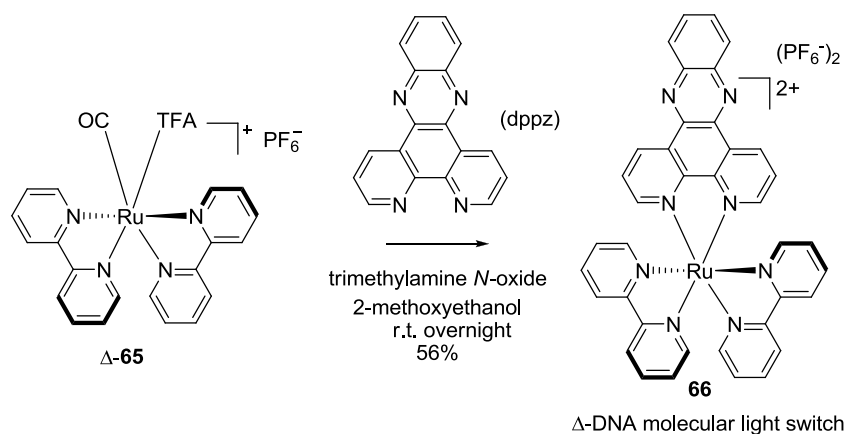
**$\Lambda$ -[Ru(bpy)<sub>3</sub>](PF<sub>6</sub>)<sub>2</sub>.**

*Synthesis from the CO-complex A-65:* The following reaction was executed in the dark, while workup and purification were performed under reduced light.  $\Lambda$ -**65** (7 mg, 0.01 mmol), 2,2'-bipyridine (11 mg, 0.07 mmol), and trimethylamine *N*-oxide (7.7 mg, 0.07 mmol) were dissolved in 2-methoxyethanol (0.2 mL) (quality: Aldrich >99%). The mixture stirred at room temperature for 4 hours. The reaction mixture was cooled to room temperature. The crude material was subjected to silica gel chromatography eluting with CH<sub>3</sub>CN: H<sub>2</sub>O: KNO<sub>3</sub>(sat) = 50: 6: 2. The product eluents were concentrated to dryness by evaporator, the resulting material was dissolved in minimal amounts of ethanol/water = 1/10 (2~3 mL), and the product was precipitated by the addition of solid NH<sub>4</sub>PF<sub>6</sub> (add NH<sub>4</sub>PF<sub>6</sub> together with shaking until the precipitate came and the colour of the solution from the orange to light yellow). The orange precipitate was centrifuged, washed twice with water, and dried under high vacuum to afford  $\Lambda$ -[Ru(bpy)<sub>3</sub>](PF<sub>6</sub>)<sub>2</sub> (4.0 mg, 47%). The enantiomeric ratio (97: 3 er) was determined by chiral HPLC analysis (Figure 57). The  $\Lambda$ -configuration of  $\Lambda$ -[Ru(bpy)<sub>3</sub>](PF<sub>6</sub>)<sub>2</sub> was verified by comparing CD spectrum with  $\Lambda$ -[Ru(bpy)<sub>3</sub>](PF<sub>6</sub>)<sub>2</sub> which was synthesized from compound  $\Lambda$ -(*S*)-**45**.

**Determination of enantiomeric ratios of ruthenium complexes by chiral HPLC analysis.** The analysis was performed with a Daicel Chiralcel OD-R (250 × 4 mm) HPLC column on an Agilent 1200 Series HPLC System. The flow rate was 0.5 mL/min, the column temperature 40 °C, and UV-absorption was measured at 254 nm. Solvent A = 0.087% H<sub>3</sub>PO<sub>4</sub>, solvent B = MeCN, with a linear gradient of 4% to 10%.



**Figure 57.** Synthesis of  $\Delta$ -[Ru(bpy)<sub>3</sub>](PF<sub>6</sub>)<sub>2</sub> from CO-complex  $\Delta$ -65. Integration of peak areas = 97: 3.

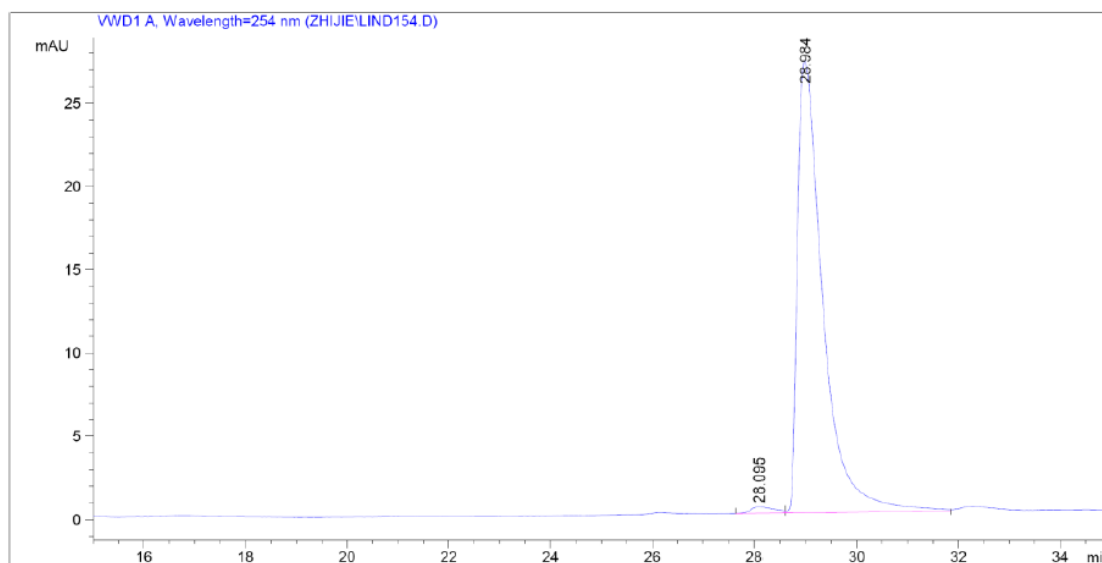


### $\Delta$ -[Ru(bpy)<sub>2</sub>(dppz)](PF<sub>6</sub>)<sub>2</sub> (**66**).

The following reaction was executed in the dark, while workup and purification were performed under reduced light. The CO-complex  $\Delta$ -65 (7 mg, 0.01 mmol), dppz (17 mg, 0.06 mmol) and an excess of trimethylamine *N*-oxide (6.6 mg, 0.06 mmol) were dissolved in 2-methoxyethanol (0.2 mL). The reaction mixture was cooled to room temperature. The crude material was subjected to silica gel chromatography eluting with CH<sub>3</sub>CN: H<sub>2</sub>O: KNO<sub>3</sub>(sat) = 50: 3: 1. The product eluents were concentrated to dryness by evaporator, the resulting material was dissolved in minimal amounts of ethanol/water = 1/10 (2~3 mL), and the product was precipitated by the addition of

solid  $\text{NH}_4\text{PF}_6$  (add  $\text{NH}_4\text{PF}_6$  together with shaking until the precipitate came and the colour of the solution from the orange to light yellow). The orange precipitate was centrifuged, washed twice with water, and dried under high vacuum to afford  $\Delta\text{-}[\text{Ru}(\text{bpy})_2(\text{dppz})](\text{PF}_6)_2$  (5.5 mg, 56%). The enantiomeric ratio (98.7: 1.3 er) was determined by chiral HPLC analysis (Figures 58 and 59). And the stereochemistry of  $\Delta\text{-}66$  was same with the precursor  $\Delta\text{-}65$  owing to the retained configuration in the substituted reaction, which was confirmed by previous results.

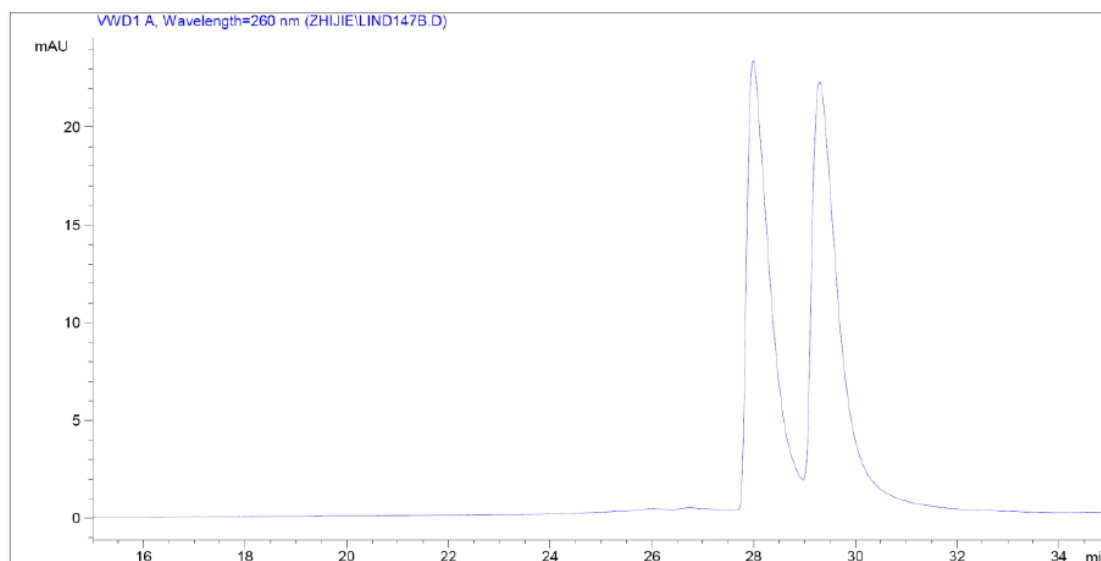
**Determination of enantiomeric ratios of ruthenium complexes by chiral HPLC analysis.** The analysis was performed with a Daicel Chiralcel OD-R (250 × 4 mm) HPLC column on an Agilent 1200 Series HPLC System. The flow rate was 0.5 mL/min, the column temperature 40 °C, and UV-absorption was measured at 254 nm. Solvent A = 0.087%  $\text{H}_3\text{PO}_4$ , solvent B = MeCN, a linear gradient of 10% to 25% B in 20 min and thereafter isocratic 25% B.



**Figure 58.** Synthesis of  $\Delta\text{-}[\text{Ru}(\text{bpy})_2(\text{dppz})](\text{PF}_6)_2$  from the CO-complex  $\Delta\text{-}66$ .

Integration of peak areas = 98.7: 1.3.

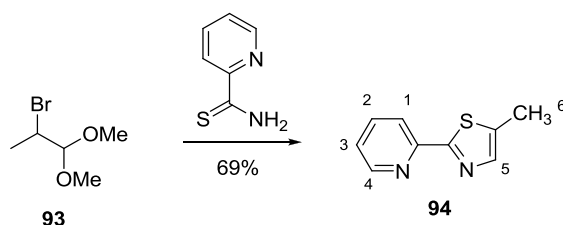




**Figure 59.** HPLC trace of the racemic reference complex  $[\text{Ru}(\text{bpy})_2(\text{dppz})](\text{PF}_6)_2$ .

## 5.3 Development of octahedral chiral-at-metal complexes for asymmetric catalysis

### 5.3.1 Synthesis of DMAP-ligands

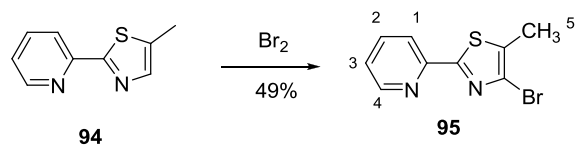


#### 5-Methyl-2-(pyridin-2-yl)thiazole (**94**).

A solution of pyridine-2-thiocarboxamide (2.5 g, 18.1 mmol) and 2-bromopropanal (4.1 g, 22.6 mmol) dimethyl acetal in acetic acid (18.1 mL) was brought to 100 °C and kept at 100 °C overnight under stirring. After removal of the acetic acid, the 100 mL  $\text{H}_2\text{O}$  was added. The pH of the mixture was adjusted to 8 with solid  $\text{Na}_2\text{CO}_3$ , and the mixture was then extracted with  $\text{Et}_2\text{O}$ . The brown  $\text{Et}_2\text{O}$  phase was decolorized with activated carbon and dried over  $\text{Na}_2\text{SO}_4$ . Evaporating the  $\text{Et}_2\text{O}$  afforded the crude product 5-methyl-2-(pyridin-2-yl)thiazole (**94**) (2.2g 71%) which used in next step without further purification.

$^1\text{H-NMR}$  (300.1 MHz,  $\text{CDCl}_3$ ):  $\delta$  (ppm) 8.59 (dq,  $J = 4.8, 0.9$  Hz, 1H, 4-H), 8.13 (dt,

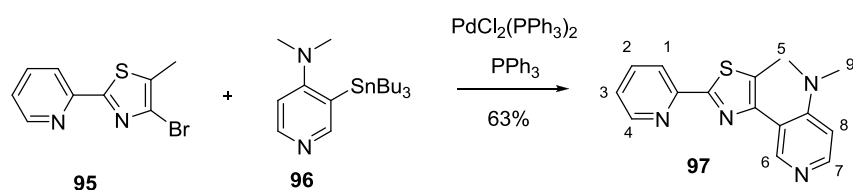
$J = 8.0, 1.0$  Hz, 1H, 1-H), 7.78 (td,  $J = 7.65, 1.7$  Hz, 1H, 2-H), 7.56 (d,  $J = 1.1$ Hz, 1H, 5-H), 7.28 (ddd,  $J = 7.5, 4.9, 1.1$  Hz, 1H, 3-H), 2.53 (d,  $J = 1.1$  Hz, 3H, 6-H). HRMS (ESI) calcd for  $C_9H_8N_2SNa$  ( $M+Na$ )<sup>+</sup> 199.0300, found: 199.0300.



#### 4-Bromo-5-methyl-2-(pyridin-2-yl)thiazole (95).

To a solution of 5-methyl-2-(pyridin-2-yl)thiazole (**94**) (2110 mg, 12 mmol) in 25 mL  $CHCl_3$  and 25 mL MeCN was slowly added  $Br_2$  (1.25 mL, 24 mmol). The reaction was refluxed for 48 hours. Then the solvents were removed under vacuum.  $H_2O$  (100 mL) and DCM (50mL) were added to the solid residue and the pH of the aqueous phase was adjusted to 8 with solid  $Na_2CO_3$ . The aqueous phase was washed once again with 50 mL DCM. The combined organic phase was washed with brine and dried over. After removal of DCM, the residue was purified by flash chromatography (hexane: EtOAc 1: 1) to give the 4-bromo-5-methyl-2-(pyridin-2-yl)thiazole (**95**). (1.5 g, 49%)

$^1H$ -NMR (300.1 MHz,  $CDCl_3$ ):  $\delta$  (ppm) 8.58 (dq,  $J = 4.8, 0.95$  Hz, 1H, 4-H), 8.13 (dt,  $J = 7.95, 1.0$  Hz, 1H, 1-H), 7.78 (td,  $J = 7.6, 1.7$  Hz, 1H, 2-H), 7.31 (ddd,  $J = 7.5, 4.9, 1.2$  Hz, 1H, 3-H), 2.48 (s, 3H, 5-H). HRMS (ESI) calcd for  $C_9H_7BrN_2SNa$  ( $M+Na$ )<sup>+</sup> 276.9406, 278.9385, found: 276.9405, 278.9384.

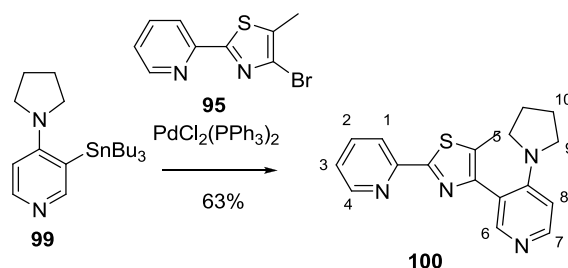


#### *N,N*-Dimethyl-3-(5-methyl-2-(pyridin-2-yl)thiazol-4-yl)pyridin-4-amine (97).

The 4-bromo-5-methyl-2-(pyridin-2-yl)thiazole (**95**) (155 mg, 0.607 mmol) , *N,N*-dimethyl-3-(tributylstannyl)pyridin-4-amine (**96**)<sup>80</sup> (300 mg, 0.728 mmol),  $PdCl_2(PPh_3)_2$  (106.5 mg, 0.152 mmol) and  $PPh_3$  (79.5 mg, 0.3 mmol) were dissolved in the xylene (12.1 mL) and degassed with argon. The reaction was stirred at 158 °C

overnight. Then the solvent was evaporated and the residue was purified by flash chromatography (DCM: MeOH 15: 1) to give the *N,N*-dimethyl-3-(5-methyl-2-(pyridin-2-yl)thiazol-4-yl)pyridin-4-amine (**97**) as a yellow solid (113 mg, 63%) contaminated with a little bit of  $\text{HSnBu}_3$ .

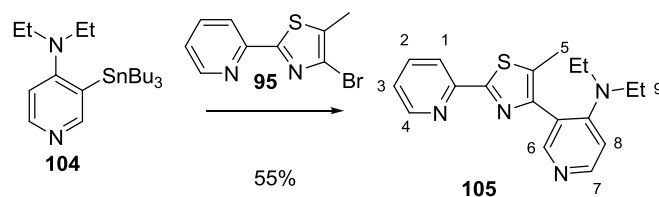
$^1\text{H-NMR}$  (300.1 MHz,  $\text{CDCl}_3$ ):  $\delta$  (ppm) 8.58-8.62 (m, 1H, 4-H), 8.25-8.30 (m, 2H, 6-H, 7-H), 8.16 (d,  $J = 7.95$  Hz, 1H, 1-H), 7.76 (td,  $J = 7.6, 1.7$  Hz, 1H, 2-H), 7.29 (ddd,  $J = 7.5, 4.8, 1.2$  Hz, 1H, 3-H), 6.72 (d,  $J = 6.2$  Hz, 1H, 8-H), 2.75 (s, 6H,  $\text{Me}_2\text{-N}$ ), 2.45 (s, 3H, 5-H). HRMS (ESI) calcd for  $\text{C}_{16}\text{H}_{16}\text{N}_4\text{SH}$  ( $\text{M}+\text{H}$ ) $^+$  297.1168, found: 297.1169.



#### 5-Methyl-2-(pyridin-2-yl)-4-(4-(pyrrolidin-1-yl)pyridin-3-yl)thiazole (**100**).

The 4-bromo-5-methyl-2-(pyridin-2-yl)thiazole (**95**) (155 mg, 0.607 mmol), 4-(pyrrolidin-1-yl)-3-(tributylstannyl)pyridine (**99**)<sup>80</sup> (300 mg, 0.728 mmol),  $\text{PdCl}_2(\text{PPh}_3)_2$  (106.5 mg, 0.152 mmol) and  $\text{PPh}_3$  (79.5 mg, 0.3 mmol) were dissolved in the xylene (12.1 mL) and degassed with argon. The reaction was stirred at 158 °C overnight. Then the solvent was evaporated and the residue was purified by flash chromatography (DCM: MeOH 15: 1) to give the 5-methyl-2-(pyridin-2-yl)-4-(4-(pyrrolidin-1-yl)pyridin-3-yl)thiazole (**100**) as a yellow solid (113 mg, 63%) contaminated with a little bit of  $\text{HSnBu}_3$ .

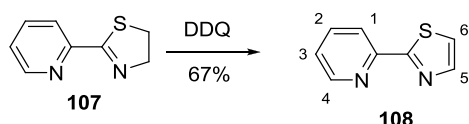
$^1\text{H-NMR}$  (300.1 MHz,  $\text{CDCl}_3$ ):  $\delta$  (ppm) 8.55-8.61 (m, 1H, 4-H), 8.05-8.18 (m, 3H, 6-H, 7-H, 1-H), 7.75 (td,  $J = 7.6, 1.7$  Hz, 1H, 2-H), 7.29 (ddd,  $J = 7.5, 4.9, 1.1$  Hz, 1H, 3-H), 6.61 (d,  $J = 4.4$  Hz, 1H, 8-H), 3.05-3.15 (m, 4H, 9-H), 2.32 (s, 3H, 5-H), 1.80-1.88 (m, 4H, 10-H). HRMS (ESI) calcd for  $\text{C}_{18}\text{H}_{18}\text{N}_4\text{SH}$  ( $\text{M}+\text{H}$ ) $^+$  323.1325, found: 323.1326.



***N,N*-Diethyl-3-(5-methyl-2-(pyridin-2-yl)thiazol-4-yl)pyridin-4-amine (105).**

The 4-bromo-5-methyl-2-(pyridin-2-yl)thiazole (**95**) (100 mg, 0.39 mmol), *N,N*-diethyl-3-(tributylstannyl)pyridin-4-amine (**104**)<sup>80</sup> (206 mg, 0.47 mmol), PdCl<sub>2</sub>(PPh<sub>3</sub>)<sub>2</sub> (68.4 mg, 0.097 mmol) and PPh<sub>3</sub> (51.1 mg, 0.19 mmol) were dissolved in the xylene (7.8 mL) and degassed with argon. The reaction was stirred at 158 °C overnight. Then the solvent was evaporated and the residue was purified by flash chromatography (DCM: MeOH 15: 1) to give the *N,N*-diethyl-3-(5-methyl-2-(pyridin-2-yl)thiazol-4-yl)pyridin-4-amine (**105**) as a yellow solid (70 mg, 55%) contaminated with a little bit of HSnBu<sub>3</sub>.

<sup>1</sup>H-NMR (300.1 MHz, CDCl<sub>3</sub>): δ (ppm) 8.57 (dq, *J* = 4.9, 0.9 Hz, 1H, 4-H), 8.21 (d, *J* = 6.1 Hz, 1H, 6-H), 8.09-8.18 (m, 2H, 7-H, 1-H), 7.73 (td, *J* = 7.6, 1.7 Hz, 1H, 2-H), 7.29 (ddd, *J* = 7.5, 4.9, 1.1 Hz, 1H, 3-H), 6.74 (d, *J* = 6.1 Hz, 1H, 8-H), 3.11 (q, *J* = 7.1 Hz, 4H, N-(CH<sub>2</sub>CH<sub>3</sub>)<sub>2</sub>), 2.31 (s, 3H, 5-H), 0.99 (t, *J* = 7.1 Hz, 6H, N-(CH<sub>2</sub>CH<sub>3</sub>)<sub>2</sub>). HRMS (ESI) calcd for C<sub>18</sub>H<sub>20</sub>N<sub>4</sub>SH (M+H)<sup>+</sup> 325.1481, found: 325.1486.

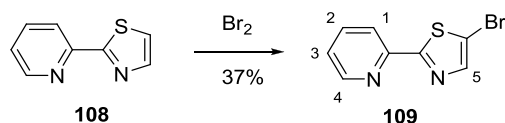


**2-(Pyridin-2-yl)thiazole (108).**

To a solution of the 2-(pyridin-2-yl)-4,5-dihydrothiazole (**107**)<sup>73</sup> (3.0 g, 18.3 mmol) in benzene (83 mL) was added DDQ (4.9 g, 21.9 mmol). The reaction was refluxed for 2 hours. Then the solvent was evaporated and the residue was purified by flash chromatography (hexane: EtOAc 10: 1 to 2: 1) to give the 2-(pyridin-2-yl)thiazole (**108**) as a white solid (2.0 g, 67 %).

<sup>1</sup>H-NMR (300.1 MHz, CDCl<sub>3</sub>): δ (ppm) 8.51 (dq, *J* = 4.8, 0.9 Hz, 1H, 4-H), 8.10 (dt, *J* = 7.9, 1.0 Hz, 1H, 1-H), 7.83 (d, *J* = 3.2 Hz, 1H, 5-H), 7.67 (td, *J* = 7.65, 1.8 Hz, 1H, 2-H), 7.34 (d, *J* = 3.2 Hz, 1H, 6-H), 7.19 (ddd, *J* = 7.5, 4.9, 1.1 Hz, 1H, 3-H). HRMS

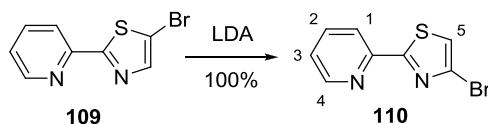
(ESI) calcd for  $C_8H_6N_2SNa$  ( $M+Na$ )<sup>+</sup> 185.0144, found: 185.0143.



#### 5-Bromo-2-(pyridin-2-yl)thiazole (**109**).

To a solution of the 2-(pyridin-2-yl)thiazole (**108**) (800 mg, 4.9 mmol) in  $CHCl_3$  (14 mL) was added bromine (0.28 mL, 5.4 mmol) in  $CHCl_3$  (5.5 mL). After stirring at room temperature for overnight, another 0.5 eq of the bromine was added stirring for another 2 hours. Then the solvent was evaporated and the residue was purified by flash chromatography (hexane: EtOAc 2: 1) to give the 5-bromo-2-(pyridin-2-yl)thiazole (**109**) (440 mg, 37 %).

<sup>1</sup>H-NMR (300.1 MHz,  $CDCl_3$ ):  $\delta$  (ppm) 8.55-8.62 (m, 1H, 4-H), 8.08-8.15 (m, 1H, 1-H), 7.76-7.85 (m, 2H, 5-H, 2-H), 7.34 (ddd,  $J = 7.5, 4.8, 1.0$  Hz, 1H, 3-H). HRMS (ESI) calcd for  $C_8H_5BrN_2SNa$  ( $M+Na$ )<sup>+</sup> 262.9249, 264.9228, found: 262.9248, 264.9227.

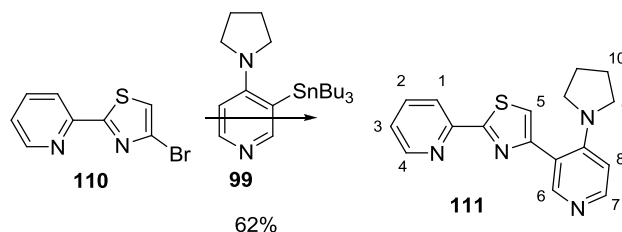


#### 4-Bromo-2-(pyridin-2-yl)thiazole (**110**).

A LDA (0.51 mL, 1.8M) in THF was added to a solution of 5-bromo-2-(pyridin-2-yl)thiazole (**109**) in THF (3.1 mL) at  $-80^\circ C$  under argon. After stirring at  $-80^\circ C$  for 0.5 hours, the reaction was quenched with  $H_2O$  and warmed to room temperature. Then Brine was added and the 2/3 THF was removed. The aqueous phase was extracted by DCM. The organic phase was dried by  $Na_2SO_4$ . Then the solvent was evaporated and the residue was purified by flash chromatography (hexane: EtOAc 4: 1) to give the 4-bromo-2-(pyridin-2-yl)thiazole (**110**) (133 mg, 100 %).

<sup>1</sup>H-NMR (300.1 MHz,  $CDCl_3$ ):  $\delta$  (ppm) 8.60 (dq,  $J = 4.8, 0.9$  Hz, 1H, 4-H), 8.18 (dt,  $J = 7.95, 1.0$  Hz, 1H, 1-H), 7.81 (td,  $J = 7.7, 1.7$  Hz, 1H, 2-H), 7.32-7.37 (m, 2H, 3-H,

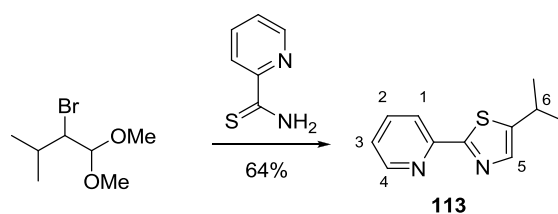
5-H). HRMS (ESI) calcd for  $C_8H_5BrN_2SNa$  ( $M+Na$ )<sup>+</sup> 262.9249, 264.9228, found: 262.9251, 264.9230.



**2-(Pyridin-2-yl)-4-(4-(pyrrolidin-1-yl)pyridin-3-yl)thiazole (111).**

The 4-bromo-2-(pyridin-2-yl)thiazole (**110**) (100 mg, 0.415 mmol), 4-(pyrrolidin-1-yl)-3-(tributylstannyl)pyridine (**99**)<sup>80</sup> (218 mg, 0.49 mmol),  $PdCl_2(PPh_3)_2$  (72.8 mg, 0.104 mmol) and  $PPh_3$  (54.3 mg, 0.2 mmol) were dissolved in the xylene (8.2 mL) and degassed with argon. The reaction was stirred at 158 °C overnight. Then the solvent was evaporated and the residue was purified by flash chromatography (DCM: MeOH 20: 1) to give the 2-(pyridin-2-yl)-4-(4-(pyrrolidin-1-yl)pyridin-3-yl) thiazole (**111**) as a yellow solid (80 mg, 62%) contaminated with a little bit of  $HSnBu_3$ .

<sup>1</sup>H-NMR (300.1 MHz,  $CDCl_3$ ):  $\delta$  (ppm) 8.64 (dq,  $J = 4.8, 0.9$  Hz, 1H, 4-H), 8.18-8.26 (m, 3H, 6-H, 7-H, 1-H), 7.79 (td,  $J = 7.6, 1.7$  Hz, 1H, 2-H), 7.31-7.39 (m, 2H, 3-H, 5-H), 6.59 (d,  $J = 6.3$  Hz, 1H, 8-H), 3.16 (t,  $J = 6.7$  Hz, 4H, 9-H), 1.80-1.88 (m, 4H, 10-H). HRMS (ESI) calcd for  $C_{17}H_{16}N_4SH$  ( $M+H$ )<sup>+</sup> 309.1168, found: 309.1171.

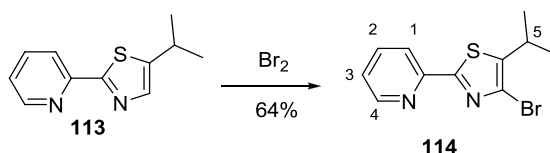


**5-Isopropyl-2-(pyridin-2-yl)thiazole (113).**

A solution of pyridine-2-thiocarboxamide (2.5 g, 18.1 mmol) and 2-bromo-1,1-dimethoxy-3-methylbutane (4.7 g, 22.6 mmol) dimethyl acetal in acetic acid (18.1 mL) was brought to 100 °C and kept at 100 °C overnight under stirring. After removal of the acetic acid, the 100mL  $H_2O$  was added. The pH of the mixture was adjusted to 8 with solid  $Na_2CO_3$ , and the mixture was then extracted with  $Et_2O$ . The brown  $Et_2O$

phase was decolorized with activated carbon and dried over  $\text{Na}_2\text{SO}_4$ . Evaporating the  $\text{Et}_2\text{O}$  afforded the crude product 5-isopropyl-2-(pyridin-2-yl)thiazole (**113**) (2.3 g, 64%) which used in next step without further purification.

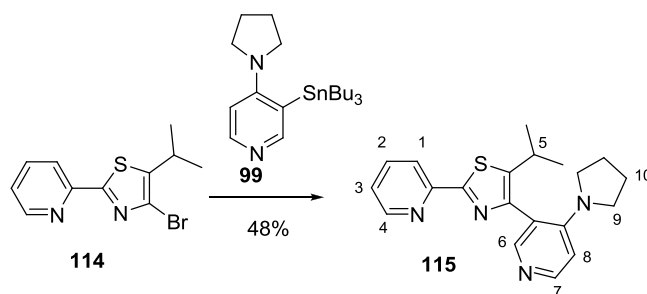
$^1\text{H-NMR}$  (300.1 MHz,  $\text{CDCl}_3$ ):  $\delta$  (ppm) 8.59 (dq,  $J = 4.8, 0.9$  Hz, 1H, 4-H), 8.15 (dt,  $J = 7.95, 1.0$  Hz, 1H, 1-H), 7.79 (td,  $J = 7.6, 1.7$  Hz, 1H, 2-H), 7.60 (d,  $J = 0.9$  Hz, 1H, 5-H), 7.29 (ddd,  $J = 7.5, 4.9, 1.1$  Hz, 1H, 3-H), 3.20-3.35 (m, 1H, 6-H), 1.39 (d,  $J = 6.8$  Hz, 6H,  $\text{CH}-(\text{CH}_3)_2$ ). HRMS (ESI) calcd for  $\text{C}_{15}\text{H}_{16}\text{N}_4\text{ONa}$  ( $\text{M}+\text{Na}$ ) $^+$  227.0613, found: 227.0616.



#### 4-Bromo-5-isopropyl-2-(pyridin-2-yl)thiazole (**114**).

To a solution of 5-isopropyl-2-(pyridin-2-yl)thiazole (**113**) (1000 mg, 4.89 mmol) in 10 mL  $\text{CHCl}_3$  and 10 mL MeCN was slowly added  $\text{Br}_2$  (0.503 mL, 9.7 mmol). The reaction was refluxed for 48 hours. Then the solvents were removed under vacuum.  $\text{H}_2\text{O}$  (50 mL) and DCM (25 mL) were added to the solid residue and the pH of the aqueous phase was adjusted to 8 with solid  $\text{Na}_2\text{CO}_3$ . The aqueous phase was washed once again with 25 mL DCM. The combined organic phase was washed with brine and dried over. After removal of DCM, the residue was purified by flash chromatography (hexane: EtOAc 10: 1) to give the 4-bromo-5-isopropyl-2-(pyridin-2-yl)thiazole (**114**) (1.5 g, 49%).

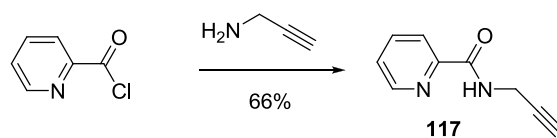
$^1\text{H-NMR}$  (300.1 MHz,  $\text{CDCl}_3$ ):  $\delta$  (ppm) 8.57 (dq,  $J = 4.8, 0.9$  Hz, 1H, 4-H), 8.13 (dt,  $J = 7.95, 1.0$  Hz, 1H, 1-H), 7.76 (td,  $J = 7.6, 1.7$  Hz, 1H, 2-H), 7.30 (ddd,  $J = 7.5, 4.9, 1.1$  Hz, 1H, 3-H), 3.25-3.40 (m, 1H, 5-H), 1.35 (d,  $J = 6.8$  Hz, 6H,  $\text{CH}-(\text{CH}_3)_2$ ). HRMS (ESI) calcd for  $\text{C}_{11}\text{H}_{11}\text{BrN}_2\text{SNa}$  ( $\text{M}+\text{Na}$ ) $^+$  304.9719, 306.9698, found: 304.9715, 306.9695.



### 5-Isopropyl-2-(pyridin-2-yl)-4-(4-(pyrrolidin-1-yl)pyridin-3-yl)thiazole (**115**).

The 4-bromo-5-isopropyl-2-(pyridin-2-yl)thiazole (**114**) (100 mg, 0.35 mmol), 4-(pyrrolidin-1-yl)-3-(tributylstannyl)pyridine (**99**)<sup>80</sup> (183 mg, 0.422 mmol), PdCl<sub>2</sub>(PPh<sub>3</sub>)<sub>2</sub> (61.7 mg, 0.088 mmol) and PPh<sub>3</sub> (46.1 mg, 0.176 mmol) were dissolved in the xylene (7.0 mL) and degassed with argon. The reaction was stirred at 158 °C overnight. Then the solvent was evaporated and the residue was purified by flash chromatography (DCM: MeOH 15: 1) to give the 5-isopropyl-2-(pyridin-2-yl)-4-(4-(pyrrolidin-1-yl)pyridin-3-yl)thiazole (**115**) as a yellow solid (60 mg, 48%) contaminated with a little bit of HSnBu<sub>3</sub>.

<sup>1</sup>H-NMR (300.1 MHz, CDCl<sub>3</sub>): δ (ppm) 8.58 (dq, *J* = 4.8, 0.9 Hz, 1H, 4-H), 8.00-8.18 (m, 3H, 6-H, 7-H, 1-H), 7.70-7.78 (m, 1H, 2-H), 7.29 (ddd, *J* = 7.5, 4.9, 1.1 Hz, 1H, 3-H), 6.59 (d, *J* = 6.3 Hz, 1H, 8-H), 3.00-3.20 (m, 5H, 5-H, 9-H), 1.75-1.85 (m, 4H, 10-H), 1.20-1.30 (m, 6H, CH-(CH<sub>3</sub>)<sub>2</sub>). HRMS (ESI) calcd for C<sub>20</sub>H<sub>22</sub>N<sub>4</sub>SH (M+H)<sup>+</sup> 351.1638, found: 351.1643.

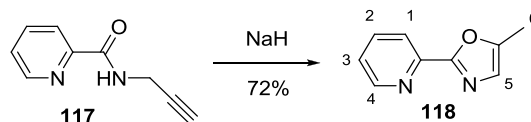


### *N*-(Prop-2-ynyl)picolinamide (**117**).

To a solution of propargylic amine (773.5 mg, 14.04 mmol) in DCM (28 mL) was added Et<sub>3</sub>N (3.9 mL, 28.0 mmol) and DMAP (8.5 mg, 0.07 mmol). After cooling to 0 °C, picolinoyl chloride (2500 mg, 14.04 mmol) was added and the mixture was stirred for 15 min at 0 °C and for further 3 hours at room temperature. Then water was added and the aqueous phase was extracted with DCM. After drying the solvent by Na<sub>2</sub>SO<sub>4</sub>, the solvent was evaporated and the residue was purified by recrystallization (EtOAc) to give the *N*-(prop-2-ynyl)picolinamide (**117**) (1500 mg, 66%). (use the crude



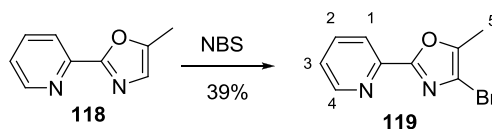
compound for next step). HRMS (ESI) calcd for  $C_9H_8N_2ONa$  ( $M+Na$ )<sup>+</sup> 183.0529, found: 183.0528.



#### 5-Methyl-2-(pyridin-2-yl)oxazole (**118**).

To a solution of *N*-(prop-2-ynyl)picolinamide (**117**) (500 mg, 3.12 mmol) in dioxane (6.2 mL) was added NaH (60%) (137.4 mg, 3.4 mmol). The reaction refluxed for overnight. After quenching by water, the aqueous phase was extracted by EtOAc. The organic phase was dried by  $Na_2SO_4$ , the solvent was evaporated and the residue was purified by flash chromatography (EtOAc: hexane 1: 1) to give the 5-methyl-2-(pyridin-2-yl)oxazole (**118**) (360 mg, 72%).

<sup>1</sup>H-NMR (300.1 MHz,  $CDCl_3$ ):  $\delta$  (ppm) 8.70 (dq,  $J = 4.8, 0.9$  Hz, 1H, 4-H), 8.09 (dt,  $J = 8.0, 1.0$  Hz, 1H, 1-H), 7.79 (td,  $J = 7.7, 1.7$  Hz, 1H, 2-H), 7.33 (ddd,  $J = 7.5, 4.9, 1.1$  Hz, 1H, 3-H), 6.90 (d,  $J = 1.1$  Hz, 1H, 5-H), 2.45 (d,  $J = 1.1$  Hz, 3H, 6-H). HRMS (ESI) calcd for  $C_9H_8N_2ONa$  ( $M+Na$ )<sup>+</sup> 183.0529, found: 183.0530.

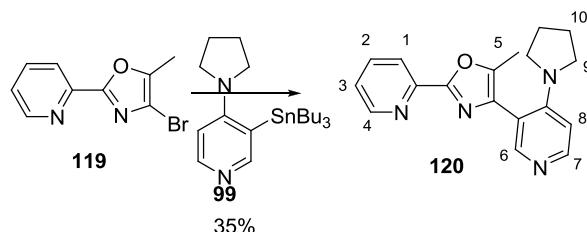


#### 4-Bromo-5-methyl-2-(pyridin-2-yl)oxazole (**119**).

To a solution of 5-methyl-2-(pyridin-2-yl)oxazole (**118**) (360 mg, 1.1 mmol) in DMF (2.1 mL) was added NBS (208.0 mg 1.2 mmol). The reaction stirred at room temperature for overnight. After it quenching by water, the aqueous phase was extracted by EtOAc. The organic phase was dried by  $Na_2SO_4$ , the solvent was evaporated and the residue was purified by flash chromatography (EtOAc: hexane 1: 4 to 1: 1) to give the 4-bromo-5-methyl-2-(pyridin-2-yl)oxazole (**119**) (100 mg, 39%).

<sup>1</sup>H-NMR (300.1 MHz,  $CDCl_3$ ):  $\delta$  (ppm) 8.70 (dq,  $J = 4.8, 0.9$  Hz, 1H, 4-H), 8.09 (dt,  $J = 8.0, 1.0$  Hz, 1H, 1-H), 7.80 (td,  $J = 7.7, 1.7$  Hz, 1H, 2-H), 7.35 (ddd,  $J = 7.6, 4.8,$

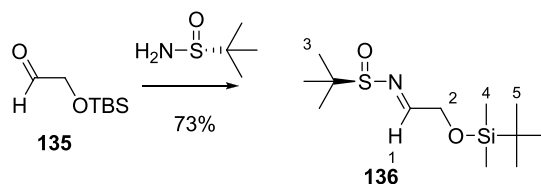
1.1 Hz, 1H, 3-H), 2.43 (s, 3H, 5-H). HRMS calcd for  $C_9H_7BrN_2ONa$  ( $M+Na$ )<sup>+</sup> 260.9634, 262.9614, found: 260.9640, 262.9620.



**5-Methyl-2-(pyridin-2-yl)-4-(4-(pyrrolidin-1-yl)pyridin-3-yl)oxazole (120).**

The 4-bromo-5-methyl-2-(pyridin-2-yl)oxazole (**119**) (100 mg, 0.42 mmol), 4-(pyrrolidin-1-yl)-3-(tributylstannyl)pyridine (**99**)<sup>80</sup> (220.9 mg, 0.5 mmol),  $PdCl_2(PPh_3)_2$  (72.8 mg, 0.1 mmol) and  $PPh_3$  (55.0 mg, 0.21 mmol) were dissolved in the xylene (8.4 mL) and degassed with argon. The reaction was stirred at 158 °C overnight. Then the solvent was evaporated and the residue was purified by flash chromatography (DCM: MeOH 15: 1) to give the 5-methyl-2-(pyridin-2-yl)-4-(4-(pyrrolidin-1-yl)pyridin-3-yl)oxazole (**120**) as the yellow solid (45 mg, 35%).

<sup>1</sup>H-NMR (300.1 MHz,  $CDCl_3$ ):  $\delta$  (ppm) 8.74 (dq,  $J = 4.8, 0.9$  Hz, 1H, 4-H), 8.07-8.19 (m, 3H, 6-H, 7-H, 1-H), 7.82 (td,  $J = 7.6, 1.7$  Hz, 1H, 2-H), 7.39 (ddd,  $J = 7.5, 4.9, 1.1$  Hz, 1H, 3-H), 6.62 (d,  $J = 6.6$  Hz, 1H, 8-H), 3.28 (t,  $J = 6.7$  Hz, 4H, 9-H), 2.42 (s, 3H, 5-H), 1.86-1.92 (m, 4H, 10-H). HRMS calcd for  $C_{20}H_{22}N_4SH$  ( $M+H$ )<sup>+</sup> 351.1638, found: 351.1643. HRMS (ESI) calcd for  $C_{18}H_{18}N_4OH$  ( $M+H$ )<sup>+</sup> 307.1553, found: 307.1555.

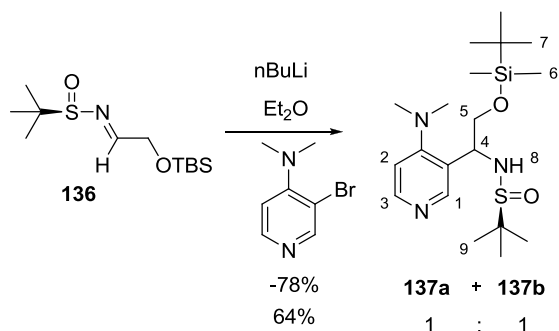


**(*R*)-*N*-(2-(*tert*-Butyldimethylsilyloxy)ethylidene)-2-methylpropane-2-sulfonamide (136).**

A mixture of 2-(*tert*-butyldimethylsilyloxy)acetaldehyde (**135**)<sup>75</sup> (700 mg, 3.7 mmol) in DCM (7.4 mL) was treated with (*R*)-2-methylpropane-2-sulfonamide (429.5 mg, 4.1 mmol) followed by copper sulfate (1461.5 mg, 9.3 mmol). After stirring at room

temperature for 2 days, the mixture was filtered through Celite and washed with DCM. The solvent was evaporated and the residue was purified by flash chromatography to give the (*R*)-*N*-(2-(tert-butyldimethylsilyloxy)ethylidene)-2-methylpropane-2-sulfonamide (**136**) (753 mg, 73%).

$^1\text{H-NMR}$  (300.1 MHz,  $\text{CDCl}_3$ ): 8.05 (t,  $J = 3.0$  Hz, 1H, 1-H), 4.52 (d,  $J = 3.0$  Hz, 2H, 2-H), 1.20 (s, 9H, 3-H), 0.91 (s, 9H, 5-H), 0.10 (s, 6H, 4-H). HRMS (ESI) calcd for  $\text{C}_{12}\text{H}_{27}\text{NO}_2\text{SSiNa}$  ( $\text{M}+\text{Na}$ ) $^+$  300.1424, found: 300.1425.



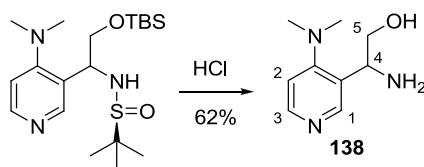
### Compound **137a**, **137b**.

To a solution of compound 3-bromo-DMAP (50 mg, 0.25 mmol) in  $\text{Et}_2\text{O}$  (0.8 mL) was added *n*-BuLi (0.11 mL, 2.5 M) at  $-78^\circ\text{C}$ . The mixture was stirred at  $-78^\circ\text{C}$  for 0.5 hour. Then the (*R*)-*N*-(2-(tert-butyldimethylsilyloxy)ethylidene)-2-methylpropane-2-sulfonamide (**136**) (76 mg, 0.27 mmol) in  $\text{Et}_2\text{O}$  (0.5 mL) was added, and stirred for further 1 hour at  $-78^\circ\text{C}$ . After quenching the reaction by water, the mixture warmed to room temperature. The aqueous phase was extracted by EtOAc and dried by  $\text{Na}_2\text{SO}_4$ . The solvent was evaporated and the residue was purified by flash chromatography (EtOAc) to give the compound **137a** (21 mg 32%), **137b** (21 mg, 32%).

Compound **137a**  $^1\text{H-NMR}$  (300.1 MHz,  $\text{CDCl}_3$ ): 8.45 (s, 1H, 3-H), 8.32 (d,  $J = 5.6$  Hz, 1H, 1-H), 6.35 (d,  $J = 5.6$  Hz, 1H, 2-H), 4.94-5.01 (m, 1H, 4-H), 4.30 (d,  $J = 0.17$  Hz, 1H, 8-H), 3.78 (dd,  $J = 10.05, 4.0$  Hz, 1H, 5-H), 3.60 (dd,  $J = 9.9, 8.5$  Hz, 1H, 5-H), 2.85 (s, 6H,  $\text{N}(\text{CH}_3)_2$ ), 1.20 (s, 9H, 9-H), 0.89 (s, 9H, 7-H), 0.05 (d,  $J = 4.5$  Hz, 6H, 6-H). HRMS (ESI) calcd for  $\text{C}_{19}\text{H}_{37}\text{N}_3\text{O}_2\text{SSiH}$  ( $\text{M}+\text{H}$ ) $^+$  400.2449, found: 400.2447.

Compound **137b**  $^1\text{H-NMR}$  (300.1 MHz,  $\text{CDCl}_3$ ): 8.51 (s, 1H, 3-H), 8.34 (d,  $J = 5.7$  Hz, 1H, 1-H), 6.89 (d,  $J = 5.6$  Hz, 1H, 2-H), 4.87 (q,  $J = 4.6$ , 1H, 4-H), 4.15 (br, 1H, 8-H),

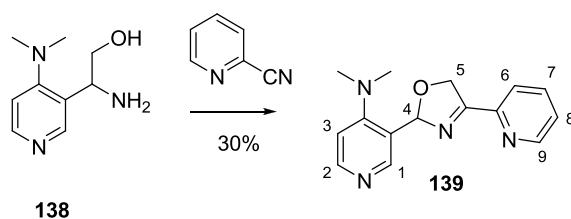
3.95 (dd,  $J = 10.0, 5.65$  Hz, 1H, 5-H), 3.80 (dd,  $J = 10.0, 6.0$  Hz, 1H, 5-H), 2.83 (s, 6H, N-(CH<sub>3</sub>)<sub>2</sub>), 1.20 (s, 9H, 9-H), 0.80 (s, 9H, 7-H), -0.05 (d,  $J = 6.4$  Hz, 6H, 6-H). HRMS (ESI) calcd for C<sub>19</sub>H<sub>37</sub>N<sub>3</sub>O<sub>2</sub>SSiH (M+H)<sup>+</sup> 400.2449, found: 400.2441.



### 2-Amino-2-(4-(dimethylamino)pyridin-3-yl)ethanol (**138**).

To a solution of compound **137** (320 mg, 0.81 mmol) in MeOH (4.2 mL) was added 3*N* HCl (1 mL) at 0 °C. The mixture stirred at room temperature for overnight. Then the NaHCO<sub>3</sub> (aq) was added to adjust pH to 8 and evaporated the solvent. The solid was washed with MeOH and DCM. The solvent was evaporated and the residue was purified by flash chromatography (DCM/MeOH/NH<sub>3</sub>(aq) = 10: 1: 0.1) to give the 2-amino-2-(4-(dimethylamino)pyridin-3-yl)ethanol (**138**) (90 mg, 62%).

<sup>1</sup>H-NMR (300.1 MHz, CDCl<sub>3</sub>): 8.44 (s, 1H, 1-H), 8.25 (d,  $J = 5.6$  Hz, 1H, 3-H), 6.80 (d,  $J = 5.6$  Hz, 1H, 2-H), 4.38 (dd,  $J = 8.1, 4.6$ , 1H, 5-H), 3.65-3.75 (m, 2H, 5-H, 4-H), 2.80 (s, 6H, N(CH<sub>3</sub>)<sub>2</sub>). HRMS (ESI) calcd for C<sub>9</sub>H<sub>15</sub>N<sub>3</sub>OH (M+H)<sup>+</sup> 182.1288, found: 182.1287.



### *N,N*-Dimethyl-3-(4-(pyridin-2-yl)-2,5-dihydrooxazol-2-yl)pyridin-4-amine (**139**).

To a solution of 2-amino-2-(4-(dimethylamino)pyridin-3-yl)ethanol **138** (90 mg, 0.49 mmol) in toluene (0.5 mL) was added ZnCl<sub>2</sub> (6.7 mg) and degassed with argon. The mixture was heated at 134 °C for overnight. The solvent was evaporated and the residue was purified by flash chromatography (DCM/MeOH/NH<sub>3</sub>(aq) = 10: 1: 0.1) to give the *N,N*-dimethyl-3-(4-(pyridin-2-yl)-2,5-dihydrooxazol-2-yl)pyridin-4-amine (**139**) (40 mg, 30%).

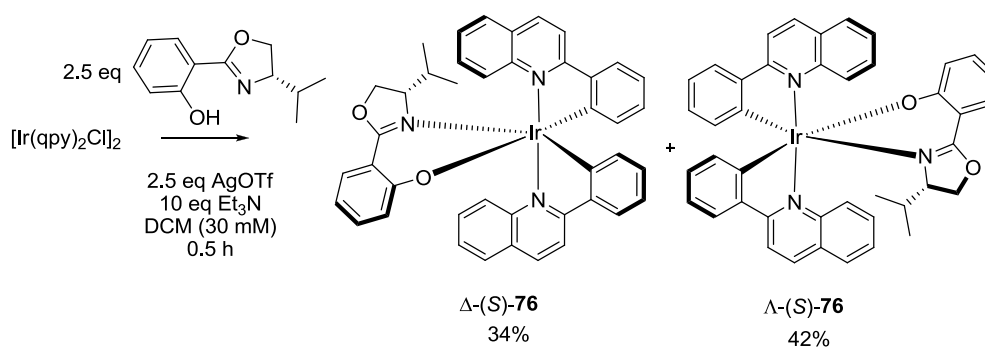
<sup>1</sup>H-NMR (300.1 MHz, MeOD): 8.69 (d,  $J = 4.6$  Hz, 1H, 9-H), 7.99-8.19 (m, 4H, 1-H,

2-H, 6-H, 7-H), 7.59-7.65 (m, 1H, 8-H), 6.72 (d,  $J = 6.7$  Hz, 1H, 3-H), 5.76 (dd,  $J = 9.8, 5.0$ , 1H, 5-H), 4.15 (t,  $J = 10.9$  Hz, 1H, 5-H), 3.81 (dd,  $J = 11.5, 4.5$ , 1H, 4-H), 3.34 (s, 6H,  $N(CH_3)_2$ ). HRMS (ESI) calcd for  $C_{15}H_{16}N_4OH$  ( $M+H$ )<sup>+</sup> 269.1397, found: 269.1398.

### 5.3.2 Synthesis of metal chiral DMAP catalysts

#### 5.3.2.1 Synthesis of enantiopure iridium precursor

Method of resolving iridium dimer



$\Delta$ -[Ir((S)-2-(4-isopropyl-4,5-dihydrooxazol-2-yl)phenol)(qp)<sub>2</sub>](PF<sub>6</sub>)( $\Lambda$ -(S)-76) and  $\Lambda$ -[Ir((S)-2-(4-isopropyl-4,5-dihydrooxazol-2-yl)phenol)(qp)<sub>2</sub>](PF<sub>6</sub>)( $\Delta$ -(S)-76).

The phenylquinoline Ir-dimer (30 mg, 0.023 mmol)<sup>83</sup>, (S)-5-isopropyl-2-(2'-hydroxyphenyl)oxazoline (10.6 mg, 0.052 mmol)<sup>35</sup> and  $AgOTf$  (13.2 mg, 0.052 mmol) were dissolved in  $CH_2Cl_2$  (0.78 mL).  $Et_3N$  (32.0  $\mu$ l, 0.23 mmol) was then added to the reaction mixture and stirred at room temperature for 0.5 hour. The crude product was subjected to silica gel chromatography with (hexane:  $EtOAc = 2: 1$ ) to afford complex  $\Lambda$ -(S)-76 (16 mg, 42%) (the first fraction eluted from the column). Complex  $\Delta$ -(S)-76 (13 mg, 34%) (the second fraction eluted from the column). The absolute metal centered configuration of complex  $\Lambda$ -(S)-76 was verified by two aspects. Firstly, it was confirmed by the crystal structure of the  $\Lambda$ -[Ir(bpy)(qp)<sub>2</sub>](PF<sub>6</sub>) (qp = 2-phenylquinoline) which was formed in the reaction with complex  $\Lambda$ -(S)-76. Secondly, the literature which was published by Chepelin and co-workers demonstrated that the configuration of the iridium center was retained during the

substitution reaction<sup>55</sup>. The absolute stereochemistry of complex  $\Delta$ -(S)-**76** was verified by the CD spectrum after comparing with the complex  $\Lambda$ -(S)-**76**.

$\Lambda$ -[Ir((S)-2-(4-isopropyl-4,5-dihydrooxazol-2-yl)phenol)(qp)<sub>2</sub>](PF<sub>6</sub>) ( $\Lambda$ -(S)-**76**) (90% purity)

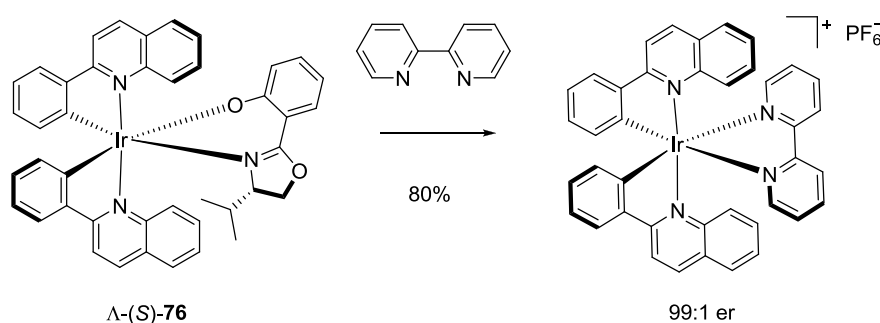
<sup>1</sup>H-NMR (300.1 MHz, CDCl<sub>3</sub>):  $\delta$  (ppm) 9.91 (d,  $J$  = 8.8 Hz, 1H), 8.23 (dd,  $J$  = 8.7, 18.6 Hz, 2H), 8.09 (d,  $J$  = 8.9 Hz, 1H), 7.87- 7.92 (m, 3H), 7.77 (dd,  $J$  = 7.8, 1.6 Hz, 1H), 7.72 (dd,  $J$  = 7.8, 0.9 Hz, 1H), 7.59 (dd,  $J$  = 7.5, 1.4 Hz, 1H), 7.52 (td,  $J$  = 6.9, 1.7 Hz, 1H), 7.34 – 7.47 (m, 3H), 7.08 (dd,  $J$  = 8.5, 0.8 Hz, 1H), 6.85- 6.97 (m, 2H), 6.73 - 6.81 (m, 2H), 6.66 (td,  $J$  = 7.8, 1.3 Hz, 1H), 6.60 (td,  $J$  = 7.3, 1.3 Hz, 1H), 6.27 (dd,  $J$  = 9.0, 1.2 Hz, 1H), 6.07 (dd,  $J$  = 7.6, 0.8 Hz, 1H), 5.88 (td,  $J$  = 6.9, 1.0 Hz, 1H), 4.05 – 4.21 (m, 2H), 3.75 – 3.84 (m, 1H), 0.35 (d,  $J$  = 6.9 Hz, 3H), 0.15 – 0.26 (m, 1H), -0.20 (d,  $J$  = 6.7 Hz, 3H) <sup>13</sup>C-NMR (125 MHz, CDCl<sub>3</sub>)  $\delta$  (ppm) 171.3, 171.2, 170.7, 165.3, 155.1, 151.5, 150.7, 147.9, 147.0, 146.4, 138.7, 137.8, 136.6, 132.9, 132.5, 131.9, 129.3, 128.9, 128.75, 128.71, 128.6, 128.2, 127.9, 127.5, 127.2, 126.8, 126.2, 126.1, 125.2, 125.0, 123.1, 121.6, 119.9, 116.8, 116.2, 112.1, 71.5, 66.6, 29.4, 19.1, 13.3, 1.0. IR (thin film):  $\nu$  (cm<sup>-1</sup>) 3052, 2959, 2921, 2856, 1608, 1597, 1538, 1512, 1463, 1439, 1377, 1336, 1259, 1224, 1150, 1098, 1063, 1030, 961, 906, 825, 796, 756, 721, 687, 639, 568, 506. CD ( $\Delta\epsilon$ /M<sup>-1</sup>cm<sup>-1</sup>, CHCl<sub>3</sub>): 240 nm (+19.5), 268 nm (-24), 278 nm (-5), 283 nm (-8), 293 nm (+19), 306 nm (+5), 356 nm (+44). HRMS (ESI) calcd for C<sub>42</sub>H<sub>34</sub>IrN<sub>3</sub>O<sub>2</sub> (M+H)<sup>+</sup> 806.2356, found: 806.2363.

$\Delta$ -[Ir((S)-2-(4-isopropyl-4,5-dihydrooxazol-2-yl)phenol)(qp)<sub>2</sub>](PF<sub>6</sub>) ( $\Delta$ -(S)-**76**)

<sup>1</sup>H-NMR (300.1 MHz, CDCl<sub>3</sub>):  $\delta$  (ppm) 9.92 (dd,  $J$  = 8.6, 0.7 Hz, 1H), 8.61 (dd,  $J$  = 6.5, 4.2 Hz, 1H), 8.28 (d,  $J$  = 8.5 Hz, 1H), 8.15 (d,  $J$  = 8.8 Hz, 1H), 8.02 (s, 2H), 7.82 (dd,  $J$  = 7.8, 1.1 Hz, 2H), 7.75 (dd,  $J$  = 7.9, 1.0 Hz, 1H), 7.59- 7.63 (m, 1H), 7.43- 7.56 (m, 2H), 7.31- 7.38 (m, 2H), 6.80- 6.92 (m, 4H), 6.62- 6.69 (m, 1 H), 6.58 (tt,  $J$  = 7.44, 3.2, 1.4 Hz, 2H), 6.09- 6.16 (m, 2H), 5.90- 5.98 (m, 1H), 4.15 (t,  $J$  = 7.1 Hz, 1H), 3.38 (t,  $J$  = 8.9 Hz, 1H), 2.79 (ddd,  $J$  = 9.8, 4.2, 1.5 Hz, 1H), 1.32- 1.45 (m, 1H), 0.92 (d,  $J$  = 6.7 Hz, 3H), 0.31 (d,  $J$  = 7.0 Hz, 3H) <sup>13</sup>C-NMR (125 MHz, CDCl<sub>3</sub>)  $\delta$  (ppm) 171.4, 170.8, 170.3, 164.7, 152.7, 152.2, 150.5, 148.5, 147.1, 146.0, 139.1, 138.0, 136.0, 133.0, 132.5, 132.3, 129.58, 129.56, 129.1, 127.90, 127.87, 127.6, 127.5,

127.4, 126.5, 126.3, 126.0, 125.3, 122.3, 121.6, 120.1, 117.0, 116.0, 114.1, 112.3, 69.7, 67.3, 28.6, 20.8, 15.0, 1.0. IR (thin film):  $\nu$  ( $\text{cm}^{-1}$ ) 3054, 2958, 2192, 1614, 1581, 1540, 1513, 1465, 1440, 1376, 1325, 1281, 1233, 1150, 1063, 1033, 993, 954, 908, 827, 792, 759, 725, 638, 574, 508, 440. CD ( $\Delta\epsilon/M^{-1}\text{cm}^{-1}$ ,  $\text{CHCl}_3$ ): 252 nm (-6), 267 nm (+30), 291 nm (-5), 356 nm (-29). HRMS (ESI) calcd for  $\text{C}_{42}\text{H}_{34}\text{IrN}_3\text{O}_2$  ( $\text{M}+\text{H}$ )<sup>+</sup> 806.2356, found: 806.2373.

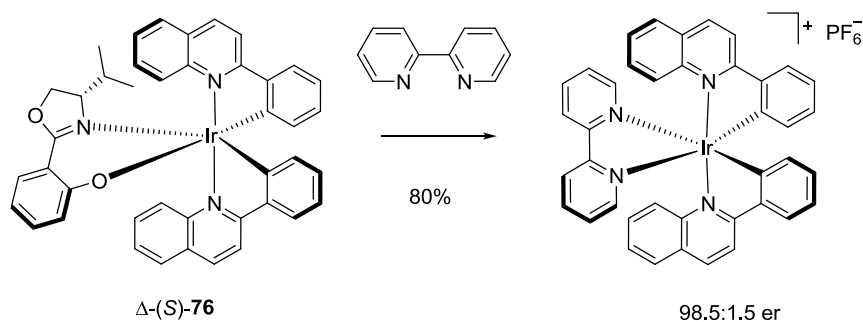
Evaluation of the enantiopurity of iridium center of the complex  $\Lambda$ -(*S*)-**76** and  $\Delta$ -(*S*)-**76**:



#### $\Lambda$ -[Ir(bpy)<sub>2</sub>(qp)<sub>2</sub>](PF<sub>6</sub>).

In a closed glass 1.5 mL vial fitted with a septum (brand: MACHEREY-NAGEL), the complex  $\Lambda$ -(*S*)-**76** (6 mg, 0.007 mmol), 2,2'-bipyridine (5.8 mg, 0.037 mmol) and TFA (2.8  $\mu\text{L}$ , 0.037 mmol) were dissolved in DCM (0.4 mL) and stirred at rt for 1 hour. The crude material was subjected to silica gel chromatography with DCM and later MeCN: DCM = 1: 10 to MeOH: DCM = 1: 10. The product eluents were concentrated to dryness. Then water and  $\text{NH}_4\text{PF}_6$  were added to the resulting material and shake in the ultrasound cleaner. The orange precipitate was centrifuged, washed twice with water to afford  $\Lambda$ -[Ir(bpy)<sub>2</sub>(qp)<sub>2</sub>](PF<sub>6</sub>) (5.4 mg, 80%). The enantiopurity (1.1: 98.9 er) was determined by chiral HPLC analysis (Figure 61). The absolute configuration of the complex  $\Lambda$ -[Ir(bpy)<sub>2</sub>(qp)<sub>2</sub>](PF<sub>6</sub>) was verified by crystal structure (Figure 62).

CD ( $\Delta\epsilon/M^{-1}\text{cm}^{-1}$ , MeCN): 213 nm (-71), 227 nm (-19), 235 nm (-44), 252 nm (+57), 264 nm (-15), 274 nm (+47), 283 nm (-24), 298 nm (+67), 320 nm (+3.9), 345 nm (+51). Other analysis data was already published<sup>84</sup>.



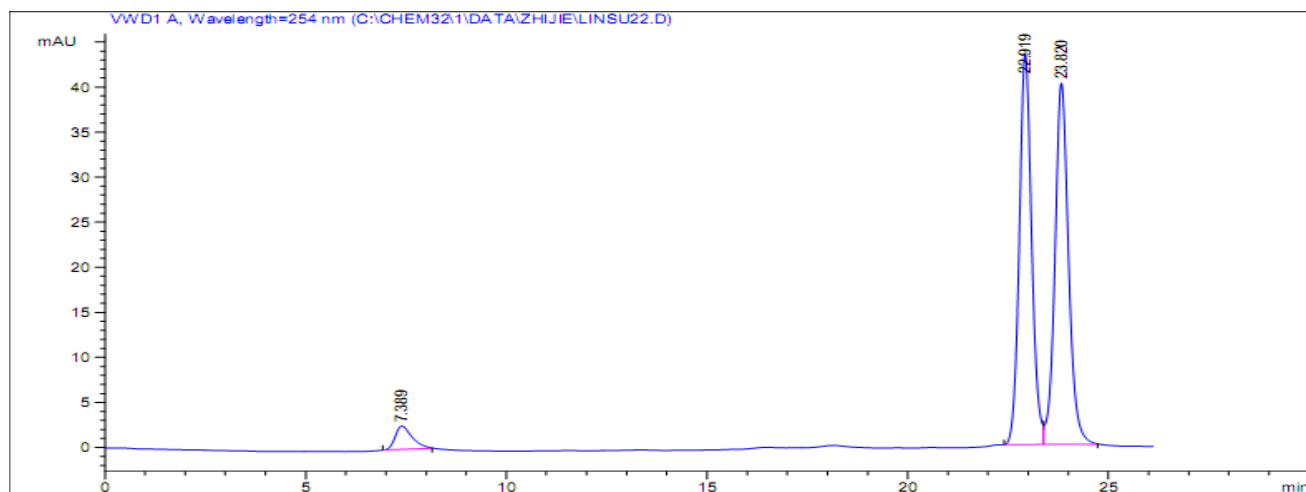
### $\Delta$ -[Ir(bpy)(qp)<sub>2</sub>](PF<sub>6</sub>).

The procedure was same with  $\Lambda$ -[Ir(bpy)<sub>2</sub>(qp)<sub>2</sub>](PF<sub>6</sub>). Complex  $\Delta-(S)-76$  (5.4 mg, 0.007 mmol), 2,2'-bipyridine (5.2 mg, 0.034 mmol), TFA (2.5  $\mu$ l, 0.034 mmol) DCM (0.34 mL). Yield: (4.6 mg, 76%) The enantiopurity (98.5: 1.5 er) was determined by chiral HPLC analysis analysis (Figure 62) The absolute configuration of the complex  $\Delta$ -[Ir(bpy)(qp)<sub>2</sub>](PF<sub>6</sub>) was verified by CD spectrum after comparing with  $\Lambda$ -[Ir(bpy)(qp)<sub>2</sub>](PF<sub>6</sub>).

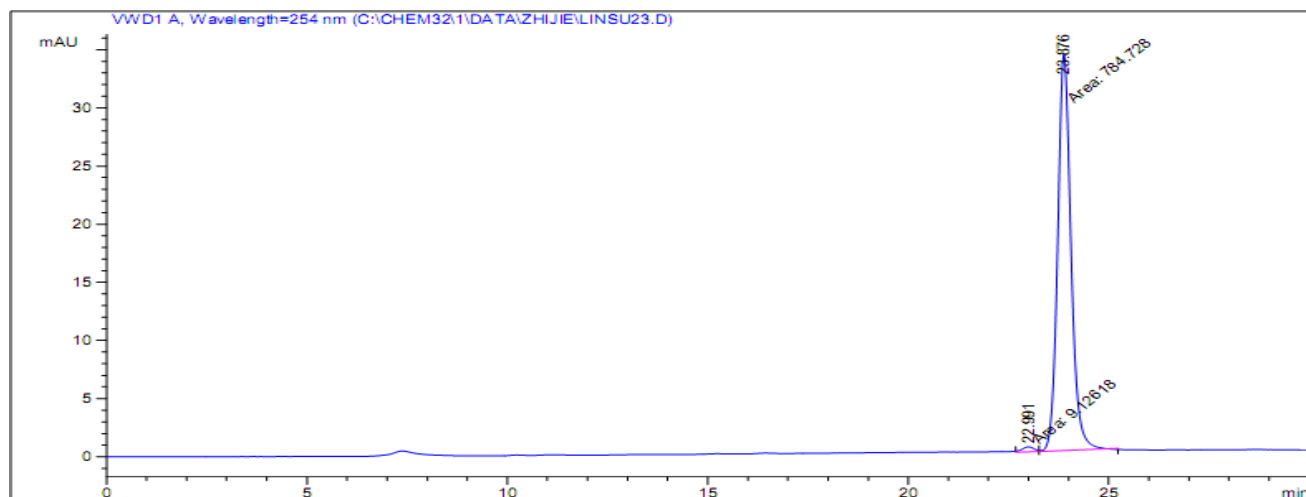
CD ( $\Delta\epsilon/M^{-1}cm^{-1}$ , MeCN): 213 nm (+81), 227 nm (+24), 235 nm (+46), 252 nm (-60), 264 nm (+15), 274 nm (-47), 283 nm (+32), 298 nm (-66), 320 nm (-1), 345 nm (-52).

Determination of enantiomeric ratio of  $\Lambda$ -[Ir(bpy)(qp)<sub>2</sub>](PF<sub>6</sub>),  $\Delta$ -[Ir(bpy)(qp)<sub>2</sub>](PF<sub>6</sub>) by chiral HPLC. The Iridium complex was analyzed with a Chiralpak IA (250  $\times$  4 mm) HPLC column on an Agilent 1200 Series HPLC System. The flow rate was 0.5 mL/min, the column temperature 40  $^{\circ}C$ , and UV-absorption was measured at 254 nm. Solvent A = 0.1% TFA, solvent B = MeCN, with a linear gradient of 45% to 60% B in 20 min.

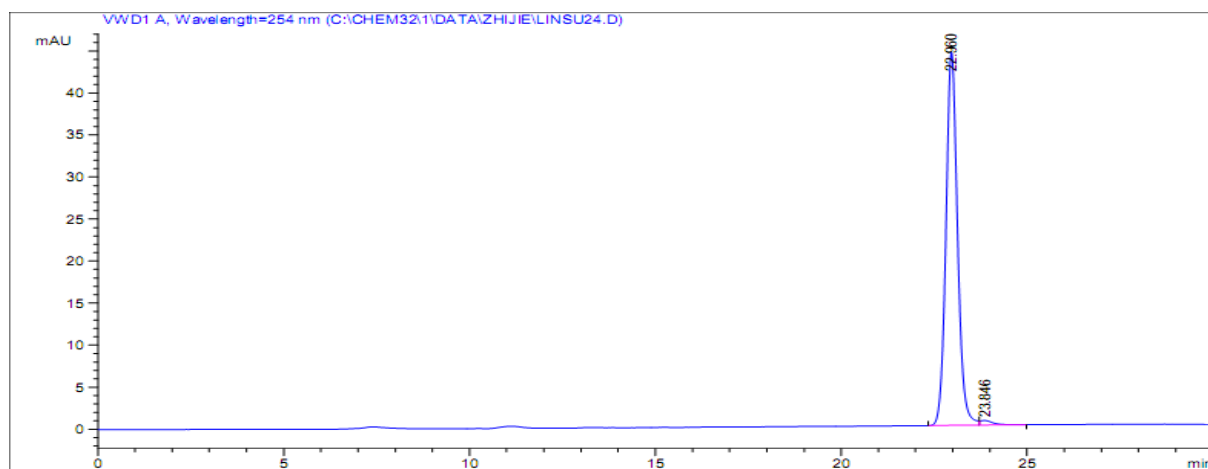




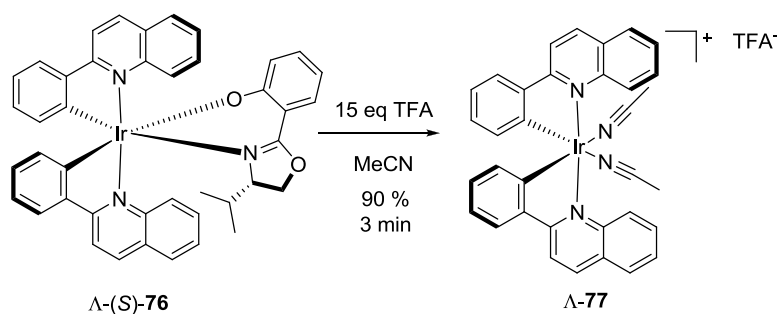
**Figure 60.** HPLC trace for  $(rac)\text{-}[\text{Ir}(\text{bpy})(\text{qp})_2](\text{PF}_6)$ .



**Figure 61.** HPLC trace for  $\Lambda\text{-}[\text{Ir}(\text{bpy})(\text{qp})_2](\text{PF}_6)$  Integration of peak areas: 1.1: 98.9  
er.



**Figure 62.** HPLC trace for  $\Delta\text{-}[\text{Ir}(\text{bpy})(\text{qp})_2](\text{PF}_6)$  Integration of peak areas: 98.5: 1.5  
er.



### $\Lambda$ -[Ir(bpy)(MeCN)<sub>2</sub>](TFA) ( $\Lambda$ -77).

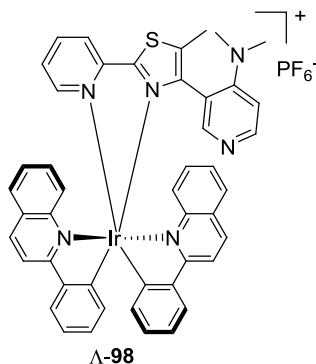
Complex  $\Lambda$ -(S)-76 (20 mg, 0.025 mmol) was dissolved in 3 mL MeCN. And 5 eq TFA was added to the acetonitrile solvent stirring for 3 min. Then the mixture was subjected to silica gel chromatography and eluted with hexane: EtOAc: MeCN (4: 2: 1) later MeOH: DCM (10: 1). The crude product was redissolved in MeCN. After evaporating the solvent, the reaction provided the complex  $\Lambda$ -77 as the orange color solid (18 mg, 90%). The absolute configuration of the complex  $\Lambda$ -77 was relative from the starting material  $\Lambda$ -(S)-76 together with the configuration retention in the substitution reaction<sup>55</sup>. Other precursor  $\Lambda$ -Ir(polypyridyl)<sub>2</sub>(MeCN)<sub>2</sub> was synthesized in the same procedure with the complex  $\Lambda$ -77.

<sup>1</sup>H-NMR (300.1 MHz, CD<sub>3</sub>CN):  $\delta$  (ppm) 8.82 (d,  $J$  = 8.9 Hz, 2H), 8.56 (d,  $J$  = 8.8 Hz, 2H), 8.24 (d,  $J$  = 8.8 Hz, 2H), 8.09 (d,  $J$  = 8.0 Hz, 2H), 7.89 (t,  $J$  = 7.5 Hz, 2H), 7.82 (d,  $J$  = 7.8 Hz, 2H), 7.74 (t,  $J$  = 7.7 Hz, 2H), 6.95 (t,  $J$  = 7.5 Hz, 2H), 6.65 (t,  $J$  = 7.4 Hz, 2H), 6.11 (d,  $J$  = 7.7 Hz, 2H), 1.97 (s, 6H).

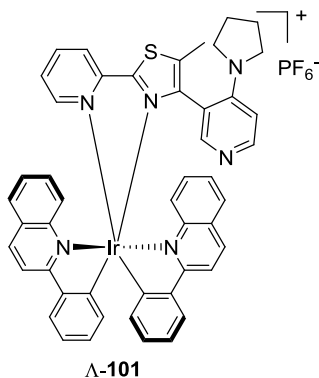
#### 5.3.2.2 General procedure for synthesis of chiral-at-metal DMAP catalysts

In a closed glass vial fitted with a septum, the compound  $\Lambda$ -Ir(polypyridyl)<sub>2</sub>(MeCN)<sub>2</sub> (1 eq) (20 mg~35 mg), directing ligand (1 eq) were dissolved in DCM and MeOH (1: 1) (50 mM) stirred at 70 °C for 2 hours. The crude material was subjected to silica gel chromatography with DCM and later CH<sub>3</sub>CN: H<sub>2</sub>O: KNO<sub>3</sub>(sat) = 100: 4: 1. The product eluents were concentrated to dryness by evaporator. Then water and NH<sub>4</sub>PF<sub>6</sub> were added to the resulting material and was shaken in the ultrasound cleaner. The orange precipitate was centrifuged, washed twice with water and Et<sub>2</sub>O to afford  $\Lambda$ -Ir catalyst.

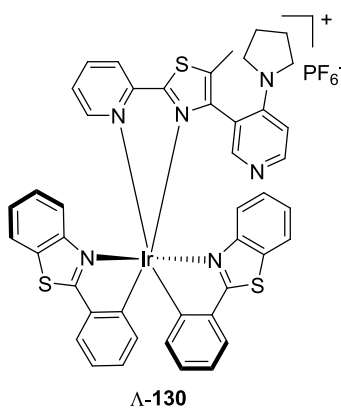
For  $\Lambda$ -Ir(polypyridyl)<sub>2</sub>(MeCN)<sub>2</sub> precursor, when the polypyridyl ligand is 2-phenylquinoline, the first elution in the column chromatography resolution was  $\Lambda$ -configuration. Considering the metal configuration is retained in the substitution reaction, the catalysts which formed from the precursor  $\Lambda$ -Ir(2-phenylquinoline)<sub>2</sub>(MeCN)<sub>2</sub> are  $\Lambda$ -configuration. For other ligands (2-phenylbenzo[d]thiazole (Aldrich); 5-methyl-2-phenylbenzo[d]thiazole<sup>77</sup>; 2,5-diphenylpyridine<sup>78</sup>; 2-(4-(trifluoromethyl)phenyl)quinoline<sup>74</sup>; 2-(2,4-difluorophenyl)quinoline<sup>74</sup>; 2-p-tolylquinoline<sup>74</sup>; 2-(naphthalen-2-yl)quinoline<sup>74</sup>), we also used the first elution in the column chromatography resolution. Thus, we proposed that the catalysts which formed from these precursors are also  $\Lambda$ -configuration. Additionally, these precursors were synthesized using a similar procedure as the precursor  $\Lambda$ -Ir(2-phenylquinoline)<sub>2</sub>(MeCN)<sub>2</sub> ( $\Lambda$ -77).



**Compound  $\Lambda$ -98** (61%). <sup>1</sup>H-NMR (300.1 MHz, CD<sub>3</sub>CN):  $\delta$  (ppm) 8.55 (d,  $J$  = 8.8 Hz, 1H), 8.33 (d,  $J$  = 8.8 Hz, 1H), 8.13 (t,  $J$  = 9.4 Hz, 2H), 8.03 (dd,  $J$  = 8.1, 1.35 Hz, 1H), 7.87- 7.99 (m, 4H), 7.83- 7.87 (m, 1H), 7.71 (dd,  $J$  = 7.6, 1.3 Hz, 1H), 7.48- 7.63 (m, 6H), 7.36- 7.44 (m, 1H), 7.29 (d,  $J$  = 8.8 Hz, 1H), 7.18- 7.25 (m, 1H), 7.08 (td,  $J$  = 8.0, 1.1 Hz, 1H), 6.91 (td,  $J$  = 8.0, 1.1 Hz, 1H), 6.63 – 6.76 (m, 3H), 6.39 (dd,  $J$  = 7.7, 0.8 Hz, 1H), 5.89 (dd,  $J$  = 7.8, 0.75 Hz, 1H), 2.28 (s, 3H), 1.8 – 2.5 (br, 6H). HRMS (ESI) calcd for C<sub>46</sub>H<sub>36</sub>IrN<sub>6</sub>S (M)<sup>+</sup> 897.2347, found: 897.2335.

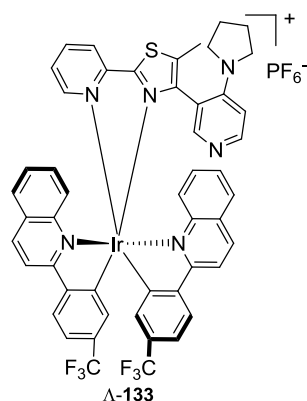


**Compound A-101** (54%).  $^1\text{H-NMR}$  (300.1 MHz,  $\text{CD}_3\text{CN}$ ):  $\delta$  (ppm) 8.54 (d,  $J = 8.8$  Hz, 1H), 8.29 (d,  $J = 8.8$  Hz, 1H), 8.14 (d,  $J = 8.9$  Hz, 1H), 8.07 (d,  $J = 8.9$  Hz, 1H), 8.03 (dd,  $J = 8.05, 1.2$  Hz, 1H), 7.85- 7.96 (m, 4H), 7.75 (dd,  $J = 5.4, 0.75$  Hz, 1H), 7.70 (dd,  $J = 7.5, 1.2$  Hz, 1H), 7.48- 7.68 (m, 6H), 7.35- 7.41 (m, 1H), 7.19- 7.26 (m, 2H), 7.04 (td,  $J = 8.3, 1.1$  Hz, 1H), 6.94 (td,  $J = 8.2, 1.1$  Hz, 1H), 6.64– 6.75 (m, 2H), 6.52 (d,  $J = 7.5$  Hz, 1H), 6.46 (d,  $J = 7.7$  Hz, 1H), 5.61 (dd,  $J = 7.8, 0.6$  Hz, 1H), 2.35 (s, 3H), 2.01 – 2.50 (br, 6H), 1.16 (br, 2H). HRMS (ESI) calcd for  $\text{C}_{48}\text{H}_{38}\text{IrN}_6\text{S}$  ( $\text{M}$ ) $^+$  923.2504, found: 923.2476.

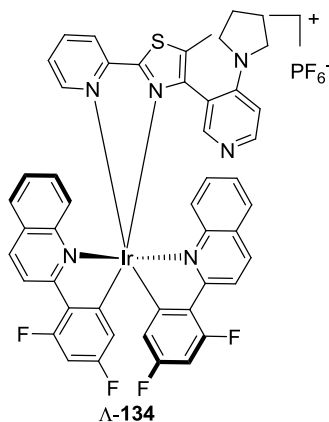


**Compound A-130** (23%).  $^1\text{H-NMR}$  (300.1 MHz,  $\text{CD}_3\text{CN}$ ):  $\delta$  (ppm) 8.32 (d,  $J = 7.4$  Hz, 1H), 8.05- 8.14 (m, 3H), 7.87 (d,  $J = 5.5$  Hz, 1H), 7.76 (dd,  $J = 8.5, 0.9$  Hz, 1H), 7.72 (s, 1H), 7.63 (d,  $J = 6.5$  Hz, 1H), 7.44- 7.55 (m, 5H), 7.19- 7.26 (m, 1H), 7.03 (td,  $J = 7.5, 1.0$  Hz, 1H), 6.75 – 6.85 (m, 2H), 6.62 (td,  $J = 7.5, 1.3$  Hz, 1H), 6.39 (d,  $J = 8.3$  Hz, 1H), 6.30 (d,  $J = 6.75$  Hz, 1H), 6.04 (d,  $J = 7.4$  Hz, 1H), 5.89 (d,  $J = 7.5$  Hz, 1H), 2.38 (s, 3H), 2.01 – 2.38 (br, 6H), 1.30 (br, 2H). (mixture with the other diastereomer in the proton NMR; the ratio was 5.5:1). HRMS (ESI) calcd for

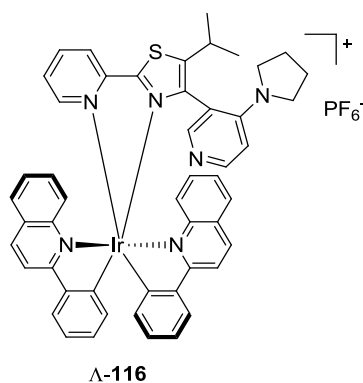
$C_{44}H_{34}IrN_6S_3 (M)^+$  935.1629, found: 935.1626.



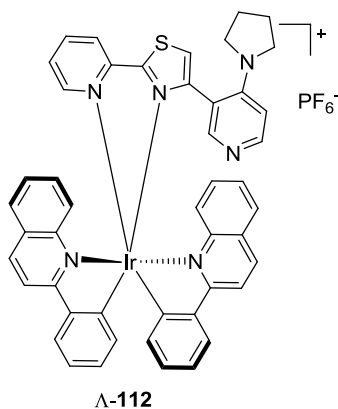
**Compound Λ-133** (53%).  $^1H$ -NMR (300.1 MHz,  $CD_3CN$ ):  $\delta$  (ppm) 8.68 (d,  $J = 8.7$  Hz, 1H), 8.39 (d,  $J = 8.7$  Hz, 1H), 8.28(d,  $J = 8.9$  Hz, 1H), 8.08- 8.15 (m, 2H), 7.96- 8.05 (m, 2H), 7.89- 7.94 (m, 2H), 7.84 (d,  $J = 8.25$  Hz, 1H), 7.73 (d,  $J = 7.0$  Hz, 1H), 7.59- 7.72 (m, 5H), 7.48 (d,  $J = 8.85$  Hz, 1H), 7.20- 7.40 (m, 5H), 6.64 (s, 1H), 6.45(d,  $J = 6.8$  Hz, 1H), 5.63 (s, 1H), 2.38 (s, 3H), 2.20 – 2.60 (br, 6H), 1.04 (br, 2H). HRMS (ESI) calcd for  $C_{50}H_{36}F_6IrN_6S (M)^+$  1059.2252, found: 1059.2225.



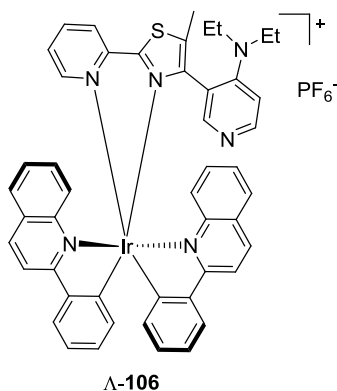
**Compound Λ-134** (60%).  $^1H$ -NMR (300.1 MHz,  $CD_3CN$ ):  $\delta$  (ppm) 8.62 (d,  $J = 8.9$  Hz, 1H), 8.47 (dd,  $J = 9.0, 4.4$  Hz, 1H), 8.26- 8.36 (m, 2H), 8.06 (dd,  $J = 8.1, 2.2$  Hz, 1H), 7.86- 7.96 (m, 5H), 7.79 (d,  $J = 1.05$  Hz, 1H), 7.52- 7.66 (m, 3H), 7.39- 7.48 (m, 2H), 7.20- 7.29 (m, 2H), 6.54- 6.75 (m, 3H), 6.10 (dd,  $J = 8.9, 2.4$  Hz, 1H), 4.98 (dd,  $J = 9.0, 2.2$  Hz, 1H), 2.38 (s, 3H), 2.20 – 2.60 (br, 6H), 1.09 (br, 2H). HRMS (ESI) calcd for  $C_{48}H_{34}F_4IrN_6S (M)^+$  995.2127, found: 995.2114.



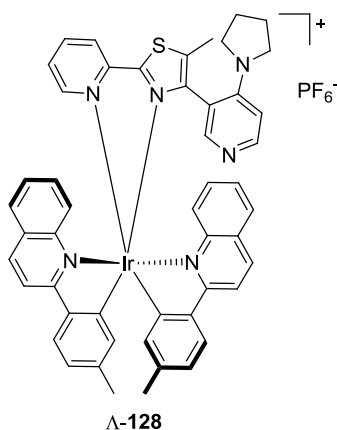
**Compound A-116** (58%).  $^1\text{H-NMR}$  (300.1 MHz,  $\text{CD}_3\text{CN}$ ):  $\delta$  (ppm) 8.54 (d,  $J = 8.8$  Hz, 1H), 8.28 (d,  $J = 8.8$  Hz, 1H), 8.14 (d,  $J = 8.85$  Hz, 1H), 8.00- 8.09 (m, 2H), 7.84- 7.94 (m, 4H), 7.76 (d,  $J = 5.3$  Hz, 1H), 7.72 (dd,  $J = 7.4, 1.0$  Hz, 1H), 7.50- 7.68 (m, 5H), 7.36- 7.45 (m, 2H), 7.17- 7.24 (m, 2H), 7.04 (td,  $J = 8.2, 1.1$  Hz, 1H), 6.95 (td,  $J = 8.0, 1.0$  Hz, 1H), 6.65- 6.75 (m, 2H), 6.52 (d,  $J = 7.5$  Hz, 1H), 6.48 (d,  $J = 7.8$  Hz, 1H), 5.60 (dd,  $J = 7.8, 0.7$  Hz, 1H), 2.92- 3.02 (m, 1H), 2.20- 2.60 (br, 6H), 1.34 (d,  $J = 6.8$  Hz, 3H), 1.27 (d,  $J = 6.8$  Hz, 3H), 1.16 (br, 2H). HRMS (ESI) calcd for  $\text{C}_{50}\text{H}_{42}\text{IrN}_6\text{S}$  ( $\text{M}$ ) $^+$  951.2817, found: 951.2800.



**Compound A-112** (83%).  $^1\text{H-NMR}$  (300.1 MHz,  $\text{CD}_3\text{CN}$ ):  $\delta$  (ppm) 8.54 (d,  $J = 8.8$  Hz, 1H), 8.29 (d,  $J = 8.8$  Hz, 1H), 8.14 (d,  $J = 8.8$  Hz, 1H), 7.97- 8.10 (m, 4H), 7.86- 7.95 (m, 3H), 7.77 (d,  $J = 5.5$  Hz, 1H), 7.37- 7.70 (m, 8H), 7.18- 7.26 (m, 2H), 7.04 (td,  $J = 8.2, 1.1$  Hz, 1H), 6.91 (td,  $J = 8.0, 1.0$  Hz, 1H), 6.68 (t,  $J = 6.8$  Hz, 2H), 6.48 (d,  $J = 7.35$  Hz, 1H), 6.43 (d,  $J = 7.8$  Hz, 1H), 5.64 (d,  $J = 7.7$  Hz, 1H), 2.52- 2.68 (br, 6H), 1.16 (br, 2H). HRMS (ESI) calcd for  $\text{C}_{47}\text{H}_{36}\text{IrN}_6\text{S}$  ( $\text{M}$ ) $^+$  909.2347, found: 909.2336.



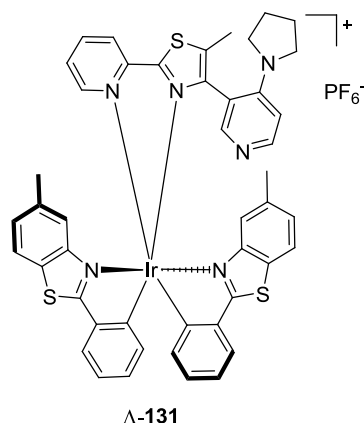
**Compound A-106** (40%).  $^1\text{H-NMR}$  (300.1 MHz,  $\text{CD}_3\text{CN}$ ):  $\delta$  (ppm) 8.52 (d,  $J = 8.8$  Hz, 1H), 8.29 (d,  $J = 8.8$  Hz, 1H), 8.15 (d,  $J = 8.9$  Hz, 1H), 8.09 (d,  $J = 8.9$  Hz, 1H), 8.01 (d,  $J = 8.1$  Hz, 1H), 7.84- 7.95 (m, 4H), 7.77 (d,  $J = 5.5$  Hz, 1H), 7.73 (d,  $J = 7.1$  Hz, 1H), 7.48- 7.64 (m, 6H), 7.36- 7.42 (m, 1H), 7.18- 7.26 (m, 2H), 7.04 (t,  $J = 7.2$  Hz, 1H), 6.91 (t,  $J = 8.1$  Hz, 1H), 6.63- 6.74 (m, 3H), 6.44 (d,  $J = 7.7$  Hz, 1H), 5.66 (d,  $J = 7.8$  Hz, 1H), 2.40- 2.50 (m, 7H), 0.57 (t,  $J = 7.1$  Hz, 6H). HRMS (ESI) calcd for  $\text{C}_{48}\text{H}_{40}\text{IrN}_6\text{S}$  ( $\text{M}$ ) $^+$  925.2660, found: 925.2645.



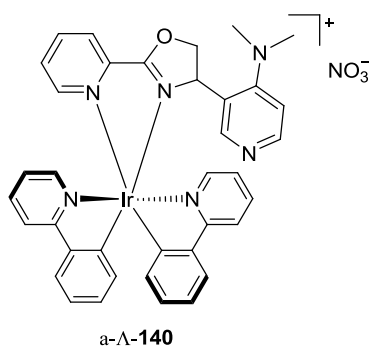
**Compound A-128** (53%).  $^1\text{H-NMR}$  (300.1 MHz,  $\text{CD}_3\text{CN}$ ):  $\delta$  (ppm) 8.49 (d,  $J = 8.8$  Hz, 1H), 8.23 (d,  $J = 8.7$  Hz, 1H), 8.08 (d,  $J = 8.9$  Hz, 1H), 7.99 (d,  $J = 8.8$  Hz, 2H), 7.78- 7.92 (m, 3H), 7.70- 7.77 (m, 3H), 7.64 (d,  $J = 1.1$  Hz, 1H), 7.42- 7.61 (m, 5H), 7.33- 7.39 (m, 1H), 7.15- 7.25 (m, 2H), 6.87 (dd,  $J = 8.0, 1.0$  Hz, 1H), 6.76 (dd,  $J = 8.0, 1.0$  Hz, 1H), 6.51 (d,  $J = 7.45$  Hz, 1H), 6.29 (s, 1H), 5.41 (s, 1H), 2.40- 2.70 (br, 6H), 2.48 (s, 3H), 1.99 (s, 3H), 1.85 (s, 3H), 1.16 (br, 2H). HRMS (ESI) calcd for  $\text{C}_{50}\text{H}_{42}\text{IrN}_6\text{S}$  ( $\text{M}$ ) $^+$  951.2817, found: 951.2827.



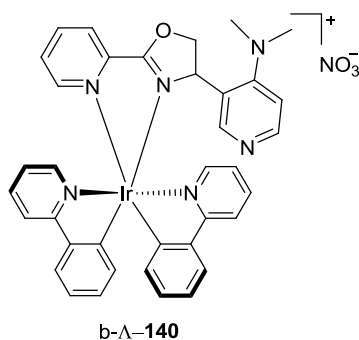




**Compound Λ-131** (31%).  $^1\text{H-NMR}$  (300.1 MHz,  $\text{CD}_3\text{CN}$ ):  $\delta$  (ppm) 8.36 (d,  $J = 7.9$  Hz, 1H), 8.14 (td,  $J = 7.9, 1.5$  Hz, 1H), 7.89- 8.00 (m, 3H), 7.73 (dd,  $J = 7.7, 1.0$  Hz, 1H), 7.60- 7.70 (m, 2H), 7.47- 7.53 (m, 1H), 7.45 (dd,  $J = 6.1, 0.8$  Hz, 1H), 7.37 (d,  $J = 8.3$  Hz, 1H), 7.30 (d,  $J = 7.3$  Hz, 1H), 7.02 (td,  $J = 7.5, 1.0$  Hz, 1H), 6.74- 6.85 (m, 2H), 6.61 (td,  $J = 7.6, 1.3$  Hz, 1H), 6.26 (d,  $J = 7.0$  Hz, 1H), 5.96- 6.03 (m, 3H), 5.89 (d,  $J = 7.7$  Hz, 1H), 2.50- 2.70 (br, 6H), 2.44 (s, 3H), 2.33 (s, 3H), 2.03 (s, 3H), 1.30 (br, 2H). HRMS (ESI) calcd for  $\text{C}_{46}\text{H}_{38}\text{IrN}_6\text{S}_3$  ( $\text{M}$ ) $^+$  963.1942, found: 963.1935.



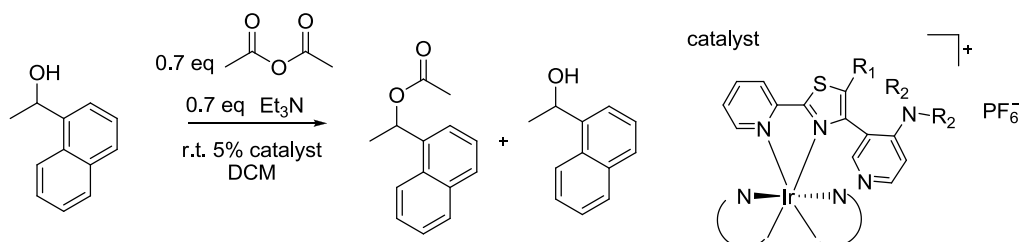
**Compound a-Λ-140** (90%).  $^1\text{H-NMR}$  (300.1 MHz,  $\text{CD}_3\text{CN}$ ):  $\delta$  (ppm) 8.63 (dd,  $J = 5.8, 0.7$  Hz, 1H), 8.24 (dd,  $J = 7.1, 0.6$  Hz, 1H), 7.93- 8.04 (m, 2H), 7.80- 7.88 (m, 2H), 7.65- 7.74 (m, 2H), 7.52- 7.60 (m, 4H), 7.34 (dd,  $J = 7.8, 1.4$  Hz, 1H), 7.25- 7.31 (m, 1H), 7.16- 7.23 (m, 1H), 7.00- 7.06 (m, 1H), 6.91 (td,  $J = 7.7, 1.2$  Hz, 1H), 6.60- 6.80 (m, 4H), 6.53 (d,  $J = 5.4$  Hz, 1H), 6.34 (dd,  $J = 7.2, 0.9$  Hz, 1H), 6.01 (dd,  $J = 7.6, 0.75$  Hz, 1H), 5.96 (d,  $J = 6.9$  Hz, 1H), 4.04 (dd,  $J = 10.8, 7.2$  Hz, 1H), 3.76 (t,  $J = 10.8$  Hz, 1H), 3.52- 3.58 (m, 1H), 2.20 (br, 6H). HRMS (ESI) calcd for  $\text{C}_{37}\text{H}_{32}\text{IrN}_6\text{O}$  ( $\text{M}$ ) $^+$  769.2263, found: 769.2277.




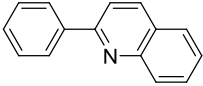
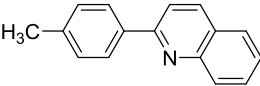
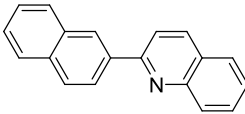
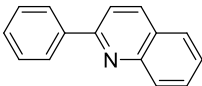
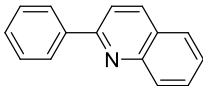
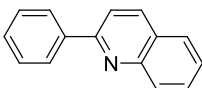
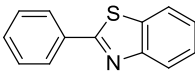
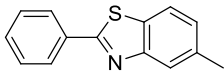
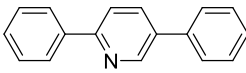
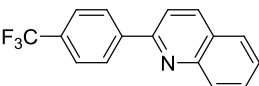
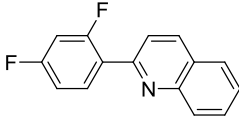
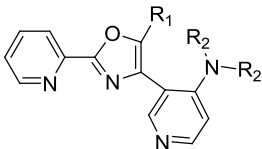
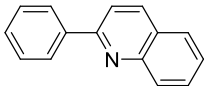
**Compound b-Λ-140** (64%).  $^1\text{H-NMR}$  (300.1 MHz,  $\text{CD}_3\text{CN}$ ):  $\delta$  (ppm) 8.79 (d,  $J = 5.6$  Hz, 1H), 8.14 (d,  $J = 7.7$  Hz, 1H), 8.06 (d,  $J = 8.1$  Hz, 1H), 7.87- 7.98 (m, 3H), 7.80 (td,  $J = 8.3, 1.4$  Hz, 1H), 7.65- 7.72 (m, 2H), 7.58- 7.64 (m, 2H), 7.51 (d,  $J = 6.0$  Hz, 1H), 7.20- 7.31 (m, 2H), 7.09- 7.16 (m, 1H), 6.91 (td,  $J = 7.4, 1.1$  Hz, 1H), 6.72- 6.85 (m, 3H), 6.51 (td,  $J = 7.4, 1.1$  Hz, 1H), 6.15 (d,  $J = 7.5$  Hz, 1H), 5.95 (d,  $J = 7.0$  Hz, 1H), 5.85 (d,  $J = 7.5$  Hz, 1H), 5.55 (dd,  $J = 10.9, 4.6$  Hz, 1H), 3.68 (t,  $J = 10.7$  Hz, 1H), 2.80 (dd,  $J = 10.8, 4.7$  Hz, 1H), 2.19 (s, 6H). HRMS (ESI) calcd for  $\text{C}_{37}\text{H}_{32}\text{IrN}_6\text{O}$  ( $\text{M}$ ) $^+$  769.2263, found: 769.2264.

### 5.3.3 Evaluation of chiral-at-metal DMAP catalysts

To a solution of 1-(naphthalen-1-yl)ethanol (1 eq) (15~30 mg) and catalyst (0.05 eq) in DCM (0.3M) were added  $\text{Et}_3\text{N}$  (0.7 eq) and acetic anhydride (0.7 eq). The reaction was carried out at room temperature for 2 hours (catalyst **134** for 8 hours). The residue was purified by flash chromatography (EtOAc: hexane = 1: 2) to give the remaining alcohol. The enantiomeric excess of the remaining alcohol was determined by HPLC. Conditions: Chiralpak IB (0.46cm $\times$  25cm) HPLC column on an Agilent 1200 Series HPLC System. The flow rate was 0.5 mL/min, the column temperature 40  $^\circ\text{C}$ , and UV-absorption was measured at 254 nm. Solvent A = *i*PrOH, solvent B = hexane, with 10% A in 25 min. The result was showed in the Table 21.



**Table 21.** Evaluation of metal chiral DMAP catalysts <sup>a</sup>.

Entry	R <sub>1</sub> ,R <sub>2</sub>		yeild of the remaining alcohol	ee of the remaining alcohol	s <sup>b</sup>
1	R <sub>1</sub> =Me, R <sub>2</sub> =pyrrolidine		33%	50%	2.6
2	R <sub>1</sub> =Me, R <sub>2</sub> =pyrrolidine		27%	65%	2.9
3	R <sub>1</sub> =Me, R <sub>2</sub> =pyrrolidine		35%	41%	2.2
4	R <sub>1</sub> =Me, R <sub>2</sub> =Et,		35%	15%	1.3
5	R <sub>1</sub> =H, R <sub>2</sub> =pyrrolidine		23%	3%	1.0
6	R <sub>1</sub> =i-Pr, R <sub>2</sub> =pyrrolidine		35%	14% (reverse)	1.3
7	R <sub>1</sub> =Me, R <sub>2</sub> =pyrrolidine		34%	40%	2.1
8	R <sub>1</sub> =Me, R <sub>2</sub> =pyrrolidine		43%	30%	2.0
9	R <sub>1</sub> =Me, R <sub>2</sub> =pyrrolidine		35%	6%	2.9
10	R <sub>1</sub> =Me, R <sub>2</sub> =pyrrolidine		49%	21%	1.8
11	R <sub>1</sub> =Me, R <sub>2</sub> =pyrrolidine		40%	56%	3.7
					
12	R <sub>1</sub> =Me, R <sub>2</sub> =pyrrolidine		24%	60%	2.2

<sup>a</sup>The catalyst a- $\Lambda$ -**140** and b- $\Lambda$ -**140** provide 2.2 and 1.6 selectivity factor respectively, which are not in the Table 21.

<sup>b</sup> Selectivity factor (s) =  $K_{\text{fast}}/K_{\text{slow}} = \{\ln[(1-\text{conv})(1-\text{ee})]\}/\{\ln[(1-\text{conv})(1+\text{ee})]\}$

## Chapter 6 References

### 6.1 Literature

- (1) *On the knowledge of asymmetrical cobalt atom. III.*; Werner, A. *Berichte Der Deutschen Chemischen Gesellschaft* **1911**, *44*, 3272.
- (2) *Information on asymmetric cobalt atoms. I.*; Werner, A. *Berichte Der Deutschen Chemischen Gesellschaft* **1911**, *44*, 1887.
- (3) *On the knowledge of asymmetrical cobalt atoms. IV.*; Werner, A. *Berichte Der Deutschen Chemischen Gesellschaft* **1911**, *44*, 3279.
- (4) *The information about the asymmetric cobalt atom. II.*; Werner, A. *Berichte Der Deutschen Chemischen Gesellschaft* **1911**, *44*, 2445.
- (5) *Metallo-intercalators and metallo-insertors*; Zeglis, B. M.; Pierre, V. C.; Barton, J. K. *Chem. Commun.* **2007**, 4565.
- (6) *Structurally Sophisticated Octahedral Metal Complexes as Highly Selective Protein Kinase Inhibitors*; Feng, L.; Geisselbrecht, Y.; Blanck, S.; Wilbuer, A.; Atilla-Gokcumen, G. E.; Filippakopoulos, P.; Kraling, K.; Celik, M. A.; Harms, K.; Maksimoska, J.; Marmorstein, R.; Frenking, G.; Knapp, S.; Essen, L. O.; Meggers, E. *J. Am. Chem. Soc.* **2011**, *133*, 5976.
- (7) *Nonenzymatic Dynamic Kinetic Resolution of Secondary Alcohols via Enantioselective Acylation: Synthetic and Mechanistic Studies*; Lee, S. Y.; Murphy, J. M.; Ukai, A.; Fu, G. C. *J. Am. Chem. Soc.* **2012**, *134*, 15149.
- (8) *Enantiomeric Resolution of Ru(Phen)<sub>3</sub>(2+) and Ru(Bpy)<sub>2</sub>ppz<sub>2</sub>+ on a DNA Hydroxylapatite Column*; Baker, A. D.; Morgan, R. J.; Streckas, T. C. *J. Am. Chem. Soc.* **1991**, *113*, 1411.
- (9) *Dynamic HPLC of Stereolabile Iron(II) Complexes on Chiral Stationary Phases*; Villani, C.; Gasparini, F.; Pierini, M.; Mortera, S. L.; D'Acquarica, I.; Ciogli, A.; Zappia, G. *Chirality* **2009**, *21*, 97.
- (10) *The Spontaneous Resolution of Cis-Bis(Ethylenediamine)Dinitrocobalt(II) Salts - Werner, Alfred Overlooked Opportunity*; Bernal, I.; Kauffman, G. B. *J. Chem. Educ.* **1987**, *64*, 604.
- (11) *Efficient resolution of a dinuclear triple helicate by asymmetric extraction/precipitation with TRISPHAT anions as resolving agents*; Jodry, J. J.; Lacour, J. *Chem.--Eur. J.* **2000**, *6*, 4297.
- (12) *Efficient enantioselective extraction of tris(diimine)ruthenium(II) complexes by chiral, lipophilic TRISPHAT anions*; Lacour, J.; Goujon-Ginglinger, C.; Torche-Haldimann, S.; Jodry, J. J. *Angew. Chem. Int. Ed.* **2000**, *39*, 3695.
- (13) *Resolution of Conformationally Chiral me-[Ru(dqp)(2)](2+) and Crystallographic Analysis of [delta,delta-Ru(dqP)(2)][Delta-TRISPHAT](2) (dqp=2,6-Di(quinolin-8-yl)pyridine; TRISPHAT =Tris(tetrachlorocatecholate)phosphate)*; Sharma, S.; Lombeck, F.; Eriksson, L.; Johansson, O. *Chem.--Eur. J.* **2010**, *16*, 7078.
- (14) *Anion-Exchange Studies of Copper(2) Acetate Glycolate + Tartrate Systems*; Lundqvist, I. *Acta Chem. Scand.* **1964**, *18*, 858.
- (15) *Anion-Exchange Behavior of Indium(III) in Citrate and Tartrate Solutions - Separation from*

- Mixtures; Sitaram, R.; Khopkar, S. M. *Anal. Chim. Acta* **1974**, *71*, 472.
- (16) *Chiral recognition and resolution of the enantiomers of supramolecular triangular hosts: Synthesis, circular dichroism, NMR, and X-ray molecular structure of [Li subset of (R,R,R)-{Cp\*Rh(5-chloro-2,3-dioxopyridine)}(3)][Delta-trisphat];* Mimassi, L.; Guyard-Duhayon, C.; Rager, M. N.; Amouri, H. *Inorg. Chem.* **2004**, *43*, 6644.
- (17) *Structural Study of Optical Resolution .15. Chiral Discrimination of the Facial Isomer of the Tris((R,S)-1,2-Cyclohexanediamine)Cobalt(Iii) Cation with (R,R)-Tartrate Anion;* Mizuta, T.; Toshitani, K.; Miyoshi, K. *Bull. Chem. Soc. Jpn.* **1991**, *64*, 1183.
- (18) *Anion Exchange Separations of Iron ( 2 ) + Iron 3 ) in Tartrate Medium;* Morie, G. P.; Sweet, T. R. *Anal. Chem.* **1964**, *36*, 140.
- (19) *Preparation of Optically-Active Cation Exchangers with L-Tartrate Groups and Its Application to Resolution of [Co(En)3]3+ Ion;* Fujita, M.; Yoshikawa, Y.; Yamatera, H. *Chem. Lett.* **1974**, 1515.
- (20) *Preparation of New Cation-Exchangers Derived from Toyopearl Gel and Their Application to the Resolution of Cobalt(Iii) Complexes;* Fujita, M.; Yoshikawa, Y.; Yamatera, H. *Chem. Lett.* **1982**, 437.
- (21) *Self-Association of [Pt-II(1,10-Phenanthroline)(N-pyrrolidyl-N-(2,2-dimethylpropanoyl)thiourea)](+) and Non-Covalent Outer-Sphere Complex Formation with Fluoranthene through pi-Cation Interactions: A High-Resolution H-1 and DOSY NMR Study (pg 1626, 2009);* Kotze, I. A.; Gerber, W. J.; Mckenzie, J. M.; Koch, K. R. *Eur. J. Inorg. Chem.* **2009**, 2560.
- (22) *Diastereoselective ion pairing of TRISPHAT anions and tris(4,4 '-dimethyl-2,2 '-bipyridine)iron(II);* Lacour, J.; Jodry, J. J.; Ginglinger, C.; Torche-Haldimann, S. *Angew. Chem. Int. Ed.* **1998**, *37*, 2379.
- (23) *"Chiral-at-metal" octahedral ruthenium(II) complexes with achiral ligands: A new type of enantioselective catalyst;* Chavarot, M.; Menage, S.; Hamelin, O.; Charnay, F.; Pecaut, J.; Fontecave, M. *Inorg. Chem.* **2003**, *42*, 4810.
- (24) *On the stereochemistry of plantium atoms : On the relatively assymmetric with anorganic complexes;* Smirnoff, A. P. *Helv. Chim. Acta* **1920**, *3*, 177.
- (25) *Asymmetric Synthesis of Coordination Compounds: Back to the Roots. Diastereoselective Synthesis of Simple Platinum(IV) Complexes;* Drahoňovský, D.; Zelewsky, A. v. *Helv. Chim. Acta* **2005**, 496.
- (26) *Stereoselective Synthesis of Octahedral Complexes with Predetermined Helical Chirality;* Hayoz, P.; Vonzelewsky, A.; Stoecklievans, H. *J. Am. Chem. Soc.* **1993**, *115*, 5111.
- (27) *Catalytic, highly enantio- and diastereoselective pinacol coupling reaction with a new tethered bis(8-quinolinolato) ligand;* Takenaka, N.; Xia, G. Y.; Yamamoto, H. *J. Am. Chem. Soc.* **2004**, *126*, 13198.
- (28) *Iron-catalyzed asymmetric olefin cis-dihydroxylation with 97 % enantiomeric excess;* Suzuki, K.; Oldenburg, P. D.; Que, L. *Angew. Chem. Int. Ed.* **2008**, *47*, 1887.
- (29) *Self-assembling optically pure Fe(A-B)(3) chelates;* Howson, S. E.; Allan, L. E. N.; Chmel, N. P.; Clarkson, G. J.; van Gorkum, R.; Scott, P. *Chem. Commun.* **2009**, 1727.
- (30) *Square planar (SP-4) and octahedral (OC-6) complexes of platinum(II) and -(IV) with predetermined chirality at the metal center;* Gianini, M.; Forster, A.; Haag, P.; vonZelewsky, A.; StoeckliEvans, H. *Inorg. Chem.* **1996**, *35*, 4889.

- (31) *The Stereochemistry of Complex Inorganic Compounds* .9. *The Diastereoisomers of Dextro-Tartrato-Bis-Ethylenediamine Cobaltic Ion*; Jonassen, H. B.; Bailar, J. C.; Huffman, E. H. *J. Am. Chem. Soc.* **1948**, *70*, 756.
- (32) *Stereochemistry of Complex Inorganic Compounds* .27. *Asymmetric Syntheses of Tris(Bipyridine) Complexes of Ruthenium (2) + Osmium (2)*; Liu, C. F.; Liu, N. C.; Bailar, J. C. *Inorg. Chem.* **1964**, *3*, 1085.
- (33) *Diastereoselective preparation and characterization of ruthenium bis(bipyridine) sulfoxide complexes*; Heseck, D.; Inoue, Y.; Everitt, S. R. L.; Ishida, H.; Kunieda, M.; Drew, M. G. B. *Inorg. Chem.* **2000**, *39*, 317.
- (34) *Highly diastereoselective preparation of ruthenium bis(diimine) sulfoxide complexes: New concept in the preparation of optically active octahedral ruthenium complexes*; Pezet, F.; Daran, J. C.; Sasaki, I.; Ait-Haddou, H.; Balavoine, G. G. A. *Organometallics* **2000**, *19*, 4008.
- (35) *Chiral-Auxiliary-Mediated Asymmetric Synthesis of Tris-Heteroleptic Ruthenium Polypyridyl Complexes*; Gong, L.; Mulcahy, S. P.; Harms, K.; Meggers, E. *J. Am. Chem. Soc.* **2009**, *131*, 9602.
- (36) *2-Diphenylphosphino-2'-hydroxy-1,1'-binaphthyl as a chiral auxiliary for asymmetric coordination chemistry*; Gong, L.; Muller, C.; Celik, M. A.; Frenking, G.; Meggers, E. *New J. Chem.* **2011**, *35*, 788.
- (37) *Inorganic asymmetric synthesis: Asymmetric synthesis of a two-bladed propeller, octahedral metal complex*; Warr, R. J.; Willis, A. C.; Wild, S. B. *Inorg. Chem.* **2006**, *45*, 8618.
- (38) *Enantiomeric programming in tripodal transition metal scaffolds*; Fletcher, N. C.; Martin, C.; Abraham, H. J. *New J. Chem.* **2007**, *31*, 1407.
- (39) *A boronic acid-diol interaction is useful for chiroselective transcription of the sugar structure to the Delta- versus Lambda-[Co-III(bpy)(3)](3+) ratio*; Mizuno, T.; Takeuchi, M.; Hamachi, I.; Nakashima, K.; Shinkai, S. *Journal of the Chemical Society-Perkin Transactions 2* **1998**, 2281.
- (40) *Phase transfer of enantiopure Werner cations into organic solvents: An overlooked family of chiral hydrogen bond donors for enantioselective catalysis*; Ganzmann, C.; Gladysz, J. A. *Chem.--Eur. J.* **2008**, *14*, 5397.
- (41) *Chiral-at-metal ruthenium complex as a metalloligand for asymmetric catalysis*; Hamelin, O.; Rimboud, M.; Pecaut, J.; Fontecave, M. *Inorg. Chem.* **2007**, *46*, 5354.
- (42) *Highly enantioselective asymmetric autocatalysis induced by chiral cobalt complexes due to the topology of the coordination of achiral ligands*; Sato, I.; Kadowaki, K.; Ohgo, Y.; Soai, K.; Ogino, H. *Chem. Commun.* **2001**, 1022.
- (43) *Thermal and photochemical racemization of chiral aromatic sulfoxides via the intermediacy of sulfoxide radical cations*; Aurisicchio, C.; Baciocchi, E.; Gerini, M. F.; Lanzalunga, O. *Org. Lett.* **2007**, *9*, 1939.
- (44) *Diastereoselective preparation of chiral-at-metal organometallic complexes using a chelating sulfoxide-carboxylate ligand*; Otto, M.; Parr, J.; Slawin, A. Z. *Organometallics* **1998**, *17*, 4527.
- (45) *Recent developments in the synthesis and utilization of chiral sulfoxides*; Fernandez, I.; Khair, N. *Chem. Rev.* **2003**, *103*, 3651.
- (46) *Asymmetric Synthesis of Alkane- and Arenesulfinates of Diacetone-D-glucose (DAG): An Improved and General Route to Both Enantiomerically Pure Sulfoxides* Fernández, I.;

- Khlar, N.; Llera, J. M.; Alcudia, F. *Journal of Organic Chemistry* **1992**, *57*.
- (47) *Chiral [Ru(Pp)(2)(Co)(2)](2+) Species (Pp=Bidentate Polypyridyl Ligand) and Their Use in the Stereoselective Synthesis of Ligand-Bridged Dinuclear Complexes*; Rutherford, T. J.; Quagliotto, M. G.; Keene, F. R. *Inorg. Chem.* **1995**, *34*, 3857.
- (48) *Preparation and Characterization of Cis- $\alpha$ -[Ru(Bpy)(2)(Py)(O)](2+)*; Hua, X.; Lappin, A. G. *Inorg. Chem.* **1995**, *34*, 992.
- (49) *Synthesis of Polypyridyl Complexes of Ruthenium(II) Containing 3 Different Bidentate Ligands*; Strouse, G. F.; Anderson, P. A.; Schoonover, J. R.; Meyer, T. J.; Keene, F. R. *Inorg. Chem.* **1992**, *31*, 3004.
- (50) *Molecular Light Switch for DNA - Ru(Bpy)<sub>2</sub>(Dppz)<sub>2</sub><sup>+</sup>*; Friedman, A. E.; Chambron, J. C.; Sauvage, J. P.; Turro, N. J.; Barton, J. K. *J. Am. Chem. Soc.* **1990**, *112*, 4960.
- (51) *An effective route to cycloruthenated N-ligands under mild conditions*; Fernandez, S.; Pfeffer, M.; Ritleng, V.; Sirlin, C. *Organometallics* **1999**, *18*, 2390.
- (52) *Proline as Chiral Auxiliary for the Economical Asymmetric Synthesis of Ruthenium(II) Polypyridyl Complexes*; Fu, C.; Wenzel, M.; Treutlein, E.; Harms, K.; Meggers, E. *Inorg. Chem.* **2012**, *51*, 10004.
- (53) *Solvent Effects on Isomerization in a Ruthenium Sulfoxide Complex*; Grusenmeyer, T. A.; McClure, B. A.; Ziegler, C. J.; Rack, J. J. *Inorg. Chem.* **2010**, *49*, 4466.
- (54) *Photoracemization of Ru(Bipyridine)<sub>3</sub><sup>2+</sup>*; Porter, G. B.; Sparks, R. H. *Journal of Photochemistry* **1980**, *13*, 123.
- (55) *Luminescent, Enantiopure, Phenylatopyridine Iridium-Based Coordination Capsules*; Chepelin, O.; Ujma, J.; Wu, X. H.; Slawin, A. M. Z.; Pitak, M. B.; Coles, S. J.; Michel, J.; Jones, A. C.; Barran, P. E.; Lusby, P. J. *J. Am. Chem. Soc.* **2012**, *134*, 19334.
- (56) *Nonenzymatic kinetic resolution of propargylic alcohols by a planar-chiral DMAP derivative: Crystallographic characterization of the acylated catalyst (vol 121, pg 5091, 1999)*; Tao, B.; Ruble, J. C.; Hoic, D. A.; Fu, G. C. *J. Am. Chem. Soc.* **1999**, *121*, 10452.
- (57) *The kinetic resolution of allylic alcohols by a non-enzymatic acylation catalyst; application to natural product synthesis*; Bellemin-Laponnaz, S.; Tweddell, J.; Ruble, J. C.; Breitling, F. M.; Fu, G. C. *Chem. Commun.* **2000**, 1009.
- (58) *Enantioselective nucleophilic catalysis with "planar-chiral" heterocycles*; Fu, G. C. *Acc. Chem. Res.* **2000**, *33*, 412.
- (59) *A new benchmark for the non-enzymatic enantioselective acylation of amines: use of a planar-chiral derivative of 4-pyrrolidinopyridine as the acylating agent*; Ie, Y.; Fu, G. C. *Chem. Commun.* **2000**, 119.
- (60) *Kinetic resolution of amines by a nonenzymatic acylation catalyst*; Arai, S.; Bellemin-Laponnaz, S.; Fu, G. C. *Angew. Chem. Int. Ed.* **2001**, *40*, 234.
- (61) *Applications of "planar-chiral" heterocycles in asymmetric catalysis*; Fu, G. C. *Pure Appl. Chem.* **2001**, *73*, 1113.
- (62) *Asymmetric catalysis with "planar-chiral" heterocycles.*; Fu, G. C. *Abstracts of Papers of the American Chemical Society* **2001**, *221*, U102.
- (63) *Asymmetric catalysis with "planar-chiral" heterocycles*; Fu, G. C. *Pure Appl. Chem.* **2001**, *73*, 347.
- (64) *Applications of planar-chiral heterocycles in enantioselective catalysis: Cu(I)/bisazaferrocene-catalyzed asymmetric ring expansion of oxetanes to tetrahydrofurans*;



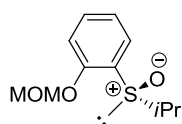
- Lo, M. M. C.; Fu, G. C. *Tetrahedron* **2001**, *57*, 2621.
- (65) *Asymmetric catalysis with "planar-chiral" derivatives of 4-(dimethylamino)pyridine*; Fu, G. C. *Acc. Chem. Res.* **2004**, *37*, 542.
- (66) *Kinetic resolutions of indolines by a nonenzymatic acylation catalyst*; Arp, F. O.; Fu, G. C. *J. Am. Chem. Soc.* **2006**, *128*, 14264.
- (67) *Asymmetric [3+2] annulations catalyzed by a planar-chiral derivative of DMAP*; Bappert, E.; Muller, P.; Fu, G. C. *Chem. Commun.* **2006**, 2604.
- (68) *Cyclometalated Ir(III) complexes containing N-aryl picolinamide ancillary ligands*; Chandrasekhar, V.; Mahanti, B.; Bandipalli, P.; Bhanuprakash, K.; Nair, N. N. *J. Organomet. Chem.* **2011**, *696*, 2711.
- (69) *The Stability of Acylpyridinium Cations and Their Relation to the Catalytic Activity of Pyridine Bases*; Zipse, H.; Held, I.; Villinger, A. *Synthesis* **2005**, 1425.
- (70) *Configurational Stability of Biaryl Analogues of 4-(Dimethylamino)pyridine: A Novel Class of Chiral Nucleophilic Catalysts*; Spivey, A. C.; Fekner, T.; Spey, S. E.; Adams, H. *Journal of Organic Chemistry* **1999**, *64*, 9430.
- (71) *Kinetic Resolution*; Eliel, E. L.; Wilen, S. H.; Kagan, H. B.; Fiaud, J. C. *book* **2007**.
- (72) *Theoretical Prediction of Selectivity in Kinetic Resolution of Secondary Alcohols Catalyzed by Chiral DMAP Derivatives*; Larionov, E.; Mahesh, M.; Spivey, A. C.; Wei, Y.; Zipse, H. *J. Am. Chem. Soc.* **2012**, *134*, 9390.
- (73) *Solvent-Free Tandem Synthesis of 2-Thiazolines and 2-Oxazolines Catalyzed by a Copper Catalyst*; Li, X. N.; Zhou, B. Y.; Zhang, J.; She, M. Y.; An, S. J.; Ge, H. X.; Li, C.; Yin, B.; Li, J. L.; Shi, Z. *Eur. J. Org. Chem.* **2012**, 1626.
- (74) *PdCl<sub>2</sub>(dppf)-catalyzed in situ coupling of 2-hydroxypyridines with aryl boronic acids mediated by PyBroP and the one-pot chemo- and regioselective construction of two distinct aryl-aryl bonds*; Li, S.-M.; Huang, J.; Chen, G.-J.; Han, F.-S. *Chem. Commun.* **2011**, *47*, 12840.
- (75) *A Ring-Closing Metathesis (RCM)-Based Approach to Mycolactones A/B*; Gersbach, P.; Jantsch, A.; Feyen, F.; Scherr, N.; Dangy, J. P.; Pluschke, G.; Altmann, K. H. *Chem.--Eur. J.* **2011**, *17*, 13017.
- (76) *Mixed Phosphine 2,2'-Bipyridine Complexes of Ruthenium*; Sullivan, B. P.; Salmon, D. J.; Meyer, T. J. *Inorg. Chem.* **1978**, *17*, 3334.
- (77) *Conversion of thiobenzamides to benzothiazoles via intramolecular cyclization of the aryl radical cation*; Downer-Riley, N. K.; Jackson, Y. A. *Tetrahedron* **2008**, *64*, 7741.
- (78) *Cross-Coupling in the Preparation of Pharmaceutically Relevant Substrates using Palladium Supported on Functionalized Mesoporous Silicas*; El Kadib, A.; McEleney, K.; Seki, T.; Wood, T. K.; Crudden, C. M. *Chemcatchem* **2011**, *3*, 1281.
- (79) *Ketene Chemistry .2. A General Procedure for the Synthesis of 2-Alkoxypropyl-Carboxylic Esters and Acids Starting from Aldehydes and Ketene*; Rasmussen, P. B.; Bowadt, S. *Synthesis* **1989**, 114.
- (80) *Efficient C-3 functionalization of 4-dimethylaminopyridine (DMAP). A straightforward access to new chiral nucleophilic catalysts*; Poisson, T.; Oudeyer, S.; Levacher, V. *Tetrahedron Lett.* **2012**, *53*, 3284.
- (81) *NMR Chemical Shifts of Trace Impurities: Common Laboratory Solvents, Organics, and Gases in Deuterated Solvents Relevant to the Organometallic Chemist*; Fulmer, G. R.; Miller,

- A. J. M.; Sherden, N. H.; Gottlieb, H. E.; Nudelman, A.; Stoltz, B. M.; Bercaw, J. E.; Goldberg, K. I. *Organometallics* **2010**, *29*, 2176.
- (82) *Chiral Salicyloxazolines as Auxiliaries for the Asymmetric Synthesis of Ruthenium Polypyridyl Complexes*; Gong, L.; Mulcahy, S. P.; Devarajan, D.; Harms, K.; Frenking, G.; Meggers, E. *Inorg. Chem.* **2010**, *49*, 7692.
- (83) *US2004/127710 A1*; Park, S. J.; Lee, K. H.; Kim, J. I.; Lee, J. K.; Kwon, J. H. *Patent* **2004**, 8.
- (84) *New Approach Toward Fast Response Light-Emitting Electrochemical Cells Based on Neutral Iridium Complexes via Cation Transport*; Kwon, T. H.; Oh, Y. H.; Shin, I. S.; Hong, J. I. *Adv. Funct. Mater.* **2009**, *19*, 711.

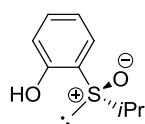
## 6.2 List of synthesized compounds

### Novel chiral auxiliaries for the asymmetric synthesis of the ruthenium polypyridyl complexes

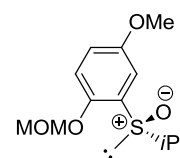
#### i) Ligands



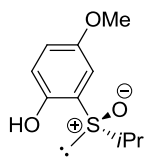
41



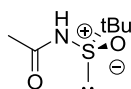
> 99%ee  
(*R*)-2-(isopropylsulfinyl)phenol  
(*R*)-SO



51

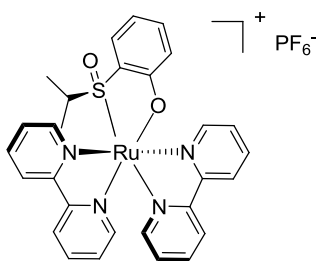


>99ee%  
(*R*)-2-(isopropylsulfinyl)-  
5-methoxyphenol  
(*R*)-SO'

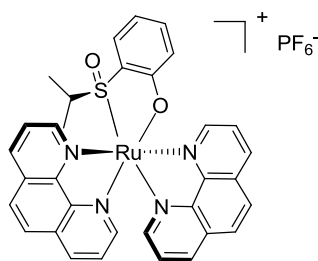


(R)-ASA

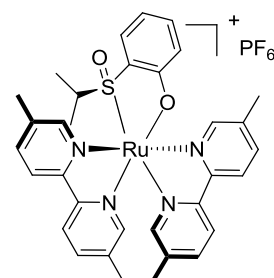
#### ii) Chiral-auxiliary-mediate ruthenium complexes



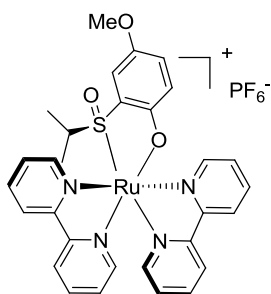
Λ-(S)-45



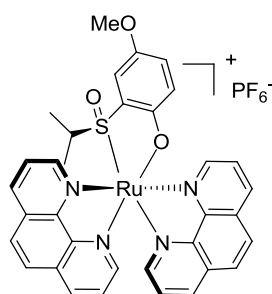
Λ-(S)-44



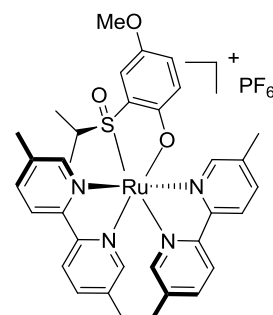
Λ-(S)-49



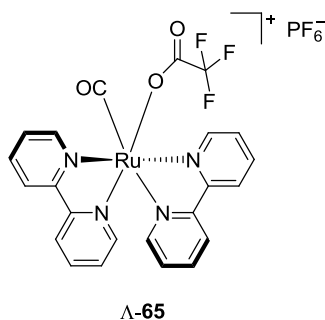
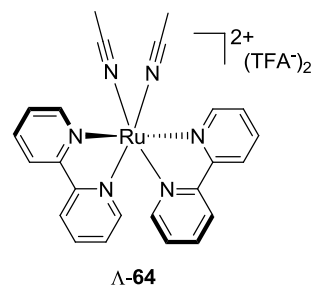
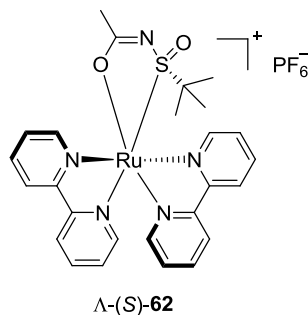
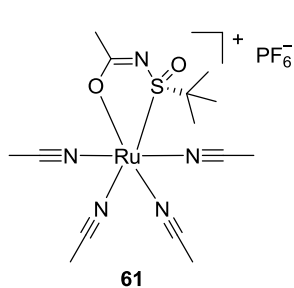
Λ-(S)-53



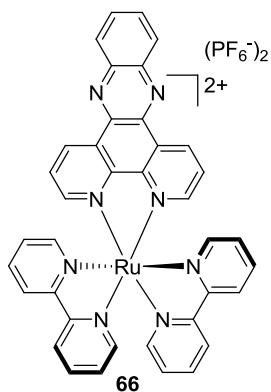
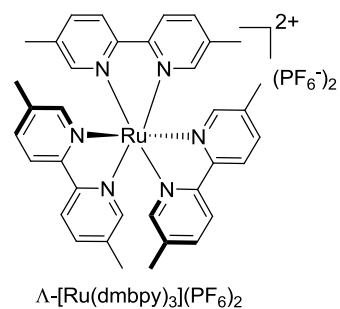
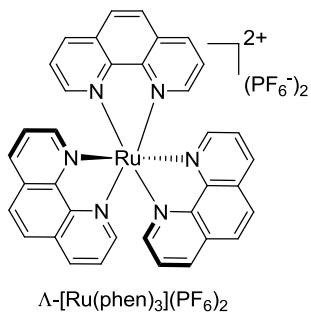
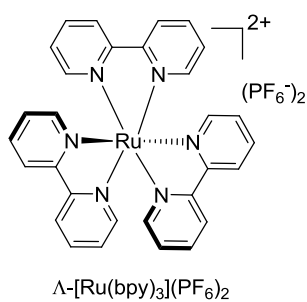
Λ-(S)-54



Λ-(S)-55



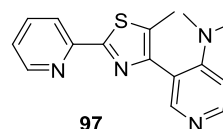
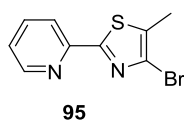
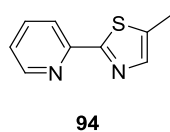
### iii) Enantiopure polypyridyl ruthenium complexes

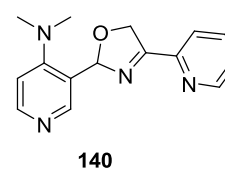
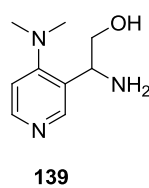
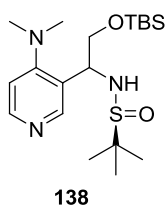
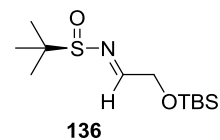
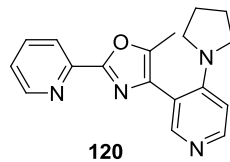
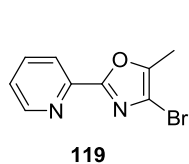
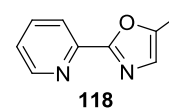
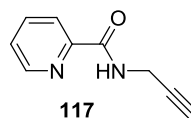
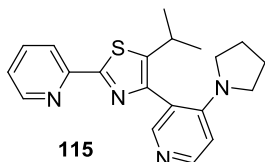
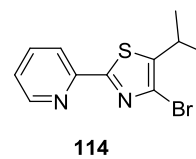
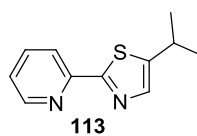
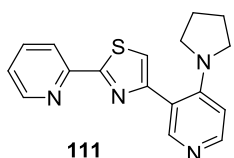
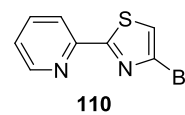
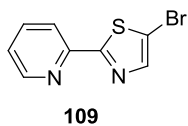
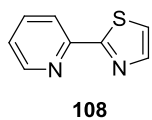
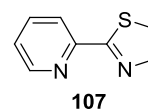
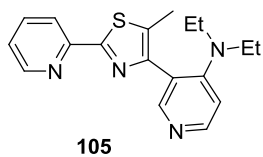
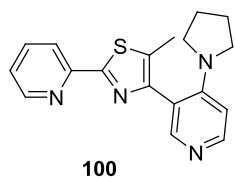


Δ-DNA molecular light switch

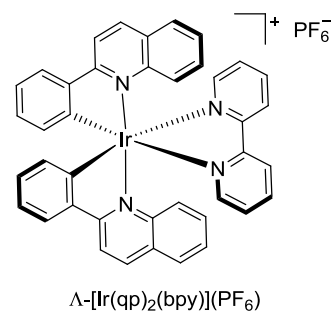
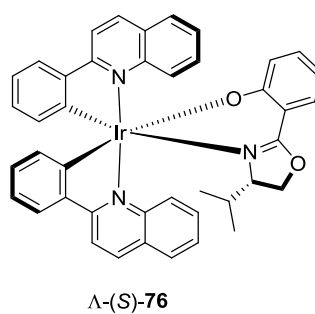
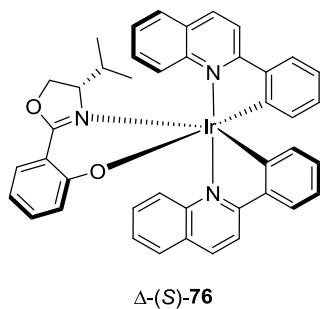
## Development of octahedral chiral-at-metal complexes for asymmetric catalysis

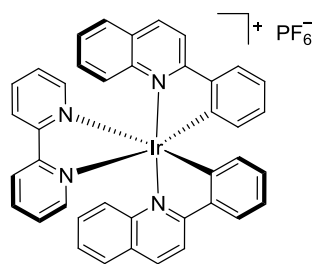
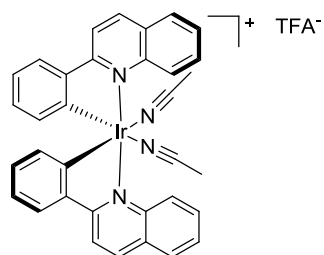
### i) Compounds for synthesizing DMAP-ligands



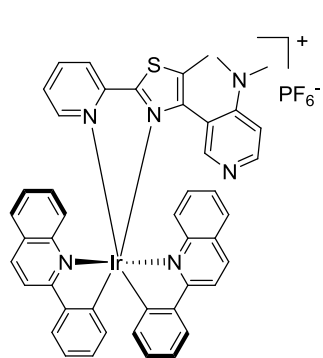
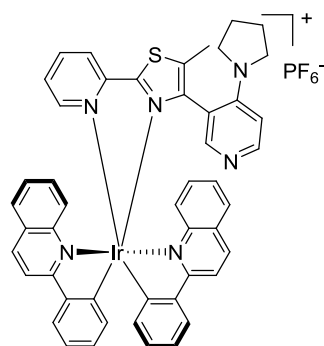
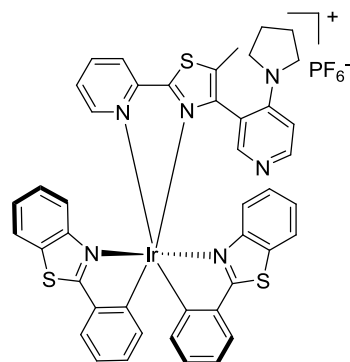
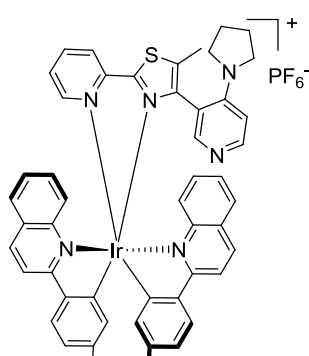
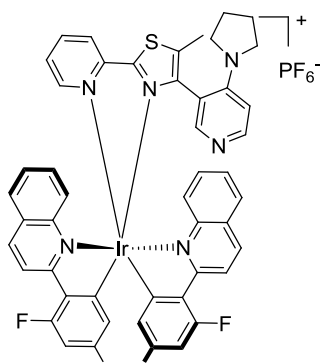
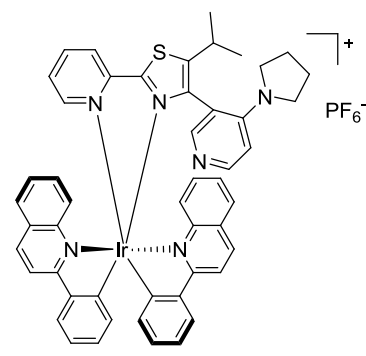
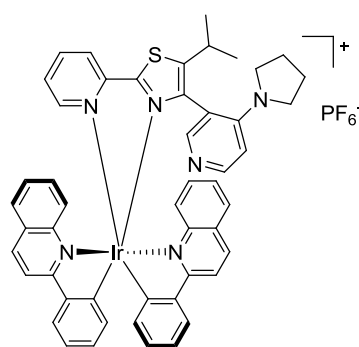
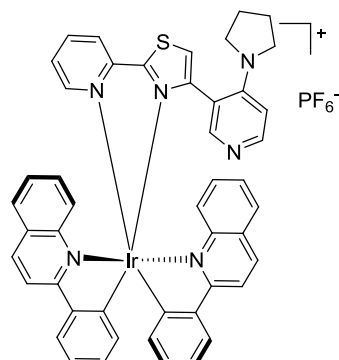
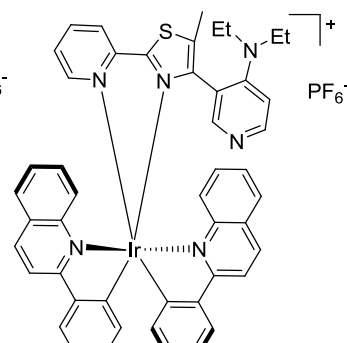


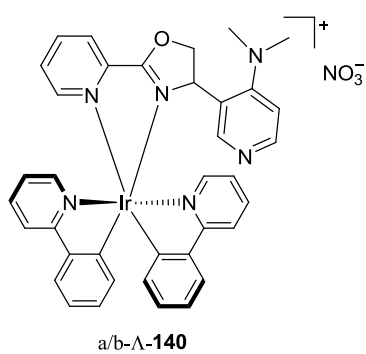
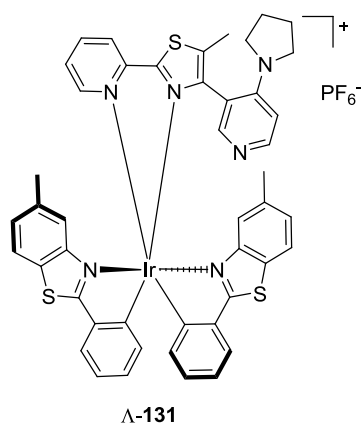
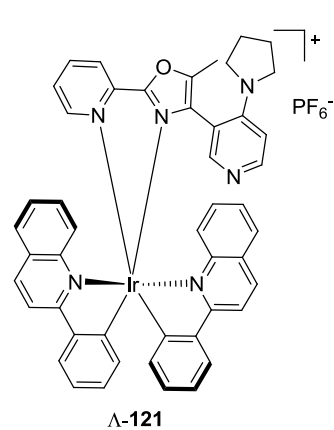
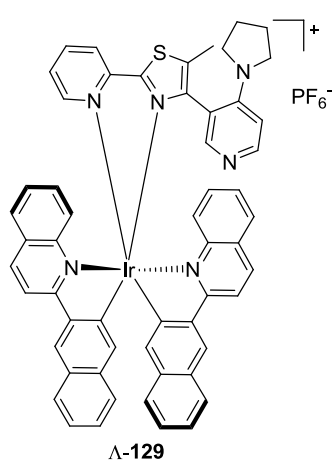
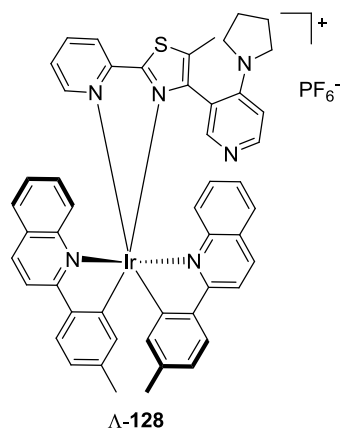
## ii) Complexes for synthesizing enantiopure iridium precursor




 $\Delta$ -[Ir(qp)<sub>2</sub>(bpy)](PF<sub>6</sub>)

 $\Lambda$ -77

### iii) Catalysts


 $\Lambda$ -98

 $\Lambda$ -101

 $\Lambda$ -130

 $\Lambda$ -133

 $\Lambda$ -134

 $\Lambda$ -116

 $\Lambda$ -116

 $\Lambda$ -112

 $\Lambda$ -106



### 6.3 Abbreviations and symbols

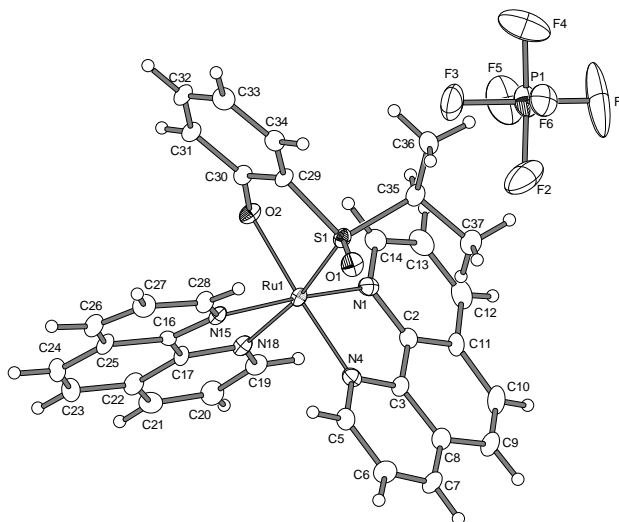
$^1\text{H-NMR}$	Proton nuclear magnetic resonance spectroscopy
$^{13}\text{C-NMR}$	Carbon-13 nuclear magnetic resonance spectroscopy
ASA	N -acetyl-tert -butanesul-finamide
bpy	2,2'-bipyridine
CD	circular dichroism
$\text{CHCl}_3$	chloroform
$\text{CH}_2\text{Cl}_2$	Dichloromethane
DMF	dimethylformamide
DCM	Dichloromethane
DMSO	dimethyl sulfoxide
DIPEA	<i>N,N</i> -Diisopropylethylamine
DNA	deoxyribonucleic acid
DDQ	2,3-Dichloro-5,6-dicyano-1,4-benzoquinone
DMAP	4-Dimethylaminopyridine
dmbpy	5,5'-dimethyl-2,2'-bipyridine
dppz	dipyrido[3,2-a:2',3'-c]phenazine
dr	Diastereomeric ratio
$\text{Et}_2\text{NH}$	Diethyl amine
$\text{Et}_3\text{N}$	Triethyl amine
EDCI	1-Ethyl-3-(3-dimethylaminopropyl)carbodiimide
EtOAc	ethyl acetate
EtOH	ethanol
$\text{Et}_2\text{O}$	Diethyl ether
en	ethylene diamine
ee	Enantiomeric excesses
er	Enantiomeric ratio
HPLC	high-performanc liquid chromatography



IR spectra	infrared spectra
LDA	Lithium diisopropylamide
mCPBA	3-chloroperoxybenzoic acid
MeOH	methanol
NBS	<i>N</i> -Bromosuccinimide
NaH	Sodium hydride
NaOAc	Sodium acetate
NaOMe	Sodium methoxide
<i>n</i> -BuLi	<i>n</i> -Butyllithium
phen	1,10-phenanthroline
s	Selective factor
TBS	tert-butyldimethylsilyl
THF	tetrahydrofuran
TFA	Trifluoroacetic acid
TLC	Thin layer chromatography
UV	Ultraviolet

## 6.4 Appendix

Crystal structure data:



Crystal data

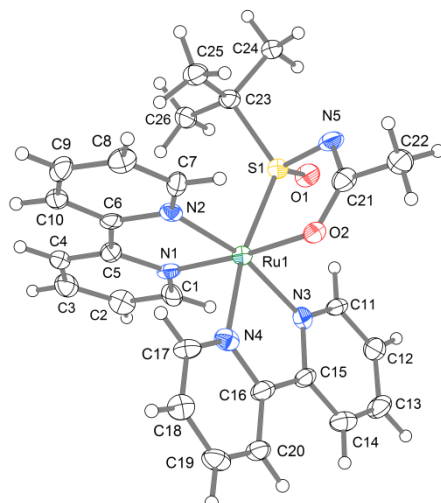
Identification code	linb43	
Habitus, colour	prism, red	
Crystal size	0.25 x 0.12 x 0.09 mm <sup>3</sup>	
Crystal system	Orthorhombic	
Space group	P 2 <sub>1</sub> 2 <sub>1</sub> 2 <sub>1</sub>	Z = 4
Unit cell dimensions	a = 10.0326(2) Å	α = 90 °
	b = 16.7149(4) Å	β = 90 °
	c = 18.0433(6) Å	γ = 90 °
Volume	3025.75(14) Å <sup>3</sup>	
Cell determination	15823 peaks with Theta 4.6 to 26 °	
Empirical formula	C <sub>33</sub> H <sub>27</sub> F <sub>6</sub> N <sub>4</sub> O <sub>2</sub> P Ru S	
Formula weight	789.69	
Density (calculated)	1.734 Mg/m <sup>3</sup>	
Absorption coefficient	0.718 mm <sup>-1</sup>	
F(000)	1592	

Data collection:

Diffractometer type	STOE IPDS 2T
Wavelength	0.71073 Å
Temperature	100(2) K
Theta range for data collection	4.64 to 25.00 °
Index ranges	-11 ≤ h ≤ 11, -17 ≤ k ≤ 19, -21 ≤ l ≤ 21
Data collection software	STOE X-AREA

---

Cell refinement software	STOE X-AREA
Data reduction software	STOE X-AREA
Solution and refinement:	
Reflections collected	13494
Independent reflections	5301 [R(int) = 0.0539]
Completeness to theta = 25.00 °	99.0 %
Observed reflections	4684[I>2(I)]
Reflections used for refinement	5301
Extinction coefficient	X = 0.0004(2)
Absorption correction	Integration
Max. and min. transmission	0.9638 and 0.8877
Flack parameter (absolute struct.)	-0.04(3)
Largest diff. peak and hole	0.640 and -0.608 e.Å <sup>-3</sup>
Solution	Direct methods
Refinement	Full-matrix least-squares on F <sup>2</sup>
Treatment of hydrogen atoms	Calculated positions, riding model
Programs used	SIR2008 (Giaccovazzo, 2009) SHELXL-97 (Sheldrick, 2008) DIAMOND 3.2 (Crystal Impact) STOE IPDS2 software
Data / restraints / parameters	5301 / 0 / 436
Goodness-of-fit on F <sup>2</sup>	0.961
R index (all data)	wR2 = 0.0646
R index conventional [I>2sigma(I)]	R1 = 0.0333



## Crystal data

Identification code	line20	
Habitus, colour	prism, red	
Crystal size	0.10 x 0.08 x 0.05 mm <sup>3</sup>	
Crystal system	Orthorhombic	
Space group	P 21 21 21	Z = 4
Unit cell dimensions	a = 9.6858(5) Å	α = 90 °
	b = 17.8814(6) Å	β = 90 °
	c = 18.3615(6) Å	γ = 90 °
Volume	3180.1(2) Å <sup>3</sup>	
Cell determination	6785 peaks with Theta 2.2 to 25 °	
Empirical formula	C <sub>27</sub> H <sub>30</sub> Cl <sub>2</sub> F <sub>6</sub> N <sub>5</sub> O <sub>2</sub> P Ru S	
Formula weight	805.56	
Density (calculated)	1.683 Mg/m <sup>3</sup>	
Absorption coefficient	0.848 mm <sup>-1</sup>	
F(000)	1624	

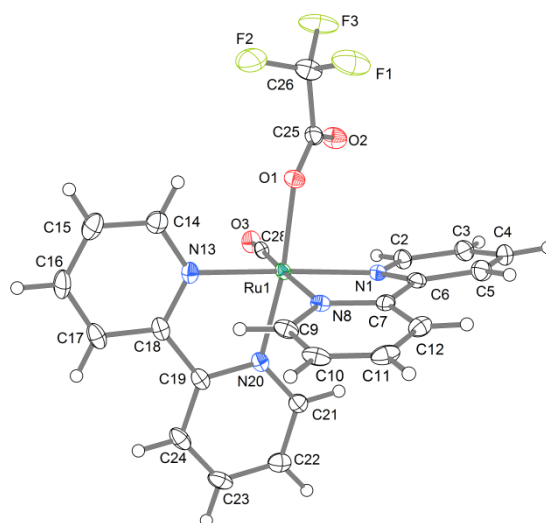
## Data collection:

Diffractometer type	STOE IPDS 2
Wavelength	0.71073 Å
Temperature	100(2) K
Theta range for data collection	1.59 to 25.00 °
Index ranges	-10 ≤ h ≤ 11, -21 ≤ k ≤ 20, -20 ≤ l ≤ 21
Data collection software	STOE X-AREA
Cell refinement software	STOE X-AREA
Data reduction software	STOE X-AREA

## Solution and refinement:

---

Reflections collected	12487
Independent reflections	5601 [R(int) = 0.0510]
Completeness to theta = 25.00 °	100.0 %
Observed reflections	4127[I>2(I)]
Reflections used for refinement	5601
Absorption correction	Semi-empirical from equivalents
Max. and min. transmission	0.9492 and 0.9251
Flack parameter (absolute struct.)	-0.02(3)
Largest diff. peak and hole	0.495 and -0.391 e.Å <sup>-3</sup>
Solution	Direct methods
Refinement	Full-matrix least-squares on F <sup>2</sup>
Treatment of hydrogen atoms	Calculated positions, constr. ref.
Programs used	SIR2008 (Giacovazzo et al, 2008) SHELXL-97 (Sheldrick, 2008) DIAMOND 3.2g STOE IPDS2 software
Data / restraints / parameters	5601 / 0 / 410
Goodness-of-fit on F <sup>2</sup>	0.755
R index (all data)	wR2 = 0.0580
R index conventional [I>2sigma(I)]	R1 = 0.0344



## Crystal data

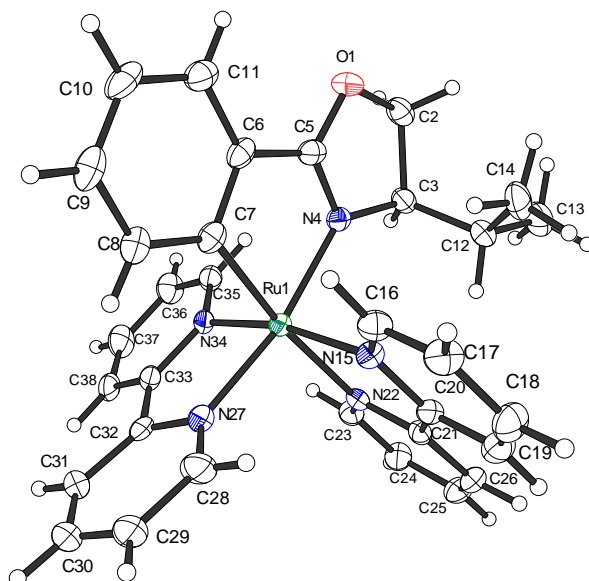
Identification code	lind136	
Habitus, colour	needle, yellow	
Crystal size	0.40 x 0.06 x 0.05 mm <sup>3</sup>	
Crystal system	Orthorhombic	
Space group	P 2 <sub>1</sub> 2 <sub>1</sub> 2 <sub>1</sub>	Z = 4
Unit cell dimensions	a = 8.1401(2) Å	α = 90 °
	b = 15.0325(4) Å	β = 90 °
	c = 20.6894(6) Å	γ = 90 °
Volume	2531.68(12) Å <sup>3</sup>	
Cell determination	22327 peaks with Theta 1.6 to 27 °	
Empirical formula	C <sub>23</sub> H <sub>16</sub> F <sub>9</sub> N <sub>4</sub> O <sub>3</sub> P Ru	
Formula weight	699.44	
Density (calculated)	1.835 Mg/m <sup>3</sup>	
Absorption coefficient	0.784 mm <sup>-1</sup>	
F(000)	1384	

## Data collection:

Diffractometer type	STOE IPDS 2T
Wavelength	0.71073 Å
Temperature	100(2) K
Theta range for data collection	1.67 to 26.73 °
Index ranges	-9 ≤ h ≤ 10, -18 ≤ k ≤ 18, -26 ≤ l ≤ 26
Data collection software	STOE X-AREA
Cell refinement software	STOE X-AREA
Data reduction software	STOE X-AREA

## Solution and refinement:

Reflections collected	19411
Independent reflections	5362 [R(int) = 0.0484]
Completeness to theta = 25.00 °	100.0 %
Observed reflections	4938[I>2(I)]
Reflections used for refinement	5362
Absorption correction	Integration
Max. and min. transmission	0.9659 and 0.8281
Flack parameter (absolute struct.)	-0.040(17)
Largest diff. peak and hole	0.455 and -0.455 e.Å <sup>-3</sup>
Solution	Direct methods
Refinement	Full-matrix least-squares on F <sup>2</sup>
Treatment of hydrogen atoms	Calculated positions, constr. ref.
Programs used	SIR-2008 SHELXL-97 (Sheldrick, 2008) DIAMOND 3.2 STOE IPDS2 software
Data / restraints / parameters	5362 / 0 / 370
Goodness-of-fit on F <sup>2</sup>	0.988
R index (all data)	wR2 = 0.0461
R index conventional [I>2sigma(I)]	R1 = 0.0198



## Crystal data

Identification code	linb152	
Habitus, colour	prism, purple	
Crystal size	0.32 x 0.23 x 0.20 mm <sup>3</sup>	
Crystal system	Monoclinic	
Space group	P 2 <sub>1</sub>	Z = 2
Unit cell dimensions	a = 10.0148(4) Å	α = 90 °
	b = 15.0807(5) Å	β = 99.396(4) °
	c = 11.8108(5) Å	γ = 90 °
Volume	1759.86(12) Å <sup>3</sup>	
Cell determination	14774 peaks with Theta 4.6 to 25 °	
Empirical formula	C <sub>33</sub> H <sub>32</sub> Cl <sub>2</sub> F <sub>6</sub> N <sub>5</sub> O P Ru	
Formula weight	831.58	
Density (calculated)	1.569 Mg/m <sup>3</sup>	
Absorption coefficient	0.710 mm <sup>-1</sup>	
F(000)	840	

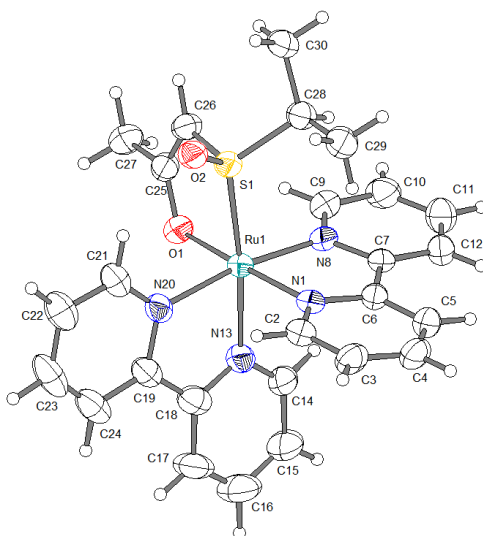
## Data collection:

Diffractometer type	STOE IPDS 2T
Wavelength	0.71073 Å
Temperature	100(2) K
Theta range for data collection	4.63 to 25.00 °
Index ranges	-11 ≤ h ≤ 11, -17 ≤ k ≤ 17, -14 ≤ l ≤ 11
Data collection software	STOE X-AREA
Cell refinement software	STOE X-AREA
Data reduction software	STOE X-AREA



## Solution and refinement:

Reflections collected	9438
Independent reflections	6093 [R(int) = 0.0313]
Completeness to theta = 25.00 °	99.1 %
Observed reflections	5691[I>2(I)]
Reflections used for refinement	6093
Absorption correction	Integration
Max. and min. transmission	0.9429 and 0.8686
Flack parameter (absolute struct.)	-0.03(2)
Largest diff. peak and hole	0.489 and -0.580 e.Å <sup>-3</sup>
Solution	direct/ difmap
Refinement	Full-matrix least-squares on F <sup>2</sup>
Treatment of hydrogen atoms	geom, noref
Programs used	SIR92 (Giacovazzo et al, 1993) SHELXL-97 (Sheldrick, 2008) DIAMOND 3.2 (Crystal Impact)
STOE IPDS2 software	
Data / restraints / parameters	6093 / 12 / 471
Goodness-of-fit on F <sup>2</sup>	1.086
R index (all data)	wR2 = 0.0788
R index conventional [I>2sigma(I)]	R1 = 0.0302



## Crystal data

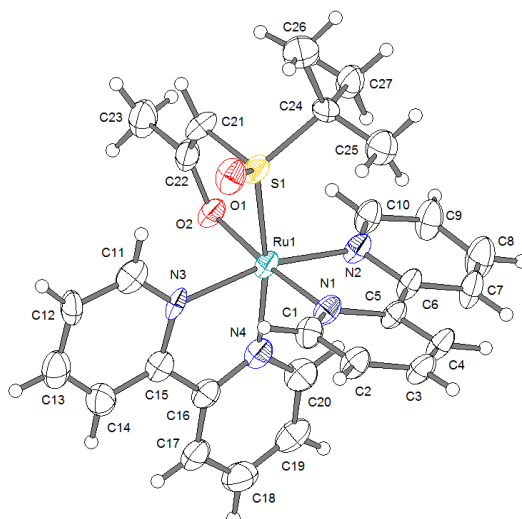
Identification code	linc163	
Habitus, colour	prism, red	
Crystal size	0.40 x 0.39 x 0.18 mm <sup>3</sup>	
Crystal system	Monoclinic	
Space group	P 21/n	Z = 4
Unit cell dimensions	a = 13.4066(7) Å	α = 90 °
	b = 15.3033(6) Å	β = 105.060(4) °
	c = 15.9511(7) Å	γ = 90 °
Volume	3160.2(2) Å <sup>3</sup>	
Cell determination	6449 peaks with Theta 1.8 to 25 °	
Empirical formula	C <sub>27</sub> H <sub>29.50</sub> Cl <sub>2</sub> F <sub>6</sub> N <sub>4</sub> O <sub>2.25</sub> P Ru S	
Formula weight	795.05	
Density (calculated)	1.671 Mg/m <sup>3</sup>	
Absorption coefficient	0.852 mm <sup>-1</sup>	
F(000)	1602	

## Data collection:

Diffractometer type	STOE IPDS2
Wavelength	0.71073 Å
Temperature	100(2) K
Theta range for data collection	1.77 to 25.00 °
Index ranges	-14 ≤ h ≤ 15, -18 ≤ k ≤ 16, -18 ≤ l ≤ 18
Data collection software	STOE X-AREA
Cell refinement software	STOE X-AREA
Data reduction software	STOE X-AREA

## Solution and refinement:

Reflections collected	10249
Independent reflections	5254 [R(int) = 0.0410]
Completeness to theta = 25.00 °	94.4 %
Observed reflections	3373[I>2(I)]
Reflections used for refinement	5254
Absorption correction	Semi-empirical from equivalents
Max. and min. transmission	0.8025 and 0.7392
Largest diff. peak and hole	0.770 and -0.379 e.Å <sup>-3</sup>
Solution	Direct methods
Refinement	Full-matrix least-squares on F <sup>2</sup>
Treatment of hydrogen atoms	Calculated positions, constr. ref.
Programs used	SIR92 (Giacovazzo et al, 1993) SHELXL-97 (Sheldrick, 2008) DIAMOND 3.2 (Crystal Impact) STOE IPDS2 software
Data / restraints / parameters	5254 / 35 / 486
Goodness-of-fit on F <sup>2</sup>	0.777
R index (all data)	wR2 = 0.0711
R index conventional [I>2sigma(I)]	R1 = 0.0344



## Crystal data

Identification code	lind5	
Habitus, colour	prism, colourless	
Crystal size	0.16 x 0.16 x 0.04 mm <sup>3</sup>	
Crystal system	Triclinic	
Space group	P -1	Z = 2
Unit cell dimensions	a = 11.0138(11) Å	α = 68.685(9) °
	b = 13.5021(16) Å	β = 68.780(8) °
	c = 13.8380(15) Å	γ = 70.451(8) °
Volume	1737.6(3) Å <sup>3</sup>	
Cell determination	5247 peaks with Theta 1.6 to 25 °	
Empirical formula	C <sub>28.56</sub> H <sub>32.12</sub> Cl <sub>3.12</sub> F <sub>6</sub> N <sub>4</sub> O <sub>2</sub> P Ru S	
Formula weight	852.13	
Density (calculated)	1.629 Mg/m <sup>3</sup>	
Absorption coefficient	0.863 mm <sup>-1</sup>	
F(000)	859	

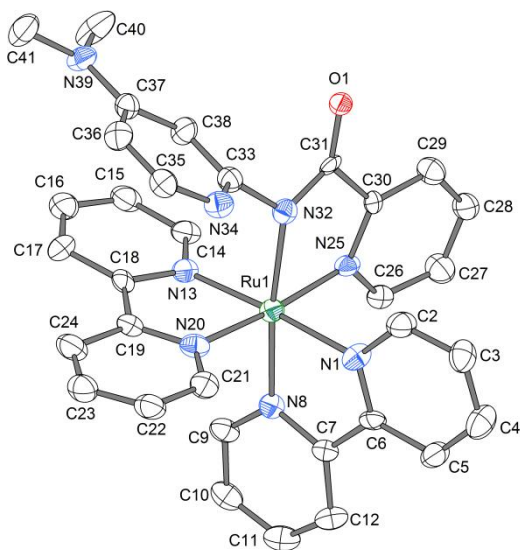
## Data collection:

Diffractometer type	STOE IPDS 2T
Wavelength	0.71073 Å
Temperature	100(2) K
Theta range for data collection	1.67 to 25.00 °
Index ranges	-13 ≤ h ≤ 12, -16 ≤ k ≤ 16, -13 ≤ l ≤ 16
Data collection software	STOE X-AREA
Cell refinement software	STOE X-AREA
Data reduction software	STOE X-AREA

## Solution and refinement:

---

Reflections collected	12376
Independent reflections	6055 [R(int) = 0.1184]
Completeness to theta = 25.00 °	99.0 %
Observed reflections	2723[I>2(I)]
Reflections used for refinement	6055
Extinction coefficient	X = 0.0016(2)
Absorption correction	Semi-empirical from equivalents
Max. and min. transmission	0.9115 and 0.8808
Largest diff. peak and hole	0.553 and -0.828 e.Å <sup>-3</sup>
Solution	Direct methods
Refinement	Full-matrix least-squares on F <sup>2</sup>
Treatment of hydrogen atoms	Calculated positions, constr. ref.
Programs used	SIR92 (Giacovazzo et al, 1993) SHELXL-97 (Sheldrick, 2008) DIAMOND 3.2 (Crystal Impact) STOE IPDS2 software
Data / restraints / parameters	6055 / 0 / 438
Goodness-of-fit on F <sup>2</sup>	0.736
R index (all data)	wR2 = 0.0876
R index conventional [I>2sigma(I)]	R1 = 0.0522



## Crystal data

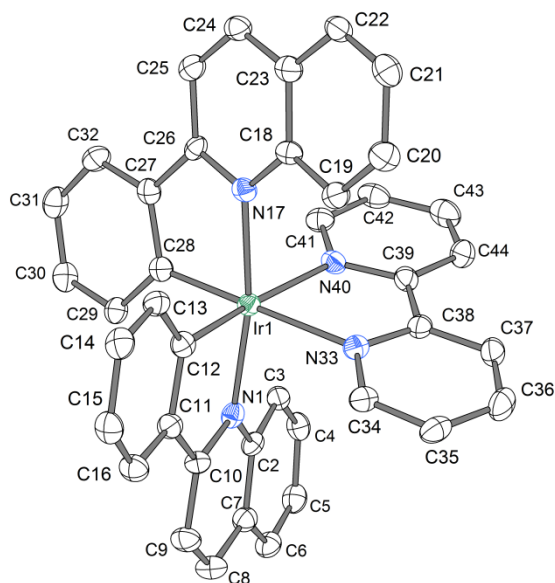
Identification code	ling52b	
Habitus, colour	block, orange	
Crystal size	0.16 x 0.15 x 0.07 mm <sup>3</sup>	
Crystal system	Orthorhombic	
Space group	P c a 2 <sub>1</sub>	Z = 8
Unit cell dimensions	a = 20.6272(8) Å	α = 90 °
	b = 11.3486(4) Å	β = 90 °
	c = 37.6770(17) Å	γ = 90 °
Volume	8819.8(6) Å <sup>3</sup>	
Cell determination	7848 peaks with Theta 1.9 to 26.0 °	
Empirical formula	C <sub>33</sub> H <sub>30</sub> N <sub>8</sub> O Ru, 2(F <sub>6</sub> P), 2(C H <sub>2</sub> Cl <sub>2</sub> )	
Formula weight	1115.51	
Density (calculated)	1.680 Mg/m <sup>3</sup>	
Absorption coefficient	0.762 mm <sup>-1</sup>	
F(000)	4464	

## Data collection:

Diffractometer type	STOE IPDS 2
Wavelength	0.71073 Å
Temperature	100(2) K
Theta range for data collection	1.79 to 25.25 °
Index ranges	-24 ≤ h ≤ 23, -13 ≤ k ≤ 13, -43 ≤ l ≤ 45
Data collection software	STOE X-AREA
Cell refinement software	STOE X-AREA
Data reduction software	STOE X-RED

## Solution and refinement:

Reflections collected	37385
Independent reflections	15542 [R(int) = 0.1025]
Completeness to theta = 25.25 °	100.0 %
Observed reflections	5475[I>2sigma(I)]
Reflections used for refinement	15542
Absorption correction	Integration
Max. and min. transmission	0.9452 and 0.8896
Flack parameter (absolute struct.)	0(2)
Largest diff. peak and hole	0.360 and -0.544 e.Å <sup>-3</sup>
Solution	Direct methods
Refinement	Full-matrix least-squares on F <sup>2</sup>
Treatment of hydrogen atoms	Calculated positions, constr. ref.
Programs used	SIR 2011 SHELXL-97 (Sheldrick, 1997) DIAMOND 3.2h STOE IPDS2 software
Data / restraints / parameters	15542 / 1165 / 1177
Goodness-of-fit on F <sup>2</sup>	0.481
R index (all data)	wR2 = 0.0657
R index conventional [I>2sigma(I)]	R1 = 0.0355



## Crystal data

Identification code	linsu23	
Habitus, colour	block, orange	
Crystal size	0.44 x 0.35 x 0.12 mm <sup>3</sup>	
Crystal system	Orthorhombic	
Space group	P 2 <sub>1</sub> 2 <sub>1</sub> 2 <sub>1</sub>	Z = 4
Unit cell dimensions	a = 14.3262(4) Å	α = 90 °
	b = 14.4257(6) Å	β = 90 °
	c = 17.8459(5) Å	γ = 90 °
Volume	3688.1(2) Å <sup>3</sup>	
Cell determination	22014 peaks with Theta 1.8 to 27.1 °	
Empirical formula	C <sub>41</sub> H <sub>30</sub> Cl <sub>2</sub> F <sub>6</sub> Ir N <sub>4</sub> P	
Formula weight	986.76	
Density (calculated)	1.777 Mg/m <sup>3</sup>	
Absorption coefficient	3.877 mm <sup>-1</sup>	
F(000)	1936	

## Data collection:

Diffractometer type	STOE IPDS 2
Wavelength	0.71073 Å
Temperature	100(2) K
Theta range for data collection	1.82 to 26.69 °
Index ranges	-17 ≤ h ≤ 18, -18 ≤ k ≤ 16, -22 ≤ l ≤ 22
Data collection software	STOE X-AREA
Cell refinement software	STOE X-AREA
Data reduction software	STOE X-RED



## Solution and refinement:

Reflections collected	22353
Independent reflections	7784 [R(int) = 0.0336]
Completeness to theta = 25.50 °	100.0 %
Observed reflections	7283[I>2sigma(I)]
Reflections used for refinement	7784
Absorption correction	Integration
Max. and min. transmission	0.7902 and 0.5527
Flack parameter (absolute struct.)	-0.020(4)
Largest diff. peak and hole	0.785 and -0.444 e.Å <sup>-3</sup>
Solution	Direct methods
Refinement	Full-matrix least-squares on F <sup>2</sup>
Treatment of hydrogen atoms	Calculated positions, riding model
Programs used	SIR-2008 SHELXL-97 (Sheldrick, 1997) DIAMOND STOE IPDS2 software
Data / restraints / parameters	7784 / 0 / 496
Goodness-of-fit on F <sup>2</sup>	0.917
R index (all data)	wR2 = 0.0376
R index conventional [I>2sigma(I)]	R1 = 0.0185

---

## Curriculum Vitae

**Name:** Zhijie Lin

**Sex:** Male

**Date of the birth:** 19.10.1983

---

### Education

**2009-Present Philipps-Universität Marburg Chemistry Department**

**Ph.D. in Organic Chemistry (Eric meggers Group)**

**Research:** Asymmetric synthesis of octahedral metal complex as the inhibitor for protein kinase  
Asymmetric catalysis reaction base on octahedral metal complex

**Publications:** 1) L. Gong, Z. Lin, K. Harms, E. Meggers, *Angew. Chem. Int. Ed.* **2010**, *49*, 7955-7957  
2) Z. Lin, L. Gong, M. A. Celik, K. Harms, G. Frenking, E. Meggers, *Chem. Asian J.* **2011**, *6*, 474-481.  
3) Z. Lin, M. A. Celik, C. Fu, K. Harms, G. Frenking, E. Meggers, *Chem. Eur. J.* **2011**, *17*, 12602-12605  
4) P. Sasmal, S. Carregal-Romero, A. Han, C. Streu, Z. Lin, E. Meggers, *ChemBioChem.* **2012**, *13*, 1116-1120.

**2006-2009 Xiamen University Chemistry Department**

**M.S. in Organic Chemistry (Peiqiang Huang Group)**

**Courses:** Advanced Organic synthesis Asymmetric Organic synthesis Organic spectroscopy  
Quantum Chemistry

**Research:** Asymmetric total synthesis

**Publication:** *Chin. J. Chem.* **2010**, *28*, 1717—1724

**2002-2006 Xiamen University Chemistry Department**

**B.S. in Chemistry**

**Awards:** University Scholarship  
Personnel training base Scholarship

**Publication:** *Journal of Xiamen University (Natural Science).* **2009**, *48*, 64-68

---